Acute Anti-Allodynic Actions of Gabapentin

by

Sascha Robert Anthony Alles

A thesis submitted in partial fulfillment of the requirements for the degree of

Doctor of Philosophy

Centre for Neuroscience
University of Alberta

Abstract

This thesis examines the cellular basis of the acute (<1 hour) anti-allodynic actions of the clinically-approved neuropathic pain drug gabapentin (GBP) in rats at the level of the spinal dorsal horn and primary somatosensory cortex.

Although the clinical effectiveness of the alpha-2-delta (α2δ) ligand GBP in treatment for neuropathic pain in patients develops over a period of several days, acute administration of clinically-relevant doses (100 mg/kg) of intraperitoneal (IP)-injected GBP significantly reduces behavioural signs of neuropathic pain in rats subject to sciatic chronic constriction injury (CCI) within 30 min. We used *ex vivo* whole-cell recording and confocal Ca^{2+} imaging of spinal cord slices and *in vivo* cortical Ca^{2+} imaging from GBP-injected rats to identify the neuronal correlates of these acute drug actions.

Putative excitatory *substantia gelatinosa* neurons were identified by their delay firing pattern and putative inhibitory neurons by their tonic firing pattern. When 'neuropathic' rats (subject to 7-14 days of sciatic CCI) received an IP injection of 100 mg/kg GBP 30 min prior to euthanasia, excitatory drive to putative excitatory neurons was decreased compared to control saline-injected neuropathic rats. This involved a decreased frequency and amplitude of spontaneous excitatory post-synaptic currents (sEPSC). In contrast, excitatory drive to putative inhibitory neurons increased as a result of increased sEPSC frequency. In putative excitatory neurons from neuropathic animals, rates of action potential discharge in response to depolarising current were

decreased by GBP administration. These changes, which were not observed in sham-operated animals, led to an overall decrease in dorsal horn excitability.

In vivo imaging studies of rats subject to CCI showed that there is a significant reduction in cortical excitability 10 min following IP injection of 100mg/kg GBP. This result implies that GBP influences cortical responses and affects pain *per se* within 10 min of systemic injection.

It was also shown that bath application of 100 μM GBP to spinal cord slices from neuropathic rats reduced the frequency of sEPSCs in both putative excitatory delay and inhibitory tonic neurons, suggesting that the cell-type specific effects of GBP are lost unless the drug is delivered systemically. These results point to a peripheral or central target of GBP's acute actions.

Many previous studies of the gabapentinoids have failed to identify any major acute effects since these studies have been mainly carried out on naïve animals or with no reference to effects on specific cell types. These results suggest that the acute effectiveness of GBP is specific to neuropathic animals. Since it has been demonstrated that α2δ levels are upregulated in neuropathic rats and that GBP is a α2δ ligand, these results suggest that the levels of α2δ are related to acute gabapentin effectiveness and the rapidity of GBP's actions. Elucidation of the mechanisms of these acute, cell-type specific actions of gabapentinoids may provide a basis for development of more effective therapeutic approaches.

Preface

This thesis is an original work by Sascha R.A. Alles. The research project, of which this thesis is a part, received research ethics approval from the University of Alberta Research Ethics Board, Project Name "Cellular electrophysiology of Neuropathic Pain", No. AUP00000338, Date: July 24th, 2015.

Part of Chapter 1 and Chapter 6 of this thesis have been published as "ALLES, S.R.A. and SMITH, P.A. 2016. The anti-allodynic gabapentinoids: myths, paradoxes and acute effects. *Neuroscientist* (in press)". This is a review article written and conceptualized jointly by myself and P.A. Smith.

This thesis is dedicated to chronic pain sufferers everywhere.

Acknowledgements

To my supervisor and scientific mentor, Prof. Peter Smith. Thank you for your financial and moral support throughout my training and for providing me with guidance and wisdom in planning my future career. Special thanks for reminding me that "you have to pay your dues to play the blues".

To Prof. Greg Funk, for your expertise on my committee and providing me with support in my future career choices. Thank you for your supportive comments after my candidacy exam and helping to boost my confidence as a budding scientist.

To Prof. John Greer, for serving on my committee, for your keen eye and extensive experience in electrophysiology. Thank you for helping me to put my work into perspective.

To Dr. James Biggs for training in the defined-medium organotypic culture technique and Ca^{2+} imaging and to Dr. Lele Chen for training in electrophysiological techniques, spinal cord slice preparation and nerve-injury surgery.

To Prof. Klaus Ballanyi and Dr. Araya Ruangkittisukal for their expertise and use of equipment for Ca^{2+} imaging experiments.

To Prof. Ian Winship and his lab members Mischa Bandet and Bin Dong, for use of Ca^{2+} imaging equipment and work involving *in vivo* imaging experiments.

To Prof. Glen Baker and his technician, Gail Rauw for work involving measurements of gabapentin levels in spinal cord slices.

To Dr. Nataliya Bukhanova, for all her work involving behavioural studies, animal handling/ordering and general lab maintenance. Thank you for making these experiments a reality.

To Twinkle Joy, for assistance in behavioural studies, animal handling/ordering and surgical/dissection procedures whenever your help was needed.

To my external examiner, Prof. David Luo for coming to Edmonton in the winter from sunny California for my examination and for discussions and comments on my thesis.

To my external (internal) examiner Prof. Douglas Zochodne for his time and comments on my thesis.

To my friend Paul Boakye, for his moral and technical support. Thank you for being a great 'sounding board' and knowing what to say when I needed it.

To my friend Pat Stemkowski, for his moral support and reassurance. Thank you for encouraging me to persevere when the going was tough. Here's hoping you set up your very own lab one day!

To my friend Sam Noh, for his 'devil-may-care' attitude towards science.

To my non-scientist friends both here and abroad, for providing an ear to listen to my ideas.

Finally, I would like to thank my wonderful wife Amanda and the family we are surrounded by, for support, love and guidance.

Funding

This work was possible thanks to funding from the Canadian Pain Society, the University of Alberta's Faculty of Medicine and Dentistry 75th Anniversary Award and a National Sciences and Engineering Research Council (NSERC, Ottawa, ON, Canada) discovery grant.

TABLE OF CONTENTS

Chapter 1

Chapter 2

Chapter 4

Chapter 5

Chapter 6

List of Tables

List of Figures

List of Abbreviations

α2δ	Alpha-2-delta subunit
ACC	Anterior cingulate cortex
aCSF	Artificial cerebrospinal fluid
AP	Action potential
ATP	Adenosine triphosphate
BDNF	Brain-derived neurotrophic factor
Ca_v	Voltage-gated calcium channel
CBT	Cognitive behavioural therapy
CCI	Chronic constriction injury
CGRP	Calcitonin-gene related peptide
cHL	contralateral hindlimb
CNS	Central nervous system
CSF-1	Colony-stimulating factor 1
dF/F_0	Change in fluorescence/Baseline fluorescence (also called 'normalized fluorescence')
DMOTCs	Defined-medium organotypic cultures
DNA	Deoxyribonucleic acid
DRG	Dorsal root ganglion
EPSC	Excitatory postsynaptic current
GABA	γ-aminobutyric acid
GBP	Gabapentin

$g_{K,Ca}$	calcium-sensitive potassium conductance
GPI	Glycophosphatidylinositol
HBSS	Hank's buffered saline solution
HCN	Hyperpolarization-activated cyclic nucleotide gated channel
HPLC	High performance liquid chromatography
HVA	High-voltage activated
I_h	H-current
I_k	Delayed rectifier potassium current
IFN-γ	Interferon-γ
IL-1α	Interleukin-1α
IL-1β	Interleukin-1β
IOS	Intrinsic optical signal
IP	intraperitoneal
IR-DIC	Infrared-differential interference contrast
KCC2	Potassium-chloride cotransporter 2
LC	Locus coeruleus
LC-MS	Liquid chromatography-mass spectrometry
mEPSC	Miniature excitatory postsynaptic current
MCP-1/CCL2	Monocyte-chemoattractant-protein-1/Chemokine (C-C motif) ligand 2
MOR	μ-opioid receptor
NGF	Nerve growth factor

NK-1	Neurokinin-1
NP	Neuropathic pain
P2X	Ligand-gated purinergic receptor
PAG	Periaqueductal grey
PGB	Pregabalin
PNS	Peripheral nervous system
PSC	Primary somatosensory cortex
PWT	Paw withdrawal threshold
RNA	Ribonucleic acid
sEPSC	Spontaneous excitatory postsynaptic current
SG	*Substantia gelatinosa*
SNL	Spinal nerve ligation
SNI	Spared nerve injury
STZ	Streptozotocin
TMS	Transcutaneous magnetic stimulation
TrkA	Receptor tyrosine kinase A
TNF-α	Tumour necrosis factor α
TSP	Thrombospondin
TTX	Tetrodotoxin
VGCC	Voltage-gated calcium channel

INTRODUCTION

What is pain?

Pain is a vital physiological phenomenon, which serves to protect an individual from injury. The International Association for the Study of Pain defines pain as "an unpleasant sensory or emotional experience associated with actual or potential tissue damage or described in terms of such damage" (Merskey et al., 1994). A 'pain matrix' has been used to describe the interplay between anatomical structures responsible for the pain experience and this involves a system of interconnected networks from the spinal cord to the brain (information regarding bodily specificity of pain) as well as within the brain (conscious perception and emotional aspects of pain) (Fig. 1-1) (Garcia-Larrea and Peyron, 2013, Jones et al., 2003)

Acute Pain & Chronic Pain

Pain can be divided into two main categories: acute and chronic pain. Acute pain is the sharp, first pain one feels when one suffers an acute injury or insult such as when one stubs their toe or puts their hand on a hot surface. This type of pain is necessary as it promotes avoidance of further tissue damage and is necessary for survival of the species. For example, if we were to keep our hand in a fire, in the absence of pain irreparable damage would be caused. Chronic pain is the painful soreness felt after the acute pain as a second pain. It is unclear as to exactly how long pain must last in order for it to be deemed 'chronic, but generally pain lasting longer than 6 months is considered to be chronic (Russo and Brose, 1998). It is also useful to categorize pain as either stimulus-independent (ongoing) or stimulus-dependent pain (Woolf et al., 1998). There are many different types of chronic pain, but for the sake of simplicity, chronic pain can be divided into

neuropathic pain and non-neuropathic pain. Examples of the latter include some types of cancer pain or perioperative pain (Yan et al., 2014).

Socioeconomic cost of pain

The socioeconomic costs of pain are staggering. A 2011 Institute of Medicine (US) report has outlined the following figures associated with pain (IOM, 2011):

- 116 million US adults suffer from chronic pain
- $560-$635 billion - conservative estimated annual cost of chronic pain in America
- $99 billion - 2008 cost to federal and state governments of medical expenditures for pain
- 80% of patients undergoing surgery experience post-operative pain
- 62% of US nursing home residents report pain.

Pain pathways

Dorsal Horn of the Spinal Cord

The detection of a tissue-damaging stimulus is called nociception. Tissue damage capable of causing pain is detected by free nerve endings in peripheral and visceral structures and relayed to sensory neurons via primary afferents to the dorsal root ganglia before terminating in the dorsal horn of the spinal cord. The grey matter of the spinal cord is divided into 10 layers called the Laminae of Rexed (Figure 1-2) (Rexed, 1952).

Nociceptive information is received in lamina I, lamina II (also called the *substantia gelatinosa*) and to a lesser extent, lamina V of the spinal cord (Todd, 2010). While lamina I contains

interneurons for modulation and projections neurons for transmission of nociceptive information, lamina II contains mainly interneurons which project to lamina I (Todd, 2010). In addition, lamina I and II also contain the terminals of incoming primary afferents that distribute in a specific pattern based on function (see next section).

Neurons of the *substantia gelatinosa* can be divided into 4 main types on the basis of morphology: islet, central, radial and vertical cells as shown in Figure 1-3 (Zeilhofer et al., 2012). Islet cells extend dendritic trees rostrocaudally with a limited dorsoventral distribution; central cells are similar to islet cells but smaller; radial cells project dendrites in all directions; vertical cells possessed markedly extended dendrites in the ventral direction (Yasaka et al., 2010, Zeilhofer et al., 2012).

Yasaka et al have exhaustively characterized 74 neurons of lamina II by whole-cell recording and *post-hoc* neurobiotin labeling. Of these 74 neurons, the neurotransmitter phenotype of 67 neurons was identified and it was established that most islet cell neurons are GABAergic whereas the majority of radial and vertical cells are glutamatergic (Table 1-1 summarizes all of these results) (Yasaka et al., 2010).

The *substantia gelatinosa* consists of 5 main cell types on the basis of firing pattern: (1) tonic neurons, which fire APs continuously in response to increasing depolarizing current and possess the lowest rheobase of the cell types (2) delay neurons, which fire with a distinct delay prior to AP discharge in response to a depolarizing current (3) transient neurons, which only fire a single AP discharge in response to a depolarizing current and possess the highest rheobase of the group (4) phasic neurons, which fire three or four APs in response to depolarization, followed by accommodation and cessation of firing and (5) irregular neurons, which show no clear relationship

between AP discharge pattern or frequency and the intensity of depolarization (Figure 1-4) (Balasubramanyan et al., 2006).

In addition, neurons that fire with a delay in response to a depolarising current are usually excitatory and neurons that fire repetitively and possess a low threshold for firing are mainly inhibitory (Balasubramanyan et al., 2006, Punnakkal et al., 2014, Ruscheweyh and Sandkuhler, 2002).

Another method of classification of laminae I-III dorsal horn interneurons is on the basis of expression of neurochemical markers such as neuropeptides, calcium-binding proteins, enzymes and receptors (Todd, 2010). A summary of the various peptides and proteins found in different classes of interneurons of the dorsal horn is shown in Table 1-2.

Primary Afferents

Primary afferents are all glutamatergic and therefore, excitatory at their postsynaptic targets (Todd, 2010). Incoming primary afferents from the periphery terminate in a specific pattern in the spinal cord based on their function: A-β fibres are large myelinated mechanoreceptors that respond to touch or hair movement and innervate lamina III-V; A-δ hair follicle afferents extend on either side of the border between lamina II and III; A-δ nociceptors innervate mainly lamina I, with some branching into lamina V and lamina X; unmyelinated afferent C-fibres are thermoreceptors or nociceptors that mainly innervate lamina II (Fig. 1-2) (Todd, 2010). C-fibres carrying nociceptive information can be divided in to peptidergic fibers containing pro-inflammatory markers such as substance P, calcitonin-gene-related-peptide (CGRP) and TrkA, the high-affinity tyrosine kinase receptor for nerve growth factor (NGF) and non-peptidergic C-fibers that do not (Snider and

McMahon, 1998). Peptidergic C-fibers innervate the skin and non-peptidergic fibers innervate other tissues (Todd, 2010). Non-peptidergic C-fibers make up approximately 50% of the C-fiber population and can be identified by their ability to bind the plant lectin, IB4 (Stucky and Lewin, 1999) or by the presence of fluoride-resistant acid phosphatase (Nagy and Hunt, 1982).

Ascending Pain Pathways

Information regarding pain is carried from the spinal cord to the brain by the following major ascending pathways: the spinothalamic, spinoreticular, spinoparabrachial, spinomesencephalic, cervicothalamic and spinohypothalamic tracts (Kandel et al., 2000, Usunoff et al., 2006).

The *spinothalamic tract* is the major ascending nociceptive pathway in the spinal cord. Axons of nociceptive-specific and wide-dynamic range neurons in laminae I and V-VI of the dorsal horn project along the contralateral side of spinal cord and ascend in the anterolateral white matter to the thalamus where they terminate (Bear et al., 2007, Kandel et al., 2000). Spinothalamic neurons that project to the lateral thalamus are most likely involved in sensory-discriminative aspects of pain (Usunoff et al., 2006).

The *spinoparabrachial tract* is a significant nociceptive projection that may be as important as the spinothalamic tract. The parabrachial nucleus is a small region surrounding the superior cerebellar peduncle that is innervated by ascending spinal cord and spinothalamic nucleus neurons and sends projections to the amygdala and hypothalamus (Usunoff et al., 2006). This tract is most likely responsible for intensity of pain rather than its location or nature (Hunt and Mantyh, 2001).

In the *spinoreticular tract* axons of neurons in laminae VII and VIII ascend anterolaterally to the reticular formation and the thalamus, however many of the axons do not cross the midline (Kandel

et al., 2000). The reticular formation may function as a relay station for nociceptive information to the thalamus, which suggests that this tract may have a role in a control of pain processing (Usunoff et al., 2006).

In the *spinomesencephalic tract*, neurons of laminae I and V project anterolaterally to the mesencephalic reticular formation and periaqueductal gray matter and then to the parabrachial nucleus through the spinparabrachial tract (Kandel et al., 2000). Neurons from the parabrachial nucleus then project to the amygdala, which forms part of the limbic system involving emotion, therefore, this tract is thought to be involved in the affective experience of pain (Wall et al., 1994).

The *cervicothalamic tract* is comprised of neurons in the lateral cervical nucleus, in the upper two cervical segments of the spinal cord in the lateral white matter. Nociceptive neurons from laminae III and IV send inputs to the lateral cervical nucleus. Neurons of this tract ascend in the medial lemniscus of the brain stem to nuclei in the midbrain and the thalamus. Some axons from laminae III and IV terminate in the cuneate and gracile nuclei of the medulla (Kandel et al., 2000).

The *spinohypothalamic tract* consists of axons from laminae I, V and VIII that project directly to supraspinal autonomic centrers and activates complex neuroendocrine and cardiovascular responses (Kandel et al., 2000, Wall et al., 1994).

In addition some nociceptive information may travel through the *trigeminal pain pathway*, whereby sensory information from the head and face is carried directly to the thalamus. Small diameter fibres from the trigeminal nerve synapse on to second-order neurons in the trigeminal nucleus in the brainstem and axons ascend to the thalamus in the trigeminal lemniscus after crossing (Bear et al., 2007).

Pain Processing in the Brain

Within the brain, processing of nociceptive information occurs to produce the experience of pain and this has been attributed to the interplay between the regions described previously in the 'pain matrix' (Figure 1-1). It has also been shown by techniques such as positron emission tomography (PET), functional magnetic resonance imaging (MRI and electroencephalography (EEG) that the areas of the brain that are found to be active during the experience of acute pain are: the primary and secondary somatosensory cortices, the insular cortex, the anterior cingulate cortex and the prefrontal cortex and the thalamus (Tracey and Mantyh, 2007). In addition, depending on the circumstances of the particular individual, other areas such as the basal ganglia, cerebellum, amygdala, hippocampus and parietal and temporal cortices may be involved (Tracey and Mantyh, 2007). It is important therefore, to be aware that the 'pain matrix' is not a fixed concept and that there may be a unique 'pain signature' depending on the individual (Tracey, 2005). For example, in cases of chronic pain, specific brain activity has been associated with fluctuations of the intensity of chronic back pain (Baliki et al., 2006).

Descending Pain Pathways

The midbrain periaqueductal grey (PAG) sends descending input to midline regions of the medulla, mainly the serotonergic raphe nuclei, which in turn send projections through the dorsolateral funiculus to the dorsal horn of the spinal cord to modulate incoming nociception (Bear et al., 2007). The serotonergic neurons of the raphe magnus receive inputs from enkephalinergic neurons in the PAG and endogenous opioids released there activate descending modulatory pathways to affect nociceptive processing (Kandel et al., 2000).

There are additional projections to the spinal cord from noradrenergic cell groups in the pons and medulla and the nucleus paragigantocellularis, which receives input from the PAG (Kandel et al., 2000). These descending inputs can inhibit nociceptive projection neurons either directly or through interneurons of the superficial dorsal horn of the spinal cord.

In addition there are descending pathways that can facilitate pain transmission and it is thought that sustained activation of these pathways may contribute to chronic pain states (Porreca et al., 2002, Suzuki et al., 2004).

A number of brain areas have been implicated in descending modulation of pain including the frontal lobe, ACC, insula, amygdala, hypothalamus, PAG, nucleus cuneiformis (NCF) and rostral ventromedial medulla (RVM) (Tracey and Mantyh, 2007).

Gate Control Theory of Pain

Ronald Melzack and Patrick Wall proposed the gate control theory of pain in the 1960s (Melzack and Wall, 1965). The theory proposes that neurons of the dorsal horn of the spinal cord that send projections along the spinothalamic tract are excited by both large-diameter mechanoreceptive sensory fibres and unmyelinated small-diameter nociceptive fibers. Also, projection neurons are inhibited by interneurons, which in turn are excited by large-diameter fibres and inhibited by nociceptive fibres. As a result of this organization, nociceptive fibre activity results in excitation of projection neurons to carry painful information to the brain, however, simultaneous activity in large-diameter fibres can stimulate the interneuron which would then inhibit the nociceptive fibre and attenuate the flow of nociceptive information (Wall et al., 1994).

The gate control theory is correct with regards to the net result, however, the exact mechanism has not been proven experimentally. According to the gate theory (Figure 1-5A), incoming afferents carrying nociceptive information form an excitatory synapse on to projection neurons (E1) and an inhibitory synapse between incoming afferents and inhibitory interneurons (I1) in the dorsal horn of the spinal cord (Leitner et al., 2013). However, the existence of the proposed inhibitory synapse (I1) has not been demonstrated experimentally. As shown in Figure 1-5B, in a state of neuropathic pain I1 may instead be excitatory to inhibitory GABAergic neurons so as to decrease excitatory drive at this input to 'open' the spinal gate for nociception (Leitner et al., 2013).

Neuropathic Pain

Neuropathic pain (NP) is a type of chronic pain that is defined as "pain caused by a lesion or disease of the somatosensory system" (Jensen et al., 2011). It can be caused by traumatic nerve, spinal cord or brain injury (including stroke) or can be associated with diabetic, HIV/AIDS, post-herpetic neuropathies or multiple sclerosis (Treede et al., 2008). Clinical diagnosis of neuropathic pain depends on evaluation of the following patient criteria: 1) pain with a distinct neuroanatomical distribution 2) a history that suggests a lesion or disease of the nervous system 3) confirmatory test to demonstrate neuroanatomical distribution 4) confirmatory test to demonstrate a lesion or disease of the nervous system (Treede et al., 2008). Definite neuropathic pain is categorized as fulfilling all of these criteria, whereas probable neuropathic pain is categorized as fulfilling criteria 1 and 2 without evidence from 3 or 4.

NP is a maladaptive response of the nervous system to damage, the main symptoms of which include allodynia (pain in response to an innocuous stimulus), hyperalgesia (increased pain response to a noxious stimulus), spontaneous pain (electric-shock-like or shooting pain) and occasionally, causalgia or 'burning pain' (Costigan et al., 2009). For this reason NP is sometimes referred to as the 'disease of pain'. Exact prevalence of NP within the global population is unknown, however most studies put estimates at between 1.5% and 8%, equating to between approximately 100 million and 560 million people worldwide (Gilron et al., 2006, Torrance et al., 2013, Torrance et al., 2006). NP is marked by changes in normal sensory signalling at the level of the periphery, spinal cord and brain (thalamus and cortex) that occur over the course of weeks or months and that can lead to alterations in genomic expression and differences in cortical structures (Costigan et al., 2009, Luo et al., 2014, Tajerian et al., 2013, Sandkuhler, 2009).

Mechanisms of NP

There has been an increasing awareness of NP in the scientific literature over the past 40 years (Figure 1-6), suggesting that it is perhaps more commonplace than previously thought. As shown in Figure 1-6, the prevalence of the phrase "neuropathic pain" in books as measured using Google Ngram Viewer has increased more than 4 times between 1992 and 2008.

Marshall Devor was one of the first to show that injury to sensory axons can bring about changes in the organisation of the spinal cord sensory map (Devor and Wall, 1978) and sensory disturbances such as chronic NP that are attributed to changes in the electrical excitability of the injured neuron and abnormal ongoing and evoked discharge from "ectopic neural pacemaker sites" (Devor and Govrin-Lippmann, 1983, Wall and Devor, 1983). It was shown by Devor et al that the

molecular components of the nerve that are responsible for normal activity, such as channels and receptor proteins, “dam up” the injury site and the dorsal root ganglia so that these pacemaker sites become hyperexcitable and a source of abnormal sensory processing and pain (Devor, 1991a). These sites can be visualized as swellings or axon ‘endbulbs’ and neuromas that can be distributed throughout a nerve or its target tissue (Fried and Devor, 1988). These ideas were later confirmed by showing that ectopic neuroma discharge and dorsal root ganglia discharge following peripheral nerve axotomy could be silenced by systemic lidocaine without blocking nerve conduction to explain its mechanism of analgesia (Devor et al., 1992).

The idea of ‘central sensitization’ was first put forward by Clifford Woolf of Harvard Medical School in the early 1980s to describe the cascade of events that are attributed to the maladaptive changes in plasticity of sensory processing that occur in NP (Woolf and Mannion, 1999, Woolf and Thompson, 1991, Woolf and Walters, 1991, Woolf, 1983). NP has since come to be known as a far more complex phenomenon than once thought, with a variety of factors at the cellular and molecular level involved.

Coull et al showed that a decrease in anion gradient occurred in rat dorsal horn lamina I neurons following peripheral nerve injury as a result of a reduction in expression of the potassium-chloride exporter KCC2. The resulting accumulation of intracellular Cl^- can cause normally inhibitory GABAergic anionic outward synaptic currents to become inward excitatory currents (Coull et al., 2003). It was corroborated that this change was due to a reduction in KCC2 expression as a knockdown of spinal KCC2 in non-injured, intact rats reduced pain thresholds and resulted in NP behaviours (Coull et al., 2003). Hence, an injury that causes NP results in a marked change in dorsal horn function such that the net excitability of nociceptive lamina I neurons is increased.

Later Coull et al demonstrated that brain-derived neurotrophic factor (BDNF) release from activated, ATP (adenosine triphosphate)-stimulated spinal microglia is responsible for the aforementioned depolarising shift in anion gradient observed in lamina I neurons in NP (Coull et al., 2005). Administration of ATP-stimulated microglia or application of BDNF produces the shift in anion gradient seen after nerve injury and also, blocking signalling between BDNF and its receptor TrkB reversed pain behaviours (allodynia) and a shift in anion gradient (Coull et al., 2005). It is also possible to prevent allodynia and the shift in anion gradient by blocking release of BDNF from microglia by treatment with interfering RNA against BDNF (Coull et al., 2005). Around the same time it was confirmed that following peripheral nerve injury, there is an increase in the expression of the ATP-gated ionotropic purinoceptor P2X4-receptor (P2X4-R) by microglia and that this increase in expression parallels the increase in pain hypersensitivity (Tsuda et al., 2003, Tsuda et al., 2008, Ulmann et al., 2008). Pharmacological blockade of P2X4-Rs reverses pain hypersensitivity (Tsuda et al., 2008) and can be prevented in P2X4R null mutant mice (Ulmann et al., 2008). The mechanism by which P2X4R upregulation leads to BDNF release from microglia is attributed to influx of Ca^{2+} through P2X4Rs, activation of p38-mitogen-activated-kinase (MAPK) and consequently an increase in synthesis and SNARE-mediated exocytosis of BDNF (Trang et al., 2009).

Recently it was shown that this mechanism is specific to male mice as microglia are not required for mechanical sensitivity to pain in female mice in which adaptive immune cells are involved (Sorge et al., 2015).

The process by which microglia become activated arises from the complex series of events accompanying peripheral nerve injury whereby neurons release pro-inflammatory mediators such as ATP, CCL2, CCL21, NRG1, CX3CR1 and endogenous danger signals that initiate central

immune signaling in the spinal dorsal horn (Grace et al., 2014). ATP, from either cell damage or as a neurotransmitter, is an important early trigger for reactive microgliosis (Friedle et al., 2010).

In addition to altering the inhibitory actions of GABA, sciatic nerve injury (both chronic constriction injury and axotomy) produces an 'electrophysiological footprint' of NP and has been shown to reflect an increased excitatory drive to putative excitatory delay-firing neurons and a decreased excitatory drive to putative inhibitory tonic-firing neurons in lamina II of the spinal cord as measured by changes in spontaneous, excitatory synaptic activity (Balasubramanyan et al., 2006, Chen et al., 2009).

There is also evidence to suggest that the changes brought about by treatment of organotypic spinal cord cultures with chronic BDNF elicits electrophysiological and global network excitability changes in dorsal horn neurons that mimic those observed in the dorsal horn of chronic-constriction-injured, neuropathic rats (Lu et al., 2007, Lu et al., 2009). It was also shown that activated microglia-conditioned medium (aMCM) containing BDNF elicited an increase in overall dorsal horn excitability and that pre-incubation of slices with a TrkB (receptor for BDNF) antagonist inhibited the effects of BDNF as well as aMCM on dorsal horn excitability (Lu et al., 2009).

Ectopic activity in primary afferent neurons occurs in NP and this most likely contributes to spontaneous, stimulus independent pain (Gilron et al., 2015, Liu et al., 2000). Indeed it has been shown that following a peripheral nerve injury there is altered synaptic activity of *substantia gelatinosa* neurons with little effect on intrinsic neuronal properties suggesting that changes in the central nervous system are driven by activity of peripheral neurons (Balasubramanyan et al., 2006, Devor, 2006). In a simple yet elegant series of experiments it was shown that the hyperexcited state of dorsal horn neurons is maintained by ongoing, afferent discharges from the peripheral

nerve distal to, at and proximal to the site of injury by application of lidocaine to block nerve conduction and subsequent monitoring of spontaneous baseline discharge (Pitcher and Henry, 2008).

Other Molecules and Ion Channels involved in Neuropathic Pain

Changes in the expression and/or properties of a variety of ion channels have been implicated in this process including voltage-gated sodium channels (for example Nav1.3, 1.6 and 1.9), potassium channels (for example Kv7, KCNQ) and hyperpolarization-activated cyclic nucleotide gated (HCN) channels (Gilron et al., 2015). In addition to ion channels, changes in the expression of neuropeptides, receptors, signal transduction molecules and synaptic vesicle proteins have been reported using gene array studies (Zhang and Xiao, 2005). Table 1-3 provides a list of ion channel or receptor genes that are upregulated at least two-fold in the dorsal horn of nerve-injured rats compared to controls as measured using cDNA microarray analysis (Yang et al., 2004).

Voltage-gated Sodium Channels

In early experiments on DRG neurons from rats that had received a peripheral nerve injury it was established that an increase in voltage-gated sodium channel current underlies the increased action potential discharge (measure of intrinsic excitability) observed (Abdulla and Smith, 2001b, Abdulla and Smith, 2002). Later, genetic studies confirmed the importance of voltage-gated sodium channels by showing that gain-of-function mutations in Nav1.7, Nav1.8 and Nav1.9 are implicated in peripheral neuropathy disorders in humans by increasing the excitability of nociceptive neurons (Dib-Hajj et al., 2015). Pharmacological treatments such as carbamazepine, that are known to target Na^+ channels, have been used to effectively treat some types of NP (Gilron

and Dickenson, 2014). Novel sodium channel antagonists such as small molecule peptide blockers of Nav1.7 (e.g. μ-TRTX-Hhn1b derived from spider venom) are also of interest for treatment of NP (Rivara and Zuliani, 2015). More recently a monoclonal antibody targeting the voltage sensor 'paddle' domain of Nav1.7 has been designed to allow for greater sodium channel subtype selectivity (Lee et al., 2014). Slow-inactivation-specific ion channel modulators represent another method by which ion channels can be stabilized in their slow inactivated state to act as a 'brake' during periods of neuronal hyperexcitability and these have been applied to target sodium and calcium channel currents for treatment of NP (Hildebrand et al., 2011).

Voltage-gated Potassium channels

Early experiments also showed that delayed rectifier current (I_K) and Ca^{2+}-sensitive K^+ conductance ($g_{K,Ca}$) is reduced in DRG neurons from nerve-injured rats and that this contributes to increased excitability of these neurons (Abdulla and Smith, 2001a, Abdulla and Smith, 2001b). Furthermore, voltage-gated potassium channel subunits have been shown to be downregulated in DRG neurons in NP, which results in an inhibition of potassium channel expression and an overall net increase in excitability in primary afferents (Waxman and Zamponi, 2014). Two-pore-domain potassium channels (K2P) and voltage-gated potassium channels Kv1.1 and Kv1.2 have emerged as potential therapeutic targets for the treatment of chronic pain as knockdown of these channels has reduced pain behaviours in animals and dysfunction of these channels have been linked to neuropathies in humans (Guedon et al., 2015, Mathie and Veale, 2015, Tsantoulas, 2015).

Voltage-gated Calcium Channels

Another player in the field of NP and pain therapeutics research in general, is the voltage-gated calcium channel. Figure 1-7 shows the molecular structure of the VGCC with subunit interactions (Alles and Smith, 2016). Briefly, these channels encompass high-voltage activated (HVA) L-types ($Ca_V1.1$, $Ca_V1.2$, $Ca_V1.3$, and $Ca_V1.4$); P/Q-type ($Ca_V2.1$,) N-type ($Ca_V2.2$), and R-type ($Ca_V2.3$) as well as T-type (low-voltage-activated, LVA) Ca^{2+} channels ($Ca_V3.1$, $Ca_V3.2$, $Ca_V3.3$) (Zamponi, 2015). Influx of Ca^{2+} through high-voltage-activated (HVA) Ca^{2+} channels triggers neurotransmitter release from presynaptic vesicles and thereby determines neuronal network excitability. The importance of HVA-Ca^{2+} channels in NP is illustrated by the clinical effectiveness of the N-type Ca^{2+} channel blocker ziconotide (Zamponi *et al.*, 2015) and as will discussed below, the relationship between HVA-Ca^{2+} channel function and the actions of gabapentinoids.

Voltage-gated Ca^{2+} channels consist of five subunits: the α_1 pore-forming subunit and auxiliary subunits α_2, β, δ and γ (Figure 1-7, reviewed in Zamponi et al., 2015). The main subtype found in presynaptic terminals is Ca_v2 (Westenbroek et al., 1992). $Ca_v2.1$ and $Ca_v2.2$ both contain a synaptic protein interaction site (synprint) that interacts with SNARE proteins (syntaxin and SNAP-25) (Rettig et al., 1996, Sheng et al., 1994). By this mechanism, channels can be closely associated with synaptic vesicles that govern release of neurotransmitter.

Since these channels are responsible for depolarization-induced influx of Ca^{2+} and triggering consequent release of neurotransmitter, blocking or removing these channels in hyperexcitable nociceptive neurons would serve to reduce net excitability (Bourinet et al., 2014). For example, N-type VGCC knockout mice exhibit reduced inflammatory and NP symptoms (Saegusa et al., 2001). However, a decrease in $g_{K,Ca}$ has been reported in NP and so, it is possible that ablating VGCCs could actually increase excitability in DRG neurons by decreasing $g_{K,Ca}$ (Abdulla and

Smith, 2001a). It is also important to note that there is a classical 3-4th power relationship between Ca^{2+} influx and neurotransmitter release (Dodge and Rahamimoff, 1967); even if one were to reduce the amount of Ca^{2+} entering terminals using a VGCC blocker, there are sufficient VGCCs expressed to support substantial neurotransmitter release. This possibility is supported by the observation that overexpression of pore forming $Ca_v2.2$ channels in hippocampal neurons fails to increase excitatory postsynaptic current (EPSC) size and the suggestion that the strength of neurotransmission is saturated with regard to levels of Ca^{2+} channel expression (Cao and Tsien, 2010).

HCN Channels

The HCN channels have emerged as a promising peripheral target for neuropathic as well as inflammatory pain (Chaplan et al., 2003, Emery et al., 2011, Young et al., 2014). For example, HCN2 is expressed is expressed in about half of small somatosensory neurons, which are mainly nociceptors, and plays an important role in the control of firing frequency in response to noxious stimuli (Emery et al., 2011). Indeed deletion of HCN2 in nociceptive neurons prevents the development of inflammatory and NP (Emery et al., 2011). A blocker of HCN channels, ivabradine, has been shown to be effective in treating signs of NP in animals models through peripheral action on small sensory neurons and to decrease firing frequency in cultured DRG neurons from nerve-injured animals (Noh et al., 2014, Young et al., 2014).

Cytokines

As a result of traumatic peripheral nerve injury there is abrupt tissue damage at the site of the lesion where trauma occurred and distal nerves begin to undergo Wallerian degeneration (WD) after Waller (Waller, 1850). The injury sets the ‘cytokine network’ of WD into play and there is

release of tumour necrosis factor α (TNF-α) and interleukin-1α (IL-1α) from Schwann cells as a result of the signal from the injury site that travels along the axon distally (Rotshenker, 2011, Shamash et al., 2002). TNF-α and IL-1α production induces fibroblasts to release interleukin-6 (IL-6) and after several hours, Schwann cells begin to produce inflammatory interleukin-1β (IL-1β) (Rotshenker, 2011). Finally, chemokines such as monocyte-chemoattractant-protein-1 (MCP-1) and MCP-1α are released by Schwann cells (Rotshenker, 2011). Monocytes then migrate into nervous tissues 2-3 days after injury and eventually differentiate in to macrophages, which release some inflammatory mediators but also anti-inflammatory mediators such as IL-10, to downregulate cytokine production (Rotshenker, 2011).

Cytokines such as IL-1β and IL-6 have been implicated in mechanical and thermal hyperalgesia, TNF-α plays a role in thermal hyperalgesia and interferon-γ (IFN-γ) contributes to mechanical allodynia (Sandkuhler, 2009). IL-1β has been shown to increase excitability of DRG neurons through modulation of the activity of sodium channels, although it has been shown that these effects are only observed if IL-1β is constitutively present (Stemkowski et al., 2015, Stemkowski and Smith, 2012). In fact, nociceptors have been described as IL-1β sensors (Binshtok et al., 2008). MCP-1 has also been shown to enhance the excitability of nociceptive neurons following chronic compression of the dorsal ganglia by activation of a cation conductance and inhibition of voltage-dependent outward currents (Sun et al., 2006).

Animal Models of NP

Peripheral Nerve Injury

There are different types of peripheral nerve injury that can be used to model clinical neuropathic pain in rodents. Robustness of the pain behaviour being induced is an important factor to consider as some procedures will allow for post-operative recovery of the animal depending on the severity of the injury (Kim et al., 1997). All methods employ some form of partial or complete nerve damage.

The neuroma model was the first model of peripheral nerve injury and neuropathy (Wall and Gutnick, 1974). It is achieved by complete transection of the sciatic nerve, followed by re-sealing of the nerve with a polyethylene tube. The pain behaviour produced by this model is often accompanied by autotomy or self-mutilation of the denervated limb (Devor, 1991b, Wall et al., 1979).

Chronic constriction injury (CCI) entails the constriction of the sciatic nerve by loose ligation and can be produced by ligation with a suture of chromic gut around the sciatic nerve in the Bennett model or by constriction of the nerve with a polyethylene cuff as in the improved Mosconi-Kruger model to produce allodynia, spontaneous pain and hyperalgesia (Bennett and Xie, 1988, Mosconi and Kruger, 1996). Most rats recover to near control levels after 4 weeks post-surgery with peak pain-related behaviours related to mechanical and cold hyperalgesia occurring during the 2nd week post-surgery (Mosconi and Kruger, 1996).

Spinal nerve ligation (SNL) is achieved by tight ligation of lower lumbar vertebrae (L5 and L6) spinal nerves and produces the same symptoms as CCI, but with greater levels of allodynia (Kim et al., 1997). The Seltzer partial sciatic nerve injury model and Chung spinal segmental nerve

model utilize tight ligation of a part of a large peripheral nerve or an entire spinal segmental nerve respectively (Kim and Chung, 1992, Seltzer et al., 1990).

Spared nerve injury (SNI) is carried out by creating a lesion in two (tibial and common peroneal) of the three terminal branches of the sciatic nerve to leave the sural nerve intact (Decosterd and Woolf, 2000). Rats will recover slightly, however, they will maintain reduced, 'neuropathic' paw withdrawal thresholds for at least 220 days post-surgery (Decosterd and Woolf, 2000).

Diabetic neuropathy

Diabetes is frequently accompanied by painful peripheral neuropathy referred to as diabetic neuropathy. Transport of glucose into neurons is insulin independent, therefore neurons become hyperglycemic and this results in the activation of aberrant metabolic processes, oxidative stress and other inflammatory processes that lead to the generation of nociceptive stimuli contributing to neuropathy (Zochodne, 2015). This form of NP can be modelled in rodents through injection of streptozotocin (STZ), which destroys pancreatic insulin-secreting-β-cells through glucose transporter uptake and damaging DNA or by over-nutrition to develop obesity and consequent diabetes (Gao and Zheng, 2014).

Chemotherapy-induced Neuropathy

Chemotherapy has the unfortunate side effect of painful peripheral neuropathy. Chemotherapy drugs are thought to induce neuropathy by causing damage to DNA, alterations of cellular repair systems, mitochondrial changes, production of reactive oxygen species, ion channel alterations, glutamate signalling and activation of nociceptors (Carozzi et al., 2015). This has made cancer drugs a candidate for inducing painful peripheral neuropathy in rodents to study NP.

Intraperitoneal injection of paclitaxel (Taxol®) has been used to induce mechanical and thermal allodynia and hyperalgesia in rodents (Polomano et al., 2001).

Treatment of NP

Pharmacological Treatment

There are several treatment options for NP available. Many NP drugs were originally developed for other clinical conditions such as depression or epilepsy and these include antidepressants, anticonvulsants, opioids, NMDA receptor antagonists, local anesthetics, cannabinoids, botulinum toxin, conotoxins and capsaicin (Gilron et al., 2015).

Opioids show limited effectiveness in NP and this is supported by evidence that μ-opioid receptors (MORs) are downregulated in the DRG following peripheral nerve injury (Abdulla and Smith, 1998, Kohno et al., 2005). In addition, opioids also have the downside of producing severe side effects including sedation, nausea, constipation, development of novel pain syndromes such as rebound headache and risk of tolerance and abuse (Bril et al., 2011). In comparison, the gabapentinoids produce generally fewer and less severe side effects of dizziness and drowsiness with a low risk of abuse and tolerance.

Current recommendations and lines of treatment for NP drugs are shown in Table 1-4. The goal of NP drug design is to counteract the changes in nociceptive pathways that occur in NP, in other words to reduce both peripheral and central sensitization by reducing excitatory drive to pro-nociceptive pathways and/or increasing excitatory drive to anti-nociceptive pathways (Gilron et al., 2015).

Non-pharmacological treatment

In addition to the use of drugs, physicians may prescribe cognitive behavioural therapy (CBT), physiotherapy and/or massage therapy and occasionally, traditional medicine approaches such as acupuncture or yoga for treatment of chronic NP syndromes (Ehde et al., 2014, Holtzman and Beggs, 2013, Norrbrink and Lundeberg, 2011, Ulett, 1999).

Transcutaneous magnetic stimulation (TMS), whereby transcranial magnetic stimulation is used to modulate neuronal functions, has also been used to treat post-traumatic peripheral NP successfully (Leung et al., 2014).

A highly invasive neurosurgical technique called deep brain stimulation, originally developed and popularized for the treatment of Parkinson's disease and epilepsy, can also be used to treat severe cases of NP including phantom limb pain and post-stroke pain (Boccard et al., 2015). Regions of the brain implicated in nociceptive pathways including the periaqueductal grey, thalamus and anterior cingulate cortex are stimulated to relieve intractable NP (Boccard et al., 2015).

The Gabapentinoids

The gabapentinoids, pregabalin (PGB, second generation) and gabapentin (GBP, first generation) are a first-line pharmacological treatment clinically available for the management of NP (Moulin et al., 2007). GBP was originally used as an adjunct and monotherapy for partial and general tonic-clonic seizures, but later was approved as a treatment for post-herpetic neuralgia (Taylor et al., 1998).

PGB and GBP have been proven to be clinically effective in the treatment of NP, but they are also effective as anti-epilepsy medications (Field et al., 2006). Both pregabalin and GBP are structurally similar to the inhibitory neurotransmitter γ-aminobutyric acid (GABA), but neither drug appears to bind $GABA_A$ or $GABA_B$ receptors (Lanneau et al., 2001, Li et al., 2011, Moore et al., 2002, Sutton et al., 2002). Gabapentinoids also do not affect GABA uptake, synthesis or metabolism (Taylor et al., 2007). Gee et al isolated and sequenced a protein that bound GBP from porcine brain and this protein was identified as the $\alpha_2\delta$-1 subunit of voltage-gated calcium channels (VGCCs) or $Ca_v\alpha_2\delta_1$ (Gee et al., 1996). For this reason, the gabapentinoids are also referred to as '$\alpha_2\delta$ ligands'.

The $\alpha_2\delta$ subunit

The $\alpha_2\delta$ subunit is a structural subunit (Figure 1-7) of mature high-voltage activated (HVA) VGCCs, which encompasses L-, N-, P/Q- and R-type channels (Dolphin, 2013, Ertel et al., 2000). It does not associate with T-type channels (Dolphin, 2013). There are four mammalian genes that encode the $\alpha_2\delta$ subunits: *CACNA2D1-CACNA2D4* (Whittaker and Hynes, 2002). Although the $\alpha_2\delta$ subunit is encoded by a single gene, it is expressed as two individual proteins (α_2 and δ), which then re-assemble and associate with the VGCC as shown in Figure 1-7 (Dolphin, 2013). The $\alpha_2\delta$ subunits are glycophosphatidylinositol (GPI)-anchored which means that they are present on the extracellular surface making them potentially susceptible to extracellular modulation (Davies et al., 2010).

There are 4 main subtypes of the $\alpha_2\delta$ subunit: $\alpha_2\delta$-1, $\alpha_2\delta$-2, $\alpha_2\delta$-3 and $\alpha_2\delta$-4. The expression of $\alpha_2\delta$ subunits is fairly ubiquitous, where $\alpha_2\delta$-1 subunit is expressed in skeletal, cardiac and smooth

muscles, the CNS and PNS as well as endocrine tissues; the $\alpha_2\delta$-2 subunit is expressed in CNS, especially the cerebellum; $\alpha_2\delta$-3 is expressed in the CNS and PNS; and $\alpha_2\delta$-4 is expressed in the retina and in endocrine tissue (Dolphin, 2013). In neurons, it has been shown that the $\alpha_2\delta$-1 transcript colocalizes with mainly excitatory neurons and that $\alpha_2\delta$-2 mRNA colocalizes with GABAergic inhibitory neurons (Dolphin, 2013). Gabapentin binds with greater affinity for $\alpha_2\delta$-1 than $\alpha_2\delta$-2 subunit, with no binding affinity for $\alpha_2\delta$-3 (Marais et al., 2001).

The physiological role of the $\alpha_2\delta$ subunit

The $\alpha_2\delta$-1 subunit has been shown to be a multifunctional protein which plays numerous physiological roles including setting presynaptic release probability, stabilizing VGCCs at the plasma membrane and synapse modulation (Arikkath and Campbell, 2003, Dickman et al., 2008, Hoppa et al., 2012).

Hoppa et al have shown that the $\alpha_2\delta$ subunit can increase the amount of Ca^{2+} that the Ca^{2+} sensor for release 'sees' (without increasing total Ca^{2+} influx) at release sites to influence the probability of neurotransmitter release (Hoppa et al., 2012).

The function of the $\alpha_2\delta$ subunit as a molecular chaperone of voltage-gated calcium channels has also been proposed. Cassidy et al have shown, by exofacial (referring to the extracellular side or 'outside facing' part of the plasma cell membrane) tagging of Ca_v2 channels, that $\alpha_2\delta$-1 subunits increase Ca_v2 plasma membrane expression, which suggests that part of the role of $\alpha_2\delta$ is in trafficking of channel complexes (Cassidy et al., 2014). It has been demonstrated that while T-type (Ca_v3) channels do not require $\alpha_2\delta$ to be expressed, their expression is enhanced by the presence of $\alpha_2\delta$ (Zamponi et al., 2015). These experiments were performed in immortalized cell lines

(mouse neuroblastoma cells), therefore the role of $\alpha_2\delta$ in a physiological setting where the presynaptic terminals may be rather remote compared to the position of the cell body, as is the case with the dorsal root ganglia and the primary afferent terminals in the dorsal horn of the spinal cord, may yield different results especially when relating to the role of $\alpha_2\delta$-1 as a molecular chaperone for trafficking of functional VGCCs.

The $\alpha_2\delta$ subunit and NP

Luo et al first demonstrated that the α2δ-1 subunit is upregulated in the spinal cord following spinal nerve-ligation and development of NP in rats. After nerve ligation in nerve-injured (but not sham operated rats), a 17-fold increase in the $\alpha_2\delta$-1 protein in ipsilateral L5/L6 DRGs is observed (Luo et al., 2001). No increase in expression levels of other subtypes of the $\alpha_2\delta$ subunit following nerve injury have been reported.

Another spinal nerve ligation study showed that 'injury-induced discharges' that contribute to NP initiation moderate the expression of $\alpha_2\delta$ in the spinal dorsal horn (Boroujerdi et al., 2008). It was first shown that injury discharges were blocked by local application of lidocaine and then secondly that lidocaine application was able to reduce the nerve-injury induced $\alpha_2\delta$ upregulation seen in saline controls in both dorsal spinal cord and dorsal root ganglia (Boroujerdi et al., 2008).

In mice, $\alpha_2\delta$ gene deletion results in deficits in behavioural signs of mechanical and cold sensitivity and delayed mechanical hypersensitivity in response to peripheral nerve injury (Patel et al., 2013). In addition, mice that overexpress $\alpha_2\delta$ develop mechanical allodynia similar to nerve injury models and this has been shown to be mediated by a presynaptic mechanism involving an increase in

excitatory synaptic transmission as is also the case with nerve-injury (Nguyen et al., 2009, Zhou and Luo, 2014, Zhou and Luo, 2015).

Therefore, it is clear that the $\alpha_2\delta$ subunit of VGCCs are important in contributing to the pathophysiology of NP.

Mechanism of action of GBP

'Classical mechanism'

The proposed 'classical' mechanism of action of GBP is that GBP enters the neuronal cytosol through the system-L-neutral amino acid transporter and binds the $\alpha_2\delta$-1 subunit, resulting in a reduction in the forward trafficking of functional VGCCs to nerve terminals, which would consequently result in a decrease in net Ca^{2+} influx and hence a reduction in neurotransmitter release (Field et al., 2006). Studies using a mutant mouse containing a single-point mutation (a substitution of arginine for alanine on residue 217 or R217A) in the gene encoding the $\alpha_2\delta$ subunit have shown a reduction in pregabalin and gabapentin binding and a lack of analgesic efficacy (inhibition of allodynia) compared to wild-type mice (Field et al., 2006).

In the context of NP, where nociceptive neurons become hyperexcitable, it is expected that GBP reduces depolarization-induced neurotransmitter release to reduce net excitability and normalize pain thresholds (Hendrich et al., 2008). Most of the reported actions of GBP suggest that its effect on VGCC trafficking would be expected to occur over a long-term time course (>17 hours or more) (Biggs et al., 2014a, Biggs et al., 2014b, Hendrich et al., 2012) and this mechanism would also support clinical observations that GBP takes several days to produce meaningful pain reductions in NP patients (Cheshire, 2002, Sharma et al., 2010).

Paradox arguing against 'classical' mechanism

GBP appears to produce an effect on pain thresholds in a matter of minutes or hours in *in vitro* and *in vivo* animal models, which contradicts a much longer time course (>17 hours), 'classical' mechanism (Field et al., 2006, Hunter et al., 1997, Kumar et al., 2013). Therefore, a paradox exists between the acute effects of GBP *in vitro* and in animal models and its reported time course of action in the clinic. Specific examples supporting a 'classical' mechanism and their drawbacks will be outlined below in detail.

Loopholes in the literature for a 'classical' mechanism of GBP action: animal models and in vitro studies

Time course

The Dolphin group at University College London has shown that a chronic (but not acute) incubation with gabapentin or pregabalin *in vitro* can reduce Ca^{2+} influx through a reduction in the forward trafficking of $\alpha_2\delta$ subunits and pore-forming α1 subunits to synaptic terminals (Bauer et al., 2010a, Hendrich et al., 2008). It was shown that incubation with 1 mM GBP for 40 h reduced currents formed with the $\alpha_2\delta$-2 subunit (another isoform of the $\alpha_2\delta$ subunit) by roughly 70% where as an acute application of 1 mM GBP for 10 min or for 3-6 h had no effect on the same system (Hendrich et al., 2008). However, these studies were carried out in tsA-201 cells transfected with Cav2.1/β4 and $\alpha_2\delta$-2, which represents an artificial, not physiologically relevant system. Furthermore, these studies were not carried out under modelled conditions of chronic or neuropathic pain and the concentration of 1 mM GBP is very high (see discussion in Chapter 3).

Also, $\alpha_2\delta$-1 is the main $\alpha_2\delta$ subunit expressed in the DRG, whereas these studies were carried out on exclusively $\alpha_2\delta$-2-mediated currents (Bauer et al., 2009).

The time course of the effect of GBP was narrowed down to less than 1 day but more than 6 h as it was shown that incubation with 1 mM GBP for 3-6 hours failed to produce inhibition of calcium currents, but longer incubation times of 17-20 hours produced significant inhibition (Heblich et al., 2008). The authors had also shown that there was no effect after 10 min incubation with GBP. This does, however, leave a rather large period of between 10 min and 3 h that is left unresolved (Fig. 1-8).

Luo et al reported a significant increase in paw withdrawal threshold as early as 20 min (and reaching a maximal effect at 100 min) post-IP-injection with 100 mg/kg GBP in a CCI model of NP (Luo et al., 2002). These findings are supported by more recent findings by Patel et al who observed an acute effect on mechanical withdrawal threshold after 30 min of 10 mg/kg injection of PGB in behavioural studies on partial sciatic nerve-ligated rats (Patel et al., 2013).

Trafficking

Incubation with 1 mM GBP for 7 days *in vitro* failed to reduce trafficking of *de novo* calcium channels to synaptic terminals (Hoppa et al., 2012). It is paradoxical that this data shows a lack of a chronic effect of GBP in reducing VGCC trafficking, which the literature has suggested is the reason why the drug takes longer than 'a few days' to exert an effect. This is also in spite of the higher than therapeutic GBP concentration used in these studies (see later). It would seem that binding of α2δ-1 by GBP does not equate to a reduction in the trafficking of de novo calcium channels.

Neurotransmitter release and Ca^{2+} currents

In experiments on organotypic spinal cord cultures it was found that the 20 μM Mn^{2+} (a pan-VGCC blocker) was significantly more effective than 10 μM pregabalin in blocking calcium channel current in the cell bodies of DRG neurons and yet did not produce a significant effect on sEPSCs, whereas pregabalin did (Biggs et al., 2014a). This suggests that the effect of the gabapentinoids on reduction of Ca^{2+} currents does not account for its ability to reduce neurotransmitter release. It might be that the gabapentinoids interact with the presynaptic release machinery as it has been shown that α2δ expression sets release probability at the synapse and an interaction with α2δ would affect this process (Hoppa et al., 2012). It is possible that the gabapentinoids somehow reduce the coupling between sources of calcium entry and the machinery for neurotransmitter release.

Role of Thrombospondins

Thrombospondins are a family of secreted matrix proteins. All five members of this group (TSP 1-5) have been implicated in excitatory synaptogenesis (Christopherson et al., 2005, Eroglu et al., 2009). One member of this group, thrombospondin 4 (TSP4) has been implicated in the etiology of NP (Kim et al., 2012, Pan et al., 2015). TSP4 is expressed in astrocytes and is upregulated in the injury side of dorsal spinal cord and this correlates with the development of signs of NP. TSP4 blockade by intrathecally delivered antibodies, antisense oligodeoxynucleotides, or inactivation of the TSP4 gene reverses or prevents behavioral hypersensitivity. Intrathecal injection of TSP4 protein into naive rats increases the frequency of mEPSCs in dorsal horn neurons (Kim et al., 2012), suggesting an increased excitatory presynaptic input that would be consistent with behavioral hypersensitivity.

Interestingly, α2δ, which is expressed extracellularly in mature Ca^{2+} channels (Figure 1-7) (Dolphin, 2013; Hendrich et al., 2008) has been implicated as a thrombospondin receptor and 7

days gabapentinoid treatment has been shown to decrease synapse formation in cortical structures (Eroglu et al., 2009). Since both NP and α2δ subunits have been associated with excitatory synaptogenesis (Bauer et al., 2010b, Crosby et al., 2015, Li et al., 2014), gabapentinoid interaction with α2δ to antagonize the actions of thrombospondins may contribute to some of its more slowly developing effects. It is not however an exclusive mechanism for the following reasons:

1. Astrocytes secrete TSPs to increase synapse number (Christopherson et al., 2005) but slowly developing, neuron-subtype specific effects from *in vitro* experiments in neuron enriched cultures of DRG neurons which do not contain astrocytes have been reported (Biggs et al., 2014a).
2. Since the effects of gabapentinoids are prevented following blockade of uptake into the neuronal cytoplasm by of 2-aminobicyclo-(2,2,1)-heptane-2-carboxylic acid (BCH) (Biggs et al., 2014a, Biggs et al., 2014b, Heblich et al., 2008), it would seem unlikely that they act exclusively at an extracellular binding site on mature HVA-Ca^{2+} channels.
3. The actions of gabapentinoids can be observed within minutes of application under appropriate experimental conditions both *in vivo* (Coderre et al., 2005, Kumar et al., 2013, Narita et al., 2012) and *in vitro* (Zhou and Luo, 2014, Zhou and Luo, 2015). Such actions are unlikely to reflect impairment of the slow process of synaptogenesis.

Clinical studies

In the clinic it has been published that the gabapentinoids take at least 3 days to exert an effect (Cheshire, 2002, Sharma et al., 2010). However, in a clinical setting, one does not follow up with a NP patient immediately after they self-administer GBP or PGB and so, it would naturally be very difficult to determine whether there is an effect in a matter of minutes or under an hour on pain levels in the patient. One could also imagine that since pain is an extremely subjective experience

that it would be difficult for even the patient to self-report an effect of the drug. As researchers, we can look at nociception by means of looking at dorsal horn excitability or paw withdrawal thresholds in lower mammals, but for a clinician, measuring these same parameters could prove to highly unethical and therefore, not possible in humans. Although, it has been shown that chronic (15 days) GBP significantly reduced the area of brush allodynia evoked by capsaicin-injection (measured over 90 min) in human subjects compared to a placebo group (Gottrup et al., 2004). It would have been interesting to repeat this study on neuropathic patients with pre-existing allodynia and to look at the effect of GBP over a 90 min time period.

Evidence from more than 100 clinical trials suggests that perioperative GBP can reduce postsurgical pain levels. The gabapentinoids have been shown to reduce "immediate postoperative pain", which would suggest that these drugs are having an effect faster than what was previously thought (Schmidt et al., 2013).

Summary Statement

In summary, the acute (< 1hr) actions of GBP are well founded in the literature (for review see Alles and Smith, 2016), but in spite of this, have remained poorly studied compared to chronic effects, most likely on account of an apparent inconsistency with clinical findings where GBP has been reported to take at least a few days in patients to produce meaningful pain relief (Cheshire, 2002, Sharma et al., 2010).

Hypothesis

My hypothesis is that the reason for the inconsistent conclusions regarding the acute actions of GBP in the literature is because most studies that have concluded a lack of effect of acute GBP did not:

1) Use neuropathic animals
2) Examine time course of application of GBP
3) Use appropriate, clinically relevant concentrations of GBP

For this reason, I will examine the effect of clinically relevant concentrations of GBP over a <1 hr time course in neuropathic versus sham-operated animals. Using electrophysiology I will examine the acute effects of GBP on different dorsal horn neuronal cell types by studying firing frequency as well spontaneous release (s/mEPSC). I will also determine the effect of acute GBP on overall dorsal horn and primary somatosensory cortex excitability using confocal and two-photon Ca^{2+} imaging respectively. I will also attempt to correlate these results to levels of the GBP-binding-protein, α2δ-1.

Goal of work

GBP is effective in approximately 35% of NP patients (Moore et al., 2014), therefore, more effective therapies are urgently needed. It is hoped that understanding the effectiveness of GBP and its acute versus chronic mechanism of action will provide a platform for developing new therapeutics for NP.

Figure 1-1

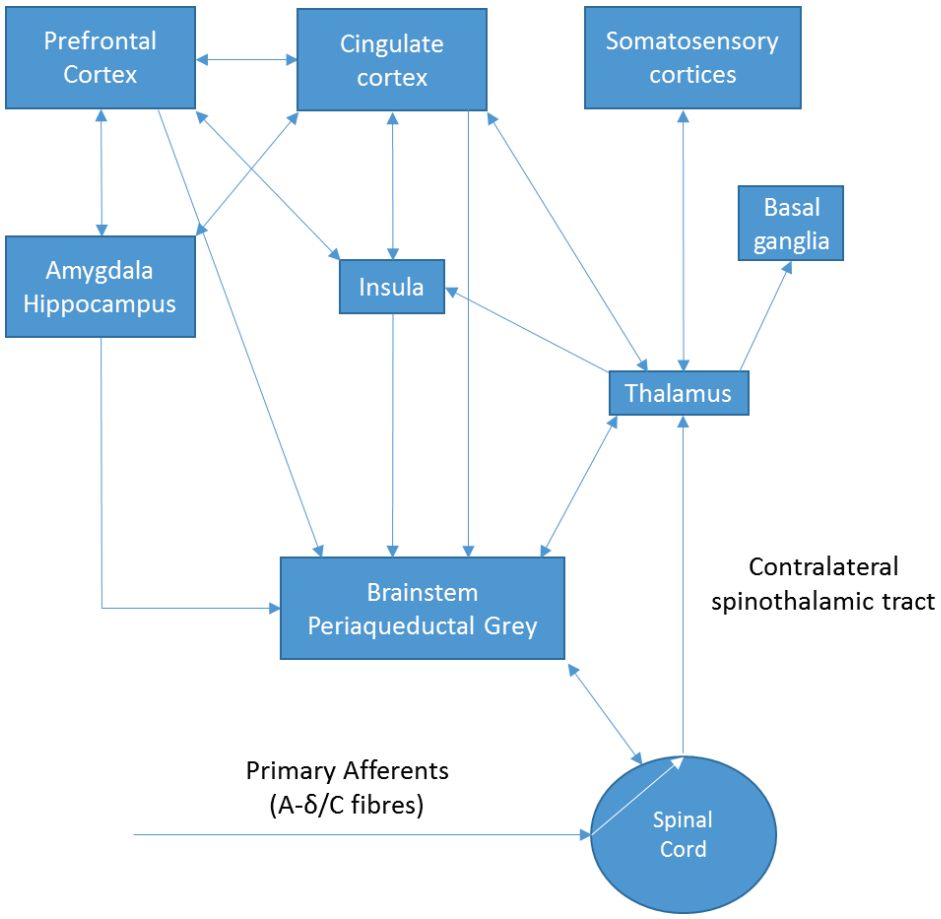

The pain matrix. A simplified schematic of a 'pain matrix' and the main anatomical components involved. A 'pain matrix' has been used to describe the interplay between anatomical structures responsible for the pain experience and this involves a system of interconnected networks from the spinal cord to the brain (information regarding bodily specificity of pain) as well as within the brain (conscious perception and emotional aspects of pain). Source: Jones et al., 2003.

Figure 1-2

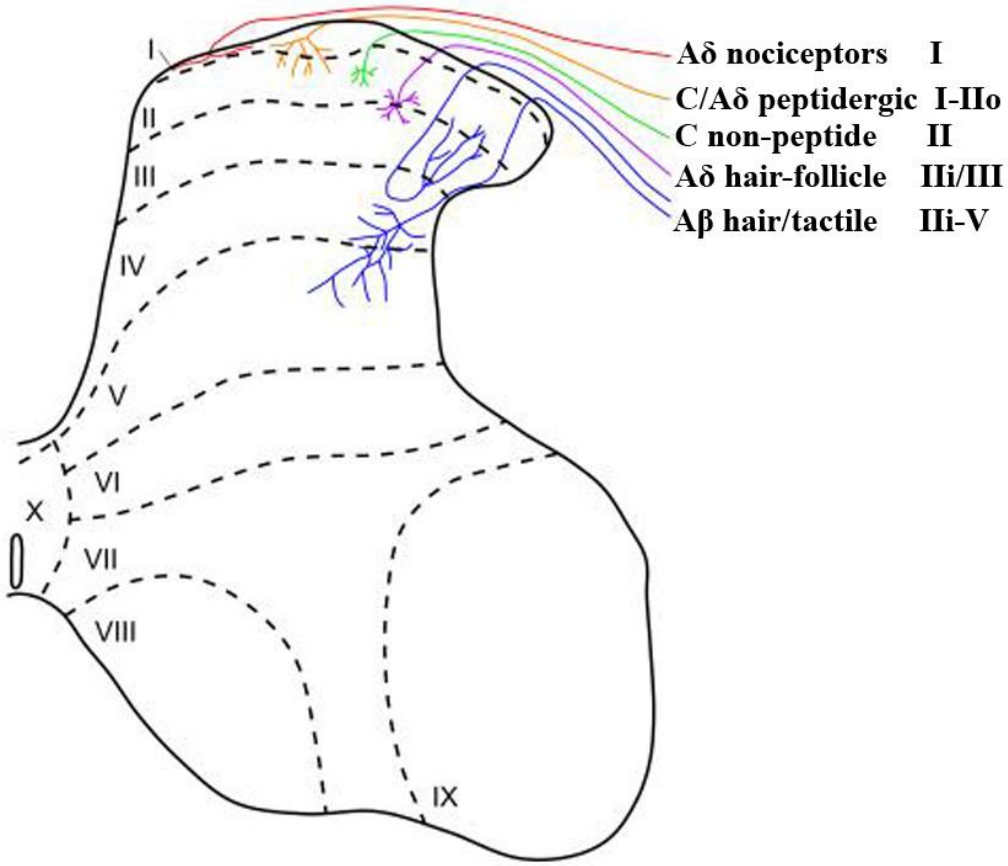

Rexed Laminae of the dorsal horn of the spinal cord. Lamina I and II form the marginal zone and *substantia gelatinosa* respectively and together these make up the superficial dorsal horn. Within the dorsal horn primary afferents arborise in an orderly laminar termination pattern based on fibre diameter and function. Aβ tactile and hair afferents end mainly in laminae III-VI with some extension into lamina IIi with distribution dependent on function. Aδ hair-follicle afferents extend across the lamina II/III border. Aδ nociceptors end mainly in lamina I, occasionally branching to laminae V and X. Peptidergic primary afferents arborise mainly in lamina I and IIo. Non-peptidergic C-fibres occupy the central part of lamina II. Modified and reproduced with permission from Todd, 2010.

Figure 1-3

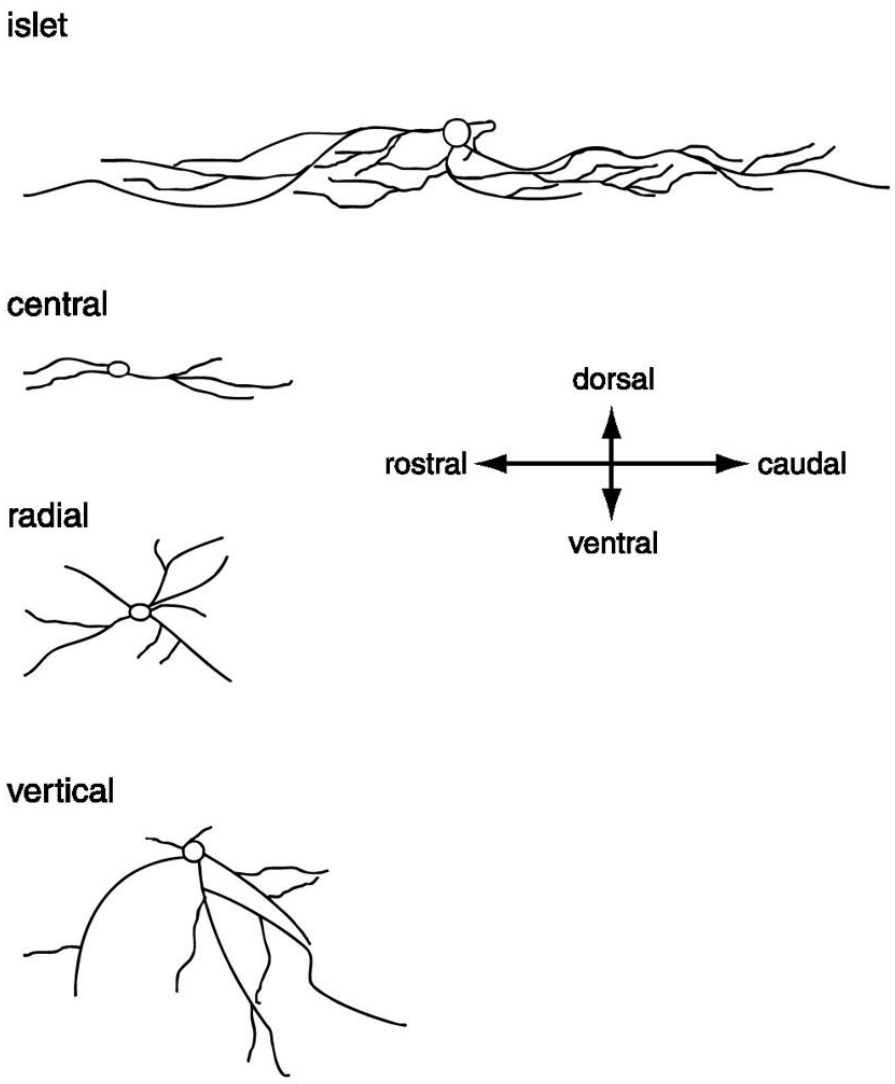

Morphology of *substantia gelatonisa* (lamina II) neurons. Islet and central cells both have rostrocaudal dendritic trees, with those of islet cells being more elaborate. Radial cells have form compact dendritic trees that radiate in all directions. Vertical cells have dendrites that extend ventrally. It has been shown that most islet cells are inhibitory and most radial and vertical cells are excitatory. Central cells form a mixed population of excitory and inhibitory neurons. Reproduced with permission from: Zeilhofer et al., 2012.

Figure 1-4

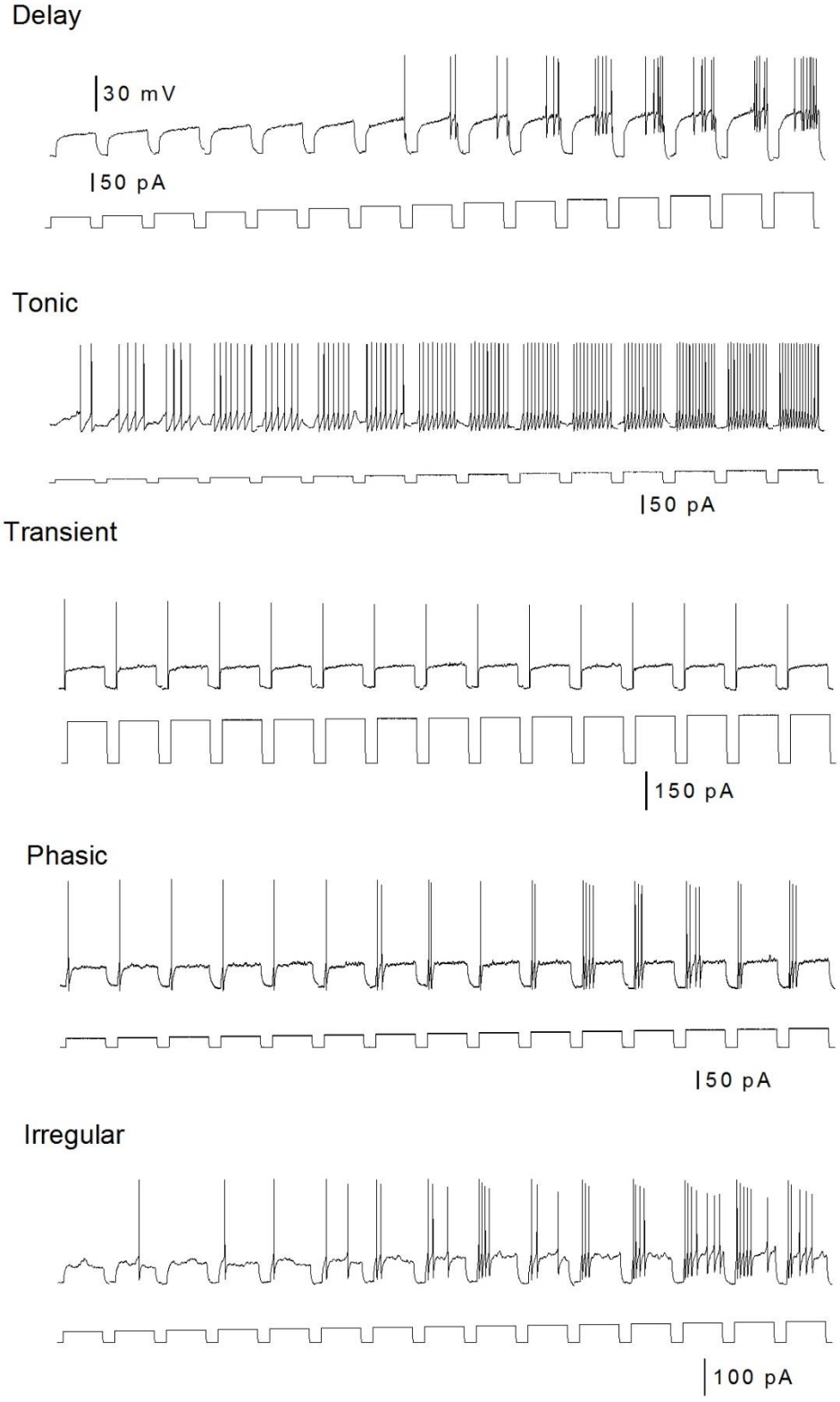
Delay
30 mV
50 pA
Tonic
50 pA
Transient
150 pA
Phasic
50 pA
Irregular
100 pA

Figure 1-4. **Neuronal cell types of the *substantia gelatinosa* based on firing pattern.** Voltage-clamp recordings are shown in response to successive depolarising current steps. Delay neurons have the highest threshold as shown by the lack of action potential firing at lower current steps and only fire after a distinct delay. Tonic neurons have the lowest threshold as shown by repetitive firing at low current steps and display a regular repeating spike pattern. Transient neurons are high threshold and only ever fire a single spike. Phasic neurons are lower threshold than delay neurons, but higher threshold than tonic neurons and usually fire 1-3 action potentials at most. Irregular neurons show no clear pattern between step size and firing pattern. Reproduced with permission from Stebbing et al., 2016.

Figure 1-5

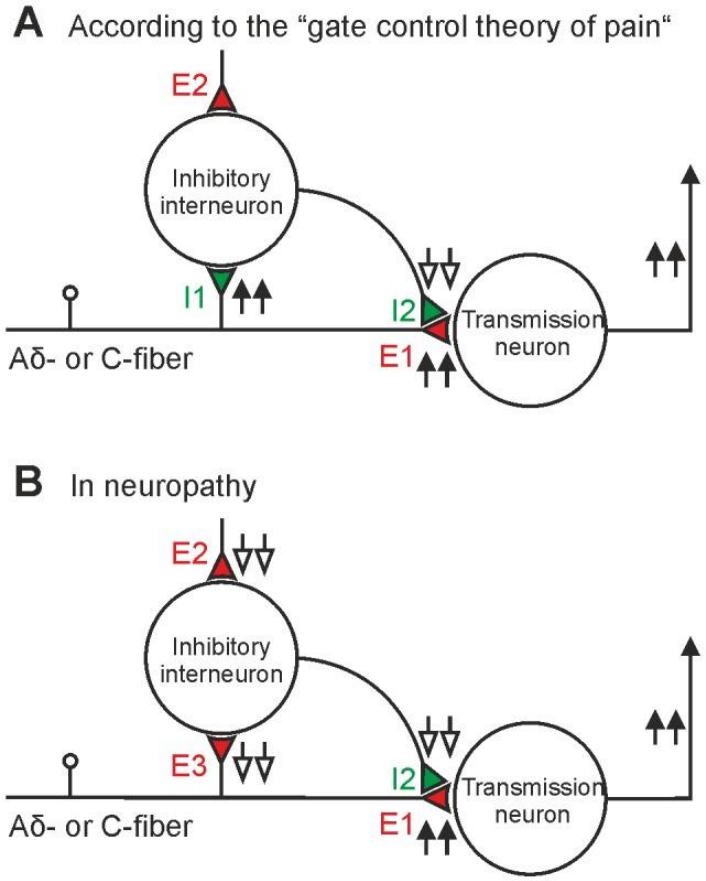

Opening a spinal gate for nociception. (A) The classical gate control theory: afferent nociceptive fibers (Aδ- and C-fibers) directly excite transmission neurons through excitatory synapse E1. Collaterals of nociceptive afferents inhibit inhibitory neurons through a proposed inhibitory synapse I1. Activity in Aδ- and C-fibers during nociception would thus depress activation of the inhibitory interneurons. This would lead to a reduced (↓↓) pre- (I2) or postsynaptic inhibition (not shown) of nociceptive transmission neurons in the spinal dorsal horn. The existence of the proposed inhibitory synapse (I1) has, however, not been shown experimentally. (B) Leitner et al demonstrated the existence of a monosynaptic excitatory input (E3) to GABAergic neurons from Aδ- and C-fiber afferents and tested the hypothesis, that in neuropathy global excitatory drive (E2 and E3) including direct excitation from presumably nociceptive Aδ- and C-fibers to GABAergic neurons is impaired. This would lead to a reduced inhibition at I2 (↓↓) and thus open the spinal gate for nociception (↑↑ E1). E2: other excitatory input from local circuits or descending pathways. (color code: green: inhibitory synapse; red: excitatory synapse). Reproduced with permission from: Leitner et al., 2013

Figure 1-6

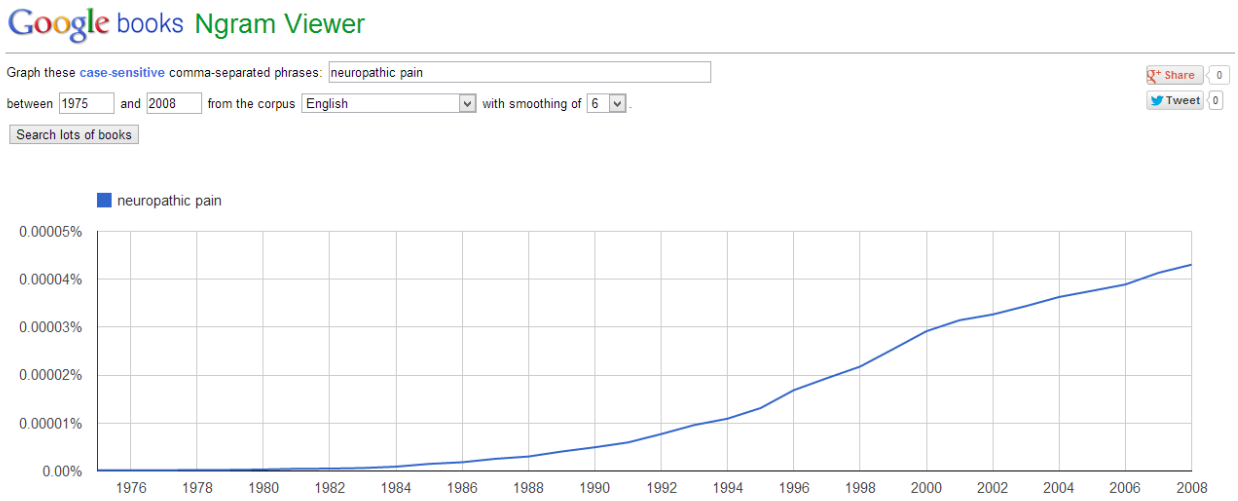

An indicator of increasing awareness of neuropathic pain. 'Google Ngram Viewer' search for term "neuropathic pain" in Google books database from 1975 to 2008. This graphic provides a loose indicator of increasing awareness and understanding of neuropathic pain of the past few decades. Prevalence of term in % is shown on the y-axis against time in years on the x-axis. Last Used: October-26-2015.

Figure 1-7

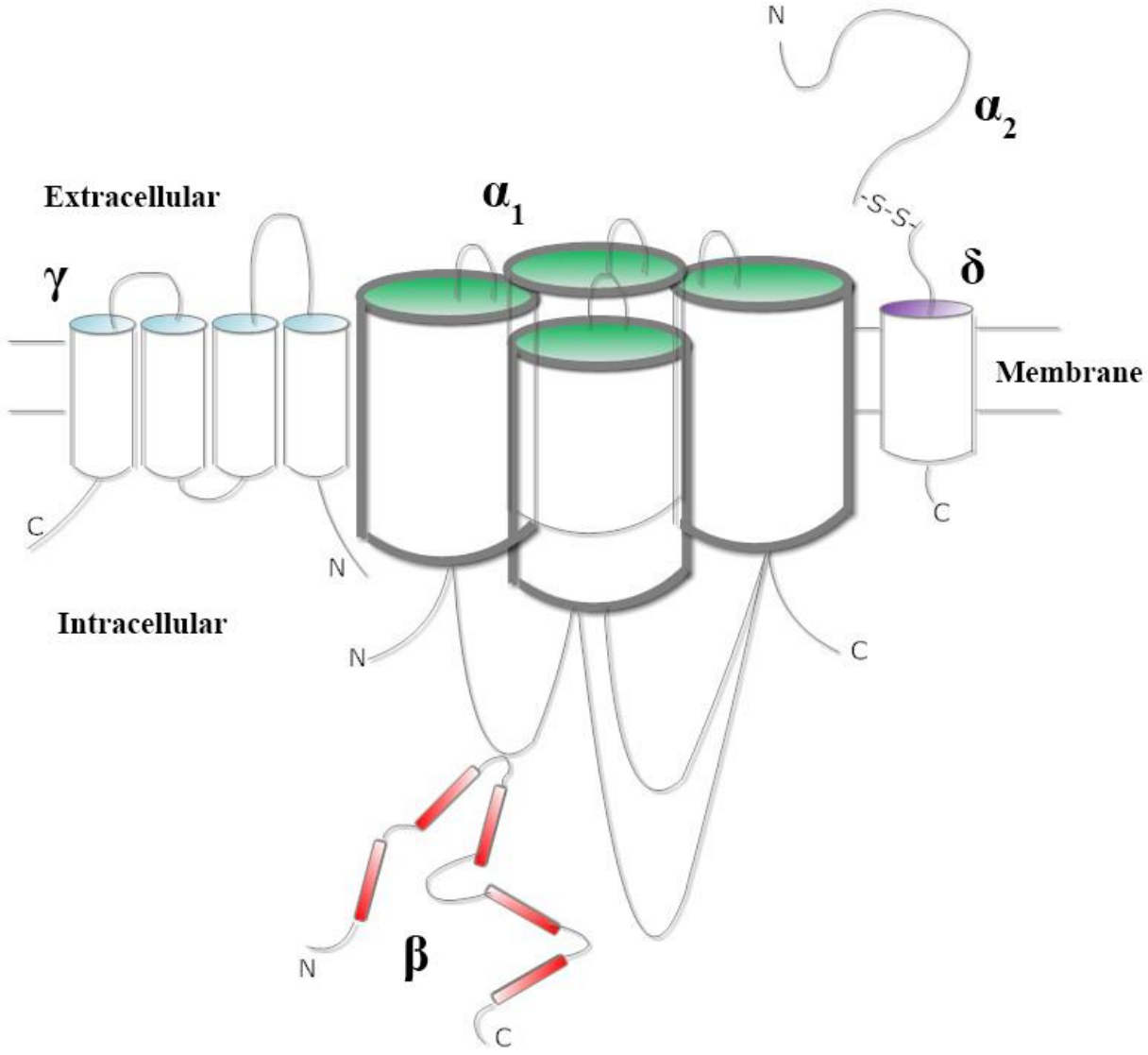

The Voltage-gated Calcium Channel. Diagram to illustrate the structure of HVA Ca^{2+} channels showing interactions of the pore-forming α_1 subunit and the auxiliary $\alpha_2\delta$, β and γ subunits. The α_2 accessory subunit is entirely extracellular and is linked by a disulfide bridge to the δ subunit which is mainly extracellular with a short transmembrane and intracellular domain. The β subunit is entirely intracellular. (Alles & Smith, 2016)

Figure 1-8

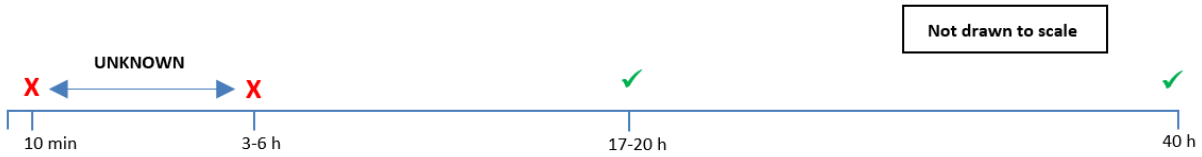

Time course of effects of GBP supporting a 'classical mechanism according to the Dolphin Group'. X=lack of effect of GBP, ✓=effect with GBP. An effect of GBP was described by a reduction of either α2δ-2-mediated current in transfected tsA-201 cells (10 min and 3-6 h time points; Hendrich et al, 2008) or by an inhibition of calcium current in cultured dorsal root ganglia (DRG) neurons (3-6 h, 17-20 h and 40 h time points; Heblich et al, 2008). The experiments were carried out in expression systems or cell cultures that were not in a 'neuropathic pain' state and this may be part of the reason why acute effects of GBP were not reported.

Table 1-1

Morphology	Excitatory (n)	Inhibitory (n)	% excitatory	% inhibitory
Islet	Nil	12	0	100%
Central	4	4	50%	50%
Vertical	12	3	80%	20%
Radial	7	Nil	100%	0

Morphology of lamina II excitatory and inhibitory neurons. 'n' indicates the number of neurons of each type identified. Percentages were calculated from these numbers. As shown above, all islet cells are inhibitory, central cells form a mixed population of excitatory and inhibitory cells, vertical cell are mainly excitatory and radial cells are all excitatory. Figure based on data from Yasaka et al., 2010.

Table 1-2

	Inhibitory (GABAergic)	Excitatory (Glutamatergic)
Neuropeptides	**NPY** **Galanin** **Enkephalin** **Endorphin**	**Somatostatin** **Neurotensin** **Neurokinin B** **Substance P** **Enkephalin** **Dynorphin**
Receptors for neuropeptides	**sst2A** **NK3**	**NK1** **NK3** **MOR** **NPY Y1**
Other proteins	**nNOS** **Parvalbumin** **ChAT**	**Calbindin** **Calretinin** **Parvalbumin** **PKC-γ**

Localization of various neuropeptides and proteins in different classes of interneurons in laminae I-III of the dorsal horn. ChAT, choline acetyltransferase; MOR-1, μ-opioid receptor 1; NK1, neurokinin 1; nNOS, neuronal form of nitric oxide synthase; NPY, neuropeptide Y; PKC-γ protein kinase C-γ. Source: Wall and Melzack, 2010.

Table 1-3

Ion Channels	Receptors	
Calcium channel, voltage-dependent, L-type, alpha 1E subunit	5-Hydroxytryptamine receptor 5B	Pyrimidinergic receptor P2Y, G protein-coupled, 6
Calcium channel, voltage-dependent, alpha2/delta subunit 1	Cholinergic receptor, nicotinic, alpha polypeptide 5	Scavenger receptor class B, member 1
Chloride channel, nucleotide-sensitive, 1A	Cholinergic receptor, nicotinic, beta polypeptide 2	Protein tyrosine phosphatase, receptor type, A
Sodium channel, nonvoltage-gated 1, beta (epithelial)	CSF-1 receptor	Purinergic receptor P2Y, G protein-coupled 1
Sodium channel, voltage-gated, type 1, alpha polypeptide	GABA-A receptor alpha-5 subunit	Vasopressin V2 receptor
ATPase, Na^+K^+ transporting, alpha 2	Glutamate receptor, ionotropic, AMPA3	Cholinergic receptor, nicotinic, delta polypeptide
Calcium channel, voltage-dependent, alpha 1C subunit	Glutamate receptor, ionotropic, 4	C-kit receptor tyrosine kinase isoform
Chloride channel protein 3 long form	Glycine receptor alpha 2 subunit	GABA-B receptor 1
Drk1 gene mRNA for potassium channel protein	Integrin, beta 1	Interleukin 13 receptor, alpha 1
Potassium channel KIR6.2	Metabotropic glutamate receptor mGluR7	Neurotensin receptor 2
Potassium voltage-gated channel, Isk-related subfamily, member 1	Neurotrophic tyrosine kinase, receptor, type 2	Opioid receptor, kappa 1
Potassium voltage gated channel, Shaw-related subfamily, member 2	Homologue to peroxisomal PTS2 receptor	Opioid receptor-like
Protein kinase C-regulated chloride channel	Prostaglandin D2 receptor	

List of the strongly regulated channels and receptors in dorsal spinal cord 14 days after peripheral axotomy of the rat sciatic nerve. The strongly regulated channels and receptors are identified with the changes in cDNA microarray ratio of axotomized dorsal horn vs. normal dorsal horn over two-fold. Quantitative analysis is based on three independent experiments. Source: Yang et al., 2004.

Table 1-4

Drug Treatment Option	Recommended Step in Treatment
Serotonin-norepinephrine reuptake inhibitors duloxetine or venlafaxine	First Line
Tricyclic antidepressants	
Gabapentin	
Gabapentin extended release or enacarbil	
Pregabalin	
Lidocaine	Second Line
Tramadol	
Capsaicin	
Opioids	Third Line
Botulinum Toxin A	

NP drugs and recommendations for line of action in treatment based on GRADE (Grading of Recommendations Assessment, Development and Evaluation). The gabapentinoids are among the first-line of treatment options available for neuropathic pain along with anti-depressant drugs. Source: Gilron et al., 2015.

METHODS

Chapter 2: Methods

The following section will describe the methods used for experiments outlined in results chapters 3, 4 and 5. I have made reference to this chapter where appropriate.

Animal Model of Neuropathic Pain

Surgery

The model of neuropathic pain I have used in my studies is the Mosconi-Kruger model of chronic constriction injury (CCI) performed on Sprague Dawley rats of between 21-23 days old (Mosconi and Kruger, 1996). Rats were shaved using an electric shaver at mid-thigh level and the exposed area of skin was sprayed with 70% ethanol. The left sciatic nerve of rats under isoflurane anesthesia was exposed at mid-thigh level (Figure 2-1A). A polyethylene cuff of 2 mm in diameter and made from PE90 tubing (ID 0.86 mm, OD 1.27 mm; Intramedic Clay Adams, Becton Dickinson and Co, Sparks MD) was slit open on one side and gently attached around the sciatic nerve using fine forceps. The cuff was carefully moved along the nerve to ensure that it had been securely fastened around the nerve (Figure 2-1B). In each rat the sciatic nerve was constricted with two cuffs. The wound was sutured with a silk suture, doused with small quantities of Betadine® (Betadine, Stamford, CT, USA) and gently wiped with a sterile gauze. In the case of sham surgery, rats were anesthetized under isoflurane and the sciatic nerve was exposed, but not touched with the forceps.

Behavioural Testing

Animals were tested for mechanical allodynia and hyperalgesia at least 7 days after surgery using von Frey hairs of 1.4 g, 2 g, 4 g, 6 g, 10 g and 15 g weights. In each case, animals were placed in

a plexi-glass box with a wire-grid bottom. Pressure was applied to the mid-plantar area of the left paw (injured side) starting with a von Frey hair of the lowest weight (1.4 g) until it bent and then held in this position for 2 seconds. This was performed 5 times and a positive result for each hair would be given if the animal withdrew its paw a minimum of 3 out of 5 times. If a negative result was obtained, the next heaviest hair would be used. A recovery period of at least 1 min between hairs was allowed. The paw withdrawal threshold (PWT) was calculated based on the weight of hair that elicited a positive result. A rat with a PWT of 6 g or less was considered to 'neuropathic'.

Preparation of acute spinal cord slices

30-40 day old CCI or sham-operated Sprague-Dawley rats were anesthetized with a large overdose of intra-peritoneal urethane (1.5 g/kg) as required by the animal welfare committee. Acute spinal cord preparation was performed as described by Moran and Smith with some minor modifications (Moran and Smith, 2002). The spinal cord was removed following decapitation of the animal via a laminectomy and then transferred to partly-frozen, 'slushy' artificial cerebrospinal fluid (aCSF) containing (in mM): 118 NaCl, 2.5 KCl, 26 $NaHCO_3$, 1.3 $MgSO_4$, 1.2 NaH_2PO_4, 1.5 $CaCl_2$, 5 $MgCl_2$, 25 D-glucose, 1 kynurenic acid. The solution was placed in a freezer at -20 ^oC for 1 hr beforehand to ensure a 'slushy' consistency and was continuously bubbled with carbogen (95% O_2, 5% CO_2) during the preparation. Kynurenic acid is a non-specific amino acid receptor antagonist that was added to reduce acute excitotoxicity during manipulation and slicing of the spinal cord (Perkins and Stone, 1982). All roots were severed using fine scissors and the dura and connective tissue was removed using No. 5 forceps from the spinal cord until the preparation was smooth. This was performed under x10 magnifying glasses. The smooth spinal cord preparation was then glued with cyanoacrylate glue ('Vetbond', WPI, Sarasota, FL, USA) to a trapezoid-

shaped block made out of 4% agar. Care was taken to add just the right amount of glue as adding too much can interfere with slicing and adding too little glue runs the risk of the spinal cord falling off the block. The block was then glued to a magnetically-attached platform submerged in the same 'slushy' aCSF described earlier in the vibratome stage (Figure 2-2). The temperature was maintained by a metal block that had been placed in the freezer for 1 hr beforehand.

Transverse slices (300 μm) were cut using Microm HM 650V vibratome (Thermo Scientific, Waltham, MA, USA). Speed and amplitude of the vibratome blade was set at 1-4 mm/min and ~1.25 mm respectively. This was increased or decreased according to the level of movement of the spinal cord slice. If the cord started to curl during slicing, the speed and/or amplitude would be reduced.

Slices were incubated in aCSF (without kynurenic acid) at 37 ºC for 1 hr prior to recording and then stored at room temperature (22-24 ºC) for the remainder of the experimental day (usually 6-7 hrs).

Recordings were made from the *substantia gelatinosa*, which was identified by its translucent appearance under IR-DIC (infrared-differential interference) optics (see Figure 2-2B) and were made from the side ipsilateral to the sciatic injury. The side ipsilateral to the nerve injury was marked by cutting a longer piece of agar along the desired side of the spinal cord after slicing was complete.

Defined-medium organotypic cultures (DMOTCs)

The method of preparation of DMOTCs was as per (Biggs et al., 2012). A caesarean section was performed on embryonic-day-13 (E13) timed-pregnant rats obtained from Charles River

(Wilmington, MA, USA; www.criver.com). Animals were induced under 5% isoflurane anesthesia until loss of paw withdrawal reflexes and the surgery was performed under 2% isoflurane anesthesia. The number of fetuses delivered per pregnant dam is between 8 and 14. Fetuses were transferred to ice-cold filtered Hank's buffered saline solution (HBSS) containing (in mM): 138 NaCl, 5.33 KCl, 0.44 KH_2PO_4, 0.5 $MgCl_2.6H_2O$, 0.41 $MgSO_4.7H_2O$, 4 $NaHCO_3$, 0.3 Na_2HPO_4, 5.6 *D*-glucose and 1.26 $CaCl_2$. The amniotic sac was punctured and the fetus was removed. The spinal cord was removed from the fetus by making 3 incisions to cut off the head, limbs and tail and ventral portion (Figure 2-3A). Slices were sectioned at 300 µm using a 'McIlwain' tissue chopper (Warner Instruments, Hamden, CT, USA; www.warneronline.com). The slices were then transferred to HBSS for trimming of connective tissue around the spinal cord under a Wild M3 light microscope (Leica Biosystems, Nussloch, Germany; www.leica-microsystems.com). Acutely isolated spinal cord is shown in Figure 2-3C. The slices were then chilled for 1 hr at 4 ^oC to allow recovery from slicing.

The slices were mounted on sterilized glass coverslips that have been soaked in 0.5 M HCl for 24 hrs, followed by 100% ethanol for 1 hr and drying in an oven at 200 ^oC for 2 hr. Slices were held in place by a clot formed between chicken plasma (Sigma, Catalogue # P-3266) and thrombin (Sigma, catalogue #T-4648). The slice was placed in a 20 µl drop of chicken plasma and then mixed well with a 30 µl drop of thrombin.

The coverslip with the slice was then placed in a flat-bottomed tube (Figure 2-3B) containing 1 ml of culture medium, composed of 82% Dulbecco's Modified Eagle Medium (DMEM; high glucose, Na pyruvate; 'Glutamax'), 10% fetal bovine serum and 8% sterile water (all from Gibco (Invitrogen, Carlsbad, CA, USA; www.invitrogen.com)). For the first 4 days of culture the medium was supplemented with 20 ng/ml NGF (Alomone Labs) as well as antibacterial and antimycotic

drugs (5 units/ml penicillin G, 5 units/ml streptomycin and 12.5 ng/ml amphotericin B: all from Gibco/Invitrogen (Grand Island, NY, USA; www.invitrogen.com). The tubes are then placed in a roller drum at 36 ºC at a rotation speed of 120 revolutions/hr.

The serum medium was gradually weaned to the defined neurotrophin- and serum-free medium that consists of Neurobasal medium with N-2 supplement and 5 mM Glutamax-1 (all from Gibco). During this time, the NGF concentration was reduced from 20 ng/ml to 2.5 ng/ml and slices were treated with 10 μM of an antimitotic drug cocktail consisting of uridine, cytosineb-D-arabinofuranoside (AraC) and 5- fluorodeoxyurindine (all from Sigma) to minimize glial overgrowth. After 1 day in anti-mitotic medium, the medium was fully exchanged to the defined medium that contains no serum or exogenous NGF. The full schedule of media exchanges is shown in Figure 2-3E.

Calcium imaging of acutely isolated spinal cord slices and DMOTCs

During calcium imaging, slices were perfused at room temperature (22-24°C) with 95% O_2 - 5% CO_2 saturated aCSF containing (in mM): 127 NaCl, 2.5 KCl, 1.2 NaH_2PO_4, 26 $NaHCO_3$, 1.3 $MgSO_4$, 2.5 $CaCl_2$, 25 *D*-glucose, pH 7.4.

Calcium imaging of acute spinal cord slices and DMOTCs was performed using a scanning confocal microscope (Olympus FV300) connected to an Argon laser (488 nm) for confocal (single-photon) imaging using a 20× objective (Olympus NA 1.0) and 2–3× optical zoom at full-frame (512 × 512 pixels). Neurons were visualized using the membrane-permeable Ca^{2+} indicator dye Fluo-4 acetyl methoxy (AM). An increase in Fluo-4 AM fluorescence intensity in response to laser excitation represented a Ca^{2+} rise. The acquisition speed was set at 1.08 frames per second.

Loading of dorsal horn neurons from acutely isolated spinal cord slices from 30-40 day old CCI and sham animals with Ca^{2+} indicator Fluo-4 AM was performed via pressure injection (25-50 mmHg) using a broken patch electrode (outer tip diameter of 5-15 μm) at a depth of 50 μm as shown in Figure 2-4. The pressure injection was applied continuously for 20 min before a desired level of loading was achieved. Occasionally, more than one injection attempt was required. A desired level of loading was defined as at least 5 clearly visible dorsal horn cells and their basic morphology in a given field of view of 200-350 μm diameter.

Loading of DMOTCs was performed in the same manner as described above, however, DMOTCs were typically more conducive to loading than acute slices with pressure of 25-mm Hg applied for 10 min. DMOTCs would only require a single injection attempt and 15-20 clearly visible dorsal horn neurons and their basic morphology within a 250-300 μm diameter field of view per DMOTC slice would be considered an acceptable level of loading.

Fluorescence traces were acquired using FluoView. Regions of interest were drawn around individual cell bodies in the field of view as shown in Figure 3-5A. The numerical values corresponding to the fluorescence traces were then exported to Microsoft Excel. Origin 2015 (Origin Lab Corp., Northampton, MA, USA, www.originlab.com) was used for measurement of normalized fluorescence ($(F_{max} - F_0)/F_0$) in response to stimulation. Finally, bar graphs were constructed in Origin 2015.

A one-way analysis of variance (ANOVA) with Bonferroni correction was used to calculate differences in $(F_{max} - F_0)/F_0$ between CCI and sham-operated animals that had received either GBP or saline.

In vivo Two-photon Cortical Imaging

This technique employs pressure injection of Ca^{2+}-indicator dyes directly in to the somatosensory cortex of anesthetized rats to measures rises in intracellular Ca^{2+} of individual neurons in response to stimulation of the hindpaw and is inspired by the work of Winship and Murphy, 2008. These experiments were carried out in the laboratory of Professor Ian Winship, Neurochemical Research Unit, University of Alberta with the help of Mischa Bandet and Bin Dong.

CCI or sham-operated rats (30-40 days old) had their head fixed to a stereotaxic frame. A surgical plane of anesthesia was achieved with 20% (w/v) urethane dissolved in saline and administered via intraperitoneal injection (1.25 g/kg; supplemented at 0.25 g/kg as needed). Body temperature was measured using a rectal probe and maintained at 37±0.5 ºC. An incision was made with a scalpel blade along the medial portion of the scalp and the skin retracted to expose the skull. Bleeding from the scalp was electro-cauterized to prevent leaking onto the exposed surface of the skull. A 4 x 4 mm region of the skull overlying the right hemisphere somatosensory region was thinned to 25-50% of original thickness using a high-speed dental drill (~1.5-4.5mm lateral, +1.5 to -2.5 mm posterior to bregma). This thinned region was covered with 1.3% low-melt agarose dissolved in aCSF at 37 ºC containing in mM: NaCl 135, KCl 5.4, $MgCl_2.6H_2O$ 1, $CaCl_2.2H_2O$ 1.8, NaHEPES 5. The region was then covered with a 5mm glass coverslip. Hemodynamic intrinsic optical signal (IOS) imaging was performed through this thin skull preparation before *in vivo* Ca^{2+} imaging (Winship and Murphy, 2008). Imaging of intrinsic optical signals and local changes in blood flow using two-photon imaging have shown that blood flow to active areas of the cerebral cortex increases within 600 ms of the onset of neuronal activity (Winship et al., 2007). For IOS imaging, the cortical surface was illuminated with a red LED (635nm). Reflected light

was captured in 12-bit format by a Dalsa Pantera 1M60 camera mounted on a Leica SP5 confocal microscope. The depth of focus was set between 200-300 μm below the cortical surface.

Custom-made piezo-electric mechanical bending actuators were used to elicit vibrotactile limb stimulation (1s, 200Hz) during IOS imaging (Winship and Murphy, 2008). A total of 40 trials of stimulation was performed on the contralateral hindlimb (cHL) to the side of nerve injury. Placement of actuators was on the glabrous skin of the cHL (nerve-injured side, Figure 2-5C), with consistent alignment relative to the flexion of wrist and ankle. Images were captured for 3.0s at 10 Hz (0.5s before and 2.5s after stimulus onset; interstimulus interval = 20s). The 40 trials were averaged in ImageJ software (NIH). Frames 1-1.5s after stimulus onset were averaged and divided by baseline frames 0.5s before stimulus onset to generate a hindlimb response map. The response map threshold was set at 50% maximal response, and overlaid on an image of surface vasculature to delineate the cHL somatosensory area (Figure 2-6). These areas were subsequently used as guides for Ca^{2+} indicator injections (Winship and Murphy, 2008).

Subsequent to IOS imaging as described above, the coverslip and agarose were removed. A metal plate was secured to the skull using cyanoacrylate glue and dental cement and then fastened to the surgical stage to prevent head movement. A 3 x 6 mm craniotomy was then performed centering over the cHL functional area, determined via IOS imaging. A dental drill was used to progressively thin the overlying skull until the bone could be removed with forceps, and the dura resected. The exposed cortical surface was bathed in saline. Pressure injections of membrane-permeant Oregon Green BAPTA-1 (OGB-1) were made 200-300μm below the cortical surface of the HL cortical region using glass micropipettes with resistances of 2-5 MΩ (Stosiek et al., 2003, Winship and Murphy, 2008). Alexa-594 was used as a tracer alongside OGB-1 to determine whether dye was being successfully ejected from the micropipette tip. Multiple injections were performed until a

desired level of loading was achieved. Typical loading is shown in Fig 2-7A. After OGB-1 injection, the cortex was incubated for 10 min with sulforhodamine 101 (SR101) dissolved in DMSO to label astrocytes (Nimmerjahn et al., 2004, Winship and Murphy, 2008, Winship et al., 2007). The craniotomy was then covered with 1.3% agarose dissolved in aCSF and sealed with a glass coverslip.

Two-photon imaging was performed using a Leica SP5 MP confocal microscope equipped with a titanium-sapphire laser tuned to 810 nm for OGB-1 and SR101 excitation (Fig. 2-7A). A Leica HCX PL APO L 20x 1.0NA water immersion objective was used. Images were acquired using Leica LAS AF using two line-averages, a zoom of 1.7x and a frame-rate of 25 Hz. Images were acquired at 256 x 256 pixels over an area of 434 x 434μm, yielding a resolution of 1.7 μm per pixel. Ca^{2+} fluctuations in neurons and astrocytes were imaged at 130-180um below the cortical surface.

Using custom scripts written in NIH ImageJ (co-credit to Mischa Bandet, Winship Lab), a median filter (radius, 1 pixel) was applied to each of the image sequences of 8 trial sweeps. The 8 filtered trails were then averaged to generate the final Ca^{2+} imaging frames to be analyzed. Regions of interest (ROIs) were drawn around visible neurons. Astrocytes were excluded from analysis by removing ROIs that co-labelled astrocytes in the SR101 channel. Numerical values representing raw neuronal fluorescence traces were exported from ImageJ and were imported into Microsoft Excel. A 5-point moving triangular smoothing filter was applied to each neuronal trace to increase signal-to-noise ratio. We found that this triangular filter did not affect the overall amplitude or main signal properties of our recorded Ca^{2+} traces, but did reduce single frame Ca^{2+} trace artifacts. ΔF/Fo traces were generated from the raw fluorescence traces as previously described (Winship and Murphy, 2008). Neuronal Ca^{2+} signals were exported from Microsoft Excel and analyzed in

Clampfit 9.0 (Molecular Devices, Silicon Valley, CA, USA). Due to the large number of signal traces that required analysis, various threshold criteria were tested to differentiate responsive from un-responsive neurons (Chen et al., 2013, Kerlin et al., 2010, Li et al., 2012, Ohki et al., 2005, Schummers et al., 2008, Winship and Murphy, 2008). A threshold criteria requiring the neuronal Ca^{2+} fluorescence to increase by 3-times the standard deviation of the baseline period (baseline defined as 1s before stimulus onset), and remain above this criteria for 160ms (4 successive frames), was found to be optimal for separating responsive neurons from noise (Fig 2-6B). Neuronal traces that met these criteria were included in subsequent analysis.

The index of excitability used for cortical excitability was the 'neural mass' or the fraction of responsive cells multiplied by the mean normalized response (Doetsch, 2000, Erickson, 1986). This measure provided a more suitable parameter for comparing neuronal population coding and excitability of the PSC between different animals.

A one-way analysis of variance (ANOVA) with Bonferonni correction was used for comparing the neural mass of CCI or sham-operated animals at each time point after GBP injection. Statistical significance was attributed if $p<0.05$.

Measurement of GBP Levels using Liquid Chromatography-Mass Spectrometry (LC-MS)

This work was carried out in the laboratory of Prof Glen Baker, Neurochemical Research Unit, University of Alberta with assistance from Nataliya Bukhanova and Gail Rauw.

21-30 day old Sprague-Dawley rats received either saline, 60 mg/kg GBP or 100 mg/kg GBP via intraperitoneal injection. After approximately 30 min, animals were anesthetized with a large overdose of intra-peritoneal urethane (1.5 g/kg) as required by the animal welfare committee.

Whole spinal cord was removed from these animals via laminectomy in the same way as for preparation of acute spinal cord slices (described previously). Whole brain was removed by making an incision along the midline of the head, peeling back the skin, cutting open the skull and dissecting out the brain.

Whole spinal cord, brain and individual spinal cord slices were stored in isopentane at -80 ºC. Samples were homogenized in ice cold methanol. For a standard control, 100 µl of the sample from saline-injected animal brain or spinal cord homogenate was used and for comparison, 100 µl of sample from GBP-injected animal brain or spinal cord homogenate was used in analysis. Samples were vortexed, placed on ice for 10 min and centrifuged at 10,000 *g* for 4 min.

The supernatant was transferred to a low volume silanized glass insert and 20µl of supernatant was injected onto the LCMS. Analysis was performed using a Waters ZQ Mass detector fitted with an ESCI Multi-Mode ionization source and coupled to a Waters 2695 Separations module (Waters, Milford, MA, USA). Mass Lynx 4.0 software was used for instrument control, data acquisition and processing. HPLC separation was performed on an Atlantis dC18 (3µm, 3.0 x 100mm) column (Waters, Milford, MA, USA) with a guard column of similar material. Mobile phase A consisted of 0.05% formic acid in water and mobile phase B was composed of 0.05% formic acid in acetonitrile. Initial conditions were 80% A and 20% B at a flow rate of 0.3ml/min. A gradient was run increasing to 80% B in 15 min followed by a return to initial conditions. The column heater and sample cooler were held at 30 ºC and 4 ºC respectively. Optimized positive electrospray parameters were as follows: capillary voltage 3.4kV; Rf lens voltage 1.0 V; source 110 ºC; desolvation temperature 350 ºC; cone gas flow (nitrogen) 100L/Hr; desolvation gas flow (nitrogen) 500 L/Hr. Cone voltage was held at 20 V. Acquisition was done in the Single Ion Monitoring

(SIM) mode and the mass:charge ratio was set at 171.2 to correspond to the molecular weight (in g/mol) of gabapentin.

Electrophysiology

For electrophysiological recording, acutely isolated spinal cord slices were superfused at room temperature (22-24°C) with 95% O_2 - 5% CO_2 saturated aCSF containing (in mM): 127 NaCl, 2.5 KCl, 1.2 NaH_2PO_4, 26 $NaHCO_3$, 1.3 $MgSO_4$, 2.5 $CaCl_2$, 25 *D*-glucose, pH 7.4. The *substantia gelatinosae* were visualized under IR-DIC (infrared-differential interference) optics as a translucent band (see Figure 2-2B). Pipettes for recording had a resistance of 6-8 MΩ when filled with an internal solution that contained (in mM): 130 potassium gluconate, 1 $MgCl_2$, 2 $CaCl_2$, 10 HEPES, 10 EGTA, 4 Mg-ATP, 0.3 Na-GTP, pH 7.18-7.20, 290-300 mOsm.

An NPI SEC-05LX amplifier was used for recording in discontinuous, single electrode, current or voltage-clamp mode. Only data from neurons that produced a clear action potential overshoot of greater than 60 mV in amplitude was collected. Neurons were characterized on the basis of firing pattern in response to 800 ms depolarizing current pulses from a holding potential of -60 mV according to criteria in Balasubramanyan et al, 2006 as either tonic, delay, phasic, transient or irregular (Figures 1-4 and 4-1) (Balasubramanyan et al., 2006).

For measurement of excitability current ramp commands were applied and discharge rates were analyzed. Current ramps were delivered at 33, 67, 100 or 133 pAs^{-1}. Only the 133 pAs^{-1} was used in analysis as this provided more discharge pattern data for comparison between cell types (Figure 4-9). Cumulative latency plots were constructed in Origin 2015 as shown in Figure 4-10. Data analysis was performed using pCLAMP 8.0 (Axon Instruments, Burlingame, CA, USA). Statistics

were performed using a one-way analysis of variance (ANOVA) with Bonferroni correction where appropriate to confirm significance. Statistical significance was attributed if $p<0.05$.

Spontaneous excitatory post-synaptic currents (sEPSCs), which encompasses action potential dependent and independent components of neurotransmitter release (Edwards et al., 1990) were recorded at -70 mV (Figure 4-3A). Miniature excitatory post-synaptic currents (mEPSCs), which represent action potential independent release (Edwards et al., 1990), were recorded in the same way but in the presence of 1 μM TTX (Figure 4-3B). The blockade of action potentials by TTX was confirmed by the failure of neurons to discharge an action potential in response a depolarising current pulse. MiniAnalysis (Synaptosoft, Decatur, GA, USA, www.synaptosoft.com) was used to identify sEPSC and mEPSC events from baseline noise. An appropriate amplitude and area threshold for events was set in the program and events were subjectively visually analysed using appropriate amplitude and area threshold for each neuron analysed for each neurons. A typical event is show in Figure 4-3C. A 3 min recording or the first 100 events were analyzed from each neuron, however, neurons that failed to produce events during a 3 min recording were excluded. The inter-event interval and amplitude of events were exported to Origin 8.5 for generation of cumulative probability plots (Figure 4-4 to 4-8). Kolmorogorv-Smirnov two-sample tests (K-S test) were used for comparison of cumulative probability plots of amplitude or inter-event interval between control or drug. The K-S test is used because it compares the entire distribution rather than the mean of the distribution (Van der Kloot, 1991). Statistical significance was attributed if $p<0.05$.

Drugs and Chemicals

Human BDNF (brain-derived neurotrophic factor; recombinant protein expressed and extracted from *E. coli*, catalogue #B-250), mouse NGF 2.5S 99% (nerve growth factor, catalogue #N-240) and TTX (tetrodotoxin, provided in citrate buffer, catalogue #T-550) were from Alomone Laboratories, Jerusalem, Israel. BDNF was made up in Neurobasal (Gibco (Invitrogen, Carlsbad, CA, USA; www.invitrogen.com)) to make a 10 µg/ml stock solution, aliquoted and stored at -80 ºC. NGF was made up in sterile Hank's buffered saline solution (HBSS, see previous) to make a 10 µg/ml stock solution, aliquoted and stored at -80 ºC. TTX was dissolved in HPLC water to make a 1mM stock solution that was stored at -80 ºC until use. On the day of each experiment, TTX was diluted to 1µM in external solution.

Kynurenic acid (Tocris) was purchased from Cedarlane Laboratories (Hornby, Ontario, Canada).

Gabapentin (>98% purity, catalogue #G0318) was from Tokyo Chemical Industry Co., Ltd. America (TCI America, Portland, Oregon).

Fluo-4 AM cell permeant (catalogue #F-14217), Oregon Green® 488 Bapta-1 (OGB-1, catalogue #O-6807) and sulforhodamine (SR-101, catalogue #S-359) were purchased from Molecular Probes, Invitrogen, Carlsbad, CA, USA.

Unless stated otherwise, all other drugs and chemicals were from Sigma, St. Louis, MO, USA.

For electrophysiological recordings, drug solutions were placed in storage reservoirs fashioned from 20 ml syringes and their flow into the recording chamber controlled manually by three way stop cocks. For Ca^{2+} imaging, drug solutions were placed in a hot water bath at 37 ºC and superfused using a motorized pump at 3 ml/min.

Statistical Analysis Software

All statistical analysis was performed using Origin 2015 (Origin Lab Corp., Northampton, MA, USA, www.originlab.com), except statistical analysis of sEPSCs and mEPSCs which was performed using MiniAnalysis (Synaptosoft, Decatur, GA, USA, www.synaptosoft.com).

Figure 2-1

A

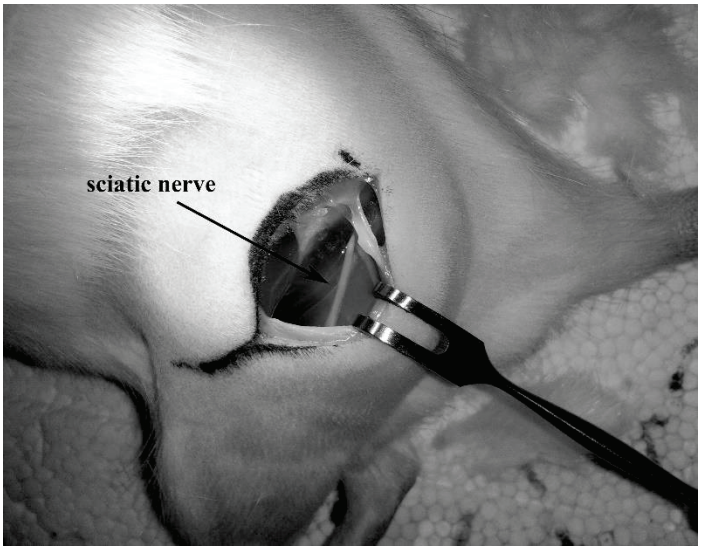

B

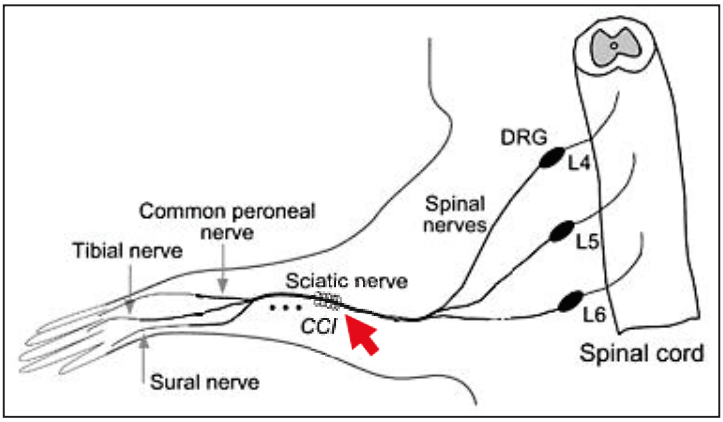

Figure 2-1. **Rodent model of neuropathic pain.** A. Sciatic nerve exposed in a 23-day-old Sprague-Dawley rat prior to Chronic Constriction Injury (CCI) surgery. The mid-thigh level position has been opened slightly more than usual to expose the sciatic nerve for demonstration purposes. B. Position of the sciatic nerve and the injury site in relation to the hindpaw and spinal cord. The red arrow indicates the placement of the 2 mm polyethylene cuffs. Figure 2-B is modified from Ueda and Rashid, 2003.

Figure 2-2

A

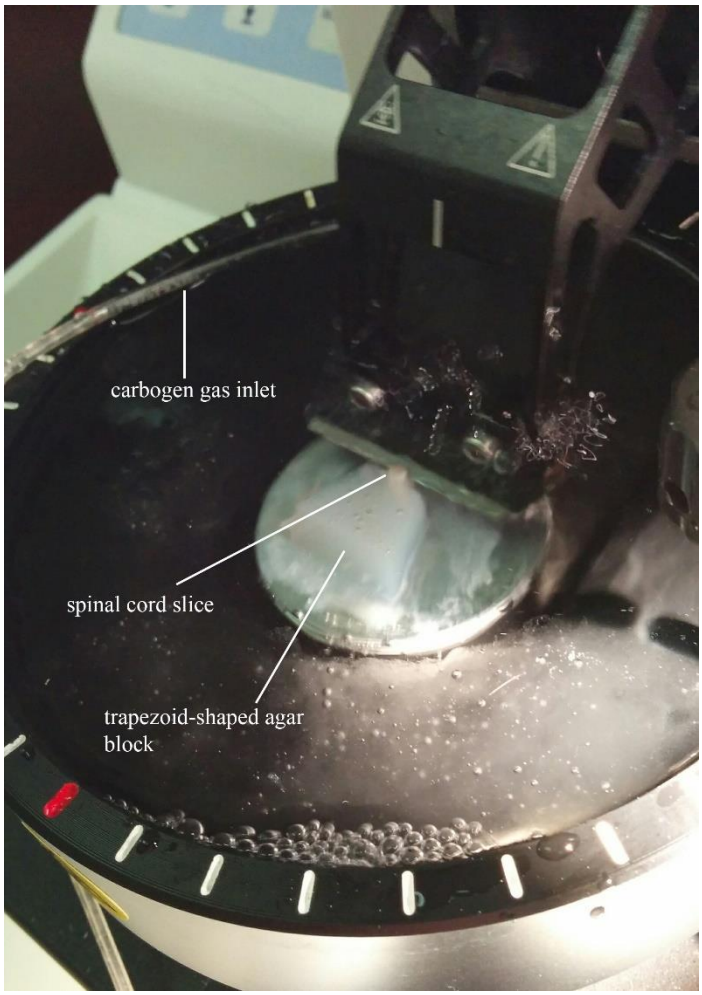

B

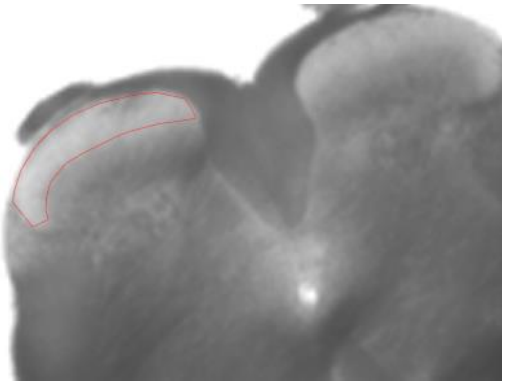

Figure 2-2. Acute spinal cord slice preparation. A. Vibratome slicing of acutely isolated spinal cord. Slices were cut transversely at 300 μm in thickness. aCSF was partly frozen and 'slushy' in consistency as it was placed in a freezer at -20 ºC for 1 hr prior to slicing. The temperature of the solution was maintained by a large metal block (the knob visible on the right hand side is attached to the block beneath the platfom to allow easy removal). Bubbles are due to carbogen gas continuously delivered to the aCSF solution. **B.** Acutely isolated spinal cord slice from a 30 day old rat. The red outlined area of the slice indicates the *substantia gelatinosa* that is clearly visible as a translucent band under IR-DIC optics.

Figure 2-3

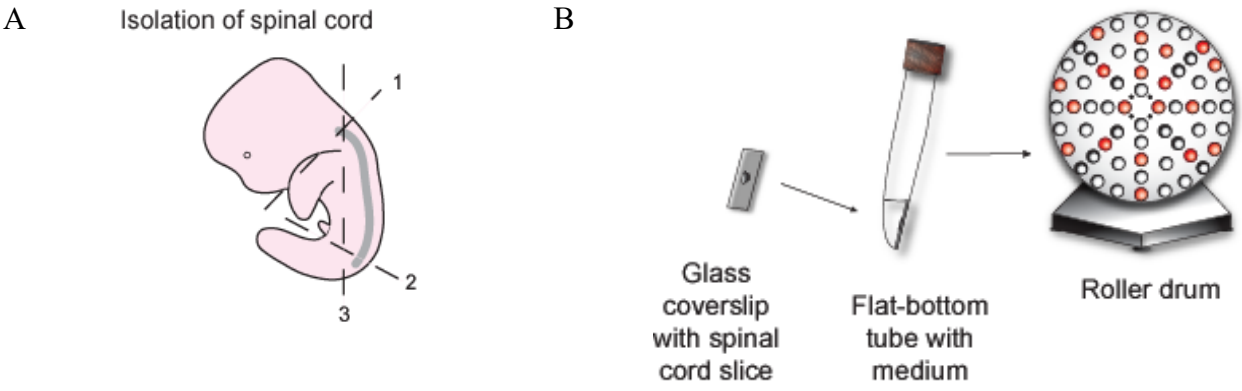
A
Isolation of spinal cord
1
2
3
B
Glass coverslip with spinal cord slice
Flat-bottom tube with medium
Roller drum

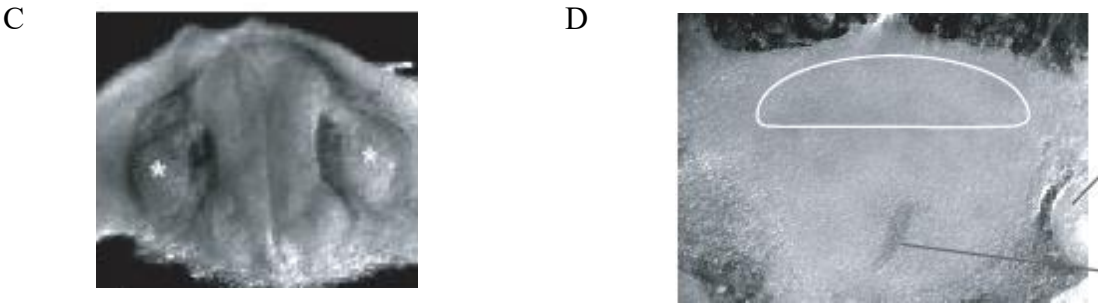
C
D

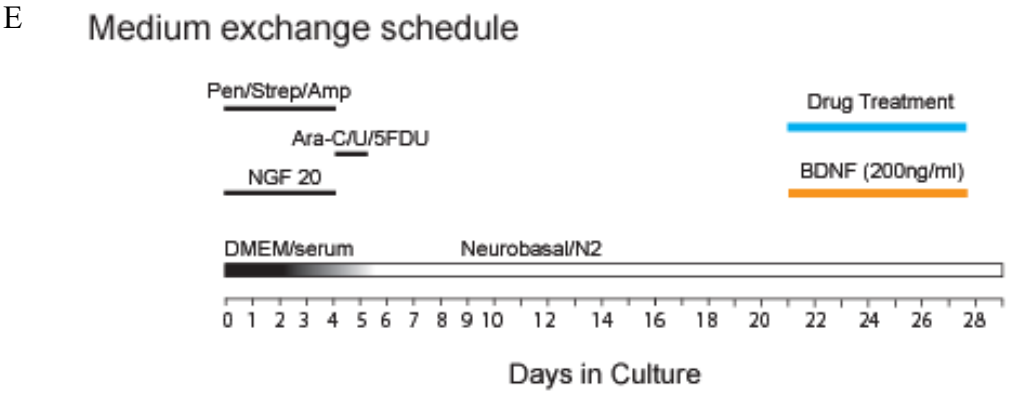
E
Medium exchange schedule
Pen/Strep/Amp
Ara-C/U/5FDU
NGF 20
Drug Treatment
BDNF (200ng/ml)
DMEM/serum
Neurobasal/N2
0 1 2 3 4 5 6 7 8 9 10 12 14 16 18 20 22 24 26 28
Days in Culture

Figure 2-3. **The Defined-Medium Organotypic Culture (DMOTC) Method.** A. Isolation of spinal cord from embryos of E13 pregnant Sprague-Dawley dams. Dotted lines indicate the sections that are made with a scalpel blade to remove the head, limbs and tail and ventral portions to extricate the spinal cord. B. The storage of DMOTCs. DMOTC slices are plated on cover slips and placed in flat-bottomed tubes to be placed in a roller rack at 37 ºC. C. An acutely isolated DMOTC at Day 0. Slices are cut at a thickness of 375 um. D. A DMOTC slice after 10 days in culture. The slice has thinned out over time. E. The schedule of media exchanges. Initially, DMOTC slices are grown in serum, DMEM, an antibiotic combination of Pen/Strep/Amp to prevent contamination and NGF to improve growth. After 4 days in this medium, an anti-mitotic cocktail is provided for 24 hrs to prevent glial overgrowth. Finally, serum is removed from the media and a neurobasal medium supplemented with N2 is used for the remainder of the life of the cultures. The cultures are now serum-free. Modified from Biggs et al, 2012.

Figure 2-4

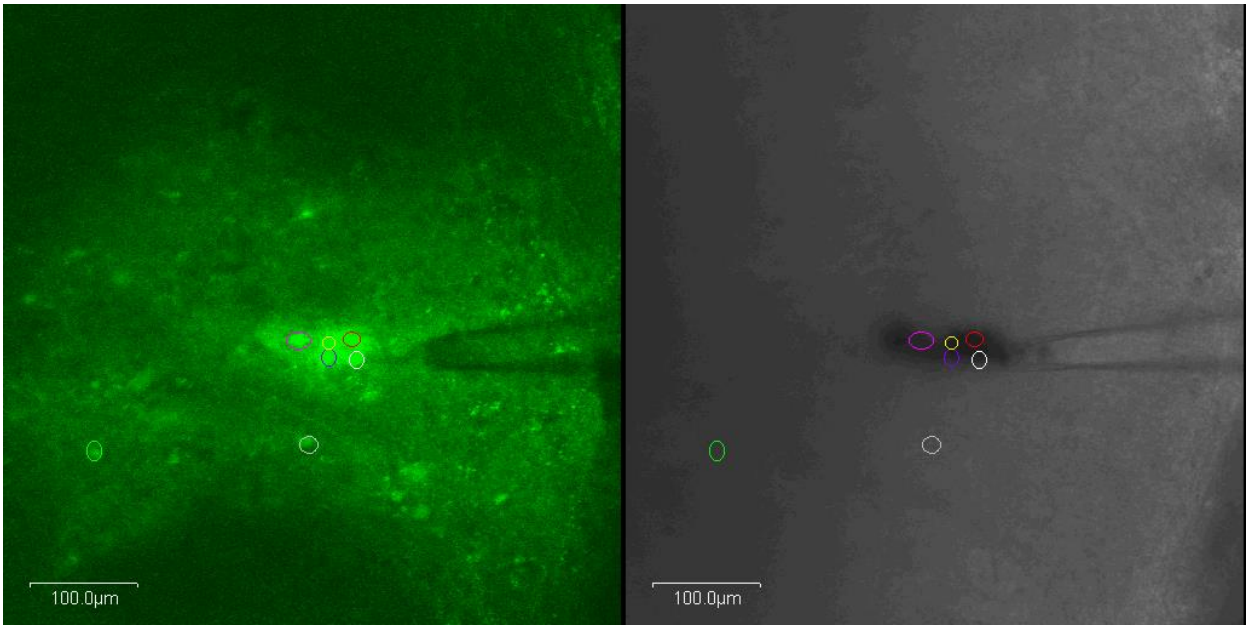

Figure 2-4. **Loading of acutely isolated spinal cord slices from adult (30-40 day old) rats.** The left panel indicates the channel for measurement of Fluo-4 AM fluorescence and the right indicates the transmitted visible light channel. In both channels dye can be seen leaving the pipette. Circles indicate random placement of regions of interest for monitoring of loading (these are not indicative of individual cells). See Figure 3-5 for individual loading of dorsal horn cells and design of stimulation protocol. Scale bar = 100 µm

Figure 2-5

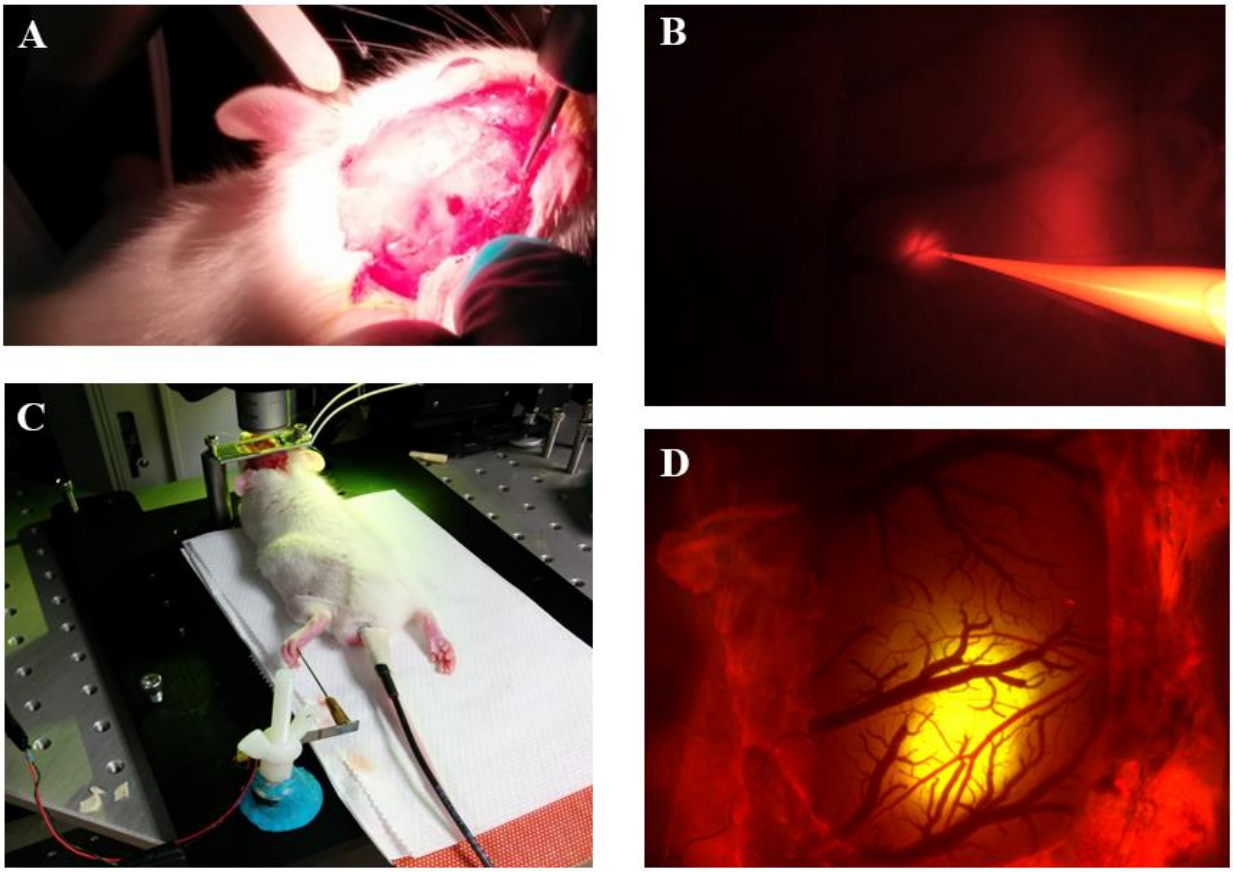

Figure 2-5. ***In vivo*** **cortical imaging. A.** Craniotomy performed after thinning of the skull and autofluorescent flavoprotein imaging to determine 'somatosensory map'. **B.** OGB-1 (Ca2+ indicator) with Alex-594 (tracer) injection into the cortex. **C.** Vibrotactile stimulation of the hindpaw. **D.** Typical loading (false colour) of the cortex with OGB-1.

Figure 2-6

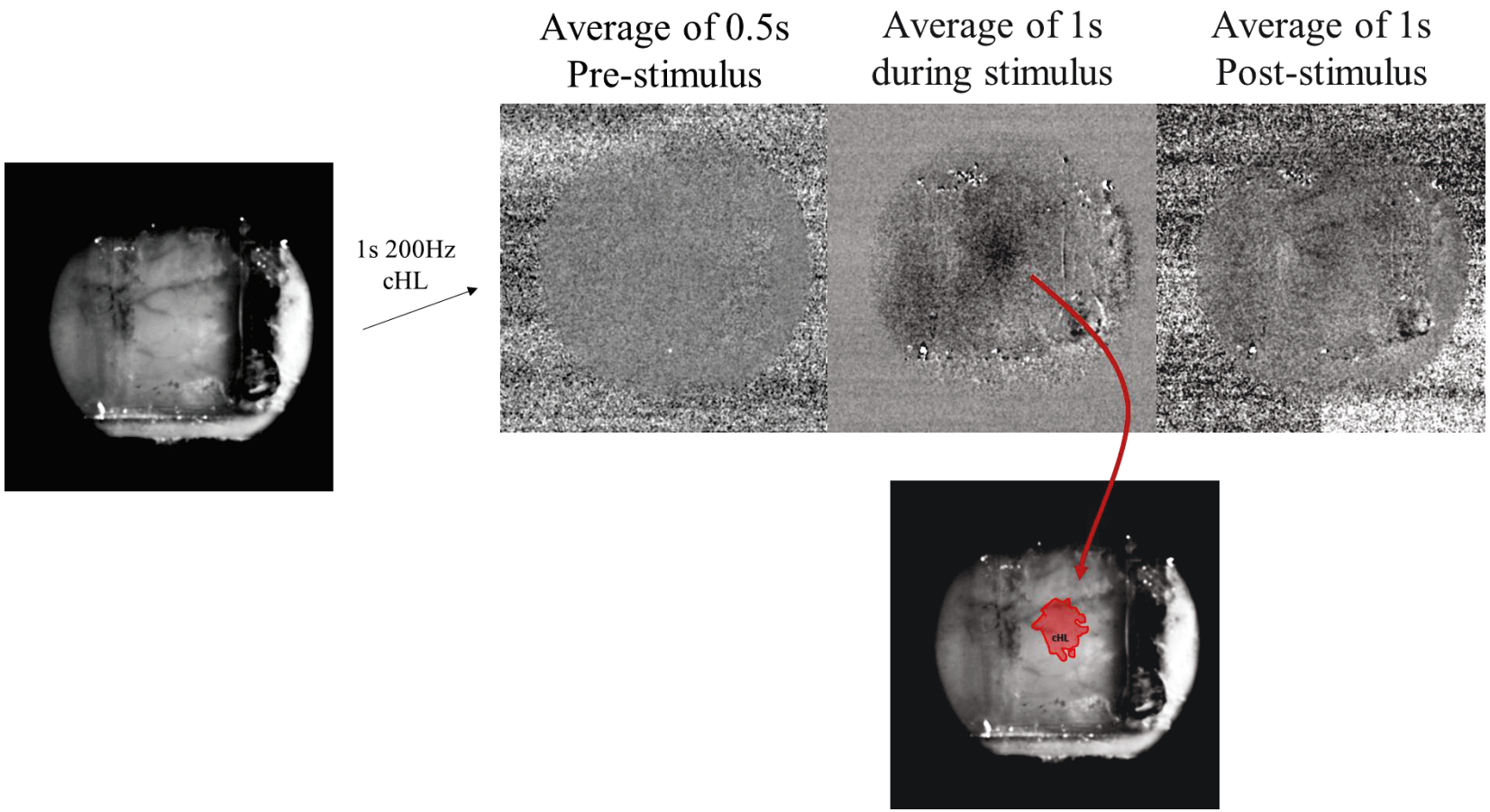

Figure 2-6. **Generation of a 'somatosensory map'.** Vibrotactile stimulation of the contralateral hindlimb (cHL) was performed at a frequency of 200 Hz for 1s to obtain a change in hemodynamic signal as indicated by the top panel. The red arrow shows the region corresponding to the cHL region on the cortex.

Figure 2-7

A

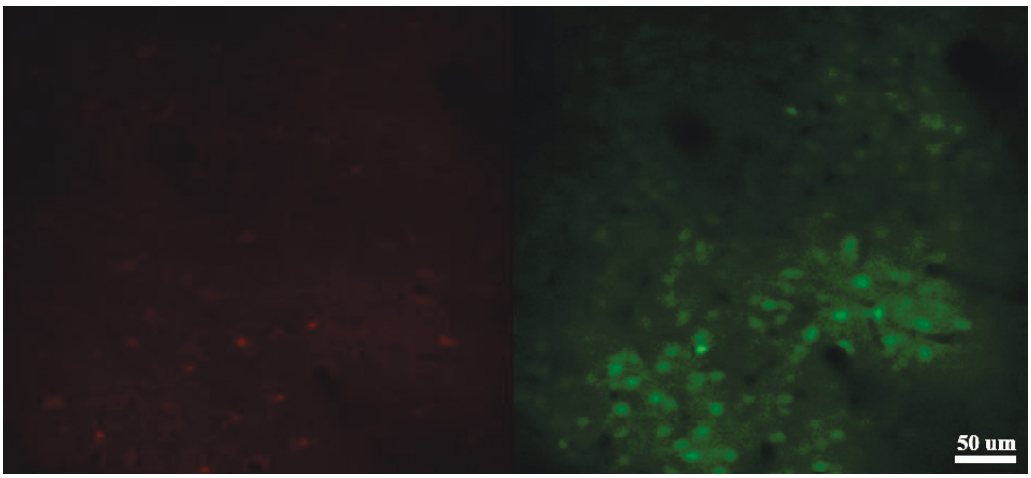

B

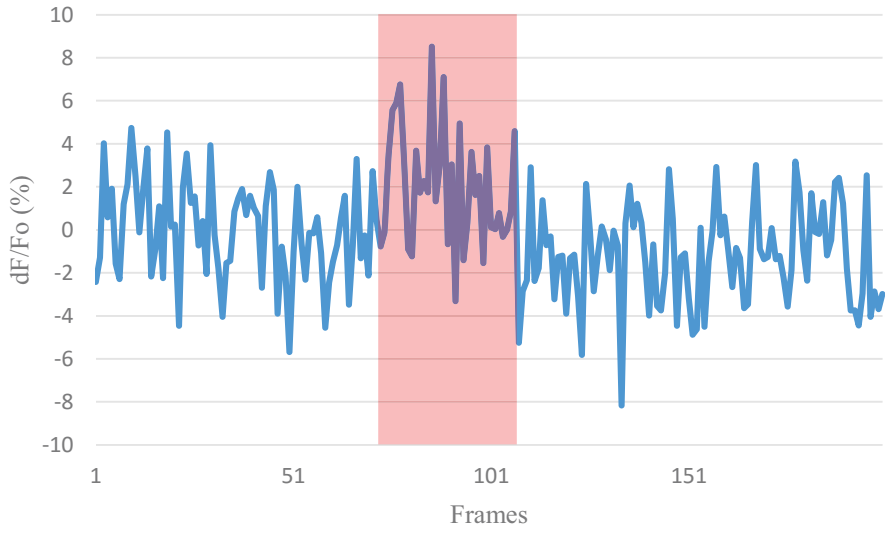

Recording of responses using *in vivo* cortical two-photon Ca^{2+} imaging. A. Loading of glial (red, left) and neuronal (green, right) cells at 100 µm depth in the primary somatosensory cortex of adult male rats for *in vivo* two-photon imaging. Glial cells are loaded by bath application of sulforhodamine and neuronal cells via pressure injection with Ca^{2+} indicator OGB-1 AM dye. B. Averaged normalized Ca^{2+} rise (shown in red) of a neuronal cell in response to repeated vibrotactile stimulation of the left hindpaw at 200 Hz.

CHAPTER 3

N.B. I carried out all nerve-injury surgeries, acute spinal cord slice preparations and *ex vivo* slice Ca^{2+} imaging experiments. LC-MS studies were carried about by Gail Rauw. *In vivo* Ca^{2+} imaging experiments were carried out with assistance from Mischa Bandet and Bin Dong. Animal behavioural studies were performed by Nataliya Bukhanova.

Chapter 3: The Acute Effects of Systemic GBP Administration on Dorsal Horn and Primary Somatosensory Cortex Excitability in Neuropathic Rats

Introduction

The proposed 'classical' mechanism of action of GBP is that GBP enters the neuronal cytosol via the system-L-neutral amino acid transporter and binds the $\alpha_2\delta$-1 subunit, an auxiliary subunit of the VGCC, resulting in a reduction in the forward trafficking of functional VGCCs to nerve terminals, which would consequently result in a decrease in net Ca^{2+} influx and hence a reduction in neurotransmitter release (Field et al., 2006). In the context of NP, where nociceptive neurons become hyperexcitable, it is expected that GBP reduces depolarization-induced neurotransmitter release to reduce net excitability and normalize pain thresholds (Hendrich et al., 2008). Most of the reported actions of GBP suggest that its effect on VGCC trafficking would be expected to occur over a long-term time course (>17 hours or more) (Biggs et al., 2014a, Biggs et al., 2014b, Hendrich et al., 2012) and this mechanism would also support clinical observations that GBP takes several days to produce meaningful pain reductions in NP patients (Cheshire, 2002, Sharma et al., 2010). However, GBP appears to produce an effect on pain thresholds in a matter of minutes or hours in *in vivo* animal models, which contradicts a much longer time course (>17 hours), 'classical' mechanism (Field et al., 2006, Hunter et al., 1997, Kumar et al., 2013). Therefore, a paradox exists between the acute effects of GBP *in vitro* and its slower effects *in vitro*. My hypothesis is that the reason for the inconsistent conclusions regarding the acute actions of GBP in the literature is because most studies that have concluded a lack of effect of acute GBP did not use neuropathic animals, examine time course of application of GBP and/or use appropriate, clinically relevant concentrations of GBP.

In order to resolve this paradox, it is necessary to examine nociceptive circuits at a time when a clinically relevant dose of GBP is exerting its acute anti-allodynic action in neuropathic animals. Therefore, I hypothesize that a clinically relevant dose of IP-injected 100 mg/kg GBP will exert anti-allodynic effects in neuropathic rats in an acute time frame and that the 'footprints' of these effects can be detected in nociceptive circuits. I will characterize an acute anti-allodynic effect of 100 mg/kg IP-injected GBP in a chronic constriction injury (CCI) model of neuropathic pain in rats by measuring paw withdrawal threshold before and 30 min after IP GBP injection.

The dorsal horn of the spinal cord forms an important site of nociceptive processing (Todd, 2010) and the primary somatosensory cortex (PSC) forms a crucial part of the 'pain matrix', where the experience of pain occurs (Jones et al., 2003). Changes in network excitability of the dorsal horn and PSC have been implicated in neuropathic pain states following peripheral nerve injury (Woolf, 1993, Navarro et al., 2007, Taylor et al., 2009). Therefore, I will test the hypothesis that GBP exerts changes in overall network excitability at the level of (1) the dorsal horn and (2) the PSC in neuropathic rats that have received a prior clinically-relevant dose of GBP via systemic IP injection. To test hypothesis (1), proposed changes in network excitability in the dorsal horn will be studied via Ca^{2+} imaging of evoked responses of *ex vivo* slices prepared from neuropathic and sham-operated rats that have been tested behaviourally and for which an acute anti-allodynic effect of GBP has been reported. To test hypothesis (2), the proposed changes in the network excitability of the PSC will be studied via *in vivo* cortical Ca^{2+} imaging of evoked responses in anesthestized neuropathic or sham-operated rats before and immediately after IP GBP injection. Understanding the proposed underlying changes in dorsal horn and PSC network excitability will provide an insight into the mechanism of acute anti-allodynic action of GBP.

Methods

The methods used in this chapter include chronic constriction injury (CCI) surgery, *ex vivo* acute spinal cord slice preparation, liquid chromatography-mass spectrometry (LC-MS), Ca^{2+} imaging of *ex vivo* acute spinal cord slices, *in vivo* Ca^{2+} imaging and statistical analysis. These methods are described in detail in Chapter 2.

Results

Repeated injection of GBP maintains reduced withdrawal thresholds in neuropathic rats

For the purposes of testing the hypothesis that GBP produces consistent acute anti-allodynic effects over the course of a few days, male Sprague-Dawley rats of 18-23 days old were subject to chronic constriction injury (CCI) of the sciatic nerve as per the Mosconi-Kruger model (Mosconi and Kruger, 1996) and developed allodynia within 7 days of surgery (see Chapter 2). Sham-operated animals were used as controls. The index of neuropathic pain used for behavioural studies was the paw withdrawal threshold or PWT, calculated by determining pattern of withdrawal of the hindpaw in response to von Frey filaments of specific weights. A score of 15 g represents a maximum score and was attributed to each sham animal, whereas a score of less than 6 g represents an animal suffering from mechanical allodynia, a sign of neuropathic pain. Figure 3-1A illustrates the time course of the development of neuropathy (reduced PWT) in CCI compared to sham rats over a 30 day period. The PWT of neuropathic versus sham-operated rat at 7 days post-surgery is shown in Figure 3-1B.

To test the hypothesis that IP GBP was effective at increasing PWTs and maintaining these increased PWTs in neuropathic CCI rats consistently over the course of a few days compared to

vehicle (saline), 100 mg/kg GBP was injected IP three times every 24 hr period into CCI neuropathic rats over the course of 3.5 days. As shown in Fig 3-1A, intraperitoneal injection of a clinically-relevant dose of GBP (100 mg/kg) increased PWTs in neuropathic rats and repeated injections (three times every 24 hr period) maintained these increased PWTs over a 3.5 day period. The effect of GBP was reversible as shown by the recovery of the PWT to neuropathic levels 3 days following cessation of GBP injections (Figure 3-1A). These results also indicate a lack of tolerance to GBP after 10 repeated injections over 3.5 days and that GBP produced a meaningful anti-allodynic effect (reduction in PWT of at least 50%) within a short-term (3.5 day) time frame. Meanwhile, an injection of saline did not produce a reduction in PWTs in neuropathic rats.

It is known that GBP produces mild, transient sedative effects as observed through a reduction in spontaneous behaviour of rodents (Vonsy et al., 2009). However, these sedative effects are not significant until at least 90 min post-GBP injection (Kayser and Christensen, 2000). Therefore, all measurements of PWT were made within 30 min of GBP injection to ensure measurement of a response that reflected mechanical allodynia as opposed to any potential motor effects.

In addition to neuropathic and sham rats, some rats (approximately 1/6) that undergo the CCI surgery did not develop mechanical allodynia and these rats are called ‘non-responders’. As another form of control for comparison to neuropathic rats, we performed experiments on non-responder rats and established that IP GBP injection did not have a significant effect on PWT compared to saline (Figure 3-1C).

A single IP injection of GBP reduces withdrawal thresholds in neuropathic rats within 30 min

In order to establish how fast GBP can produce an effect on withdrawal thresholds in neuropathic animals, we performed a single intraperitoneal injection of 100 mg/kg GBP in neuropathic CCI rats and measured pain thresholds within 30 min. As shown in Fig 3-2, a single 100 mg/kg GBP injection significantly increased the PWT score in neuropathic rats from below 6 g to near a maximum score of 15 g attributed to uninjured rats ($n=23$ rats, $P<0.05$, one way ANOVA with Bonferonni correction) within 30 min. This confirmed that GBP has a very clear acute effect in animal models of NP.

GBP detected in spinal cord (whole cord and slices) and brain of IP injected animals

GBP enters the neuronal cytosol via the system-L-neutral amino acid transporter (Su et al., 1995). However, it is not known whether GBP accumulates in tissues of the CNS within 1-1.5 h of IP injection and whether this could explain the site of acute action of GBP. The goal of this experiment was to determine if GBP was present in acutely isolated spinal cord or brain from GBP-injected animals within the first 1.5 hr of injection and to see if GBP was present in spinal cord tissue after going through the full procedure for generating slices.

For measurements of GBP from brain and spinal cord, injections of either vehicle, 60 mg/kg GBP or 100 mg/kg GBP were delivered. Whole brain and whole spinal cord were removed from naïve animals as described in Chapter 2. GBP levels were measured using liquid chromatography-mass spectrometry (LC-MS, see Chapter 2). As shown in Fig 3-3A, GBP was detected in both brain and spinal cord tissues from GBP-injected naïve rats. GBP levels in the 60 mg/kg GBP-injected animal

(n=1) were lower than in the 100 mg/kg GBP-injected animal (n=1) as expected (approximately 3.5 times lower for spinal cord and 3 times lower for brain).

We also measured GBP levels in individual *ex vivo* spinal cord slices (n=12) from a neuropathic CCI rat (Figure 3-3B) to establish whether transport mechanisms of GBP were still intact under neuropathic conditions. GBP was detected in spinal cord slices, but the variation of levels (544 ± 66 ng) through the lumbo-sacral region of the cord could be explained by the fact that it was difficult to estimate the exact weight of individual slices, hence calculating GBP levels in terms of ng per g of tissue would lead to errors.

The presence of GBP in samples of whole spinal cord, spinal cord slices and brain tissue post-injection suggests that GBP targets these tissues as part of its mechanism of acute anti-allodynic action.

In order to assess whether the rapidly developing effects of GBP *in vivo* were associated with decreased dorsal horn excitability, the scheme shown in Fig 3-4 was developed. On a given day of experiments, withdrawal thresholds were determined in a neuropathic CCI rat or a control sham-operated rat. Following IP injection with GBP (or saline as control), animals were tested again within 30 min. These same animals were then transported to from the behaviour suite to a dissection room, where the animal was euthanized via 1.5 g/kg urethane overdose and its spinal cord removed by performing a laminectomy. The intact spinal cord was cleaned of connective tissue and dura and transferred to a vibratome for slicing. Slices were then used for experiments to measure dorsal horn excitability. These experiments allowed both behavioural measurement and a corresponding cellular excitability measurement to be made on the same day and from the same animal.

Dorsal horn excitability was reduced in GBP injected rats compared to controls

The dorsal horn of the spinal cord is an important site of nociceptive processing (Todd, 2010) Changes in network excitability of the dorsal horn implicated in neuropathic pain states following peripheral nerve injury (Woolf, 1993). Therefore, I hypothesize that GBP exerts changes in overall network excitability at the level of the dorsal horn in neuropathic rats that have received a prior clinically-relevant dose of GBP via systemic IP injection.

In order to study excitability of the dorsal horn, an evoked Ca^{2+} response was compared between neuropathic and sham-operated rats that had received IP GBP or saline. A rise in intracellular Ca^{2+} was evoked in Fluo-4 AM loaded dorsal horn neurons by a 1 min bath perfusion with 35 mM K^+. Figure 3-5A shows a typical response pattern of several dorsal horn cells to this stimulus. The average of six responses to 1 min applications of 35 mM K^+ with 5 min washout between each application was obtained (Figure 3-5B). In each case the normalized fluorescence (index of dorsal horn excitability, dF/F_0) was calculated as the peak amplitude of the Ca^{2+} rise (dF) divided by the initial baseline fluorescence (F_0).

The concentration of K^+ solution used for stimulation of the dorsal horn was based on a depolarization of approximately 40 mV of neuronal membrane potential to elicit action potential firing and sufficient to open voltage-gated sodium channels for initiating the action potential upstroke as calculated using the Goldman Equation:

$$\mathbf{K_{eq} = 61.5\ mV * \log \frac{(p_K[K_{out}]+p_{Na}[Na_{out}])}{(p_K[K_{in}]+p_{Na}[Na_{in}])}}$$

where pk = 40, pNa = 1, K_{in} = 100 mM, Na_{in} = 15 mM, Na_{out} = 150 mM at rest, K_{out} = 5 mM at rest, Na_{out} = 120 mM during stimulation and K_{out} = 35 mM during stimulation (Purves, 2008). It has also been shown that 35 mM K^+ evokes a Ca^{2+} rise that is almost completely blocked by 200 uM Mn^{2+}, a pan-VGCC blocker (see Figure 5-4A), which means that 35 mM K^+ evokes a Ca^{2+} rise that is dependent almost entirely on Ca^{2+} influx via VGCCs.

As shown in Figure 3-6, dorsal horn excitability was increased in neuropathic CCI rats compared to sham rats that had received saline, which is indicative of the increase in excitability that occurs in neuronal networks in the dorsal horn under neuropathic pain conditions (Woolf, 1993). The index of dorsal horn excitability was reduced in neuropathic CCI rats that had received 100 mg/kg GBP via intraperitoneal injection compared to those that had received saline (Figure 3-6). There was no significant effect of GBP injection on excitability of slices from sham rats (Figure 3-6) compared to controls, which suggests that the effect of GBP on dorsal horn excitability is unique to neuropathic rats.

GBP reduces Primary Somatosensory Cortex Excitability in Neuropathic Rats

It may be argued that the behavioural effects of GBP described in Figure 3-1 simply reflect depression of spinal reflexes rather than suppression of pain *per* se. Therefore, in order to determine whether the acute actions of GBP impact a higher level of perception within the central nervous system, we examined the effect of intraperitoneal injection of GBP on excitability of the PSC using *in vivo* two-photon Ca^{2+} imaging of whole rat cortex that were either neuropathic (CCI) or sham-operated.

As shown in Fig 3-7, neural mass (index of excitability, see Chapter 2) of neuropathic CCI rats was approximately 2.7 times higher than in sham rats. The cortex of neuropathic rats would be expected to be more excitable compared to sham rats on account of the previously mentioned mechanism of 'central sensitization' and the changes in cortical plasticity observed in neuropathic and chronic pain (Zhuo, 2011). It was also shown that within 10 minutes of injection, 100 mg/kg IP GBP significantly reduced neural mass in neuropathic CCI rats by approximately 56% ($P<0.05$, one-way ANOVA with Bonferroni correction), but that in sham rats was not significantly affected ($P>0.05$, one-way ANOVA). After 20 minutes, a significant reduction in neural mass was observed in sham rats with no further significant reduction (compared to that at 10 minutes) observed in neuropathic rats. Finally, after 30 minutes there was a slight recovery in the excitability of the PSC in both neuropathic and sham rats, although this was not significant ($P>0.05$, one-way ANOVA). In summary, it seems that the effect of acute GBP at the cortical level was unique to neuropathic rats.

Discussion

The results of this chapter show that systemic injection of a clinically relevant dose (Alles and Smith, 2016, (Backonja and Glanzman, 2003, Coderre et al., 2005) of 100 mg/kg GBP reduces pain thresholds in neuropathic rats. The underlying basis of this effect at the level of the dorsal horn, which receives nociceptive input from the periphery, and the PSC (after 10 min), where the experience of pain occurs (Melzack and Eisenberg, 1968), is that overall network excitability is decreased compared to controls. We also see that sham animals that had received GBP do not have reduced dorsal horn network excitability or PSC excitability (after 10 min). Therefore, the acute effect of GBP on pain behaviour is supported by the cellular effects in the dorsal horn and PSC.

This suggests that neuropathic animals undergo changes in the central nervous system that confer increased effectiveness of GBP whereas sham-operated animals do not.

Reliability of results

The emotional experience of pain involves a complex system of neural structures in the brainstem reticular formation and the limbic system (Melzack and Eisenberg, 1968). One such neural structure involved in affective pain processing involves the anterior cingulate cortex (ACC) (Fuchs et al., 2014). It has been shown in humans that a cingulotomy can be used to treat intractable cancer pain (Pereira et al., 2014), lower back pain (Sharma, 1973) or neuropathic pain (Boccard et al., 2014). Furthermore, brain imaging studies have detected increased ACC activity during persistent pain states (Yuan et al., 2013).

Unfortunately for our studies of the brain, it was not possible to study the ACC as these structures are too deep (>300 μm) to image using our two-photon imaging equipment. Therefore, we must be aware that although imaging the cortical surface provided interesting results, this may not provide a 'bigger picture' of the affective or emotional experience of pain that would be obtained by studying deeper brain regions such as the ACC.

There is also the possibility that GBP suppresses neuropathic pain by increasing the excitability of serotonergic descending inhibition in higher brain centers such as the locus coeruleus (Hayashida et al., 2008), therefore one must be cautious when interpreting these cortical imaging results. As will be discussed in Chapter 5, we have data from *in vitro* experiments with GBP to suggest that this is a likely mechanism of action of systemic GBP.

Sedative effects of GBP

Studies of the sedative effects of GBP using the rotarod test, whereby animals are placed on a rotating rod and their latency to fall is measured, suggest that only chronic GBP produces a slight decrease on the latency to fall in nerve-injured rats (Vonsy et al., 2009). This suggests that the sedative effects of GBP are only mild and that the increased PWT seen in GBP-injected neuropathic animals cannot be attributed to sedation or suppression of spinal reflexes. Studies on neuropathic rats have also shown that 100 mg/kg IP GBP does not affect rotarod performance time at 20 min or 60 min post-injection and only has a significant effect at 90 min post-injection (Kayser and Christensen, 2000). This means that the sedative effects of GBP would not affect our measurement of PWT within 30 min of injection.

Consistency with other groups

Intrathecal injection of 4.2 μmoles GBP 10 min prior reduces the spinal release of excitatory neurotransmitter, glutamate, 10-40 min after a stimulus of intraplantar formalin injection in CCI rats (Coderre et al., 2005). The authors also showed that intrathecally administered GBP was more effective than IP GBP at reducing spinal glutamate release. This study helps explain our results as GBP may be reducing net dorsal horn excitability via a reduction in spinal glutamatergic transmission.

It has also been shown recently that the enhanced miniature spontaneous excitatory post-synaptic currents (mEPSCs) from deep dorsal horn neurons of nerve-injured rats can be blocked within 10 min by 100 μM GBP treatment (Zhou and Luo, 2015). Since mEPSCs provide a measure of AP-independent, neurotransmitter release, this data suggests that GBP could be reducing release by

affecting the neurotransmitter release machinery. This again corroborates our findings with acute GBP on dorsal horn excitability.

Inconsistency with other groups

Many *in vitro* studies have failed to observe acute effects of GBP and this is largely by virtue of the fact that nerve-injured animals were not used, the physiological context was not relevant to nociception or doses of GBP were not clinically relevant. For example, Moore et al have shown that GBP does not affect the frequency or amplitude of spontaneous or evoked excitatory post-synaptic currents (eEPSCs or sEPSCs) from lamina II neurons of acutely isolated spinal cord from naïve adult rats and they concluded that synaptic transmission is minimally affected by GBP (Moore et al., 2002). Biggs et al also failed to observed an acute effect of bath applied 100 μM GBP on dorsal horn excitability of organotypic spinal cord as measured by the amplitude of a Ca^{2+} rise in response to depolarizing 35 mM K^+ (Biggs et al., 2014a).

In addition, Eroglu et al demonstrated long-term effects on synaptogenesis with chronic daily administration of very high doses of GBP (400 mg/kg, 4 times as high as our studies) with no reference to acute effects and they report that only 50% of mice responded strongly to GBP injection (Eroglu et al., 2009). As discussed earlier (see *The Thrombospondin Story*, Chapter 1), the mechanism of action proposed in this study relies on the effect of GBP on α2δ function as a thrombospondin receptor to decrease excitatory synaptogenesis. Since astrocytes secrete TSPs to increase synapse number (Christopherson et al., 2005), this mechanism does not explain our neuron-specific (neurons are labeled with OGB-1 in green and astrocytes with SR-101 in red) results with *in vivo* imaging.

GBP doses used in animal studies and connection to clinical studies

The clinical dose of GBP can vary depending on the type of neuropathic pain being treated, for example doses of between 600-3600 mg/day are used for painful diabetic neuropathy, whereas doses of 1800-3600 mg/day are used in cases of post-herpetic neuralgia (Sanderson et al., 2014). However, it is generally accepted that GBP at doses of 1800 mg/day to 3600 mg/day is effective in treating neuropathic pain in adults (Backonja and Glanzman, 2003).

How do we know what dose to work with in animals based on clinical results? Let us assume that the average effective daily GBP dose for human neuropathic pain patients is 2700 mg ((1800 mg + 3600 mg)/2). Based on the half-life of GBP in humans being an average of 7 h (between 5-9 h) and that in for example, rats being 1.7 h, assuming linear pharmacokinetics, the dose of GBP for rats would need to be much higher in order to provide a 'clinically relevant' dose (Radulovic et al., 1995). Also, taking into account that the global average human body weight is 62 kg (Walpole et al., 2012), daily dose in humans would work out to approximately 44 mg/kg. If we multiply this by a factor of 4 (approximately GBP half-life in humans divided by GBP half-life in rodents), we obtain about 179 mg/kg as our equivalent 'clinical' dose in rats. However, the pharmacokinetics of GBP are non-linear, which complicates dosing for an optimal therapeutic effect, and the bioavailability of GBP can vary widely (Larsen et al., 2016). Therefore, although this conversion is not accurate, perhaps it should be considered in pain studies in animals to ensure we are working with comparable doses for humans, especially for drugs that are already clinically available but where the mechanism of action is unclear. This calculation further illustrates that although the dose of 100 mg/kg that is administered to rats in these studies may appear high when compared to human doses, they actually are not when half-life of GBP in rodents compared to humans is considered.

In a study by Ben-Menachem et al the cerebrospinal fluid (CSF) levels of GBP in 4 patients was measured after a 600 mg oral dose of GBP. It was found that the average level of GBP in the CSF after 6 h was 0.2425 μg/ml (or 1.42 μM, GBP molecular weight = 171.2 g/mol) (Ben-Menachem et al., 1992). Of course, these measures are only extracellular and only after a period of 6 h after a single dose (by which time GBP levels will have significantly depleted) and there is naturally, no measurement available in the literature for intracellular GBP in the spinal cord for humans. It would probably be more appropriate to use therapeutic plasma concentrations of GBP from neuropathic pain patients, which are typically 15-30 mg/L (or 88-175 μM), for *in vitro* studies involving GBP (Juenke et al., 2011).

Figure 3-1

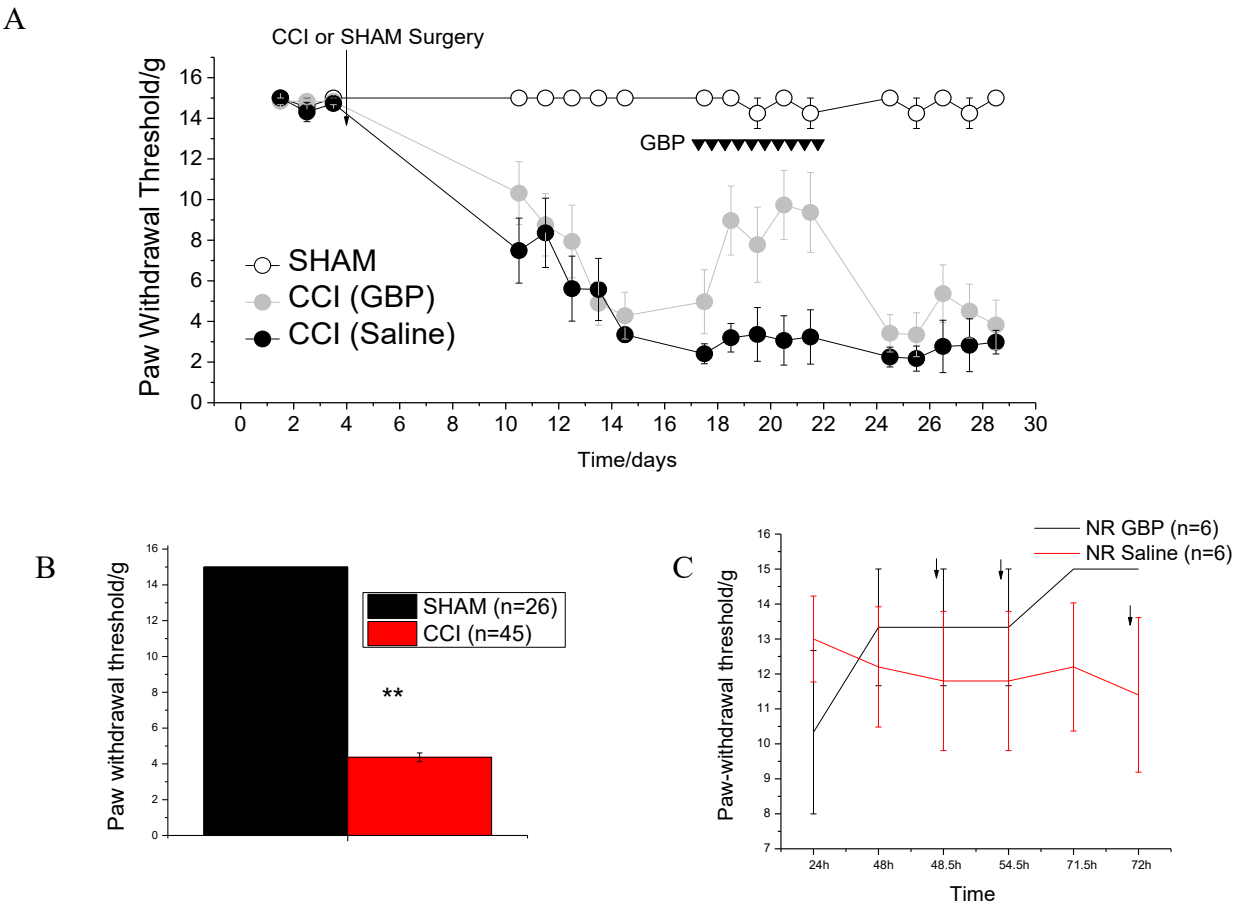

Acute anti-allodynic effects of GBP at a clinically-relevant dose of 100 mg/kg. A. Time course of effect of chronic constriction injury (CCI) on withdrawal threshold for von Frey filament stimulation and effect of repeated IP injections of 100mg/kg GBP. Animals received 3 injections per day as indicated by inverted black triangles. Treated animals displayed a rapidly developing and reversible increase in threshold. CCI (GBP) n=11, CCI (Saline) n=11, Sham n=4. Saline was injected as a control. **B.** PWT in sham versus neuropathic CCI rats at 7 days post-surgery. CCI surgery caused a lowering of withdrawal threshold and development of allodynia in rats as shown by a PWT of below 6 g. **C.** The effect of 3 repeated 100 mg/kg GBP or saline IP injections in non-responder (NR) rats. Injections of GBP are indicated by black arrows and corresponding behavioural measurements were made 30 min after injection. For comparing the von Frey responses of CCI and sham rats or non-responder rats, the one-way ANOVA with Bonferroni correction was used. **$p < 0.05$ was considered significant. All data are presented as mean ± SEM.

Figure 3-2

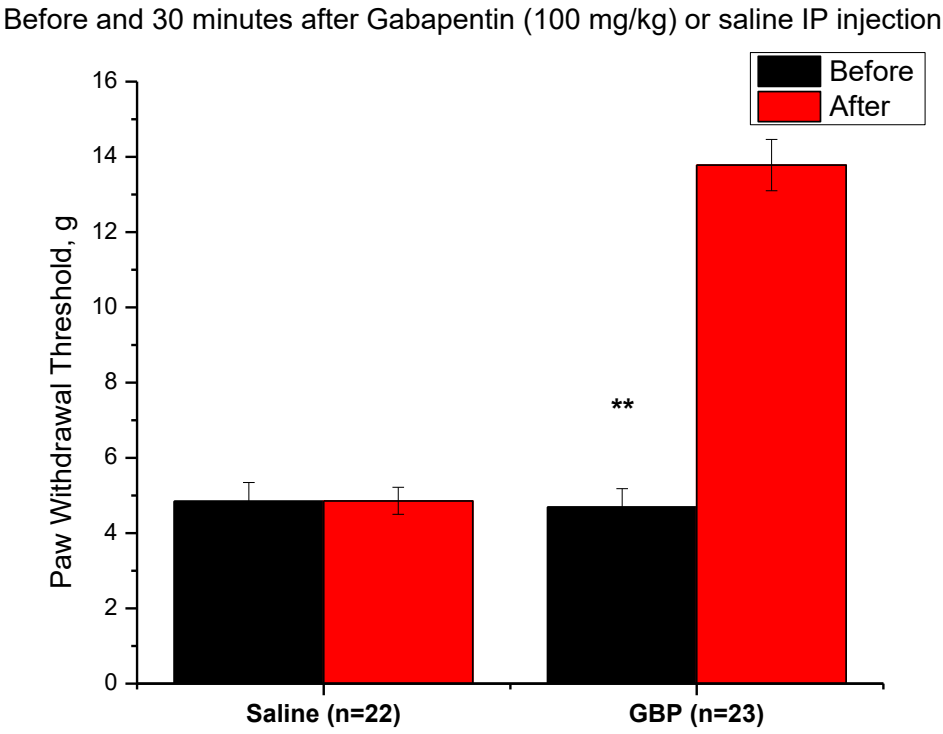

Acute (30 min) Anti-allodynic Effect of a single IP injection of 100 mg/kg GBP. A single intraperitoneal injection of 100 mg/kg GBP significantly increased PWTs within 30 min in neuropathic CCI rats, whereas saline had no effect. For comparing the von Frey responses of CCI rats, the one-way ANOVA with Bonferroni correction was used. **$p < 0.05$ was considered significant. All data are presented as mean ± SEM.

Figure 3-3

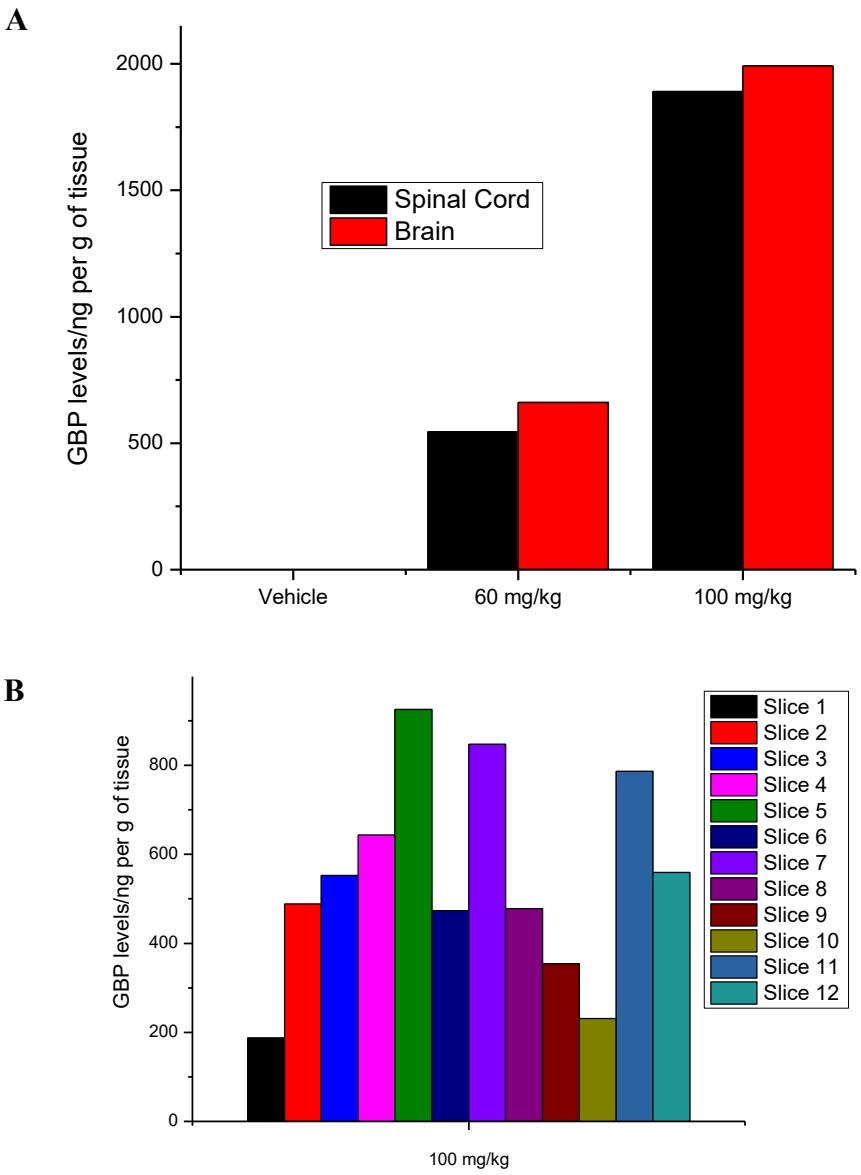

Measurement of GBP levels in spinal cord and brain tissue following IP GBP injection. A. GBP levels (in ng per g of tissue) measured using liquid chromatography-mass spectrometry (LC-MS) in whole spinal cord and brain from a naïve animal that received either vehicle, 60 mg/kg GBP or 100 mg/kg via intraperitoneal injection. **B.** GBP levels (in ng per g of tissue) measured using LC-MS in *ex vivo* spinal cord slices (n=12) from neuropathic CCI animals that received 100 mg/kg GBP via intraperitoneal injection.

Figure 3-4

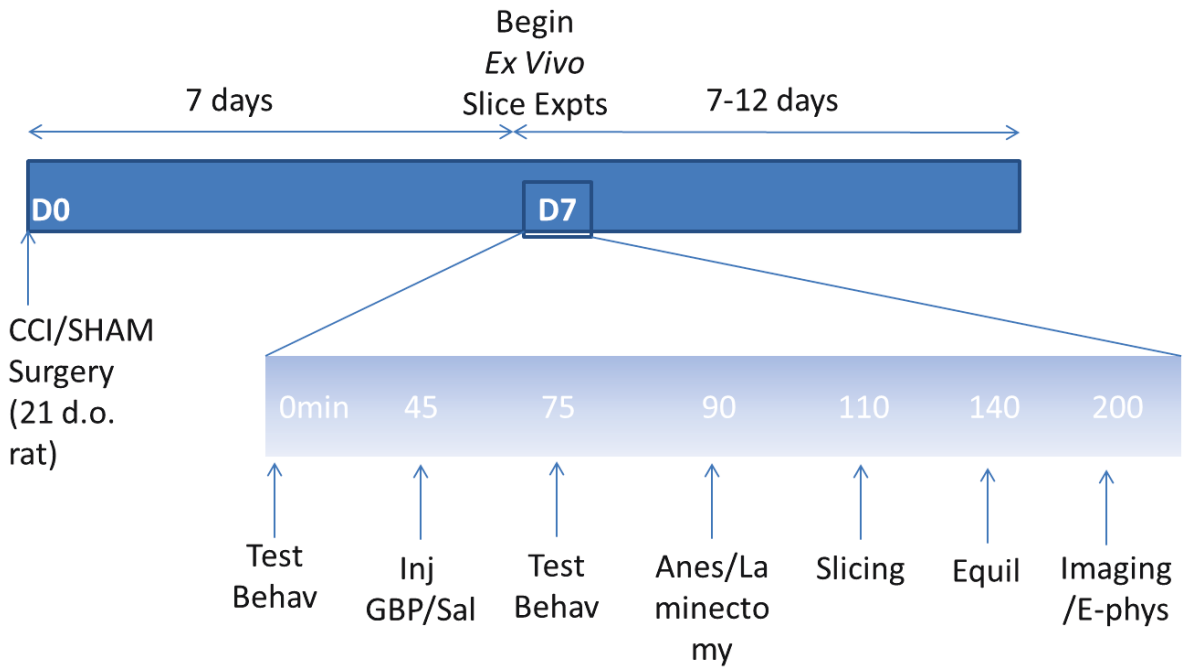

Time course of experiments for investigating the anti-allodynic actions of GBP in *ex vivo* spinal cord. Adult Sprague-Dawley rats were subject to CCI surgery and developed signs of neuropathic pain within 7 days as shown by a reduction in paw withdrawal threshold (PWT). Sham-operated rats were used as controls. On a given day of experiments, a given rat's PWT was recorded and the rat injected with either 100 mg/kg IP GBP or saline as control and the effect of the injection recorded. Following anesthesia the rat's spinal cord would be removed by laminectomy. Transverse 300 µm sections of lumbar spinal cord would be obtained and the slices equilibrate at 37 ^{o}C for 1 hr, after which experiments to study spinal cord excitability using Ca^{2+} imaging and electrophysiology (see Chapter 4) were carried out. Abbreviations: Behav=behaviour, Anes = Anesthetized, Equil = Equilibrate, E-phys = electrophysiology.

Figure 3-5

A.

Before 35 mM K^+

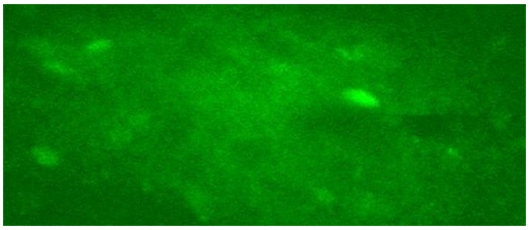

Response to 35 mM K^+

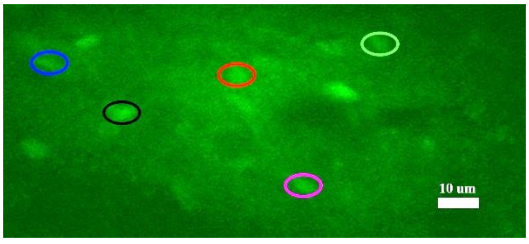

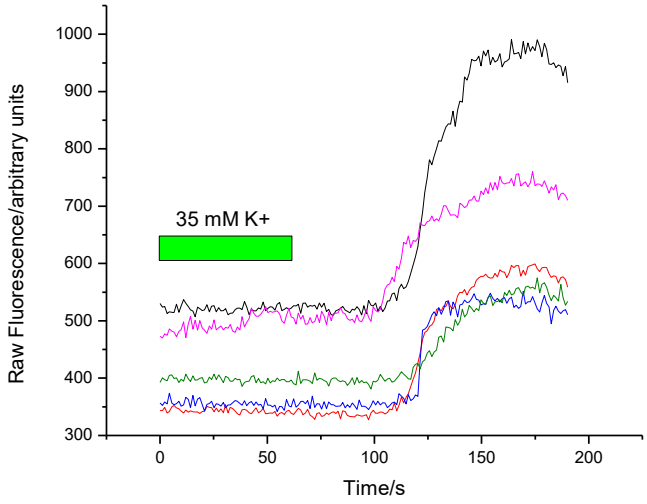

B.

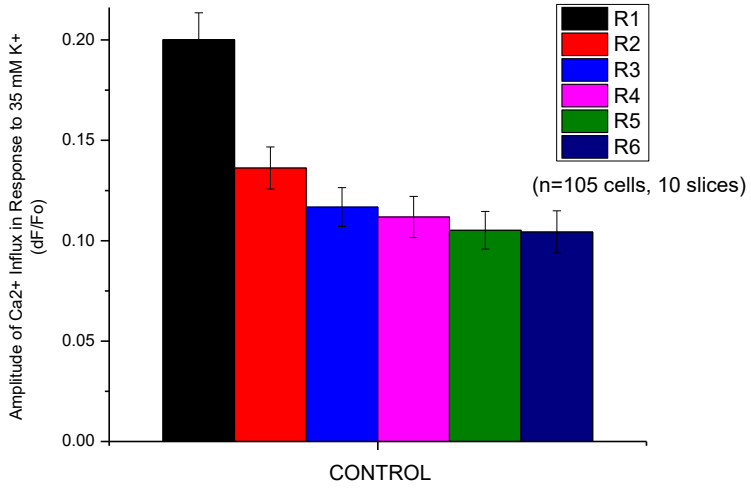

Ca^{2+} imaging of the dorsal horn of acutely isolated spinal cord slices from adult rats. A. Typical response to 35 mM K^+ (before and after). Confocal image of Fluo-4 AM loaded dorsal horn neurons before and after a response to 1 min bath perfusion with 35 mM K^+. Coloured circles indicate examples of responsive cells and the corresponding responses are shown in the traces on the right-hand side. B. Response of control (saline-injected sham-operated animals) dorsal horn neurons to six consecutive 1 min application of 35 mM K^+ with 5 min of washout between applications (R1-R6). The average of R1-R6 was used as the index of dorsal horn excitability. The average of all responses was used for each slice. All data are presented as mean ± SEM.

Figure 3-6

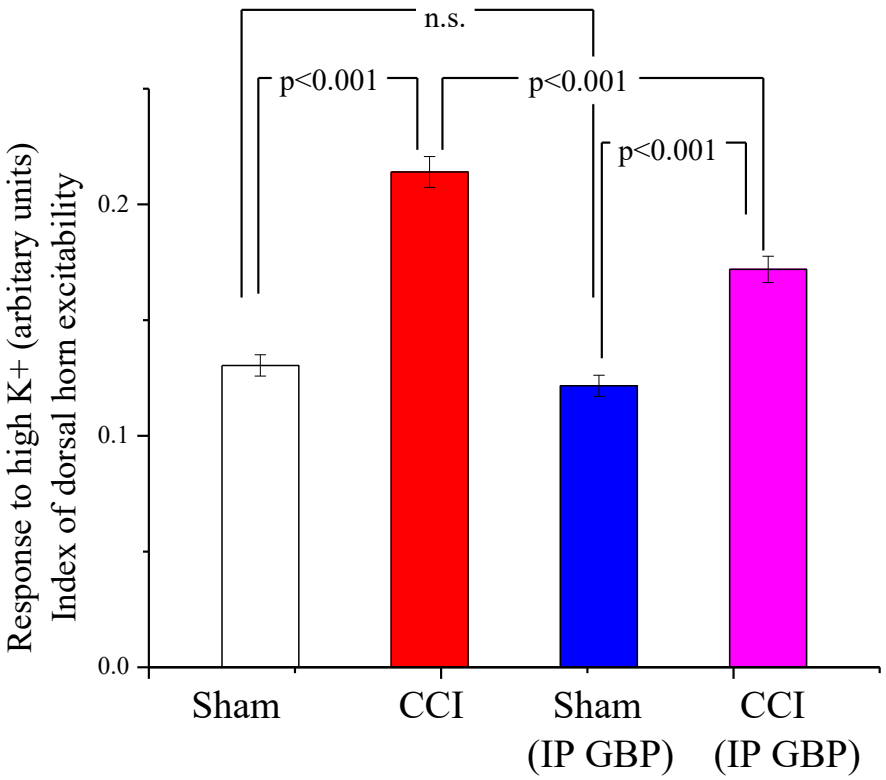

The effect of IP GBP injection on dorsal horn excitability in neuropathic CCI versus sham-operated rats. IP GBP reduces dorsal horn excitability in CCI, but not sham-operated rats. The dorsal horn excitability of CCI rats was higher than sham-operated rats. Controls for sham and CCI rats were injected with saline intraperitoneally. All experiments were performed blinded to the treatment of each rat until after analysis. CCI GBP, n = 12 slices, 107 cells; CCI (Saline Control), n = 8 slices, 80 cells; Sham GBP, n = 11 slices, 79 cells; Sham (Saline control) n = 10 slices, 105 cells. Statistically significant differences are indicated on the graph where $p<0.001$, one-way ANOVA with Bonferroni correction. All data are presented as mean ± SEM.

Figure 3-7

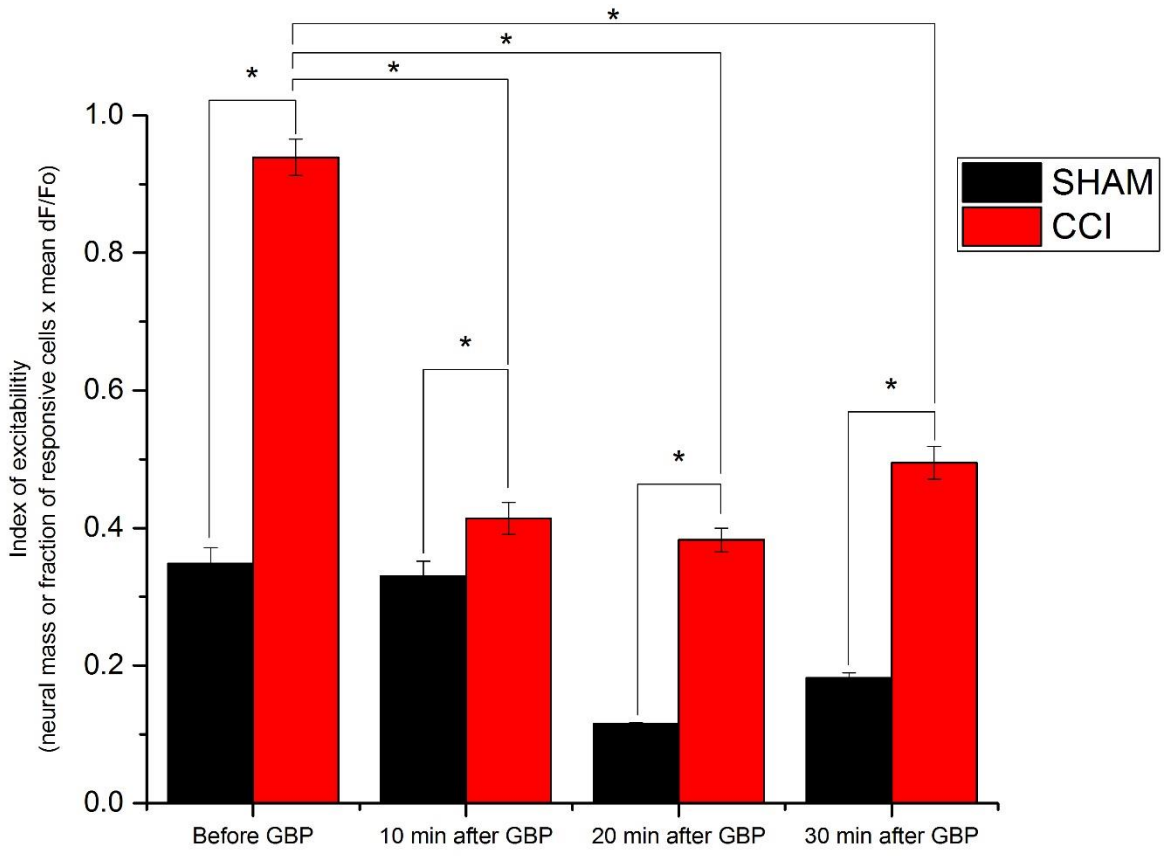

***In vivo* primary somatosensory cortical imaging in neuropathic CCI rats immediately following IP GBP.** 100 mg/kg intraperitoneal GBP injection reduced cortical excitability (neural mass) in neuropathic CCI (n=3 rats) within 10 min of injection, with no significant reduction observed in sham-operated rats (n=2 rats). A reduction in cortical excitability was observed in sham-operated rats at 20 min post-injection with no further reduction observed in neuropathic rats compared to 10 min post-injection. At 30 min post-injection there were no significant differences compared to at 20 min post-injection in cortical excitability of either CCI or sham-operated rats. *$p<0.05$, one-way ANOVA with Bonferroni correction. All data are presented as mean ± SEM.

CHAPTER 4

N.B. I carried out all nerve-injury surgeries, acute spinal cord slice preparations and electrophysiology experiments. Animal behavioural studies were performed by Nataliya Bukhanova.

Chapter 4: Dorsal horn neuronal-cell-type-specific acute actions of GBP

Introduction

Although the actions of GBP on dorsal horn neurons have been studied quite extensively (Moore et al., 2002, Patel et al., 2000, Zhou and Luo, 2014, Zhou and Luo, 2015), these studies did not address the possible differences in the effects of GBP on excitatory versus inhibitory neurons. Such studies are only now feasible in the light of recent advances in the understanding of spinal cord circuitry (Todd, 2010, Yasaka et al., 2010, Zeilhofer et al., 2012). The purpose of this chapter was to test the hypothesis that prior IP injection of GBP has differential effects on putative excitatory and inhibitory cell types in the *substantia gelatinosa* from *ex vivo* spinal cord slices. The relevance of the effects of prior IP GBP injection in neuropathic rats and sham-operated rats in the context of nociceptive processing and overall dorsal horn excitability are related to findings presented in Chapter 3.

The *substantia gelatinosa* or lamina II represents a population almost entirely of interneurons that is critical for processing of nociceptive information (Todd, 2010) and intrinsic electrophysiological changes of neurons in this region contribute to the pathophysiology of sciatic chronic constriction injury (Balasubramanyan et al., 2006). In an attempt to understand the acute anti-allodynic actions of IP GBP, acutely isolated spinal cord were be studied *ex vivo* from neuropathic or sham-operated animals that had received a prior IP injection of 100 mg/kg GBP or saline. Since I have established that GBP reduces overall dorsal horn excitability (Chapter 3), I hypothesize that prior IP GBP will inhibit synaptic transmission and reduce intrinsic excitability of *substantia gelatinosa* neuronal cell types from chronic-constriction injured neuropathic rats with no significant effects on sham-operated rats.

Neuronal cell types in the *substantia gelatinosa* of the dorsal horn were characterized on the basis of firing pattern using whole cell electrophysiology recording techniques. Delay, tonic, transient, phasic and irregular cell types were identified as in previous studies (Balasubramanyan et al., 2006, Punnakkal et al., 2014, Yasaka et al., 2010). Tonic cells possess an islet morphology and are mainly GABAergic inhibitory neurons, whereas delay neurons are mainly radial in morphology and are glutamatergic excitatory neurons (Yasaka et al., 2010). Transient neurons are most likely mainly excitatory as these cells require strong depolarising currents to fire a single AP (Punnakkal et al., 2014). Phasic cells are sometimes referred to as 'initial bursting' cells which are mainly GABAergic inhibitory neurons in the dorsal horn (Yasaka et al., 2010).

To assess whether prior IP GBP differentially affects *substantia gelatinosa* neuronal cell types, the effects of GBP on (1) frequency or amplitude of spontaneous and miniature excitatory post-synaptic currents (sEPSCs and mEPSCs) and (2) intrinsic excitability as assessed by AP firing in response to depolarising current ramps were examined. A differential effect of prior IP GBP on synaptic transmission and/or intrinsic excitability on putative excitatory and putative inhibitory *substantia gelatinosa* neurons in neuropathic and/or sham-operated rats would provide a cellular basis for the acute anti-allodynic actions of GBP.

Methods

The methods used in this chapter include chronic constriction injury (CCI) surgery, *ex vivo* acute spinal cord slice preparation, whole cell electrophysiology, Ca^{2+} imaging of *ex vivo* acute spinal cord slices and statistical analysis. These methods are described in detail in Chapter 2.

Results

Neuronal-cell types of the *Substantia Gelatinosa*

In order to study *substantia gelatinosa* cell types, it was first necessary to characterize them on the basis of previous findings in the literature. The neuronal cell types of the *substantia gelatinosa* characterized from my studies were (1) tonic neurons, which fire APs continuously in response to increasing depolarizing current and possess the lowest rheobase of the cell types (2) delay neurons, which fire with a distinct delay prior to AP discharge in response to a depolarizing current (3) transient neurons, which only fire a single AP discharge in response to a depolarizing current and possess the highest rheobase of the group (4) phasic neurons, which fire three or four APs in response to depolarization, followed by accommodation and cessation of firing and (5) irregular neurons, which show no clear relationship between AP discharge pattern or frequency and the intensity of depolarization. Typical recordings from these five cell types are shown in Figure 4-1 (inset shows the relative numbers of each neuronal phenotype based on 122 recordings). As shown from Figure 4-1 (inset) approximately 36% of neurons were tonic, 27% were delay, 20% were transient, 12% were phasic and 4% were irregular. This characterization is consistent with that of Balasubramanyan et al, 2006, Yasaka et al, 2010 and Punnakkal et al, 2014.

GBP has preferential effects on sEPSCs recorded from putative excitatory versus inhibitory neurons in the dorsal horn of neuropathic rats

To test the hypothesis that prior IP GBP has differential effects on spontaneous synaptic transmission of *substantia gelatinosa* neurons in neuropathic rats, the frequency and amplitude of

sEPSC events for each neuronal cell type from GBP-injected and saline-injected CCI rats will be compared.

In *substantia gelatinosa*, spontaneous EPSCs measured represent the excitatory post-synaptic current produced in response to spontaneous glutamate release from primary afferent nerve terminals and/or from excitatory interneurons (Santos et al., 2007). A sample sEPSC recording from a *substantia gelatinosa* neuron is shown in Figure 4-2A and a typical event is characterized by a sharp onset and a slow offset as shown in Figure 4-2C. The frequency and amplitude of sEPSC events provides a measure of neuronal spontaneous activity and the effect of GBP on these factors determine its effect on synaptic transmission. In order to help understand the acute anti-allodynic actions of IP GBP, I investigated the electrophysiological effects of prior IP GBP on spontaneous synaptic transmission of *substantia gelatinosa* neurons.

These results show that neuropathic animals that had received IP GBP exhibited specific effects on synaptic transmission on delay and tonic firing neurons (Figure 4-3). Cumulative probability plots demonstrate a significant reduction in the frequency ($p<0.05$, K-S test, Figure 4-3A, increase in inter-event interval) and amplitude ($p<0.05$, K-S test, Figure 4-3B) of sEPSCs in putative excitatory delay neurons in neuropathic animals that had received GBP compared to saline. This is confirmed by a significant decrease in the average sEPSC frequency (Figure 4-3A, inset, $p<0.05$, one-way ANOVA) and average sEPSC amplitude (Figure 4-3B, inset, $p<0.05$, one-way ANOVA) in delay neurons of GBP-injected rats compared to controls.

By contrast, in putative inhibitory tonic neurons, cumulative probability plots show that GBP increases the frequency ($p<0.05$, K-S test, Figure 4-3C, decrease in inter-event interval) of sEPSCs but that there was no significant effect on amplitude ($p>0.05$, K-S test, Figure 4-3D). This is confirmed by a significant increase in the average sEPSC frequency (Figure 4-3C, inset, $p<0.05$,

one-way ANOVA), but no significant effect on average sEPSC amplitude (Figure 4-3D, inset, $p>0.05$, one-way ANOVA) in tonic neurons of GBP-injected rats compared to controls. However, the amplitude of small sEPSC events of 22.5 pA or below from tonic neurons of CCI rats that had received IP GBP shows a statistically significant increase in amplitude compared to those that had received saline (Figure 4-3D Inset; saline: 10 neurons, 202 events, GBP: 11 neurons, 351 events; $p<0.05$, K-S test). Table 4-1 provides a summary of these findings.

GBP has preferential effects on mEPSCs recorded from putative excitatory versus inhibitory neurons in the dorsal horn of neuropathic rats

To determine whether IP GBP was affecting the neurotransmitter release process independent of depolarization-induced Ca^{2+} influx in *substantia gelatinosa* neurons, the frequency and amplitude of mEPSC events for each neuronal cell type from GBP-injected and saline-injected CCI rats were compared.

Miniature EPSCs (mEPSCs) represent sEPSCs recorded in the presence of tetrodotoxin (TTX), which blocks AP firing (by blocking Na^{+} channels), and these provide information on depolarization/Ca^{2+}-independent neurotransmitter release (Edwards et al., 1990). A sample mEPSC recording from a *substantia gelatinosa* neuron is shown in Figure 4-2B. The frequency and amplitude of mEPSCs were examined to explore any effects of IP GBP on the neurotransmitter release process in CCI compared to sham-operated rats.

To determine whether IP GBP was affecting the neurotransmitter release process independent of depolarization-induced Ca^{2+} influx, mEPSCs were recorded from the dorsal horn.

For delay neurons, Figure 4-4 shows that the effects of GBP are similar to those on sEPSCs shown in Figure 4-3. Cumulative probability plots demonstrate a significant reduction in the frequency ($p<0.05$, K-S test, Figure 4-4A, increase in inter-event interval) and amplitude ($p<0.05$, K-S test, Figure 4-4B) of mEPSCs in putative excitatory delay neurons in neuropathic animals that had received GBP compared to saline. This is confirmed by a significant decrease in the average mEPSC frequency (Figure 4-4A, inset, $p<0.05$, one-way ANOVA) and average mEPSC amplitude (Figure 4-4B, inset, $p<0.05$, one-way ANOVA) in delay neurons of GBP-injected rats compared to controls.

In tonic neurons, however, cumulative probability plots show that GBP has no significant effect on frequency ($p>0.05$, K-S test, Figure 4-4C) of mEPSCs but a significant increase in amplitude ($p<0.05$, K-S test, Figure 4-4D). This is confirmed by no significant effect on average mEPSC frequency (Figure 4-4C, inset, $p>0.05$, one-way ANOVA), but a significant increase of average mEPSC amplitude (Figure 4-4D, inset, $p<0.05$, one-way ANOVA) in tonic neurons of GBP-injected rats compared to controls.

Further analysis of mEPSC amplitude using distribution histograms (5 pA bins) as shown in Figure 4-5 demonstrates that the effect of GBP to decrease amplitude of mEPSCs from delay neurons is not specific to events of a particular size (Figure 4-5A), whereas in tonic neurons (Figure 4-5B) GBP tends to increase amplitude of larger (>20 pA) events. Table 4-1 provides a summary of these findings.

Other dorsal horn neuronal-cell-type specific effects of GBP in neuropathic rats

Transient and phasic neurons were studied in attempts to further test the hypothesis that IP GBP produces differential effects on neuronal cell types in the *substantia gelatinosa* underlying its acute anti-allodynic actions.

Specific effects of IP GBP were also observed in phasic and transient cell types as shown in Figure 4-6. Cumulative probability plots show that transient neurons from GBP-injected animals exhibited a significantly decreased sEPSC frequency (Figure 4-6A, $p<0.05$, K-S test, increase in inter-event interval) and decreased amplitude (Figure 4-6B, $p<0.05$, K-S test) compared to saline-injected controls. This is confirmed by a significant decrease in the average sEPSC frequency (Figure 4-6A, inset, $p<0.05$, one-way ANOVA) and average sEPSC amplitude (Figure 4-6B, inset, $p<0.05$, one-way ANOVA) in transient neurons of GBP-injected rats compared to controls.

With regards to phasic neurons, sEPSC amplitude was increased in GBP-injected animals, but there was no significant effect on frequency. Cumulative probability plots show that phasic neurons from GBP-injected animals exhibited no significant effect on sEPSC frequency (Figure 4-6C, $p>0.05$, K-S test) and a significant increase in amplitude (Figure 4-6D, $p<0.05$, K-S test) compared to saline-injected controls. This is confirmed by no significant effect on average sEPSC frequency (Figure 4-6C, inset, $p<0.05$, one-way ANOVA) and a significant increase in average sEPSC amplitude (Figure 4-6D, inset, $p<0.05$, one-way ANOVA) in phasic neurons of GBP-injected rats compared to controls. Table 4-1 provides a summary of these findings.

Combined sEPSC analysis of *substantia gelatinosa* cell types

In order to test the hypothesis that prior IP GBP affected putative inhibitory and excitatory neuronal cell types differentially in the *substantia gelatinosa*, I assumed based on findings in the literature that most transient neurons were excitatory (Punnakkal et al., 2014) and most phasic neurons were inhibitory (Heinke et al., 2004) and pooled these results with those from putative excitatory delay and putative inhibitory tonic neurons.

A pattern of effects shown in Figure 4-7 was observed. Cumulative probability plots show a significant decrease in sEPSC frequency (Figure 4-7A, $p<0.05$, K-S test) and amplitude (Figure 4-7B, $p<0.05$, K-S test) in delay & transient neurons and an increase in sEPSC frequency (Figure 4-7C, $p<0.05$, K-S test) and amplitude (Figure 4-7D $p<0.05$, K-S test) in tonic & phasic neurons. These results are confirmed by a significant decrease in average sEPSC frequency (Figure 4-7A, inset, $p<0.05$, one-way ANOVA) and a significant decrease in average sEPSC amplitude (Figure 4-7B, inset, $p<0.05$, one-way ANOVA) in delay and transient neurons of GBP-injected rats. In the case of tonic and phasic neurons, the results on sEPSC frequency are confirmed by a significant increase in average sEPSC frequency (Figure 4-7C, $p<0.05$, one-way ANOVA), but not in the case of average amplitude where no significant effect is observed (Figure 4-7D, $p>0.05$, one-way ANOVA). Table 4-1 provides a summary of these findings.

Effect of GBP on mEPSCs recorded from transient and phasic neurons of neuropathic rats

To further test the hypothesis that IP GBP produces differential effects on the neurotransmitter release process of *substantia gelatinosa* neuronal cell types, I determined GBP's effects on

mEPSC events from transient and phasic neurons As described earlier, mEPSCs provide information on depolarization/Ca^{2+}-independent neurotransmitter release.

mEPSCs recorded from transient and phasic neurons, as shown in Figure 4-8, cumulative probability plots do not show a significant effect in either cell type on mEPSC inter-event interval (Figure 4-8A/C, $p>0.05$, K-S test) or amplitude (Figure 4-8B/D, $p>0.05$, K-S test). However, if we compare average mEPSC inter-event interval in transient neurons, GBP causes a significant decrease in frequency (Figure 4-8A, inset, $p<0.05$, one-way ANOVA) and a significant decrease in amplitude (Figure 4-8B, inset, $p<0.05$, one-way ANOVA). For phasic neurons, GBP does not cause a significant effect on average mEPSC inter-event interval, but does cause an increase in mEPSC amplitude (Figure 4-8D, $p<0.05$, one-way ANOVA). Table 4-1 provides a summary of these findings.

GBP exerts only depressant effects on neurons from sham-operated animals

To test the hypothesis that prior IP GBP would only exert an effect on synaptic transmission in the *substantia gelatinosa* of neuropathic but not sham-operated rats, the sEPSC frequency and amplitude of *substantia gelatinosa* neurons from GBP-injected and saline-injected sham-operated animals was examined. The procedure for sham-surgery is described in detail in Chapter 2.

By contrast with results from neuropathic animals, IP GBP in sham-operated animals produced only depressant effects on individual cell types (i.e. decrease in either amplitude or frequency). Cumulative probability plots shows that in sham-operated rats there was a significant reduction in sEPSC amplitude (Figure 4-9B, $p<0.05$, K-S test), but not frequency (Figure 4-9A, $p>0.05$, K-S test) in delay neurons and a reduction in sEPSC frequency (Figure 4-9C, $p<0.05$, K-S test), but not

amplitude (Figure 4-9D, $p>0.05$, K-S test) in tonic neurons with IP GBP. These results were confirmed by the effect of GBP on average sEPSC inter-event interval (Figure 4-9A/C, insets) and amplitude (Figure 4-9B/D, insets).

The effects of IP GBP on sEPSCs in sham rats from transient and phasic neurons, as shown by cumulative probability plots, are to decrease amplitude (Figure 4-10B/D, $p<0.05$, K-S test) with no effects on frequency (Figure 4-10A/C, $p>0.05$, one-way ANOVA). This is supported in all but one case by average sEPSC interevent interval and amplitudes (Figure 4-10B/C/D insets), except in the case of average sEPSC frequency from transient neurons where GBP results in an increase compared to controls (Figure 4-10, insets, $p<0.05$, one-way ANOVA).

Effect of GBP on excitability of putative excitatory and inhibitory neurons in neuropathic and sham rats

The purpose of these experiments was to determine whether IP GBP produces differential effects on the intrinsic neuronal excitability of putative excitatory delay and putative inhibitory tonic neurons of *substantia gelatinosa* neurons in neuropathic rats. To test the hypothesis that IP GBP will produce differential effects on *substantia gelatinosa* neurons in neuropathic rats but not sham-operated rats, the intrinsic excitability of putative excitatory delay and inhibitory tonic neurons from sham-operated will be examined as well. By studying AP firing frequency and latency in response to current ramps (steadily increasing depolarizing current injection), I investigated the effects of prior IP GBP injection on the intrinsic excitability of delay and tonic neurons.

For the purpose of these studies only putative excitatory delay and putative inhibitory delay neurons were studied in neuropathic and sham-operated animals that had received IP GBP or

saline. Figure 4-11 shows a typical response of delay and tonic firing neurons to a 133pAs^{-1} depolarising current ramp injection. The time from the start of the current ramp to each AP spike was added cumulatively to obtain the cumulative latency and this was plotted against AP spike number as shown in Figure 4-12. Current ramps were delivered at 33, 67, 100 or 133 pAs^{-1}. Only the 133 pAs^{-1} was used in analysis as this provided more discharge pattern data for comparison between cell types.

After comparison it is observed that IP GBP only had an effect on putative excitatory delay firing neurons in neuropathic CCI animals, whereby the cumulative latency for action potential spike numbers 5-9 was significantly increased (Figure 4-12A, right, $p<0.05$, one-way ANOVA). No significant effect was observed on intrinsic excitability of tonic neurons (Figure 4-12A, $p>0.05$, one-way ANOVA) from neuropathic rats. There was no significant effect of IP GBP on the intrinsic excitability of delay (Figure 4-12B, right, $p>0.05$, one-way ANOVA) or tonic neurons (Figure 4-12B, left, $p>0.05$, one-way ANOVA) from sham animals. A summary of these findings is shown in Table 4-1.

Discussion

It is important to consider the neuronal phenotype from which a recording is made as an increased excitatory drive to an inhibitory neuron could translate to a net decrease in excitability. In terms of the effect on pain physiology, this is very important for establishing whether a drug has efficacy as a therapeutic for treatment.

Tonic cells mainly possess an islet morphology and are likely to be GABAergic inhibitory neurons, whereas delay cells largely possess a radial morphology and are mainly glutamatergic excitatory

interneurons and cells with a vertical or central morphology are either excitatory or inhibitory, with most excitatory cells having larger dendritic trees (Yasaka et al., 2010). It has been shown using vGluT2::eGFP and Gad-67::eGFP transgenic mice, that vGluT2 (vesicular glutamate transporter)-positive excitatory neurons require stronger depolarising currents to fire APs and fire fewer APs than GAD-67 (glutamic-acid-decarboxylase)-positive inhibitory neurons (Punnakkal et al., 2014). This supports most delay and transient neurons as being excitatory as these neurons require stronger depolarisations to fire (Figure 4-1). Transient neurons, on account of their high rheobase, are most likely excitatory (Punnakkal et al., 2014). Phasic cells are most likely a mixed population of both excitatory and inhibitory neurons (Ruscheweyh and Sandkuhler, 2002). However, a more recent paper by Heinke et al using a transgenic GAD-GFP mouse suggests that some of the presumed GABAergic cells display a phasic (initial bursting) firing pattern (Heinke et al., 2004) and another study has shown that initial bursting cells in the spinal dorsal horn are mainly inhibitory (Yasaka et al., 2010).

From these results, we see that in neuropathic animals IP GBP decreases excitatory drive to excitatory neurons (delay and transient) and increases excitatory drive to inhibitory neurons (tonic and phasic). In contrast in sham-operated animals, a depressant effect is observed across all *substantia gelatinosa* cell types. We do not know precisely how many connections each individual neuron makes or what the synaptic strength of each of these connections would be, so we cannot claim to know the net effect of these results in isolation. However, data in support of a net decrease in dorsal horn excitability from GBP-injected neuropathic animals shown in Figure 3-6, suggests that that inhibition due to IP GBP produces the dominant effect on dorsal horn excitability.

Acute effects of GBP

These results are in contrast to several studies where no acute effect of GBP is reported in an *in vitro* setting. Perhaps the most directly related to these results are those of Moore et al, who have reported no significant effect of acute bath application of 100 μM GBP on sEPSCs or inhibitory postsynaptic currents (IPSCs) recorded from naïve superficial dorsal horn neurons of the *substantia gelatinosa* (Moore et al., 2002). The study did however, report that evoked NMDA-receptor-mediated EPSCs and IPSCs were variably affected by GBP, possibly due to differences in synaptic and extrasynaptic NMDA receptor subunit composition. It is important to note that unlike Moore et al, my experiments were carried out on animals that were neuropathic or sham-operated and GBP was delivered via systemic injection prior to whole-cell recording. As will be addressed in Chapter 5, nerve-injury as well as the method of delivery may influence the effectiveness of acute GBP.

More recent studies that have been carried out on allodynic animals have reported similar findings. For example, GBP has been shown to block the increased mEPSC frequency observed in superficial and deep dorsal horn neurons from spinal nerve-ligated and α2δ-upregulated allodynic rats (Zhou and Luo, 2015, Zhou and Luo, 2014).

Several reports suggest a lack of acute effectiveness of the gabapentinoids on dorsal root ganglia as discussed in Chapter 1, however these studies were again not carried out on neuropathic animals (Biggs et al., 2014, Heblich et al., 2008, Hendrich et al., 2012, Hendrich et al., 2008).

Excitatory versus inhibitory neurons of the substantia gelatinosa

To date, no studies have addressed the effect of IP GBP on putative excitatory versus putative inhibitory cell types in the *substantia gelatinosa*. There are some studies that have addressed excitatory post-synaptic currents (glutamate-mediated) versus inhibitory post-synaptic currents (GABA-mediated) in the brain and spinal cord without a reference to the neuronal phenotype (excitatory or inhibitory) from which recordings were made (Takasu et al., 2008, Zhou and Luo, 2014).

With regards to the unexpected increase in excitatory drive to putative inhibitory tonic neurons of CCI rats with GBP, it is possible that GBP causes a disinhibition whereby tonic neurons synapse on to excitatory projection neurons so that the net result would be a reduction in nociceptive stimuli to higher brain centres and a reduction in pain. GBP has been shown to increase glutamate release via astroglial GLT-1 (glutamate-transporter-1)-dependent mechanisms, however this was in the locus coeruleus, which sends descending noradrenergic inhibition to the spinal cord to reduce pain (see Figure 6-3) (Suto et al., 2014). It could perhaps be argued that more astrocytes expressing GLT-1 are found in the vicinity of inhibitory neurons compared to excitatory neurons. This effect of GBP involving GLT-1 would explain the preferential increase of sEPSCs at excitatory synapses. This however, does not seem to be the case as GBP preferentially increased the amplitude of larger (>20 pA) mEPSCs in tonic neurons (Figure 4-5B). If GBP action depended on GLT-1 inhibition, all sizes of mEPSCs would be increased in amplitude.

Most tonic neurons in the *substantia gelatinosa* are GABAergic (Cui et al., 2011, Yasaka et al., 2010), so an increase in excitatory synaptic drive to these neurons from GBP-injected neuropathic rats suggests that GBP increases release of GABA in the dorsal horn. In support of this it has been shown that GABA levels are significantly increased in microdialysates from the spinal dorsal horn

of nerve-injured rats within 60 min of 10 mg/kg intravenous GBP injection (Yoshizumi et al., 2012).

We see a decrease in both sEPSC frequency and amplitude (quantal size) with prior IP GBP injection on putative excitatory delay neurons, but in putative inhibitory tonic neurons sEPSC frequency is increased. The effects on putative excitatory neurons are consistent with those of Biggs et al where long-term gabapentinoid exposure was shown to produce a decrease in the sEPSC amplitude in high-threshold putative excitatory *substantia gelatinosa* neurons, however this was with 5-6 day treatment with 10 μM pregabalin in spinal cord cultures (Biggs et al., 2014).

Nerve injury and acute effects of GBP

Results from CCI and sham-operated rats show clear differences in terms of the acute effects of GBP. For example, in the case of delay neurons from CCI rats, there is a significant decrease in sEPSC frequency (Figure 4-3A) whereas in sham rats there is no significant difference in frequency (Figure 4-9A). This leads to the suggestion that an effect of GBP on putative excitatory delay neuron sEPSC frequency is an α2δ-mediated effect since it is well known that α2δ-levels are upregulated following CCI in the DRG (Luo et al., 2002). Perhaps GBP has selectivity for α2δ-upregulated-DRG neurons that primarily synapse on to delay neurons of the dorsal horn in the case of CCI, but not sham-operated rat. This would make sense in terms of a pre-synaptic effect on sEPSC frequency in CCI delay neurons, but not in sham delay neurons.

The effect of GBP on delay neuron sEPSC amplitude in both CCI (Figure 4-3B) and sham rats (Figure 4-9B) may be explained by GBP causing neurons to become less sensitive to glutamate. This is supported by the observation with delay neurons where GBP causes a decrease across all

mEPSC event size categories (Figure 4-5A). This suggests that GBP may have some activity at glutamate receptors, although virtually all glutamatergic synapses in the adult superficial dorsal horn possess AMPA receptors (Yasaka et al., 2009) and only acute effects of GBP via NMDA receptors have been demonstrated (Singh et al., 2013).

The effect of GBP on delay neuron sEPSC amplitude compared to the lack of effect on tonic neuron sEPSC amplitude in both CCI and sham rats may be explained by differences in the expression of glutamate-receptor subtypes between tonic and delay neurons. Indeed, it has been shown that GluA2-lacking-Ca^{2+}-permeable-AMPA-receptors (CP-AMPARs) were associated with many GABAergic neurons but absent from some but not all putative excitatory neurons (Albuquerque et al., 1999). Another study has shown that GluA2/3 receptors associates with non-GABAergic neurons, but not with GABAergic neurons (Kerr et al., 1998).

As mentioned previously GBP may increase tonic sEPSC frequency from CCI rats in a process of disinhibition to reduce transmission of nociceptive information to higher brain centres (Figure 4-3C). However, the effects of GBP on tonic sEPSCs from sham-operated rats appear to be largely depressant as shown by either a decrease in amplitude or frequency (Figure 4-9C/D) which suggests that GBP may activate or depress different nociceptive pathways in the spinal dorsal horn under neuropathic conditions.

mEPSCs and the neurotransmitter release machinery

The neuronal SNARE (soluble N-ethylmaleimide-sensitive-factor attachment protein receptor) synaptotagmin-1 (Syt1) sets the frequency of miniature spontaneous events (Zhou et al., 2015). The effect of GBP on mEPSC frequency in delay neurons suggests that GBP may affect the release

machinery. It is well known that GBP binds the α2δ subunit of the voltage-gated calcium channel (Gee et al., 1996). In addition, there is evidence to show that α2δ is a multifunctional protein that sets release probability in central synapses (Hoppa et al., 2012). Therefore, it is possible that GBP mediates its acute effect on mEPSC frequency via binding to the α2δ protein, which interacts with the release machinery to alter neurotransmitter release. This mechanism of action will be investigated in Chapter 5.

The effects of IP GBP on tonic neuron mEPSCs from CCI rats (Figure 4-4D) may correspond to small (<22.5 pA) sEPSC events in Figure 4-3D. Amplitude of mEPSCs is increased and although this does not correspond to the overall lack of effect of IP GBP on sEPSC amplitude (Figure 4-3D) it may correspond to the significant increase in the amplitude of small (<22.5 pA) sEPSC events. This may further imply that the population of small (<22.5 pA) sEPSC events seen in Figure 4-3D are actually mEPSCs. In the case of inter-event interval, mEPSCs from tonic neurons are unaffected. Table 4-1 provides a summary of these findings.

It was shown that the effect of GBP on mEPSCs from tonic neurons is to decrease amplitude of smaller (<20 pA) events and to increase amplitude of larger (>20 pA) events (Figure 4-5B) whereas for delay neurons mEPSCs of all sizes were affected by GBP (Figure 4-5A). An effect on mEPSC amplitude is considered to be a largely post-synaptic effect (Verstreken and Bellen, 2001). Therefore, the explanation for this may be that for delay neurons, GBP may be causing neurons to become less sensitive post-synaptically to glutamate (so that inward currents mediated by glutamate receptors generate smaller amplitude currents) perhaps through an action of GBP on glutamate receptors, which in laminae I-III of the dorsal horn are mainly AMPA receptors (Polgar et al., 2008). Tonic neurons that exhibit smaller mEPSCs may have different properties from tonic neurons that exhibit larger mEPSCs. One difference may be due to the expression of CP-AMPARs

which are largely present on tonic inhibitory neurons and not delay excitatory neurons (Albuquerque et al., 1999, Kerr et al., 1998). The differential expression of CP-AMPARs across tonic neurons may influence the susceptibility of these neurons to a post-synaptic effect of GBP on large compared to small mEPSC events.

Instrinsic Excitability of Postsynaptic Neurons in Substantia Gelatinosa

The data presented in Figure 4-9 suggests that IP GBP has a preferential effect on the excitability of delay putative excitatory neurons whereby cumulative latency to firing to increased. These results suggest that delay neurons, which are mostly excitatory (Balasubramanyan et al., 2006, Punnakkal et al., 2014), will fire with an increased latency at higher potentials in the presence of GBP. However, we do not know whether this translates directly to an effect on overall excitability because again we are not aware of the exact number or strength of synaptic connections made by these neurons.

This effect of IP GBP on neuronal firing has several possible explanations. Activation of Ca^{2+}-dependent K^+-channels (K_{Ca}) have been found to increase interspike intervals in response to sustained membrane depolarisation in rat *substantia gelatinosa* neurons, but this result was only seen in tonic-firing neurons by applying blockers of K_{Ca} channels such as Mn^{2+} (Melnick et al., 2004). Since GBP does not appear to affect tonic neuron firing, this suggests that K_{Ca} channels are not involved in the mechanism of action of acute GBP.

Another possibility is that GBP has an effect on T-type Ca^{2+} channels, which are known to play a role in regulating neuronal firing and excitability as these open and elicit depolarisation near resting membrane potentials (Zamponi et al., 2015). It has been shown that although the α2δ

subunit is not required for expression of T-type channels, their expression may be enhanced by the presence of auxiliary subunits such as α2δ (Dolphin et al., 1999, Dubel et al., 2004, Zamponi et al., 2015). It is possible that in a nerve-injury situation, where α2δ levels are elevated (Li et al., 2006, Luo et al., 2001), T-type channel expression is enhanced and this may contribute to increased AP firing frequency and decreased latency. Therefore, in the presence of GBP, a ligand of α2δ, perhaps T-type expression and/or function is reduced, which results in increased latency and decreased AP firing.

The hyperpolarisation-activated cyclic nucleotide-gated cation channel (HCN) channels are also another potential target of GBP. Studies have shown that the HCN channel blocker, ivabradine, produces a weak effect on I_h in the DRG and has efficacy as an anti-allodynic agent suggesting that HCN channels are involved in neuropathic pain (Noh et al., 2014, Young et al., 2014). It is also known that HCN channels have an important role in regulating neuronal excitability as they open at near resting membrane potentials and elicit depolarisation toward AP thresholds (Benarroch, 2013, He et al., 2014). Hence, it is possible that GBP mediates its effect on AP firing via an effect on pre-synaptic HCN channels. HCN channels are found on nerve terminals in the spinal dorsal horn, so an action of GBP here could contribute to changes in sEPSCs (Huang and Trussell, 2014, Takasu et al., 2010). In addition, unpublished data from our lab demonstrates that 100 μM GBP reduces I_h density in dorsal root ganglia cultures, which is again consistent with the possibility that HCN channels play a role in mediating GBP's acute anti-allodynic actions.

Of course, with the crucial role of voltage-gated Na^+ channels and K^+ channels in action potential generation and nociceptive processing (Waxman and Zamponi, 2014), these channels cannot be ruled out as potential targets of the acute effect of GBP on neuronal firing. Indeed, it has been shown that the rat brain sodium channel $Na_v1.2$ is inhibited by exposure to 30 μM GBP (albeit

long-term) (Liu et al., 2006) and that bath application of GBP (1-20 μM) inhibited persistent sodium current (I_{NaP}) in medium-sized DRG neurons from nerve-injured animals (Yang et al., 2009). Such a peripheral action may contribute to the effect of GBP on sEPSCs in delay neurons. There is also some suggestion of the involvement of K^+ channels in GBP's mechanism of action as pre-treatment with Ca^{2+}-activated-K^+ channel or ATP-sensitive-K^+-channel blockers prevented GBP-induced anti-allodynia (Mixcoatl-Zecuatl et al., 2004).

Figure 4-1

DELAY

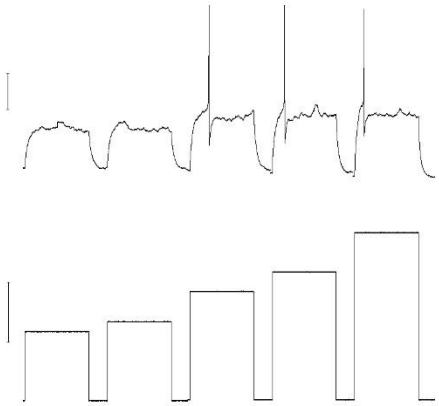

TONIC

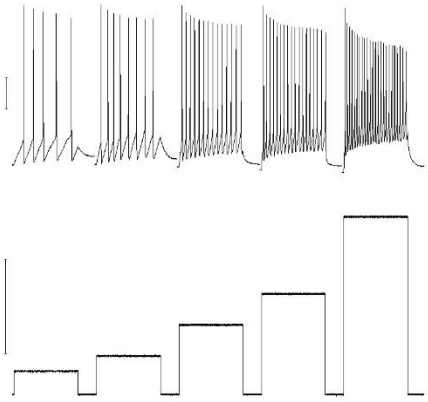

TRANSIENT

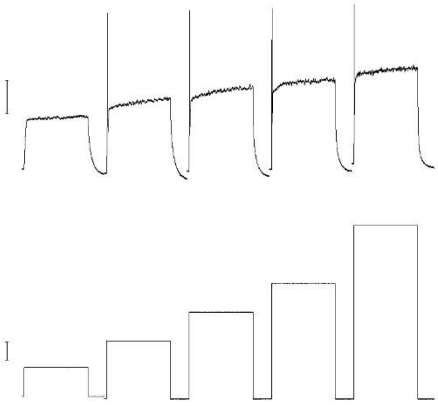

PHASIC

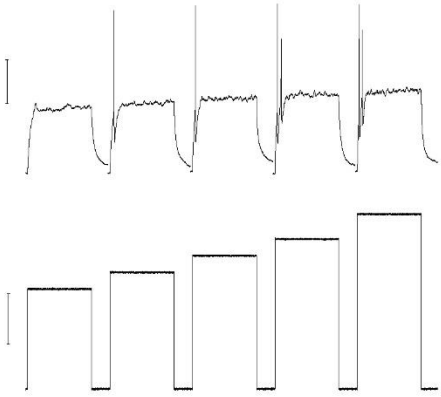

IRREGULAR

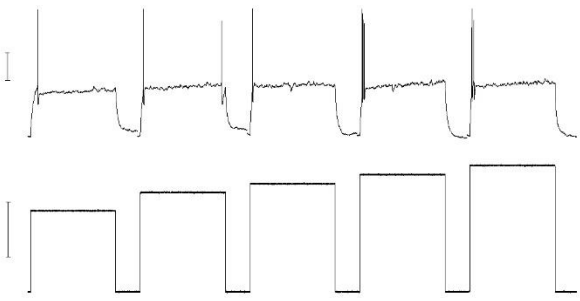

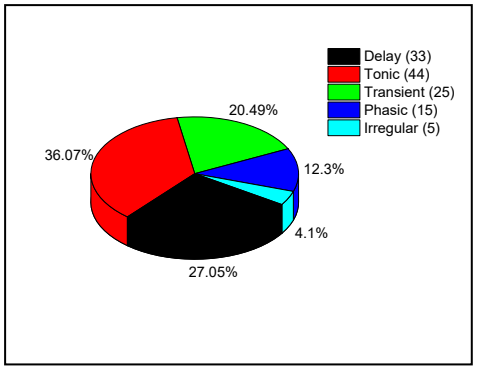

Figure 4-1. **Neuronal cell types of the *substantia gelatinosa* characterized on the basis of firing pattern.** Recordings of voltage in response to depolarising current steps are made in current clamp and neurons are held at -60 mV. Scale bar shown on the left of each set of recordings is 20 mV for voltage (top panel) and 30 pA for current (bottom panel) in each case. *(Inset)* The relative numbers of each neuronal cell type in the *substantia gelatinosa* based on 122 recordings for which a cell type could be determined. The number of each neuronal cell type is indicated in brackets.

Figure 4-2

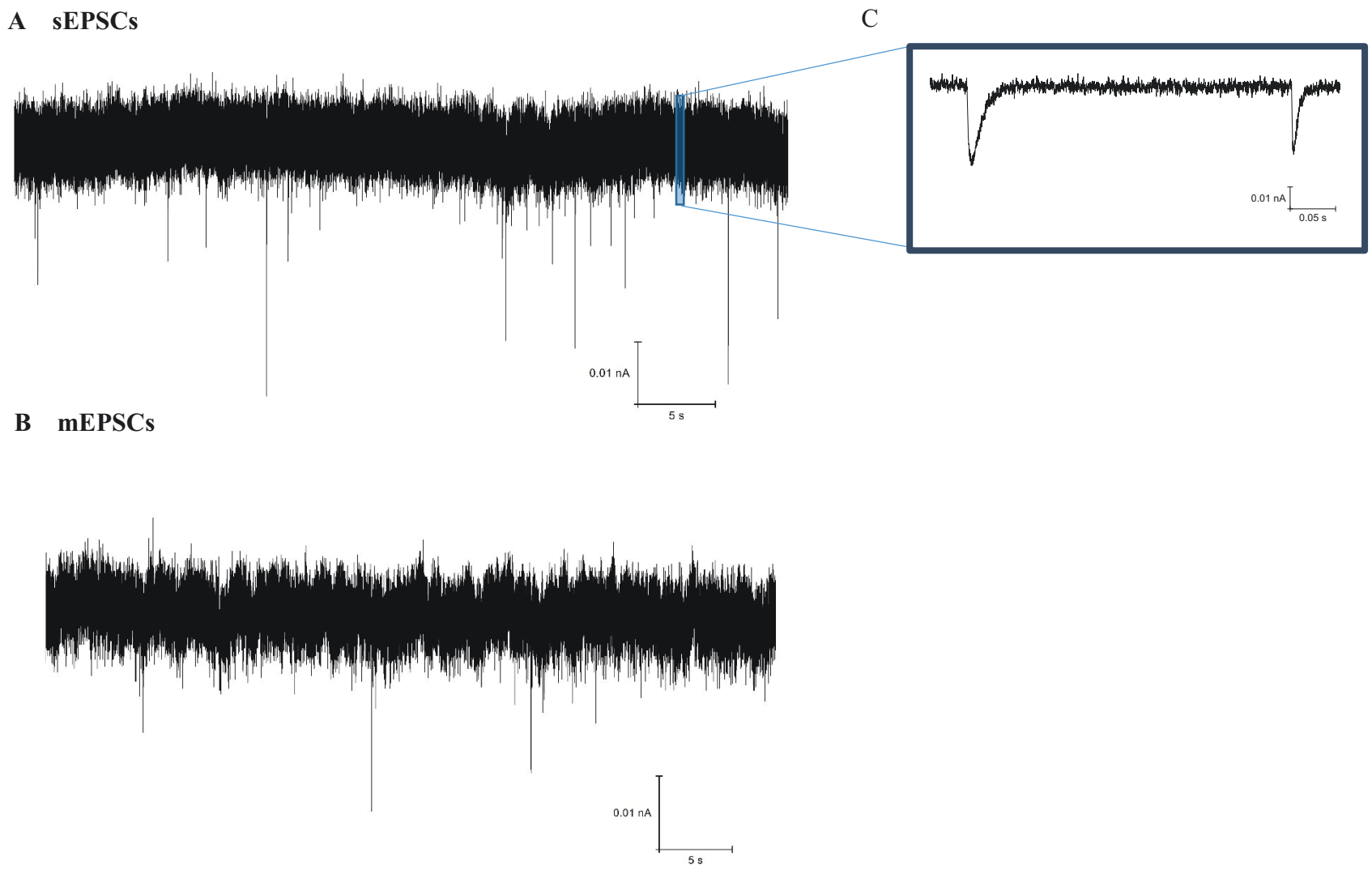

Figure 4-2. **Typical sEPSC and mEPSC recordings.** A. spontaneous excitatory post-synaptic current (sEPSC) recording and B. miniature excitatory post-synaptic current (mEPSC) recordings from a *substantia gelatinosa* neuron in voltage-clamp at -70 mV. C. mEPSCs are recorded in the presence of 10 μM tetrodotoxin (TTX). An example of an event from an sEPSC recording. Inter-event interval (i.e. inverse of frequency) and amplitude of these events was calculated after noise cancellation in MiniAnalysis. A 3 minute recording was obtained from each cell used in analysis.

Figure 4-3

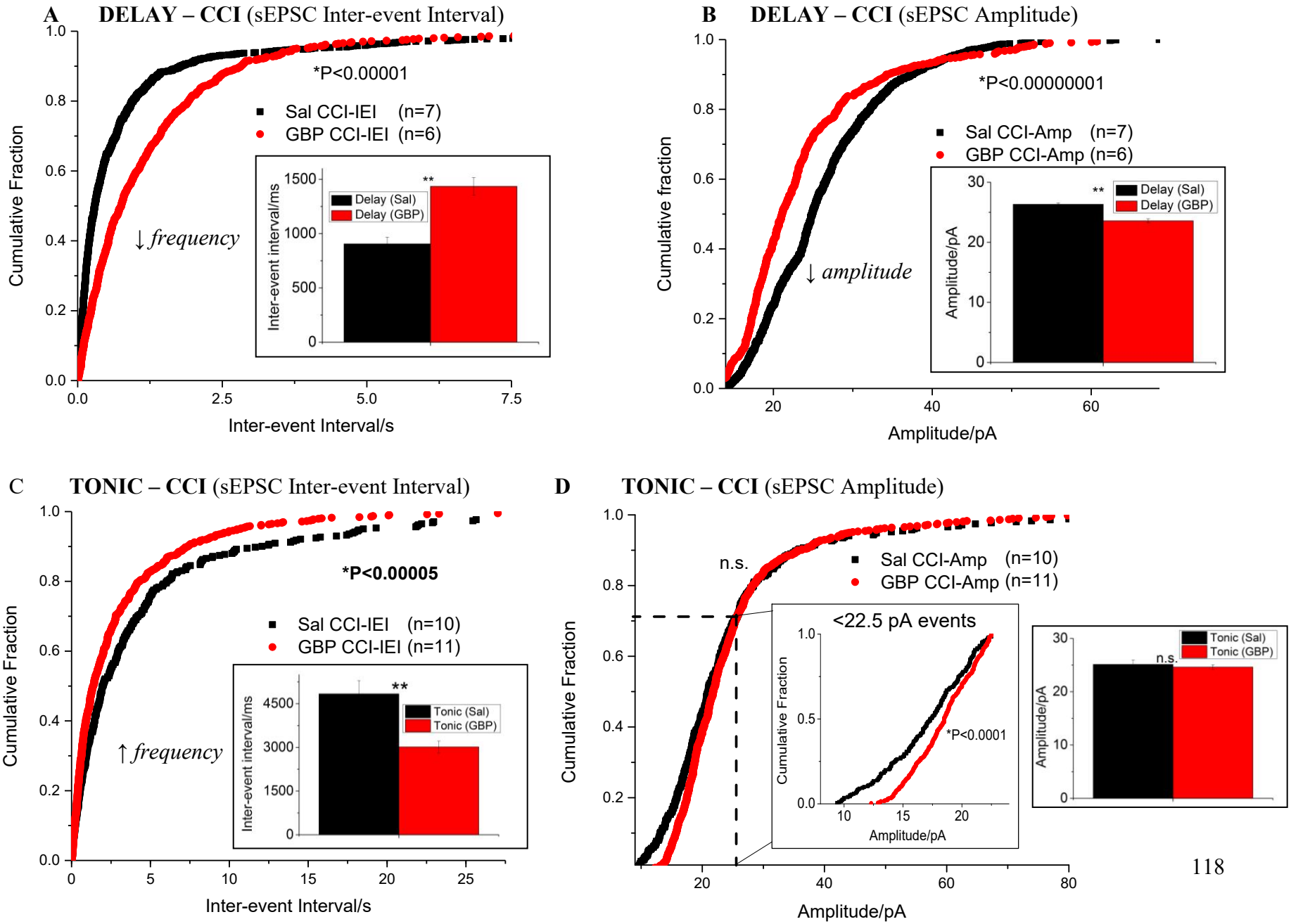
A
DELAY – CCI (sEPSC Inter-event Interval)
*P<0.00001
Sal CCI-IEI (n=7)
GBP CCI-IEI (n=6)
↓ frequency
Cumulative Fraction
Inter-event Interval/s
Inter-event interval/ms
Delay (Sal)
Delay (GBP)
**
B
DELAY – CCI (sEPSC Amplitude)
*P<0.00000001
Sal CCI-Amp (n=7)
GBP CCI-Amp (n=6)
↓ amplitude
Cumulative fraction
Amplitude/pA
C
TONIC – CCI (sEPSC Inter-event Interval)
*P<0.00005
Sal CCI-IEI (n=10)
GBP CCI-IEI (n=11)
↑ frequency
Tonic (Sal)
Tonic (GBP)
D
TONIC – CCI (sEPSC Amplitude)
n.s.
Sal CCI-Amp (n=10)
GBP CCI-Amp (n=11)
<22.5 pA events
*P<0.0001

Figure 4-3. **The effect of IP GBP on sEPSCs of delay and tonic neurons recorded from the dorsal horn of neuropathic CCI rats.** A. sEPSC inter-event interval of putative excitatory delay neurons (Inset) Average delay neuron sEPSC inter-event interval for saline versus GBP-injected rats. B. sEPSC amplitude of putative excitatory delay neurons (Inset) Average delay neuron sEPSC amplitude for saline versus GBP-injected rats. C. sEPSC inter-event interval of putative inhibitory tonic neurons (Inset) Average tonic neuron sEPSC inter-event interval for saline versus GBP-injected rats. D. sEPSC amplitude of putative inhibitory tonic neurons. (Inset, left) IP GBP increases the amplitude of 'lower-amplitude sEPSC events' (0.0225 nA or less) in tonic neurons of CCI rats. (Inset, right) Average tonic neuron sEPSC amplitude for saline versus GBP-injected rats. In each case, the red curve indicates IP GBP and black curve indicates IP saline. A shift to the right of the red compared to the black curve indicates an increase in the x-variable. Delay neurons (no. of events): Sal=1188 and GBP=753. Tonic neurons (no. of events): Sal=397 and GBP=636. No. of neurons indicated in brackets on plot. *Kolmogorov-Smirnov test, statistical significance if $p<0.05$. **One-way ANOVA with post-hoc Bonferonni correction, statistical significance if $p<0.05$.

Figure 4-4

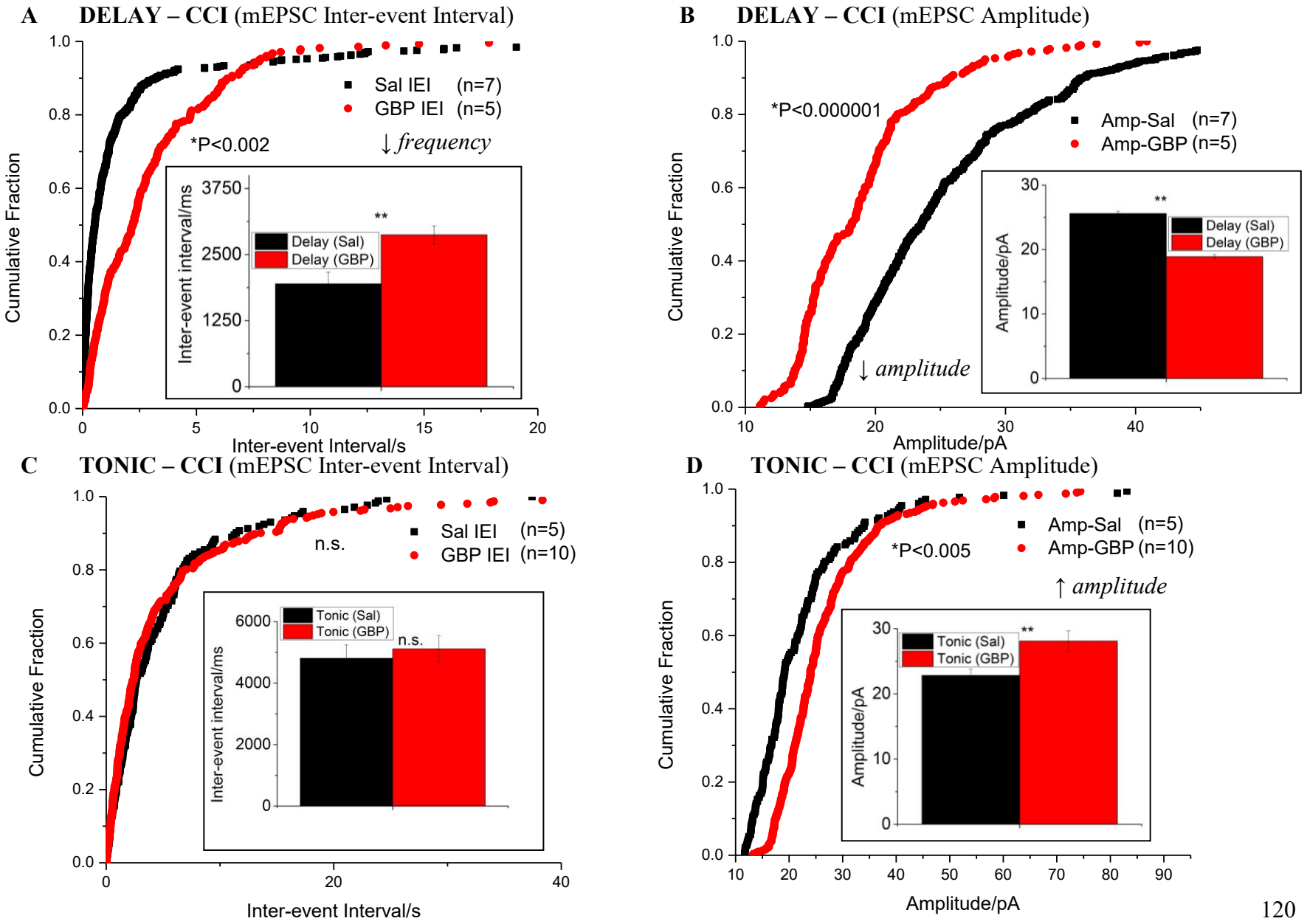
A DELAY – CCI (mEPSC Inter-event Interval)
Sal IEI (n=7)
GBP IEI (n=5)
*P<0.002
↓frequency
Cumulative Fraction
Inter-event Interval/s
Inter-event interval/ms
Delay (Sal)
Delay (GBP)
**
B DELAY – CCI (mEPSC Amplitude)
*P<0.000001
Amp-Sal (n=7)
Amp-GBP (n=5)
↓ amplitude
Amplitude/pA
C TONIC – CCI (mEPSC Inter-event Interval)
n.s.
Sal IEI (n=5)
GBP IEI (n=10)
Tonic (Sal)
Tonic (GBP)
D TONIC – CCI (mEPSC Amplitude)
*P<0.005
Amp-Sal (n=5)
Amp-GBP (n=10)
↑ amplitude

Figure 4-4. **The effect of IP GBP on mEPSCs of delay and tonic neurons recorded from the dorsal horn of neuropathic CCI rats.** A. mEPSC inter-event interval of putative excitatory delay neurons (Inset) Average delay neuron mEPSC inter-event interval for saline versus GBP-injected rats. B. mEPSC amplitude of putative excitatory delay neurons (Inset) Average delay neuron mEPSC amplitude for saline versus GBP-injected rats. C. mEPSC inter-event interval of putative inhibitory tonic neurons (Inset) Average tonic neuron mEPSC inter-event interval for saline versus GBP-injected rats. D. mEPSC amplitude of putative inhibitory tonic neurons. (Inset) Average tonic neuron mEPSC amplitude for saline versus GBP-injected rats. In each case, the red curve indicates IP GBP and black curve indicates IP saline. A shift to the right of the red compared to the black curve indicates an increase in the x-variable. Delay neurons (no. of events): Sal=580 and GBP=281. Tonic neurons (no. of events): Sal=172 and GBP=322. No. of neurons indicated in brackets on plot. *Kolmogorov-Smirnov test, statistical significance if $p<0.05$. **One-way ANOVA with post-hoc Bonferonni correction, statistical significance if $p<0.05$.

Figure 4-5

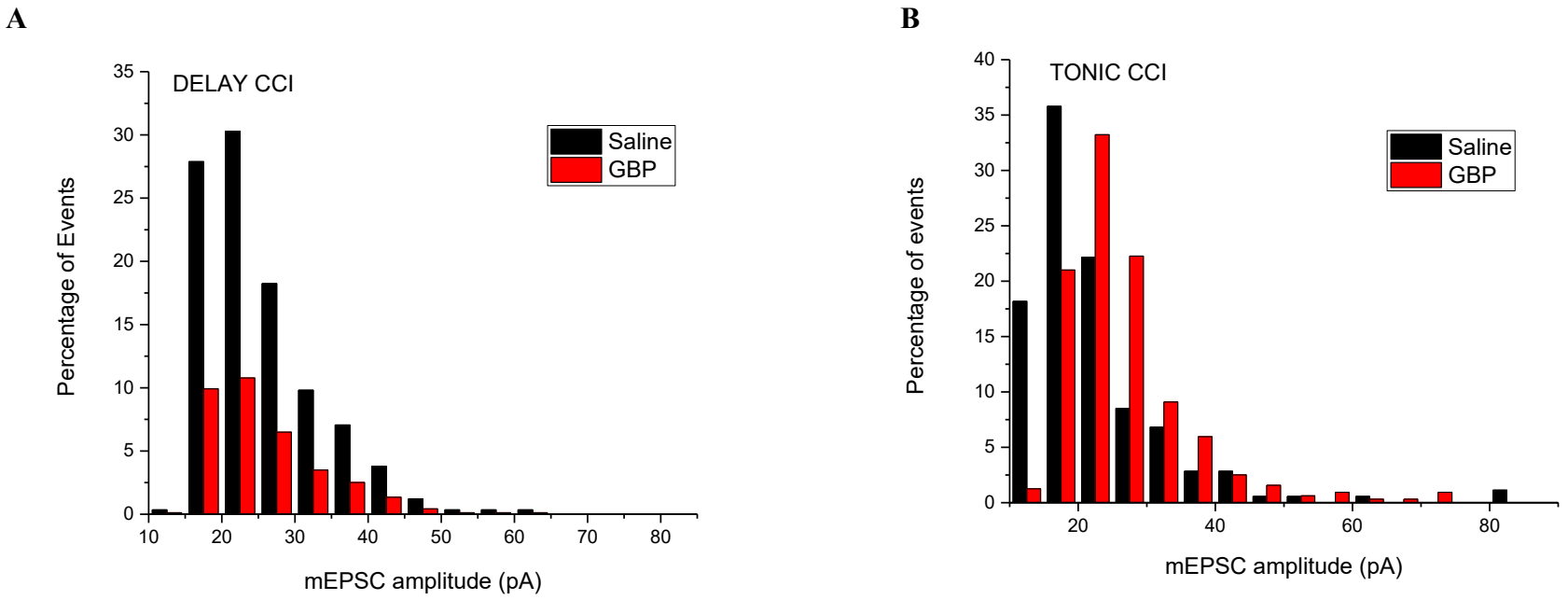

Figure 4-5. Analysis of the effects of GBP on mEPSC amplitude of delay and tonic neurons. A. Distribution histogram (5 pA bins) for amplitudes from delay neurons of 580 mEPSCs from saline-injected versus 281 mEPSCs from GBP-injected neuropathic CCI rats. The effect of GBP to decrease amplitude of mEPSCs from delay neurons is not specific to events of a particular size. **B.** Distribution histogram (5 pA bins) for amplitudes of 177 mEPSCs from tonic neurons of saline-injected versus 322 mEPSCs from GBP-injected neuropathic CCI rats. The effect of GBP on mEPSCs from tonic neurons is to decrease amplitude of smaller (<20 pA) events and to increase amplitude of larger (>20 pA) events.

Figure 4-6

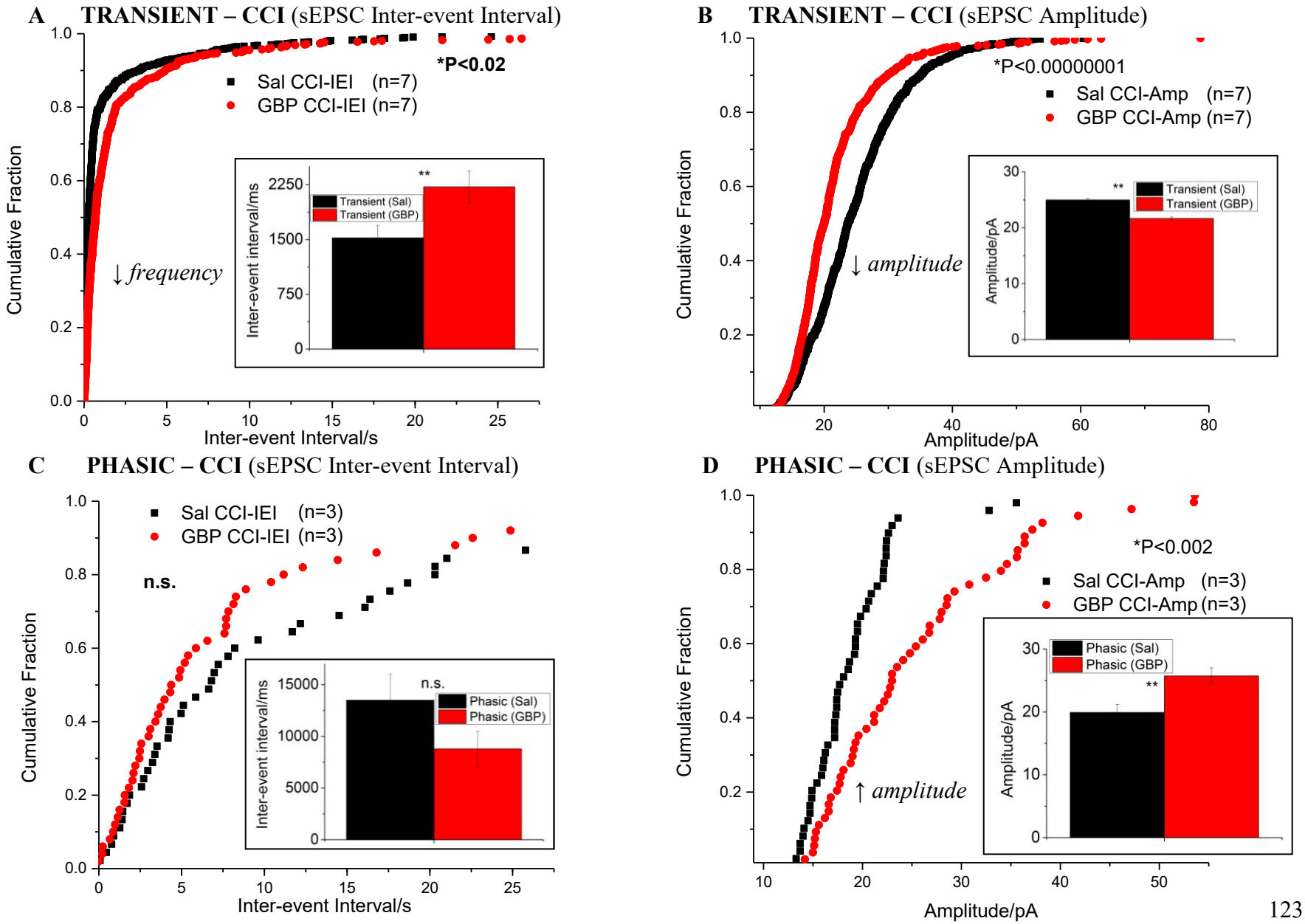
A TRANSIENT – CCI (sEPSC Inter-event Interval)
*P<0.02
Sal CCI-IEI (n=7)
GBP CCI-IEI (n=7)
↓ frequency
Transient (Sal)
Transient (GBP)
Inter-event interval/ms
Cumulative Fraction
Inter-event Interval/s
B TRANSIENT – CCI (sEPSC Amplitude)
*P<0.00000001
Sal CCI-Amp (n=7)
GBP CCI-Amp (n=7)
↓ amplitude
Amplitude/pA
C PHASIC – CCI (sEPSC Inter-event Interval)
Sal CCI-IEI (n=3)
GBP CCI-IEI (n=3)
n.s.
Phasic (Sal)
Phasic (GBP)
D PHASIC – CCI (sEPSC Amplitude)
*P<0.002
Sal CCI-Amp (n=3)
GBP CCI-Amp (n=3)
↑ amplitude

Figure 4-6. **The effect of IP GBP on sEPSCs of transient and phasic neurons recorded from the dorsal horn of neuropathic CCI rats.** A. sEPSC inter-event interval of transient neurons. (Inset) Average transient neuron sEPSC inter-event interval for saline versus GBP-injected rats. B. sEPSC amplitude of transient neurons (Inset) Average transient neuron sEPSC amplitude for saline versus GBP-injected rats. C. sEPSC inter-event interval of phasic neurons (Inset) Average phasic neuron sEPSC inter-event interval for saline versus GBP-injected rats. D. sEPSC amplitude of phasic neurons. (Inset) Average phasic neuron sEPSC amplitude for saline versus GBP-injected rats. In each case, the red curve indicates IP GBP and black curve indicates IP saline. A shift to the right of the red compared to the black curve indicates an increase in the x-variable. Transient neurons (no. of events): Sal=859 and GBP=685. Phasic neurons (no. of events): Sal=49 and GBP=54. No. of neurons indicated in brackets on plot. *Kolmogorov-Smirnov test, statistical significance if $p<0.05$. **One-way ANOVA with post-hoc Bonferonni correction, statistical significance if $p<0.05$.

Figure 4-7

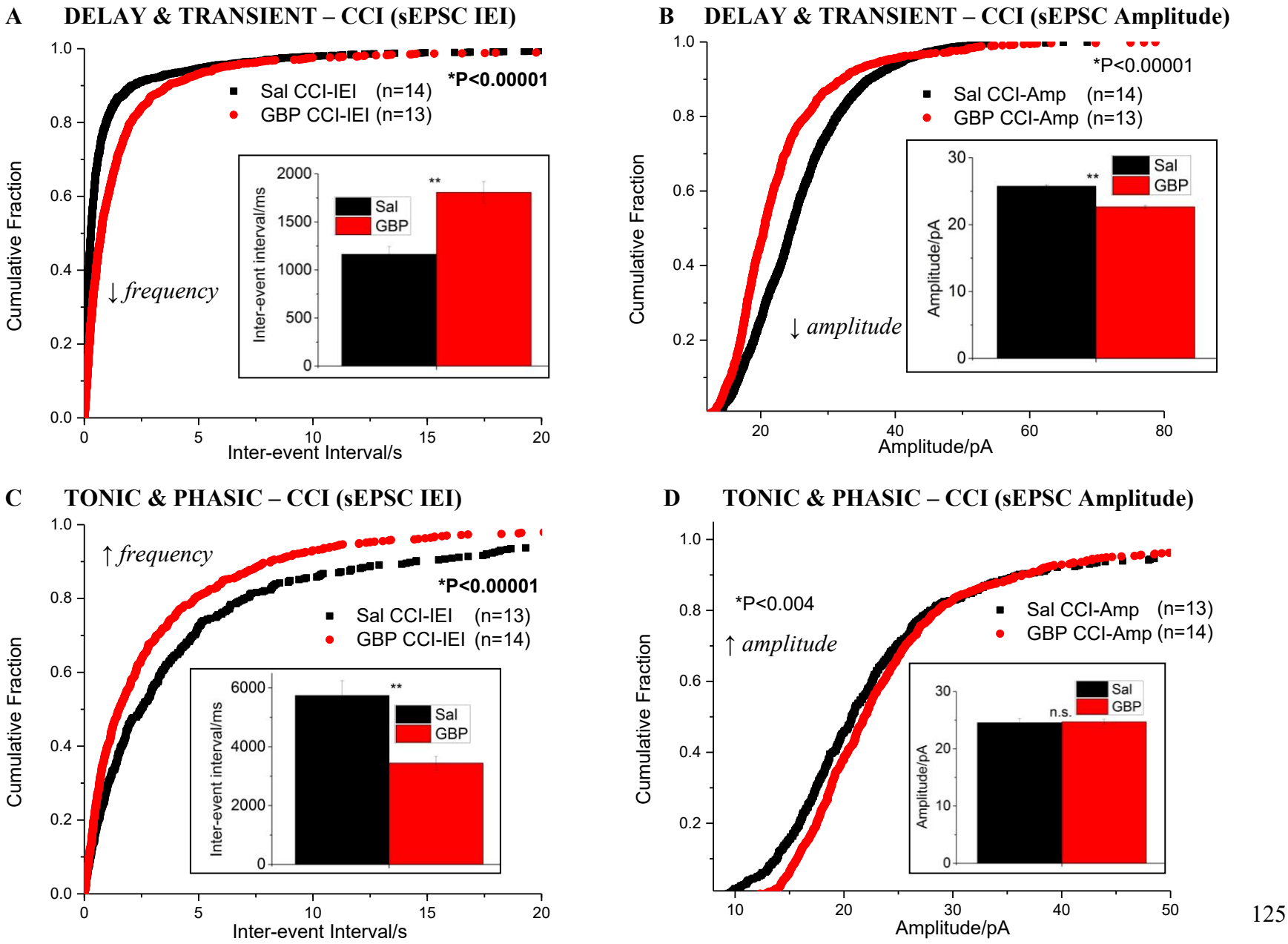
A DELAY & TRANSIENT – CCI (sEPSC IEI)
*P<0.00001
Sal CCI-IEI (n=14)
GBP CCI-IEI (n=13)
↓ frequency
Cumulative Fraction
Inter-event Interval/s
Inter-event interval/ms
Sal
GBP
**
B DELAY & TRANSIENT – CCI (sEPSC Amplitude)
*P<0.00001
Sal CCI-Amp (n=14)
GBP CCI-Amp (n=13)
↓ amplitude
Cumulative Fraction
Amplitude/pA
C TONIC & PHASIC – CCI (sEPSC IEI)
↑ frequency
*P<0.00001
Sal CCI-IEI (n=13)
GBP CCI-IEI (n=14)
Cumulative Fraction
Inter-event Interval/s
D TONIC & PHASIC – CCI (sEPSC Amplitude)
*P<0.004
↑ amplitude
Sal CCI-Amp (n=13)
GBP CCI-Amp (n=14)
n.s.
Cumulative Fraction
Amplitude/pA

Figure 4-7. **The effect of IP GBP on sEPSCs of putative excitatory (delay & transient) and putative inhibitory (tonic & phasic) neurons recorded from the dorsal horn of neuropathic CCI rats.** A. sEPSC inter-event interval of delay & transient neurons. (Inset) Average delay & transient neuron sEPSC inter-event interval for saline versus GBP-injected rats. B. sEPSC amplitude of delay & transient neurons. (Inset) Average delay & transient neuron sEPSC amplitude for saline versus GBP-injected rats. C. sEPSC inter-event interval of tonic & phasic neurons. (Inset) Average tonic & phasic neuron sEPSC inter-event interval for saline versus GBP-injected rats. D. sEPSC amplitude of tonic & phasic neurons. (Inset) Average tonic & phasic neuron sEPSC inter-event interval for saline versus GBP-injected rats. In each case, the red curve indicates IP GBP and black curve indicates IP saline. A shift to the right of the red compared to the black curve indicates an increase in the x-variable. Delay & Transient neurons (no. of events): Sal=2047 and GBP=1438. Tonic & Phasic neurons (no. of events): Sal=446 and GBP=690. No. of neurons indicated in brackets on plot. *Kolmogorov-Smirnov test, statistical significance if $p<0.05$. **One-way ANOVA with post-hoc Bonferonni correction, statistical significance if $p<0.05$.

Figure 4-8.

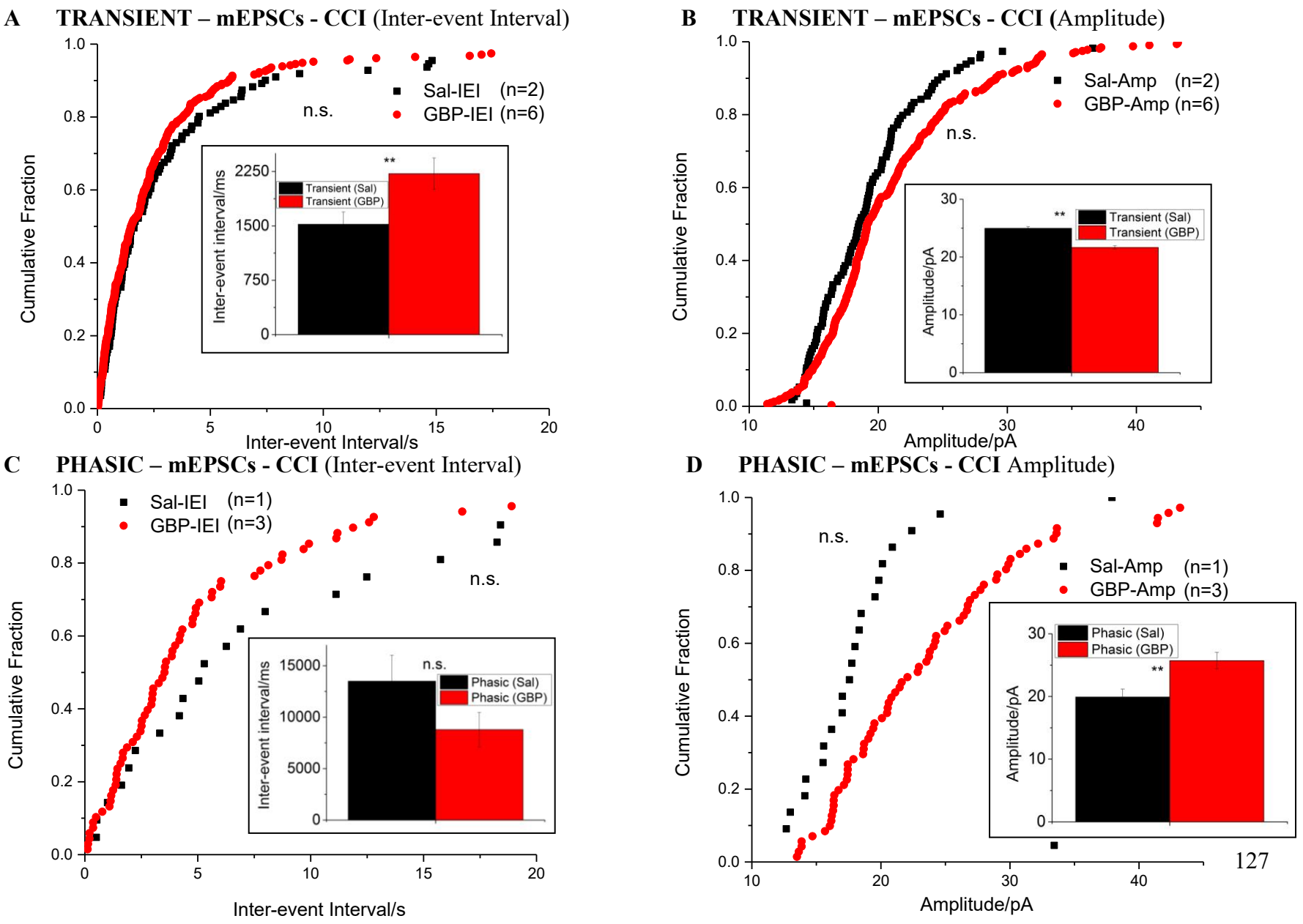
A TRANSIENT – mEPSCs - CCI (Inter-event Interval)
Cumulative Fraction
Inter-event Interval/s
Sal-IEI (n=2)
GBP-IEI (n=6)
n.s.
Inter-event interval/ms
Transient (Sal)
Transient (GBP)
**
B TRANSIENT – mEPSCs - CCI (Amplitude)
Cumulative Fraction
Amplitude/pA
Sal-Amp (n=2)
GBP-Amp (n=6)
n.s.
Amplitude/pA
Transient (Sal)
Transient (GBP)
**
C PHASIC – mEPSCs - CCI (Inter-event Interval)
Cumulative Fraction
Inter-event Interval/s
Sal-IEI (n=1)
GBP-IEI (n=3)
n.s.
Inter-event interval/ms
n.s.
Phasic (Sal)
Phasic (GBP)
D PHASIC – mEPSCs - CCI Amplitude)
Cumulative Fraction
Amplitude/pA
n.s.
Sal-Amp (n=1)
GBP-Amp (n=3)
Amplitude/pA
Phasic (Sal)
Phasic (GBP)
**

Figure 4-8. **The effect of IP GBP on mEPSCs of transient and phasic neurons recorded from the dorsal horn of neuropathic CCI rats.** A. mEPSC inter-event interval of transient neurons. (Inset) Average transient neuron mEPSC inter-event interval for saline versus GBP-injected rats. B. mEPSC amplitude of transient neurons (Inset) Average transient neuron mEPSC amplitude for saline versus GBP-injected rats. C. mEPSC inter-event interval of phasic neurons (Inset) Average phasic neuron mEPSC inter-event interval for saline versus GBP-injected rats. D. mEPSC amplitude of phasic neurons. (Inset) Average phasic neuron mEPSC amplitude for saline versus GBP-injected rats. In each case, the red curve indicates IP GBP and black curve indicates IP saline. A shift to the right of the red compared to the black curve indicates an increase in the x-variable. Transient neurons (no. of events): Sal=114 and GBP=317. Phasic neurons (no. of events): Sal=22 and GBP=71. No. of neurons indicated in brackets on plot. *Kolmogorov-Smirnov test, statistical significance if $p<0.05$. **One-way ANOVA with post-hoc Bonferonni correction, statistical significance if $p<0.05$.

Figure 4-9.

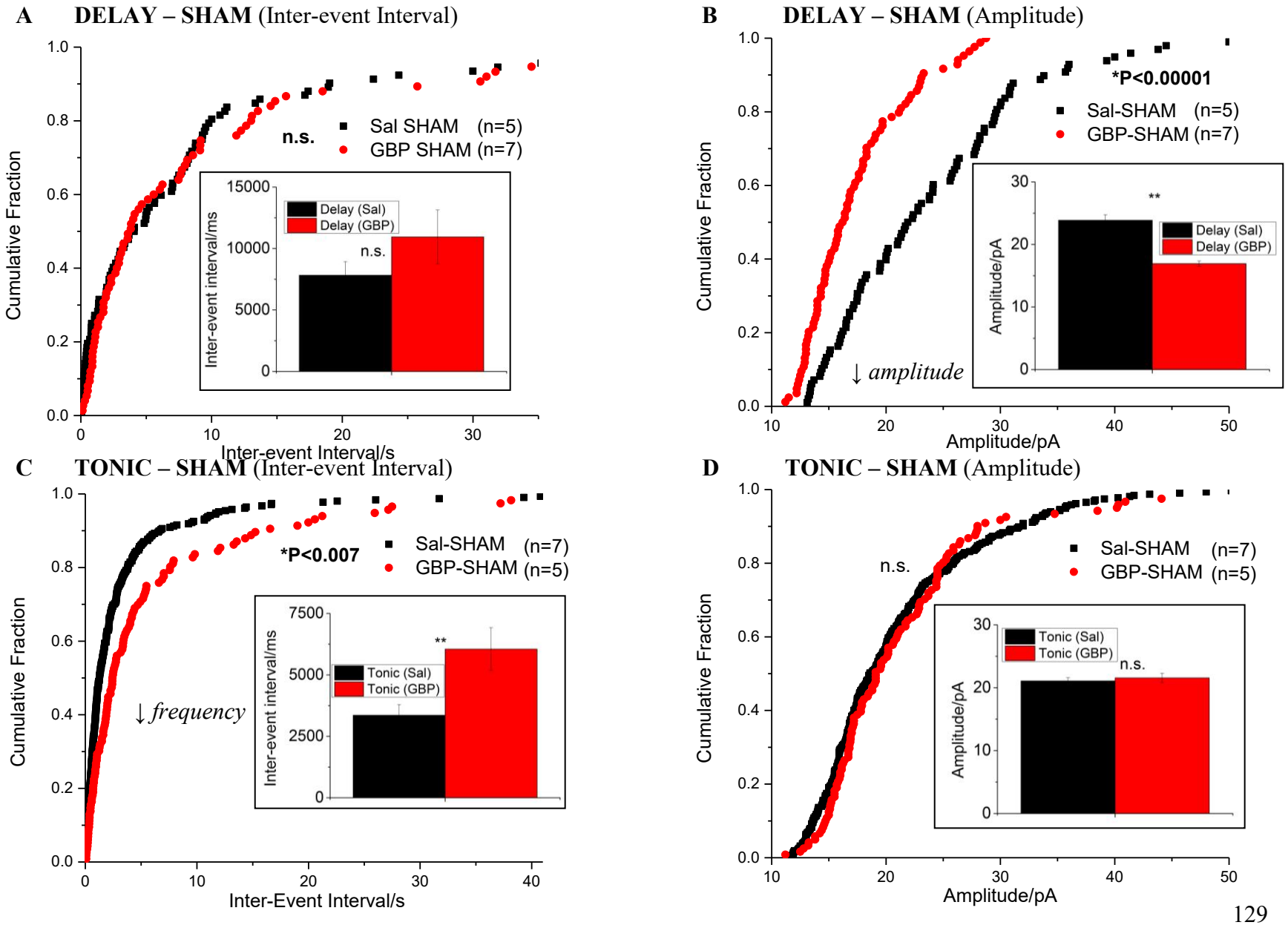
A
DELAY – SHAM (Inter-event Interval)
Cumulative Fraction
Inter-event Interval/s
n.s.
Sal SHAM (n=5)
GBP SHAM (n=7)
Inter-event interval/ms
Delay (Sal)
Delay (GBP)
n.s.
B
DELAY – SHAM (Amplitude)
*P<0.00001
Sal-SHAM (n=5)
GBP-SHAM (n=7)
↓ amplitude
Amplitude/pA
**
C
TONIC – SHAM (Inter-event Interval)
*P<0.007
Sal-SHAM (n=7)
GBP-SHAM (n=5)
↓ frequency
Tonic (Sal)
Tonic (GBP)
D
TONIC – SHAM (Amplitude)
n.s.
Sal-SHAM (n=7)
GBP-SHAM (n=5)
Tonic (Sal)
Tonic (GBP)

Figure 4-9. **The effect of IP GBP on sEPSCs of delay and tonic neurons recorded from the dorsal horn of sham-operated rats.** A. sEPSC inter-event interval of putative excitatory delay neurons. (Inset) Average delay neuron sEPSC inter-event interval for saline versus GBP-injected rats. B. sEPSC amplitude of putative excitatory delay neurons (Inset) Average delay neuron sEPSC amplitude for saline versus GBP-injected rats. C. sEPSC inter-event interval of putative inhibitory tonic neurons (Inset) Average tonic neuron sEPSC inter-event interval for saline versus GBP-injected rats. D. sEPSC amplitude of putative inhibitory tonic neurons. (Inset) Average tonic neuron sEPSC amplitude for saline versus GBP-injected rats. In each case, the red curve indicates IP GBP and black curve indicates IP saline. A shift to the right of the red compared to the black curve indicates an increase in the x-variable. Delay neurons (no. of events): Sal=98 and GBP=99. Tonic neurons (no. of events): Sal=315 and GBP=121. No. of neurons indicated in brackets on plot. *Kolmogorov-Smirnov test, statistical significance if $p<0.05$. **One-way ANOVA with post-hoc Bonferonni correction, statistical significance if $p<0.05$.

Figure 4-10.

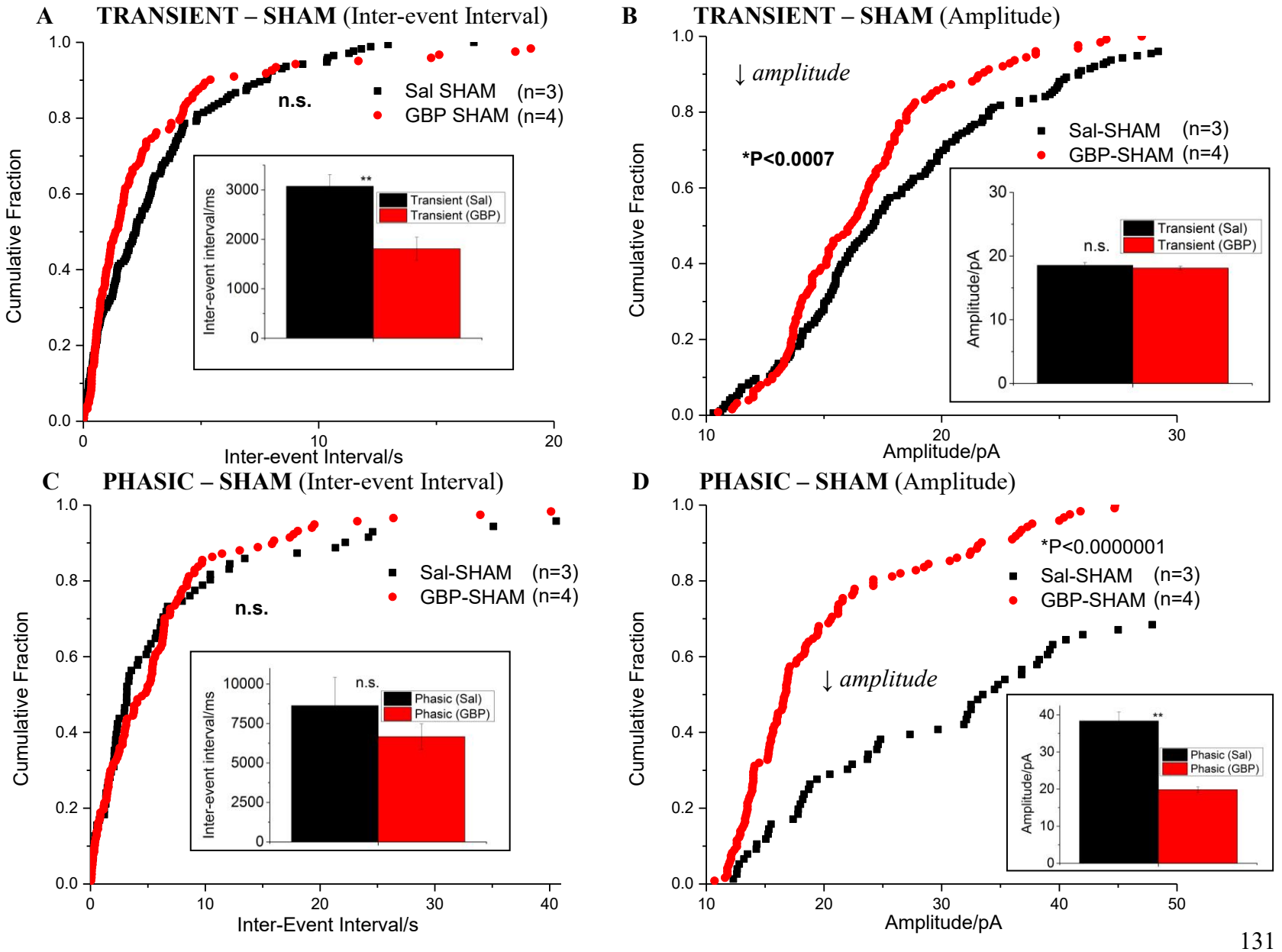
A TRANSIENT – SHAM (Inter-event Interval)
Cumulative Fraction
Inter-event Interval/s
n.s.
Sal SHAM (n=3)
GBP SHAM (n=4)
Inter-event interval/ms
**
Transient (Sal)
Transient (GBP)
B TRANSIENT – SHAM (Amplitude)
↓ amplitude
*P<0.0007
Sal-SHAM (n=3)
GBP-SHAM (n=4)
Amplitude/pA
n.s.
Transient (Sal)
Transient (GBP)
C PHASIC – SHAM (Inter-event Interval)
Cumulative Fraction
Inter-Event Interval/s
n.s.
Sal-SHAM (n=3)
GBP-SHAM (n=4)
Inter-event interval/ms
n.s.
Phasic (Sal)
Phasic (GBP)
D PHASIC – SHAM (Amplitude)
*P<0.0000001
Sal-SHAM (n=3)
GBP-SHAM (n=4)
↓ amplitude
Amplitude/pA
**
Phasic (Sal)
Phasic (GBP)

Figure 4-10. **The effect of IP GBP on sEPSCs of transient and phasic neurons recorded from the dorsal horn of sham-operated rats.** A. sEPSC inter-event interval of transient neurons. (Inset) Average transient neuron sEPSC inter-event interval for saline versus GBP-injected rats. B. sEPSC amplitude of transient neurons. (Inset) Average transient neuron sEPSC amplitude for saline versus GBP-injected rats. C. sEPSC inter-event interval of phasic neurons. (Inset) Average phasic neuron sEPSC inter-event interval for saline versus GBP-injected rats. D. sEPSC amplitude of phasic neurons. (Inset) Average phasic neuron sEPSC amplitude for saline versus GBP-injected rats. In each case, the red curve indicates IP GBP and black curve indicates IP saline. A shift to the right of the red compared to the black curve indicates an increase in the x-variable. Transient neurons (no. of events): Sal=176 and GBP=226. Phasic neurons (no. of events): Sal=76 and GBP=122. No. of neurons indicated in brackets on plot. *Kolmogorov-Smirnov test, statistical significance if $p<0.05$. **One-way ANOVA with post-hoc Bonferonni correction, statistical significance if $p<0.05$.

Figure 4-11.

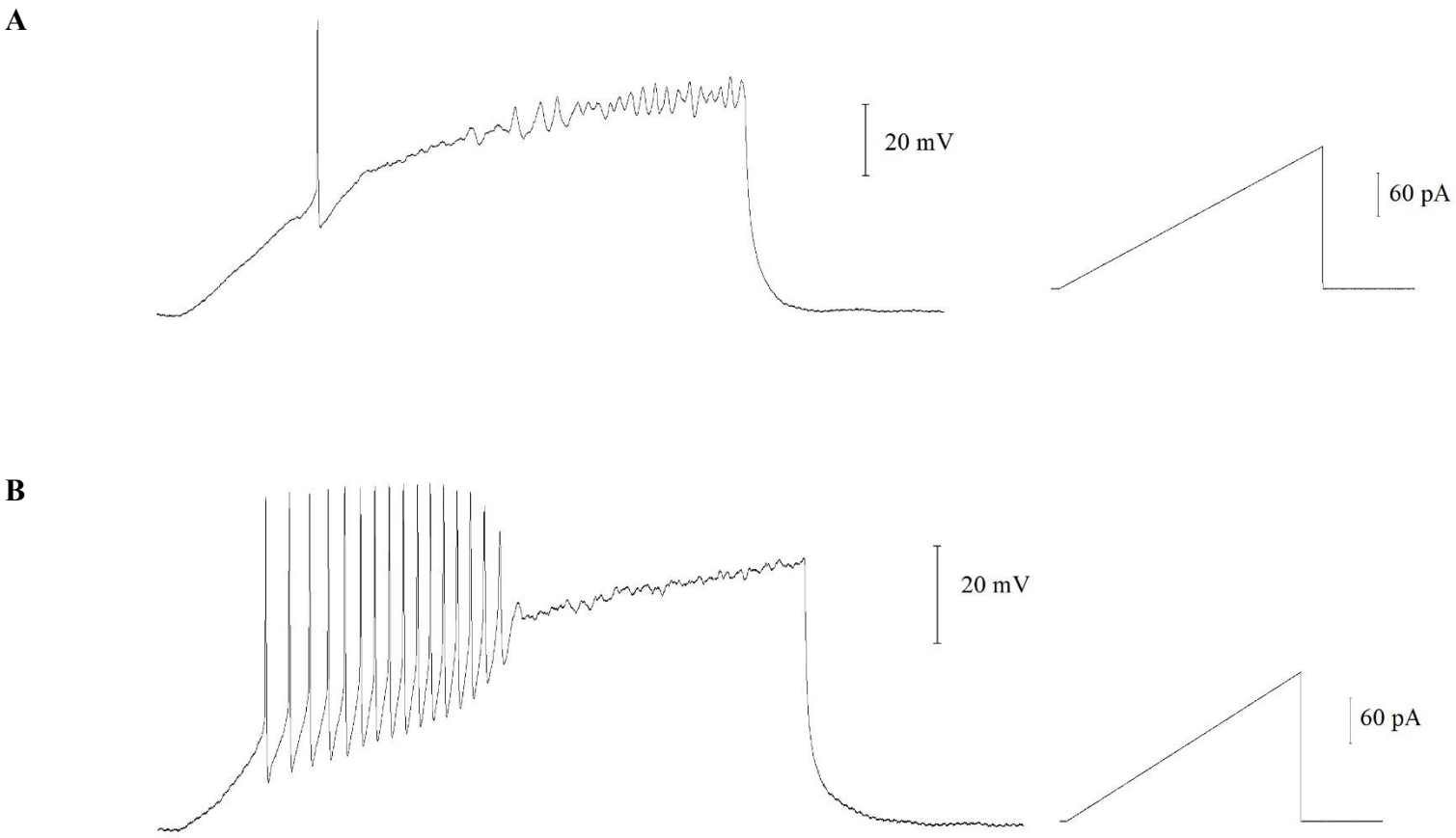

Figure 4-11. **Measurement of intrinsic neuronal excitability.** Typical depolarising current ramp (133 pAs^{-1}, right) and AP firing pattern (left) associated with **A.** putative excitatory delay firing neurons and **B.** putative inhibitory tonic firing neurons of the *substantia gelatonisa*.

Figure 4-12.

A **CCI Neuropathic Rats**

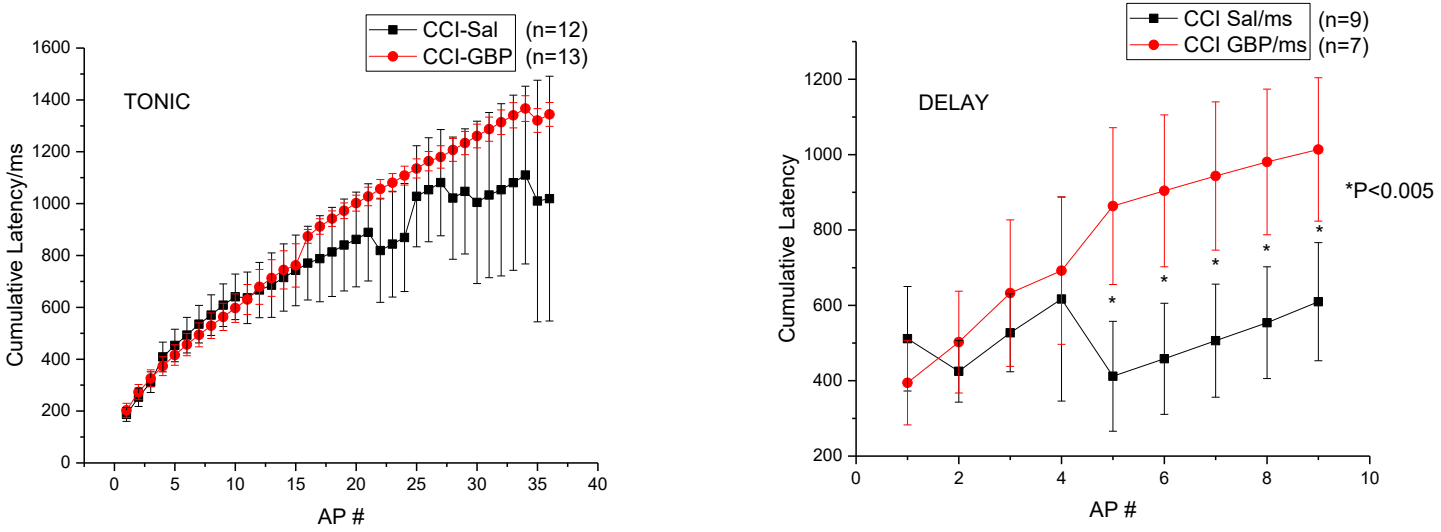

B **Sham-operated Rats**

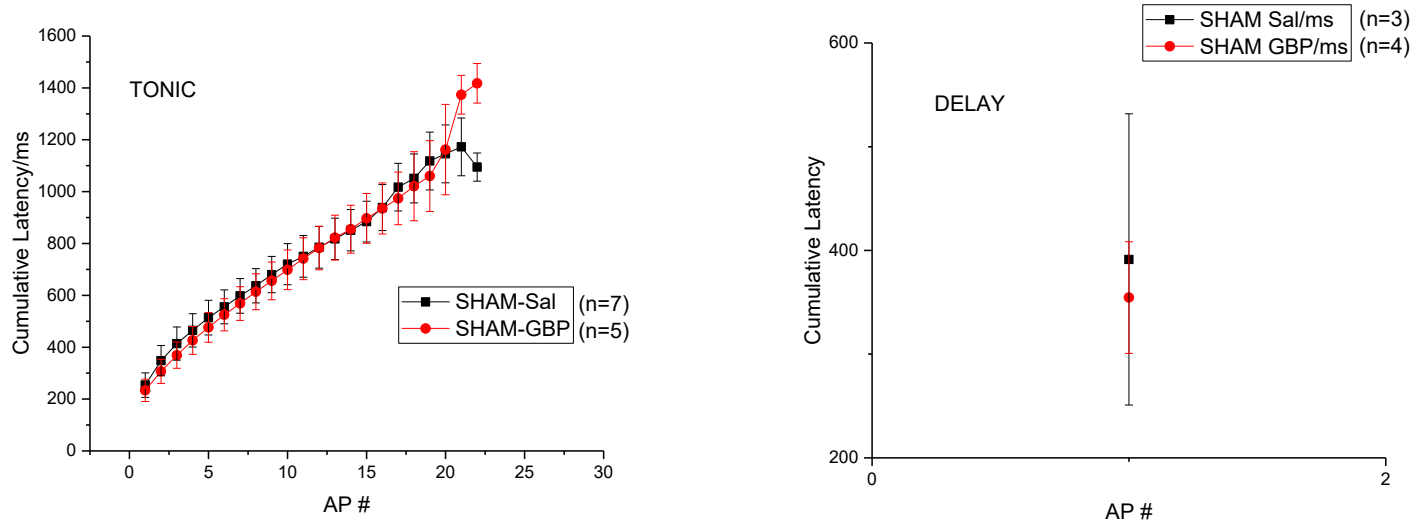

Figure 4-12. **Effect of IP GBP on intrinsic excitability of putative excitatory versus inhibitory neurons in CCI and sham-operated rats.** A. CCI neuropathic rats and B. sham-operated rats. 133 pAs-1 current ramp is used to plot cumulative latency versus AP spike number in each case. No. of neurons indicated in brackets on plot. *One-way ANOVA with Bonferroni correction, $p<0.05$ is considered significant.

Table 4-1

Lamina II Neuronal Phenotype	IP GBP (CCI)					IP GBP (Sham)		
	sEPSC frequency	sEPSC amplitude	mEPSC frequency	mEPSC amplitude	Cumulative latency	sEPSC frequency	sEPSC amplitude	Cumulative latency
Tonic (-)	↑	NC*	NC	↑	NC	↓	NC	NC
Delay (+)	↓	↓	↓	↓	↓	NC	↓	NC
Transient (+)	↓	↓	NC	NC				
Phasic (-)	NC	↓	NC	NC				
All Excitatory	↓	↓						
All Inhibitory	↑	↑						

Table 4-1. Summary of electrophysiological findings on the effects of IP GBP injection (compared to IP saline) on lamina II neurons in CCI and sham rats. The '(+)' or '(-)' indicated next to the neuronal phenotype indicates that these neurons are mostly either excitatory or inhibitory. '↑', '↓' or 'NC' means that there was an increase, decrease or no change in the property indicated. All excitatory = delay + transient. All inhibitory = tonic + phasic. *For tonic neurons there was a small increase in the amplitude of small (<22.5 pA) sEPSC events.

CHAPTER 5

N.B. I carried out all nerve-injury surgeries, acute spinal cord slice and defined-medium organotypic culture preparations, electrophysiology and Ca^{2+} imaging experiments. Animal behavioural studies were performed by Nataliya Bukhanova.

Chapter 5: Site and mechanism of action of GBP

Introduction

In chapters 3 and 4, I established that IP GBP produces effects on overall dorsal horn excitability in neuropathic rats (but not sham-operated rats) and differential effects on *substantia gelatinosa* neurons. The results of Moore et al whereby GBP was exogenously bath applied to the dorsal horn of acute spinal cord slices from naïve rats show no significant effects on synaptic transmission (Moore et al., 2002). I suggest that the reason for this was because neuropathic animals were not used. Therefore, in this chapter, I tested the hypothesis that exogenous bath application of GBP to *ex vivo* spinal cord slices from neuropathic animals will produce significant changes in synaptic transmission (as measured by the frequency and amplitude of sEPSCs) in *substantia gelatinosa* putative excitatory delay and inhibitory tonic neurons

GBP is also thought to have an effect on the neurotransmitter release process via binding to α2δ, an auxiliary subunit of VGCCs, and prevention of trafficking of functional α-subunit-containing-VGCCs to nerve terminals (Heblich et al., 2008, Hendrich et al., 2008). Reduced expression of HVA VGCCs would reduce stimulation-induced Ca^{2+} influx and this has been widely assumed to attenuate neurotransmitter release (Dodge and Rahamimoff, 1967). I tested the hypothesis that GBP produces its anti-allodynic effects via blockade of VGCCs by comparing the effects of bath applied Mn^{2+}, a pan-VGCC blocker, with bath applied GBP on the frequency and amplitude of sEPSCs of *substantia gelatinosa* neurons.

Biggs et al have shown in naïve defined-medium organotypic spinal cord cultures (DMOTCs) that chronic GBP (10 μM) is ineffective in reducing the amplitude of 35 mM K^{+}-evoked Ca^{2+} responses, but that 5-6 day treatment with 200 ng/ml BDNF confers effectiveness to chronic GBP

(10 μM) and reduces the amplitude of 35 mM K^+-evoked Ca^{2+} responses (Biggs et al., 2014). I therefore tested the hypothesis that chronic BDNF treatment confers effectiveness to acute GBP in DMOTCs by monitoring for a reduction in the amplitude of 35 mM K^+-evoked Ca^{2+} responses before and after acute GBP application

Finally, it is known that α2δ is upregulated in neuropathic pain states (Luo et al., 2002) and that BDNF is also an important driver of neuropathic pain (Coull et al., 2005, Lu et al., 2009). This leads to the hypothesis that chronic BDNF treatment of DMOTCs upregulates α2δ levels. I tested this hypothesis by performing Western blots for the α2δ-1 protein on chronic BDNF-treated versus naïve DMOTCs. If the previous hypothesis concerning chronic BDNF conferring acute effectiveness to GBP is validated, the results of these experiments will help provide a molecular basis for such an effect.

Methods

The methods used in this chapter include chronic constriction injury (CCI) surgery, *ex vivo* acute spinal cord slice preparation, defined-medium organotypic spinal cord (DMOTC) slice preparation, whole cell voltage-clamp recording, Ca^{2+} imaging of *ex vivo* acute spinal cord slices and DMOTC slices and statistical analysis. These methods are described in detail in Chapter 2.

Results

Bath applied GBP reduces sEPSC frequency in both putative excitatory and inhibitory neurons in slices from neuropathic rats

The purpose of these studies is to determine whether bath applied GBP will affect synaptic transmission of delay and tonic *substantia gelatinosa* neurons from *ex vivo* slices of nerve-injured neuropathic rats in contrast to results of Moore et al who carried out experiments on naïve acute spinal cord slices (Moore et al., 2002). These experiments will also be compared to the results of Chapter 4 where the effect of prior IP injection of GBP into neuropathic rats on *substantia gelatinosa* synaptic transmission is investigated to test the hypothesis that changing the method of delivery of GBP exerts different effects on *substantia gelatinosa* synaptic transmission. Since *ex vivo* spinal cord slices do not have intact peripheral connections and are also disconnected from higher brain centres, these experiments may provide information on the physiological site(s) of action of acute GBP.

In order to test the acute effectiveness of exogenously applied GBP on *substantia gelatinosa* putative excitatory and inhibitory neurons, a concentration of 100 μM GBP was bath applied to *ex vivo* acute spinal cord slices. This concentration of GBP mimics that reached therapeutically in the central nervous system (Bryans and Wustrow, 1999). Cumulative probability plots show that bath applied GBP produces a significant decrease in frequency (Figure 5-1A/C, $p<0.05$, K-S test), but not amplitude (Figure 5-1B/D, $p>0.05$, K-S test), in both putative excitatory delay and putative inhibitory tonic neurons. These results are confirmed by the effect of GBP on average sEPSC frequency (Figure 5-1A/C, $p<0.05$, one-way ANOVA) and average sEPSC amplitude (Figure 5-1B/D, not significant, $p>0.05$, one-way ANOVA) in delay and tonic neurons. The indiscriminate depressant effects are summarized in Table 5-1. A sample sEPSC recording of the depressant

effects of bath applied GBP on sEPSCs from a delay *substantia gelatinosa* neurons is shown in Figure 5-2. It is also worth noting that the dorsal horn neuronal cell-type specific effects of GBP (seen when GBP is injected intraperitoneally into neuropathic animals, Table 4-1) are lost when GBP is bath applied to slices from neuropathic slices instead.

Bath applied GBP does not have a significant effect on overall dorsal horn excitability in slices from neuropathic rats

Since bath applied GBP reduced excitatory drive to both *substantia gelatinosa* putative excitatory and inhibitory neurons (Figure 5-1), it was hypothesized that bath applied acute GBP would not produce a significant on overall dorsal horn excitability in neuropathic ratts. To test this hypothesis the effect of 10 min bath application of 100 μM GBP on 35 mM K^+-evoked Ca^{2+} rises in the dorsal horn from nerve-injured animals was examined (as described in Figure 3-5). The results support this hypothesis as it was shown that there was no significant effect on the amplitude of the Ca^{2+} rise after GBP perfusion compared to before (Figure 5-3). Therefore, overall dorsal horn excitability in slices from neuropathic animals was not affected by acute (10 min) bath perfusion with 100 μM GBP. This is in contrast to results in Figure 3-6 where a significant reduction in overall dorsal horn excitability ($P<0.05$, two-way ANOVA with Bonferonni correction) was produced in neuropathic animals that had received IP GBP.

Bath applied 100 μM GBP has a significant effect on sEPSCs from *substantia gelatinosa* neurons, whereas Mn^{2+}, a pan-VGCC blocker, does not

To test the hypothesis that the anti-allodynic mechanism of *ex vivo* action of acute GBP is via blockade of VGCCs, I compared the effect of 100 μM GBP on sEPSCs with 200 μM Mn^{2+}, a pan-VGCC blocker (Biggs et al., 2014). To confirm that Mn^{2+} was effective at blocking VGCCs in the dorsal horn, it was demonstrated that 200 μM Mn^{2+} significantly reduced the amplitude of K^+-evoked Ca^{2+} responses from dorsal horn neurons (Figure 5-4A). It was hypothesized that if GBP's mechanism of acute action was via a blockade of VGCC function, then effects of GBP on sEPSCs would be similar to those of 200 μM Mn^{2+}. Because GBP reduces trafficking of VGCCs to nerve terminals, it has been assumed that this will promote decreased neurotransmitter release (Cheng and Chiou, 2006, Heblich et al., 2008, Hendrich et al., 2008, Fink et al., 2000). My findings show that 200 μM Mn^{2+} did not produce a significant effect on sEPSC frequency or amplitude in acute spinal cord slices (Figure 5-4B/C, $p>0.05$, K-S test).

Chronic BDNF treatment of DMOTCs does not confer acute GBP effectiveness

Biggs et al have shown that BDNF treatment of DMOTCs confers effectiveness to chronic (10 μM) GBP as measured by a reduction of 35 mM K^+-evoked Ca^{2+} rises in dorsal horn neurons (Biggs et al., 2014). Therefore, it was hypothesized that chronic BDNF treatment of DMOTCs confers effectiveness to acute GBP. It was shown however, that acute GBP perfusion was not effective in reducing the amplitude of 35 mM K^+-evoked Ca^{2+} responses in BDNF-treated DMOTCs (Figure 5-5). This suggests that chronic BDNF treatment of DMOTCs does not confer effectiveness to acutely applied GBP.

Discussion

In vivo versus in vitro actions of acute GBP

The fact that frequency of sEPSCs and not amplitude is exclusively affected by bath applied GBP suggests that GBP acts pre-synaptically in this situation. It is also worth noting that the cell-type specific effects of GBP (seen when GBP is injected intraperitoneally into neuropathic animals, Table 4-1) are lost when GBP is bath applied to slices from neuropathic slices instead. This suggests that another target or mechanism of action exists in an *in vivo* versus an *in vitro* situation with acute GBP.

The results suggest that in nerve-injured animals GBP has different acute mechanisms *in vivo* than *in vitro*. Since GBP reduces excitatory drive to both the 'gas pedal' to nociceptive information (putative excitatory delay neurons, Figure 5-1A/B) and the 'brake' (putative inhibitory neurons, Figure 5-1C/D), it is understandable that we see no net effect on dorsal horn excitability (Figure 5-2). These results also provoke important questions regarding the context of the situation when attempting to understand mechanism of drug action. It is also important for studies to consider the effects of GBP on individual neuronal phenotypes when bath applying drugs rather than to equate the effect in an *in vitro* setting to what happens *in vivo*.

These results are consistent with those of Patel et al where in streptozocin-induced diabetic neuropathic rats 100 μM GBP acute bath application was shown to decrease mEPSC frequency (but not amplitude) in dorsal horn neurons (Patel et al., 2000). Zhou et al reported a decrease in mEPSC frequency with bath perfusion of 100 μM GBP in deep dorsal horn neurons from nerve-injured rats with no reference to neuronal phenotype, however, these results would be consistent with my findings as a decrease in frequency across all cell types was observed (Zhou and Luo, 2015). In contrast, Fink et al observed a concentration-dependent inhibition of 50 mM-K^+-induced

neuronal Ca^{2+} influx with 100 μM GBP (Fink et al., 2000). However, these experiments were carried out on rat neocortical synaptosomes, which have little relevance in the context of nociceptive circuitry.

GBP and the neurotransmitter release machinery

It has been shown that 200 μM Mn^{2+} reduces calcium current in DRG cell bodies to <20% of control amplitude (Biggs et al., 2014). In spite of this blockade of calcium current, interestingly my findings show that 200 μM Mn^{2+} did not produce a significant effect on sEPSC frequency or amplitude in acute spinal cord slices (Figure 5-4B/C). This suggests that a blockade of calcium current does not equate to a reduction in spontaneous release as measured by sEPSC frequency or amplitude. This suggests that GBP most likely utilizes a mechanism not involving calcium current blockade to affect sEPSCs.

Results in Figure 5-3 allude to an effect of GBP on a process that does not depend exclusively on the VGCC. Hoppa et al have shown that α2δ, the binding site for GBP, can increase presynaptic strength and set release probability by causing the Ca^{2+} sensor for release to experience higher levels of Ca^{2+} (Hoppa et al., 2012). GBP, when bath applied to spinal cord slices from naïve mice, has a preferential effect on presynaptic P/Q-type VGCCs (as measured by the % blockade of evoked excitatory post-synaptic currents in the presence of different VGCC blockers) and this would suggest why Mn^{2+} produces different effects than GBP on sEPSCs as Mn^{2+} is a non-specific VGCC blocker (Bayer et al., 2004). But if Mn^{2+} blocks more of the presynaptic VGCC population than GBP, then why would it not affect sEPSCs like GBP? This paradox is best explained by the 4^{th} power relationship between Ca^{2+} influx and neurotransmitter release, which essentially means that only a certain amount of Ca^{2+} influx is required for release and a reduction of Ca^{2+} influx to anything above this amount will have no effect on release (Dodge and Rahamimoff, 1967). This

is also supported with evidence showing that overexpression of $Ca_V2.2$ channels in hippocampal neurons fails to increase EPSC size suggesting that the strength of neurotransmission is saturated with regards to VGCC expression (Cao and Tsien, 2010).

GBP and BDNF: potential relationship?

There are relatively few studies to suggest a relationship between the effect of chronic BDNF exposure and GBP effectiveness. Biggs et al have shown in naïve spinal DMOTCs that chronic GBP (10 μM) is ineffective in reducing the amplitude of 35 mM K^+-evoked Ca^{2+} responses, but that 5-6 day treatment with 200 ng/ml BDNF confers effectiveness to chronic GBP (10 μM) and reduces the amplitude of 35 mM K^+-evoked Ca^{2+} responses (Biggs et al., 2014). It has been shown that cell-surface expression of the GBP ligand α2δ is reduced in the ventromedial hypothalamus of BDNF mutant mice (Cordeira et al., 2014). This study however, does not provide a direct link between levels of BDNF and α2δ in the context of nociceptive spinal cord circuitry. One study has shown that non-specific blockade of the Trk (tropomyosine receptor kinases) family (with K252a), which are critically involved in BDNF signalling, reduces GBP mediated anti-hypersensitivity in nerve-injured rats (Hayashida and Eisenach, 2011). However, this study provided GBP to rats orally, therefore dose would be difficult to control precisely, and withdrawal thresholds were measured 2 hrs after GBP was administered, which is outside the window of acute effects that we have observed (30 min or less).

Figure 5-5 shows that BDNF treatment of DMOTCs does not confer effectiveness to acute GBP (as measured via a reduction in amplitude of 35 mM-K^+-evoked Ca^{2+} rise). Further experiments would be required to determine the reason for this. One candidate molecule that may play a role in conferring effectiveness to acute GBP is α2δ. Therefore, it would be interesting to determine whether chronic BDNF treatment of DMOTCs has an effect on α2δ levels.

Figure 5-1

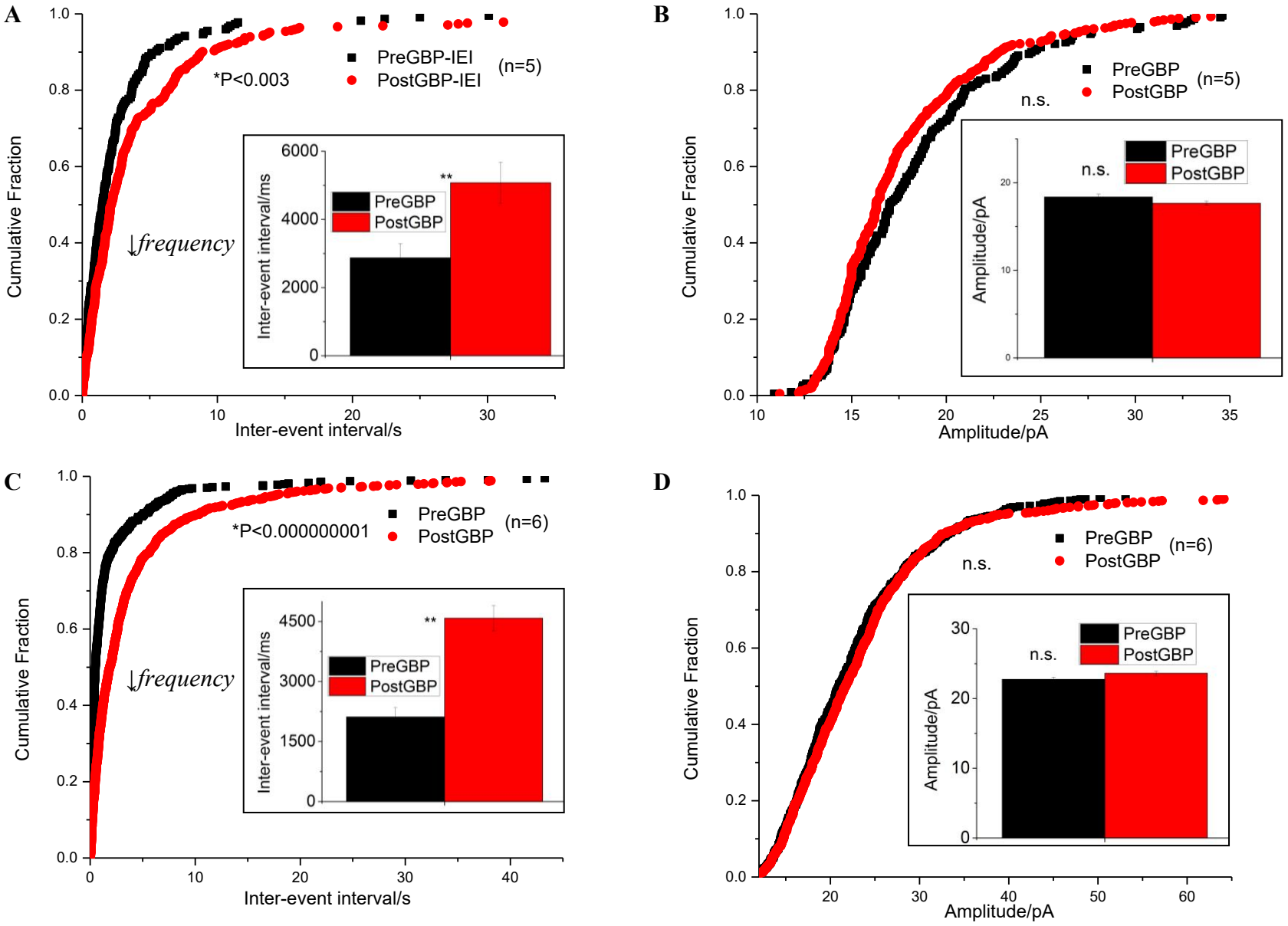
A
Cumulative Fraction
Inter-event interval/s
*P<0.003
PreGBP-IEI
PostGBP-IEI
(n=5)
↓frequency
Inter-event interval/ms
PreGBP
PostGBP
**
B
Cumulative Fraction
Amplitude/pA
PreGBP
PostGBP
(n=5)
n.s.
Amplitude/pA
C
Cumulative Fraction
Inter-event interval/s
*P<0.000000001
PreGBP
PostGBP
(n=6)
↓frequency
Inter-event interval/ms
D
Cumulative Fraction
Amplitude/pA
PreGBP
PostGBP
(n=6)
n.s.
Amplitude/pA

Figure 5-1. The effect of bath-applied 100 µM GBP on sEPSCs of delay and tonic neurons recorded from the *substantia gelatinosa* of neuropathic CCI rats. A. sEPSC inter-event interval of putative excitatory delay neurons (Inset) Average delay neuron sEPSC inter-event interval before and after GBP application. B. sEPSC amplitude of putative excitatory delay neurons. (Inset) Average delay neuron sEPSC amplitude interval before and after GBP application. C. sEPSC inter-event interval of putative inhibitory tonic neurons. (Inset) Average tonic neuron sEPSC inter-event interval before and after GBP application. D. sEPSC amplitude of putative inhibitory tonic neurons. (Inset) Average tonic neuron sEPSC amplitude before and after GBP application. Baseline recording was at least 6 min. GBP was applied for 20 min, but recording was started only after 2 min of pre-wash with GBP to ensure GBP had completely flooded the perfusion chamber. Cells were rejected if leak current >1.0 nA during bath application with GBP. The red curve indicates IP GBP and black curve indicates IP saline. A shift to the right of the red compared to the black curve indicates an increase in the x-variable. *Kolmogorov-Smirnov test, statistical significance if $p<0.05$. **One-way ANOVA with post-hoc Bonferonni correction, statistical significance if $p<0.05$.

Figure 5-2

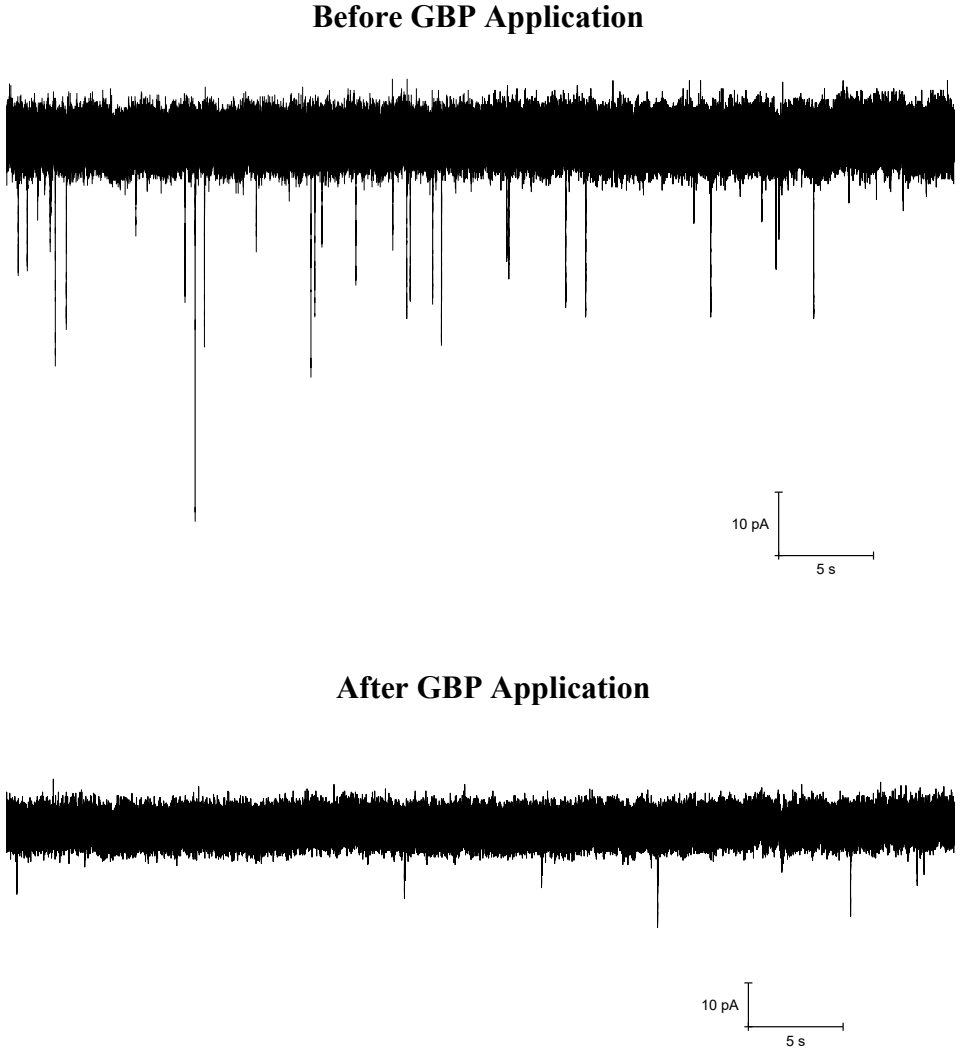

Figure 5-2. Sample recording demonstrating the acute effect of 100 µM GBP bath application on sub*stantia gelatinosa* neuron sEPSCs from a CCI rat. Acute bath GBP reduces the frequency of sEPSCs from tonic putative inhibitory and delay putative excitatory neurons, with no significant effect on amplitude. Whole-cell recordings were made in voltage-clamp at -70 mV and were obtained from *ex vivo* spinal cord slices from neuropathic CCI rats.

Figure 5-3

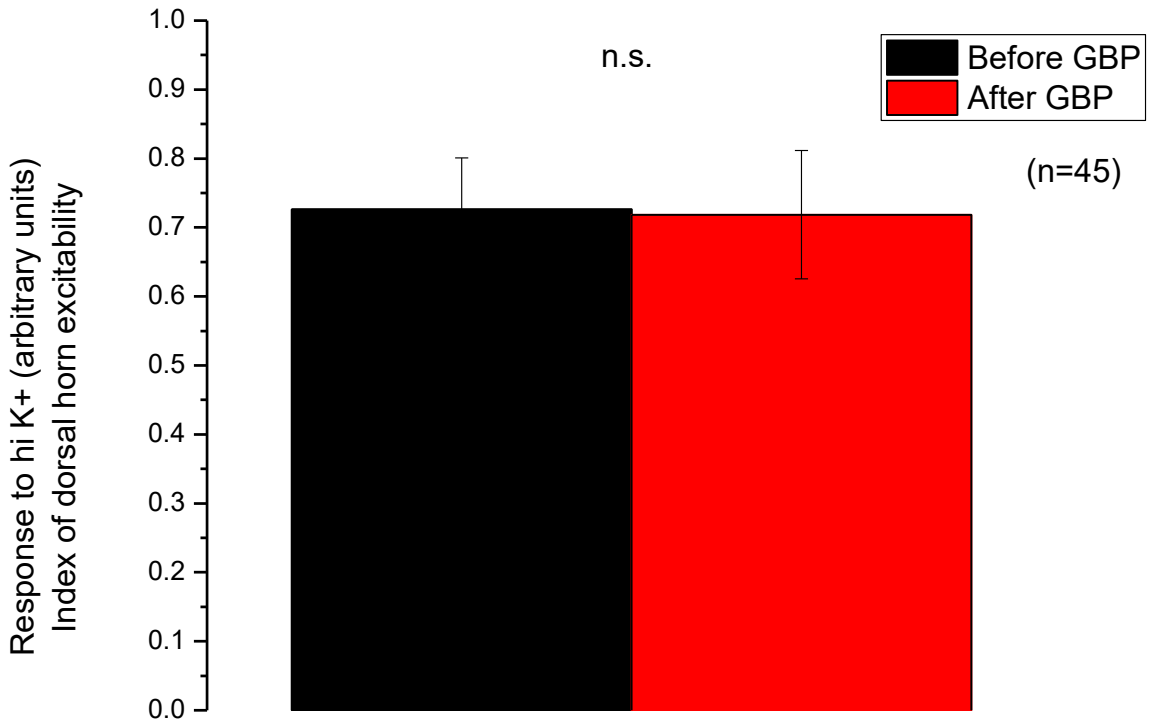

Figure 5-3. The effect of bath applied 100 µM GBP on overall dorsal horn excitability of CCI rats. Dorsal horn excitability was based on the amplitude of Ca^{2+} response to 35 mM K^{+} of dorsal horn neurons from *ex vivo* spinal cord slices obtained from CCI neuropathic rats. The average of at least 2 consistent normalized responses (dF/F_0) was obtained before and after application of 100 µM GBP for 10 min. P>0.05 one-way ANOVA was considered to be not significant (n.s.) n=45 neurons, 6 slices.

Figure 5-4

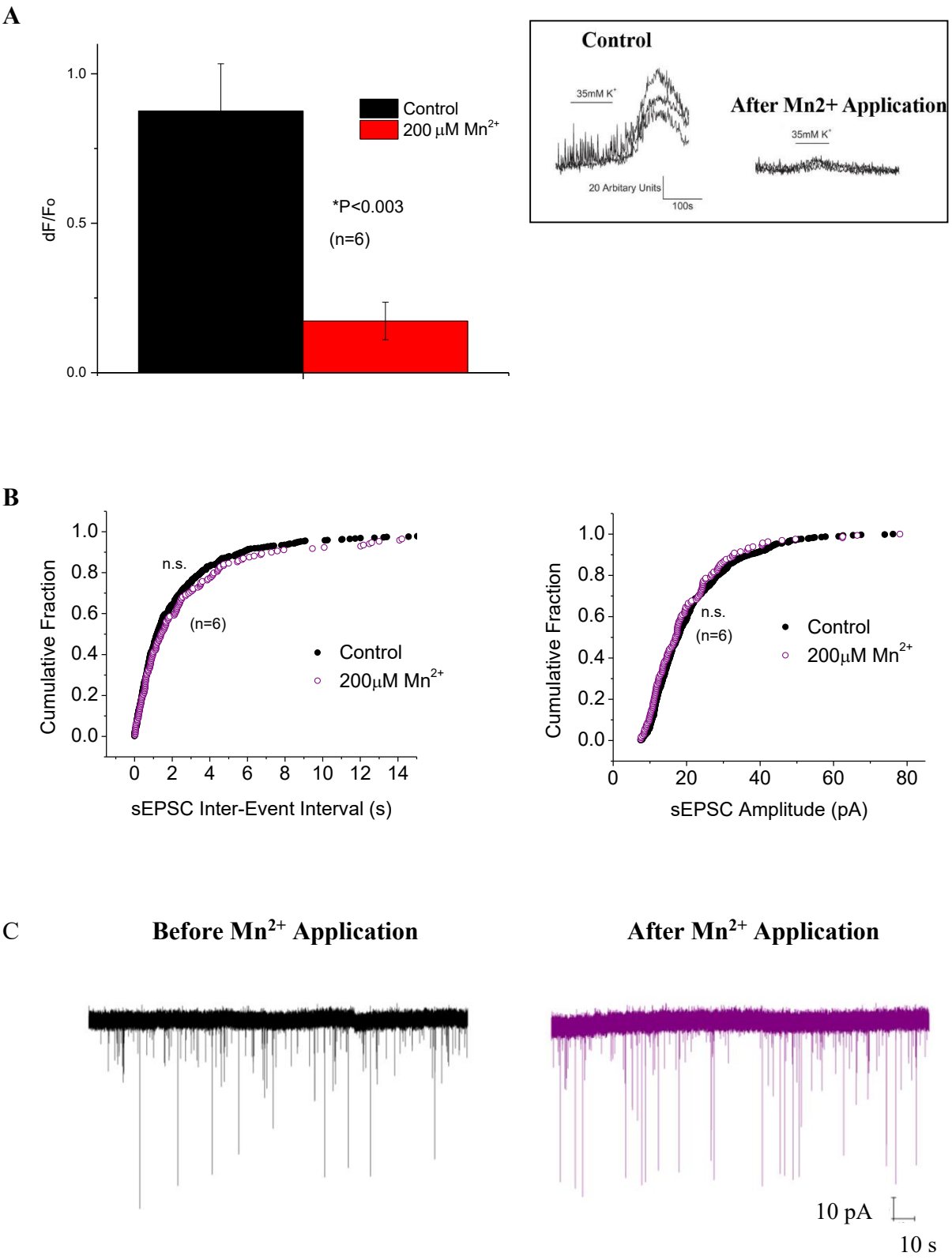
A
1.0
0.5
0.0
dF/Fo
Control
200 μM Mn2+
*P<0.003
(n=6)
Control
35mM K+
20 Arbitary Units
100s
After Mn2+ Application
35mM K+
B
Cumulative Fraction
n.s.
(n=6)
Control
200μM Mn2+
sEPSC Inter-Event Interval (s)
n.s.
(n=6)
Control
200μM Mn2+
sEPSC Amplitude (pA)
C
Before Mn2+ Application
After Mn2+ Application
10 pA
10 s

Figure 5-4. The effect of bath application of 200 µM Mn^{2+}, a pan-VGCC blocker, on spinal dorsal horn properties A. 200 µM Mn^{2+} blocks 35 mM-K^+-evoked Ca^{2+} influx in dorsal horn of DMOTCs. *statistical significance if $P<0.05$, one-way ANOVA with post-hoc Bonferonni. (Inset) Traces of 35 mM K^+-evoked Ca^{2+} responses from 3 representative neurons before and after application of 200 µM Mn^{2+}. **B.** effect of 200 µM Mn^{2+} on sEPSCs from acute spinal cord slices: sEPSC inter-event interval (left) and sEPSC amplitude (right) **C.** sample baseline recording before Mn^{2+} application (left) and sample sEPSC recording after Mn^{2+} application (right), showing no noticeable effect on event frequency or amplitude. This shows that Mn^{2+}, a blocker of VGCCs, has no effect on the neurotransmitter release machinery. Kolmogorov-Smirnov test was used to compare sEPSC inter-event interval and amplitude before and after Mn^{2+} application, n.s. (no statistical significance) if $p>0.05$.

Figure 5-5

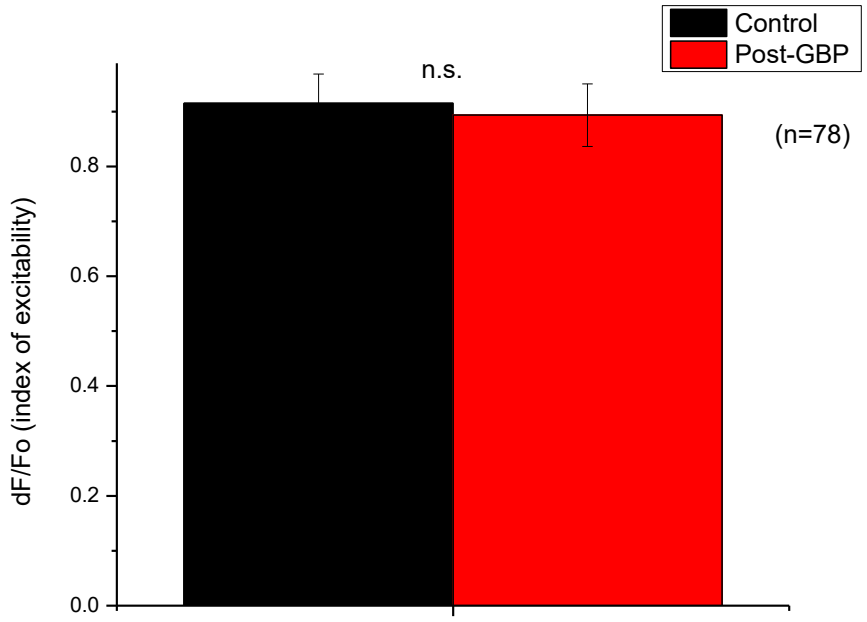

Figure 5-5. The effect of acute GBP bath application on dorsal horn excitability in BDNF-treated DMOTCs. Acute (10 min) 100 μM GBP bath application did not produce a significant effect on the amplitude of the Ca^{2+} response to 35 mM K^{+} ($P>0.05$, one way ANOVA). Dorsal horn cells n=78 (before and after GBP). The average of at least 2 responses before and after GBP application were obtained. Treated DMOTCs were treated with 200 ng/ml BDNF for 5-6 days. $P>0.05$ one-way ANOVA was considered to be not significant (n.s.) n=78 neurons, 3 slices.

Table 5-1

Lamina II Neuronal Phenotype	100 μM GBP bath application	
	sEPSC frequency	sEPSC amplitude
Tonic (-)	↓	NC
Delay (+)	↓	NC

Table 5-1. Summary of electrophysiological findings on the effects of GBP bath application (compared to before GBP) *substantia gelatinosa* neurons of CCI rats. The '(+)' or '(-)' indicated next to the neuronal phenotype indicates that these neurons are mostly either excitatory or inhibitory. '↓' or 'NC' means that there was either a decrease or no change in the property indicated.

DISCUSSION

Discussion

This thesis attempts to understand the acute (<1 hr) effects of the first-line anti-allodynic drug, gabapentin (GBP) by studying the behavioural effects in neuropathic rats and the corresponding neuronal cellular effects in spinal dorsal horn and primary somatosensory cortex. The novelty of this approach lies in the fact that we have both a behavioural and corresponding cellular measurement from each animal for an acute effect of GBP. In addition, we attempted to probe the acute mechanism of action of GBP by examining its potential site of action and relationship to levels of its ligand, α2δ (Gee et al., 1996). This chapter will summarize the findings of the previous three chapters and discuss issues arising from this work and the potential for future studies regarding the actions of GBP.

Summary of Findings

Chapter 3

In Chapter 3 the acute effects of IP injection of clinically-relevant doses of GBP on behavioural measures of mechanical allodynia in neuropathic CCI rats and the underlying changes in network excitability in the dorsal horn and primary somatosensory cortex are examined.

It was first established that a single injection of 100 mg/kg GBP increased paw withdrawal threshold (reduced allodynia) within 30 min of IP injection in CCI neuropathic rats while having no effect on sham-operated rats. GBP was still present in acute *ex vivo* spinal cord preparations and brain from injected animals.

The dorsal horn (DH) excitability of injected adult rats was determined as the amplitude of response to 35 mM K^+ stimulation by Ca^{2+} imaging of *ex vivo* spinal cord slices, a technique developed especially for this purpose (Chapter 2). DH excitability of slices from neuropathic rats that had received 100 mg/kg GBP was reduced compared to those that had received saline; whereas DH excitability of slices from sham-operated was unaffected by GBP injection.

A novel technique was established for *in vivo* cortical imaging of neuropathic rats (Chapter 2). It was shown that neuropathic rats that had received 100 mg/kg IP GBP show a reduction in 'neural mass' (an indicator of cortical excitability) (Doetsch, 2000, Erickson, 1986) in response to vibrotactile stimulation of the injury-side hindlimb within 10 minutes. There was no effect on the cortical excitability of sham-operated rats that had received GBP after the same period of time.

These results establish that there are acute actions of GBP specific to neuropathic CCI rats and provide a cellular basis for these effects at the level of the dorsal horn, where nociceptive processing occurs (Todd, 2010), and the primary somatosensory cortex, where part of the affective emotional experience of pain occurs (Wall et al., 1994).

Chapter 4

The experimental plan adopted for Chapter 4 was similar to Chapter 3, with acutely isolated spinal cord being studied *ex vivo* from neuropathic or sham-operated animals that had received 100 mg/kg IP GBP or saline. However, for these experiments spinal cord was studied using whole-cell electrophysiological recording from *substantia gelatinosa* neurons of the dorsal horn. Neurons were identified based on electrophysiological firing pattern as either delay (excitatory), tonic (inhibitory), phasic, transient or irregular (Balasubramanyan et al., 2006).

It was established that IP GBP has preferential effects on spontaneous excitatory postsynaptic currents (sEPSCs) recorded from putative excitatory delay versus inhibitory tonic neurons in the dorsal horn of neuropathic rats. Results suggest that IP GBP decreases excitatory drive to putative excitatory neurons while increasing excitatory drive to putative inhibitory neurons (see Table 4-1 for summary).

These results were corroborated by recording miniature excitatory postsynaptic currents (mEPSCs) from these neurons, which are independent of depolarisation or Ca^{2+} influx. Further analysis of mEPSC amplitude using distribution histograms (5 pA bins) as shown in Figure 4-5 demonstrates that the effect of GBP to decrease amplitude of mEPSCs from delay neurons is not specific to events of a particular size (Figure 4-5A), whereas in tonic neurons (Figure 4-5B) GBP tends to increase amplitude of larger (>20 pA) events.

In CCI rats, the effects of IP GBP on sEPSCs from high-threshold transient neurons, which are most likely excitatory (Punnakkal et al., 2014), were similar to those observed in delay neurons suggesting a decrease in excitatory drive to excitatory neurons. Phasic neurons, which have been characterized as inhibitory by one study where they are referred to as 'initial bursting' cells (Heinke et al., 2004), also saw an increase in excitatory drive in a similar way to that observed in tonic neurons. Furthermore, the summed data of delay and transient versus tonic and phasic sEPSCs (Figure 4-6A) supports a decrease in excitatory drive to putative excitatory neurons and an increase in excitatory drive to inhibitory neurons in neuropathic animals.

In sham-operated rats that had received IP GBP, sEPSCs recorded showed a decrease in excitatory drive to delay excitatory neurons as well as a decrease in excitatory drive to tonic inhibitory neurons, which suggests an overall depressant effect of GBP (see Table 4-1 for summary).

Results from CCI and sham-operated rats show clear differences in terms of the acute effects of prior IP GBP on sEPSCs on delay neurons. An effect on sEPSC frequency in CCI delay neurons (Figure 4-3A), but not in sham delay neurons (Figure 4-9A) was observed. This leads to the suggestion that an effect of GBP on putative excitatory delay neuron sEPSC frequency is an α2δ-mediated effect since it is well known that α2δ-levels are upregulated following CCI in the DRG (Luo et al., 2002). It is possible that GBP has selectivity for α2δ-upregulated-DRG neurons in CCI rats that primarily synapse on to delay neurons of the dorsal horn in the case of CCI, but not sham-operated rats.

The intrinsic excitability of *substantia gelatinosa* neurons was studied by looking at the effect of depolarising current ramps on the latency and frequency of action potential firing. Cumulative latency versus action potential number was plotted for neurons from both neuropathic and sham-operated animals that had received either IP GBP or saline. It was established that IP GBP reduced the excitability of delay excitatory neurons from neuropathic rats, while having no significant effect on tonic inhibitory neurons. In sham rats there was no significant effect of IP GBP on either delay or tonic intrinsic neuron excitability.

These electrophysiological results provide a cellular mechanism for the behavioural effect of IP GBP on reducing withdrawal thresholds in neuropathic animals and the lack of effect on withdrawal thresholds in sham-operated animals.

Chapter 5

This chapter sheds light on the acute mechanism of action of GBP by 1) investigating the potential effects of changing the method of drug delivery and 2) investigating potential molecular processes involving neurotransmitter release involved in GBP effectiveness.

Bath applied GBP reduces sEPSC frequency in both putative excitatory and inhibitory neurons in slices from neuropathic rats (see Table 5-1 for summary). This suggests that GBP decreases excitatory drive to excitatory neurons and also decreases excitatory drive to inhibitory neurons. This suggests that another target or mechanism of action exists in an *in vivo* versus an *in vitro* situation with acute GBP.

By studying overall dorsal horn excitability using confocal Ca^{2+} imaging, it was shown that bath applied GBP does not have a significant effect on the amplitude of 35 mM K^{+} evoked Ca^{2+} rises in *ex vivo* slices from neuropathic rats. These results support electrophysiological findings and again suggest that bath applied GBP does not reach its physiological target to reduce dorsal horn excitability as is the case when GBP is delivered by IP injection.

In experiments to probe the molecular mechanisms of acute GBP action, it was shown that 200 μM Mn^{2+}, a pan-VGCC blocker, did not produce a significant effect on sEPSC frequency or amplitude in acute spinal cord slices, which suggests that GBP must be doing something other than VGCC blockade to affect sEPSCs.

Chronic (5-6 day) brain-derived neurotrophic factor (BDNF) treatment of defined-medium organotypic spinal cord cultures (DMOTCs) has been used to mimic conditions of neuropathic pain (Lu et al., 2007, Lu et al., 2009). The changes that occur in BDNF-treated DMOTCs mirror some of the changes observed in the spinal cord following chronic constriction injury (CCI) (Lu

et al., 2009). Biggs et al have shown that chronic BDNF treatment of DMOTCs is effective in conferring effectiveness to chronic GBP (5-6 day treatment with 100 μM) as measured by a reduction in the amplitude of 35 mM K^+-evoked Ca^{2+} rises (Biggs et al., 2014a). In order to test whether chronic BDNF treatment of DMOTCs was effective in conferring effectiveness to acute 100 μM GBP, the amplitude of 35 mM K^+ evoked Ca^{2+} rises was measured before and 10 min after bath application of 100 μM GBP. No significant change in dorsal horn excitability were recorded following acute GBP application in BDNF-treated DMOTCs. These experiments suggest that chronic BDNF treatment of DMOTCs is not involved in conferring effectiveness to acute GBP.

Figure 6-1 shows the scheme of events accompanying a peripheral nerve injury, including the release of inflammatory mediators such as TNF-α, sensitization of primary afferents, activation of microglia and consequent release of BDNF (Biggs et al., 2010). Primary afferents terminals exhibit an upregulation of α2δ levels following peripheral nerve injury, which can be measured in the DRG and the dorsal horn of the spinal cord where these afferents terminate (Luo et al., 2001, Li et al., 2004). The release of BDNF from microglia sensitizes dorsal horn neurons to become hyperexcitable (Coull et al., 2005). It has not been tested whether α2δ upregulation precedes or brings about BDNF release or vice versa in the context of chronic neuropathic pain and this potential interaction remains to be tested. As shown in Figure 6-1 and based on my findings, GBP does not appear to interact with BDNF signaling, however this potential interaction has yet to be conclusively ruled out.

Paradoxes of the Acute Actions of Gabapentin: Comparing *In Vitro*, *In Vivo* and Clinical Results

The acute (< 1hr) actions of GBP are well founded in the literature (for review see Alles and Smith, 2016). For example, Luo et al reported a significant increase in paw withdrawal threshold as early as 20 min (and reaching a maximal effect at 100 min) post-IP-injection with 100 mg/kg GBP in a CCI model of neuropathic pain (Luo et al., 2002). GBP appears to produce an effect on pain thresholds in a matter of minutes or hours in *in vitro* and *in vivo* animal models, which contradicts a much longer time course (>17 hours), 'classical' mechanism (Field et al., 2006, Hunter et al., 1997, Kumar et al., 2013). Therefore, a paradox exists between the acute effects of GBP *in vitro* and in animal models and its reported time course of action in the clinic where GBP has been reported to take at least a few days in patients to produce meaningful pain relief (Cheshire, 2002, Sharma et al., 2010).

Why does GBP work slowly in vitro, but rapidly in vivo?

The rapid effects of GBP may be observed in an exclusively 'neuropathic pain' situation *in vivo* where its ligand, α2δ, is upregulated (Luo et al., 2002, Patel et al., 2000, Zhou and Luo, 2015) whereas in most *in vitro* studies that have reported a lack of an acute effect of GBP, α2δ levels are at baseline since neurons are from naïve, non-injured animals (Field et al., 2006, Kumar et al., 2013, Narita et al., 2012). The studies which have been carried out on neuropathic animals or where α2δ is upregulated have reported rapid effects of acute gabapentinoid application (Coderre et al., 2005, Li et al., 2006, Zhou and Luo, 2015).

Studies pertaining to the cellular mechanisms of gabapentinoid action demonstrate effects of GBP on both slow (from the cell body to the terminals; Heblich et al, 2008) and more rapid α2δ trafficking processes (from intracellular compartments to the plasma membrane; Tran-Van Minh and Dolphin 2010). Taken together with my findings, I propose the following explanation of the paradox of GBP action:

In post-Golgi compartments, α2δ subunits are complexed with pore-forming α_1 subunits and auxiliary βγ subunits (Canti et al., 2005, Tran-Van-Minh and Dolphin, 2010). Within nerve terminals, functional VGCC complexes are transported rapidly and inserted into the plasma membrane, which allows expression of VGCCs and coupling to the neurotransmitter release machinery (Cassidy et al., 2014, Heblich et al., 2008, Hoppa et al., 2012). Channel complexes may be removed from the membrane by endocytosis for targeted recycling or degradation in early endosomes (Bauer et al., 2009, Tran-Van-Minh and Dolphin, 2010). In a nerve-injured situation, where α2δ levels are upregulated, cycling of protein complexes to and from the plasma membrane may a more rapid process compared to a control situation (Figure 6-2). Therefore, surface expression of α2δ may be rendered labile and more prone to inhibition by GBP, which can elicit an acute effect within minutes instead of hours or days (Biggs et al., 2014a, Biggs et al., 2014b, Heblich et al., 2008, Hendrich et al., 2008). In a non-nerve injured situation, GBP may act more slowly (17 hrs or more) (Heblich et al., 2008) and have a gradual effect on forward trafficking of VGCC complexes from cell bodies by impairing α2δ (Bauer et al., 2009) as the rate of endocytosis would exceed the rate of replenishment and GBP does not appear to affect the rate of endocytosis (Tran-Van-Minh and Dolphin, 2010).

Results described in Chapters 3 and 4 show a preferential effect of acute GBP on nerve-injured animals, not observed in sham animals, both at the level of the spinal dorsal horn (excitability and

synaptic transmission) and the brain (primary somatosensory cortex), which most likely contribute to GBP's anti-allodynic effects. In α2δ-overexpressing mice similar rapid, acute effects of GBP are observed in deep dorsal horn neurons as well as superficial laminae of the spinal cord (Zhou and Luo, 2014, Zhou and Luo, 2015). It is likely, therefore, that GBP acts slowly in non-injured neurons and rapidly in injured neurons (Figure 6-2).

Why does GBP have different effects depending on its method of delivery?

The results of Chapter 5, which show a lack of cell-type specific effect when GBP is bath applied to *ex vivo* slices compared to when GBP is given systemically, provides information as to the potential target of GBP. It is also possible that, in spite of the acute spinal cord slice preparations for experiments with systemic injection of GBP and bath application of GBP being identical, the *ex vivo* spinal cord slice 'remembers' prior exposure to GBP delivered by IP injection to elicit cell-type specific actions on dorsal horn neurons.

Since in an *ex vivo* setting, only the primary afferent terminals are present for the drug to act on (cell bodies and peripheral nerve endings are absent), this suggests that GBP could be acting on peripheral targets when injected systemically to elicit cell-type specific effects.

There is some evidence to suggest that chronic (but not acute) GBP has an effect on peripheral targets as shown by experiments on dorsal root ganglion (DRG) cultures whereby chronic GBP has been shown to inhibit VGCC-mediated Ca^{2+} currents (Hendrich et al., 2008). Biggs et al provide a possible mechanism for cell-type specific actions of chronic gabapentinoids by explaining that these drugs exert stronger effects on the medium-sized cell bodies associated with Aδ-fibers and on small IB4- neurons, which project to excitatory *substantia gelatinosa* neurons,

whereas the cell bodies of large DRG neurons that associate with Aβ-fibers and of small IB4+ neurons that may project to inhibitory *substantia gelatinosa* neurons are less sensitive (Biggs et al., 2014a). These chronic effects of gabapentinoids may also help explain their acute actions and why cell-type specific effects are seen when GBP is delivered systemically where the DRG are present compared to when GBP is bath applied and the DRG are absent. This schematic is shown in Figure 6-3.

Another possibility is that GBP has effects on descending inputs to the spinal cord from the brain, which may influence dorsal horn synaptic transmission as shown in Figure 6-3 (Sikandar and Dickenson, 2012). Descending serotonergic and noradrenergic fibers can excite GABAergic and glycinergic inhibitory neurons in the spinal dorsal horn (Zeilhofer et al., 2012). For example in the dorsal horn, norepinephrine depolarizes GABAergic neurons via a1-adrenoreceptors (Gassner et al., 2009) and serotonin increases the frequency of GABAergic miniature inhibitory postsynaptic currents (mIPSCs) via $5HT_3$ (Abe et al., 2009).

One recent study has shown that systemic 100 mg/kg GBP inhibits descending excitatory pro-nociceptive serotonergic ($5HT_3$-mediated) pathways from the brain to spinal cord in neuropathic rats (Suzuki et al., 2005). Suzuki et al monitored the effect of GBP every 20 min for 1 hr per dose in the presence or absence of a $5HT_3$ anatagonist, which suggests that this could be a more predominant effect compared to a peripheral effect for an acute mechanism of cell-type specific action of systemically-delivered GBP (Suzuki et al., 2005). It has also been shown that GBP can increases extracellular glutamate release in the locus coeruleus via astroglial dependent mechanisms involving GLT-1 (glutamate-transporter-1) to activate descending noradrenergic inhibition to reduce nociception (Suto et al., 2014).

It has also been shown that intrathecal GBP was not effective in the treatment of chronic pain in patients, which suggests that GBP must be acting on supraspinal or peripheral targets to elicit its anti-allodynic effects (Rauck et al., 2013). Yoshizumi et al suggest a mechanism involving supraspinal targets in nerve-injured rats where GBP inhibits GABA release in the locus coeruleus but not in the spinal dorsal horn (Yoshizumi et al., 2012). This mechanism could explain the effect of GBP on spontaneous synaptic transmission of tonic neurons where in CCI dorsal horn an increase in sEPSC frequency is observed (Figure 4-3) since the locus coeruleus sends descending inhibition to the dorsal horn and a decrease in GABA release in the locus coeruleus would serve to increase excitability of dorsal spinal cord neurons.

Another study using ^{8}F-fluorodeoxyglucose-positron emission tomography supports a central mechanism of action of acute GBP in media anti-allodynia (Lin et al., 2014). It was shown that spared nerve injury-induced increases of glucose metabolism in thalamus, cerebellar vermis and medial prefrontal cortex and that these changes were attenuated by acute GBP treatment.

In a functional magnetic resonance imaging (fMRI) study acute 100 mg/kg GBP was shown to evoke changes in multiple nociceptive brain regions including the thalamus and periaqueductal grey (PAG) in anesthetized naïve rats (Governo et al., 2008). This supports a central role for GBP in eliciting its acute effects.

My results whereby a reduction in the excitability of primary somatosensory cortex is observed with systemic GBP injection (Figure 3-7) and those of others (Rauck et al., 2013, Suto et al., 2014, Suzuki et al., 2005, Yoshizumi et al., 2012, Governo et al., 2008, Lin et al., 2014) suggest a mechanism for GBP's acute anti-allodynic actions involving higher-brain centres and descending inhibition to the dorsal spinal cord (Figure 6-4). There is also the possibility that GBP affects the

thalamus, anterior cingulate cortex, paraaqueductal grey and other higher brain centres involved in pain processing.

In addition to noradrenergic and serotonergic inputs, there are also direct GABAergic and glycinergic inhibitory inputs from the rostral ventromedial medulla (RVM) to the spinal dorsal horn that have been shown to mainly inhibit excitatory neurons (Antal et al., 1996). The involvement of GBP in this pathway has not been investigated.

Another interesting possibility is the involvement of thrombospondins (TSP), which are a family of secreted matrix proteins released by astrocytes that are involved in excitatory synaptogenesis (Christopherson et al., 2005, Eroglu et al., 2009) and have been implicated in the etiology of neuropathic pain (Kim et al., 2012, Pan et al., 2015). It has also been demonstrated that α2δ may function as a receptor for thrombospondin and that GBP can decrease synapse formation in cortical structures (Eroglu et al., 2009). Since both TSPs and α2δ have been associated with neuropathic pain (Bauer et al., 2010, Crosby et al., 2015, Li et al., 2014), GBP interaction with α2δ may antagonize the actions of TSPs to contribute to its more slowly developing effects. It is also possible that a mechanism via TSPs could explain cell-type specific actions of GBP as an effect on mainly excitatory synaptogenesis would be consistent with my findings that GBP preferentially reduces synaptic transmission in delay putative excitatory dorsal horn neurons (Figure 4-3). However, a mechanism involving TSPs does not help explain the acute effects of GBP.

Clinical Paradox

Assuming that the acute effectiveness of GBP is related directly to α2δ levels, why is GBP reported to take a matter of days to work in the clinic (Cheshire, 2002, Gottrup et al., 2004, Parsons et al., 2015, Sharma et al., 2010)? It is possible that in NP patients, α2δ is no longer upregulated and

other pathological processes have taken over the maintenance of central sensitization and so, GBP may only act slowly to reduce α2δ supply to nerve terminals (Alles and Smith, 2016). In patients levels of α2δ-1 over time after injury have not been studied, however in rats it has been shown that dorsal spinal cord α2δ-1 levels are upregulated up to 5 weeks post-spinal nerve ligation injury but fall after this consistently before reaching baseline levels at week 17 (Li et al., 2004). These types of studies would be important for understanding the long-term effectiveness of the gabapentinoids in a clinical setting. In addition, the gabapentinoids only produce meaningful pain relief in 35% of neuropathic pain patients (Moore et al., 2014), so it would be interesting to know whether α2δ levels in individual patients would predict drug efficacy.

Another reason for discrepancies in clinical versus animal model data relates to differences in measuring "pain" in animals versus people (Mogil, 2009, Mogil and Crager, 2004). For example, measuring an increase in paw withdrawal threshold before and after administration of a drug may reflect attenuation of spinal reflexes. More current pre-clinical studies of potential anti-allodynic drugs make use of so-called 'operant' models to overcome these limitations (Xie et al., 2014, Yezierski et al., 2013).

There is also a good deal of interest in the use of gabapentinoids in post-surgical pain (Eipe et al., 2015). In general, the effectiveness is rather variable but rapidly developing effects have been reported (Schmidt et al., 2013). Our model posits that rapid effects of gabapentinoids will only occur under conditions where α2δ is upregulated. Interestingly, surgery itself (in the absence of nerve injury) has been reported to increase α2δ (Bauer et al., 2009) and it has also been suggested that injury-induced discharge in primary afferent fibres, as may occur during surgical manipulation, can upregulate α2δ-1 (Boroujerdi et al., 2008).

Future Work

There are only a few studies of GBP action in operant pain models (Munro et al., 2007, Yezierski et al., 2013), therefore future studies of this type may better translate findings in animal models to experiences in the clinic. In this situation, the animal needs to make a decision based on the cortical processing of a noxious stimulus. For example, rats will naturally select for a covered, darkened environment to avoid predators. If a rat is nerve injured, a mildly warm stimulus will produce thermal hyperalgesia. In an operant test, the animal is given the choice of being on a warm surface in the dark or a cool surface in the light. If the animal is experiencing thermal hyperalgesia, it would be expected to spend more time in the light than in dark; a very different response from a naïve animal.

Most NP patients may only receive GBP treatment months or years after pain onset. The clinical management of pain with GBP suggests that α2δ may play a role in the onset of neuropathic pain but that other processes take over during the maintenance phase (Alles and Smith, 2016). It is possible that α2δ may only be transiently upregulated as a result of injury, which leads to the hypothesis that GBP may work rapidly (10s of minutes) in the initial stages of NP and slowly (10s of hours) during the later stages (Alles and Smith, 2016). Future work will address this hypothesis and determine whether GBP will lose its acute effectiveness as time passes after nerve injury (Figure 6-5).

The gabapentinoids were designed as GABA mimetics to function as anti-convulsants (Field et al., 2006, Taylor et al., 2007). In spite of this, no interaction with subsynaptic $GABA_A$ receptors, $GABA_B$ receptors or GABA uptake or metabolism has been discovered (Lanneau et al., 2001, Li et al., 2006, Moore et al., 2002, Sutton et al., 2002, Taylor et al., 2007). However, little is known about GBP's interaction with extrasynaptic $GABA_A$ receptors. Therefore, future work will aim to

investigate the effect of acutely applied GBP on δ-subunit-containing extrasynaptic $GABA_A$ receptors.

Another potential target of GBP that requires further investigation are the HCN channels. These channels have been implicated in the pathophysiology of neuropathic pain and blockage of HCN channels has been shown to attenuate signs of neuropathic pain (Noh et al., 2014, Young et al., 2014). It has been shown that HCN channels are upregulated after nerve injury and it is thought that they drive spontaneous activity in the DRG (Chaplan et al., 2003, Emery et al., 2011, Emery et al., 2012, Luo et al., 2007, Young et al., 2014) to increase transmitter release from primary afferents (Antal et al., 2004, Papp et al., 2006). In addition, unpublished data from our lab demonstrates that 100 μM GBP reduces I_h density in dorsal root ganglia cultures, which again suggests that HCN channels play a role in mediating GBP's acute anti-allodynic actions. Therefore, the potential effect of GBP on HCN channels in nociceptive pathways requires further investigation.

Clinical Significance

Understanding the time course of action of GBP and cell-type specific effects may help us understand as yet unexplored mechanisms of the drug, which may shed light on its effectiveness for treating neuropathic pain and perhaps change the way and conditions for which these drugs are prescribed.

My results suggest, in support of findings in the literature, that GBP possesses multiple sites of action, which include the periphery, central descending inhibition and higher brain centres (Biggs

et al., 2014a, Suto et al., 2014, Suzuki et al., 2005) and molecular targets α2δ and thrombospondins (Eroglu et al., 2009, Hendrich et al., 2008).

Understanding these mechanisms and the variability of GBP action may provide a framework for the development of more effective therapies for the treatment of neuropathic pain.

Figure 6-1

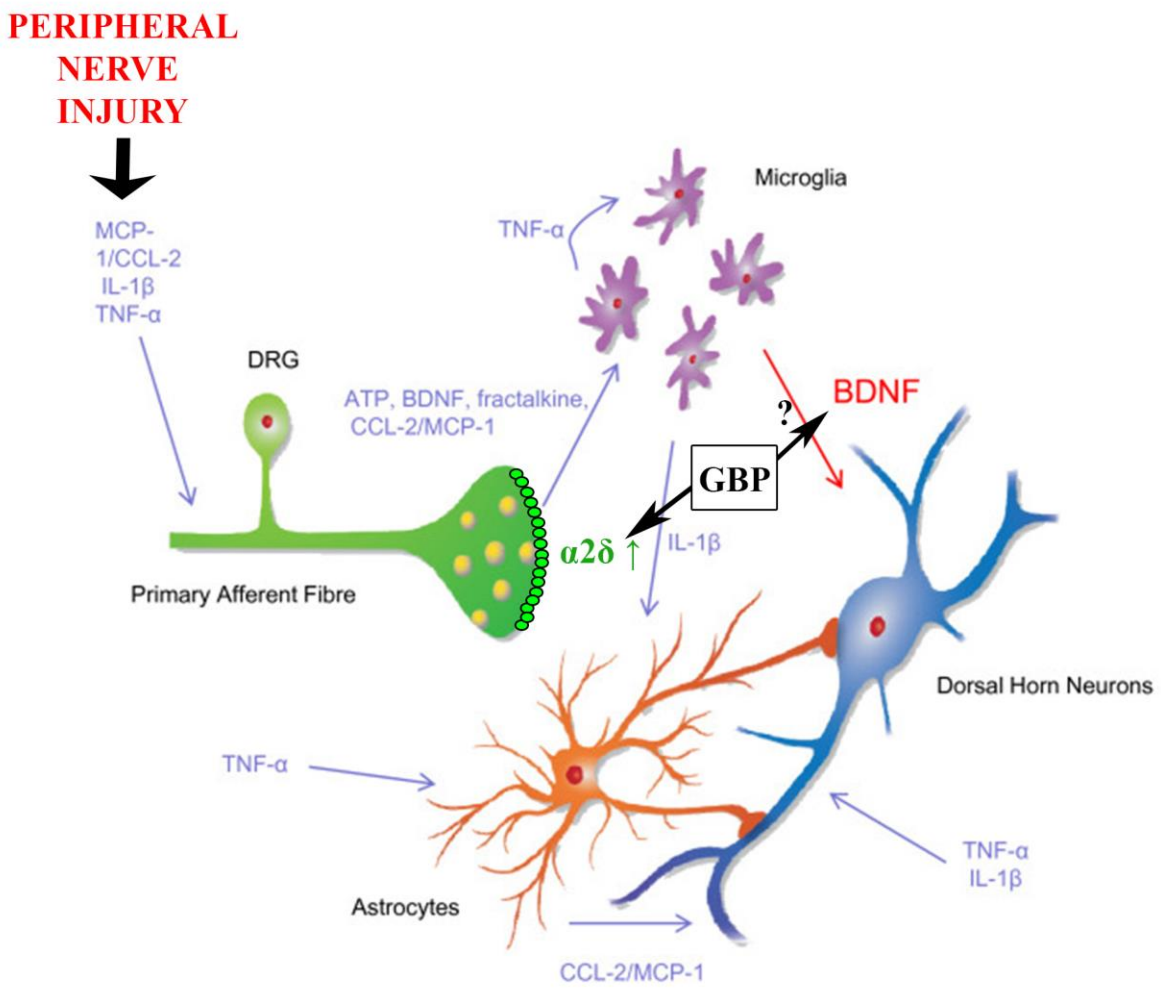

Figure 6-1. Signaling in chronic neuropathic pain showing interactions of GBP. Following a peripheral nerve injury, it is known that BDNF is released by activated microglia (Coull et al., 2005) and that α2δ is upregulated in the dorsal horn of the spinal cord in the terminals of primary afferent neurons (Luo et al., 2001; Li et al., 2004). However, a direct link between BDNF and α2δ has not been demonstrated. GBP is an α2δ ligand and is only effective in neuropathic pain, where α2δ is upregulated (Alles and Smith, 2016). My results suggest that GBP does not interact with the potential link between BDNF and α2δ in neuropathic pain. The α2δ subunit is shown as a green circle on the surface of the dorsal horn neuron. Modified with permission from Biggs et al., 2010.

Figure 6-2

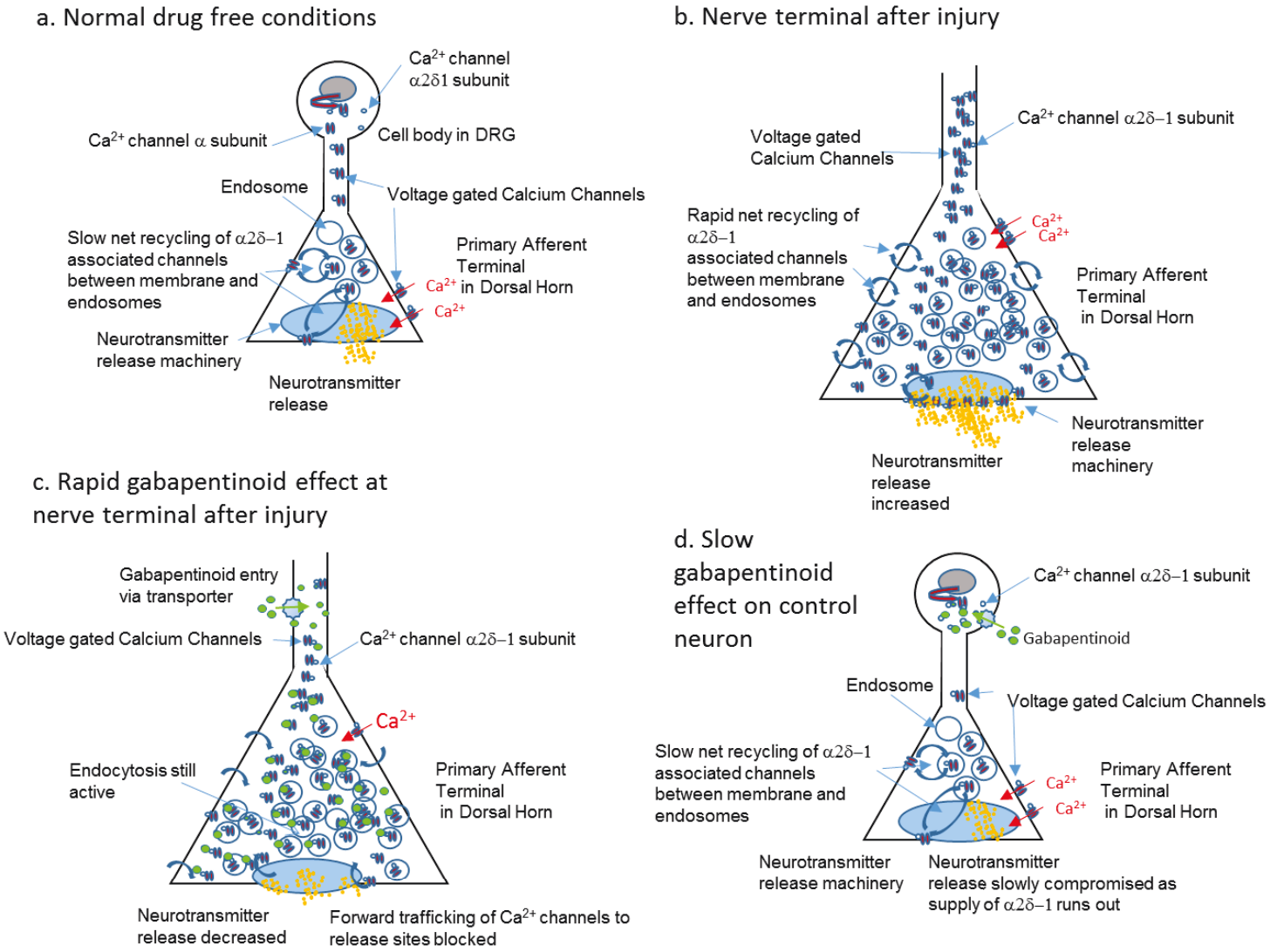
a. Normal drug free conditions
Ca2+ channel α2δ1 subunit
Ca2+ channel α subunit
Cell body in DRG
Endosome
Voltage gated Calcium Channels
Slow net recycling of α2δ–1 associated channels between membrane and endosomes
Primary Afferent Terminal in Dorsal Horn
Ca2+
Ca2+
Neurotransmitter release machinery
Neurotransmitter release
b. Nerve terminal after injury
Ca2+ channel α2δ–1 subunit
Voltage gated Calcium Channels
Rapid net recycling of α2δ–1 associated channels between membrane and endosomes
Ca2+
Ca2+
Primary Afferent Terminal in Dorsal Horn
Neurotransmitter release machinery
Neurotransmitter release increased
c. Rapid gabapentinoid effect at nerve terminal after injury
Gabapentinoid entry via transporter
Voltage gated Calcium Channels
Ca2+ channel α2δ–1 subunit
Ca2+
Endocytosis still active
Primary Afferent Terminal in Dorsal Horn
Neurotransmitter release decreased
Forward trafficking of Ca2+ channels to release sites blocked
d. Slow gabapentinoid effect on control neuron
Ca2+ channel α2δ–1 subunit
Gabapentinoid
Endosome
Voltage gated Calcium Channels
Slow net recycling of α2δ–1 associated channels between membrane and endosomes
Ca2+
Ca2+
Primary Afferent Terminal in Dorsal Horn
Neurotransmitter release machinery
Neurotransmitter release slowly compromised as supply of α2δ–1 runs out

Figure 6-2. Schematic representation of a dorsal root ganglion neuron and its terminal in the spinal dorsal horn to explain rapid and slowly developing effects of gabapentinoids. **a.** The α–subunits of HVA Ca^{2+} channels associate with α2δ–1 subunits and both are trafficked to the nerve terminal. α2δ–1 is responsible for trafficking channels to the plasma membrane thereby setting the abundance of functional HVA-Ca^{2+} channels and enabling their interaction with the neurotransmitter release machinery. Expressed channels are removed from the membrane by endocytosis into endosomes where they are targeted for recycling or degradation. With low, physiological levels of α2δ–1, the recycling of Ca^{2+} channels proceeds relatively slowly. **b.** Schematic representation of a primary afferent terminal when α2δ–1 levels are increased. The terminal becomes much more "busy", more Ca^{2+} channels may be targeted to the release machinery and neurotransmitter release is increased. The rate of channel turnover at the plasma membrane is assumed to be increased. **c.** In the presence of gabapentinoids, the rapid forward trafficking of HVA Ca^{2+} to the plasma membrane and release sites is decreased. Interruption of this rapid process may account for rapid acute effects of gabapentinoids in situations where α2δ1 is upregulated. **d.** Diagram to illustrate the slowly developing actions of gabapentinoids seen in naïve animals. Impaired trafficking of α2δ–1 subunits and α–subunits gradually depletes them at release sites and neurotransmitter release declines over a period of many hours. Reproduced with permission from Alles and Smith, 2016.

Figure 6-3

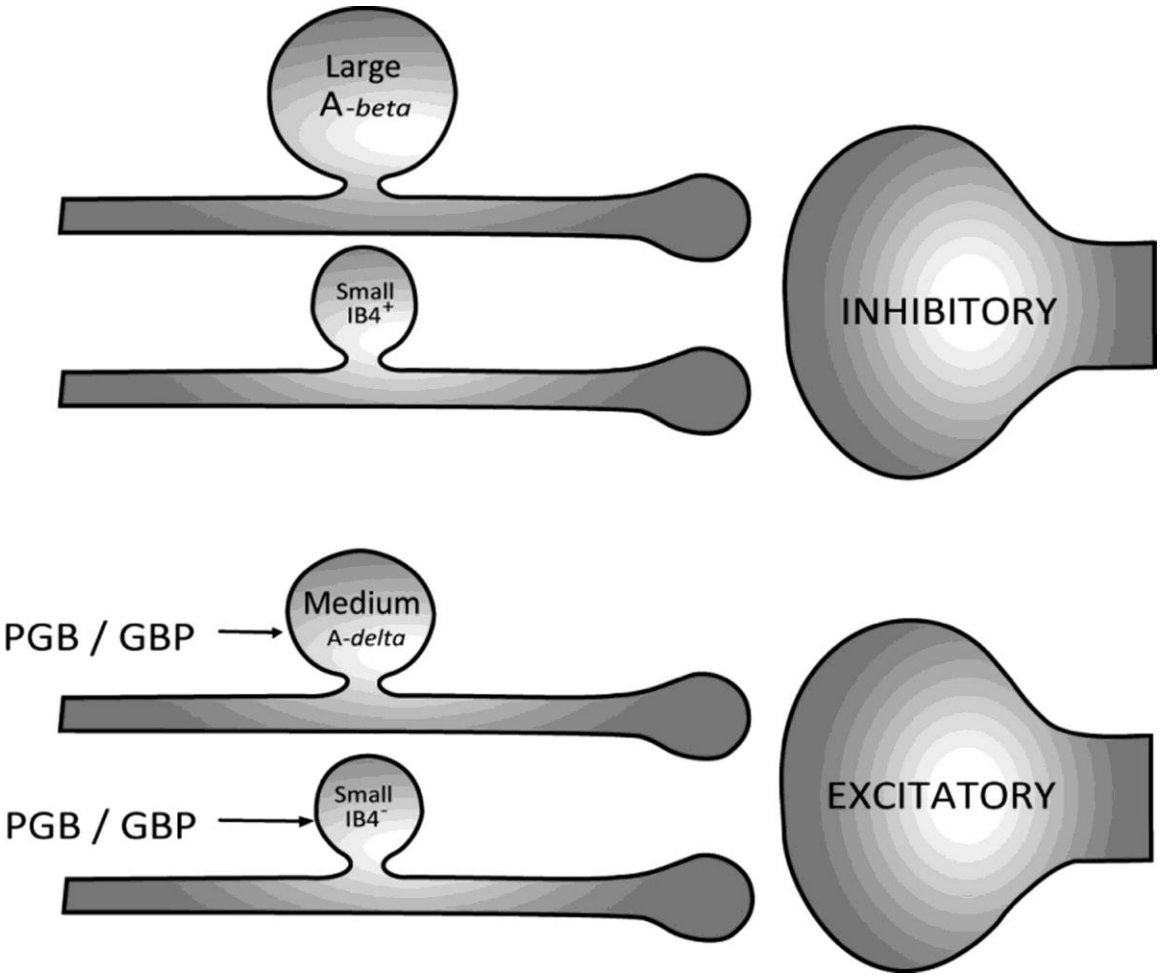

Figure 6-3. Schematic to explain the chronic effects of the gabapentinoids in the DRG and their relationship to actions in the spinal dorsal horn. The gabapentinoids (GBP and PGB) exert stronger effects on the medium-sized cell bodies associated with Aδ-fibers and on small IB4- neurons, which project to excitatory *substantia gelatinosa* neurons, whereas the cell bodies of large DRG neurons that associate with Aβ-fibers and of small IB4+ neurons that may project to inhibitory *substantia gelatinosa* neurons are less sensitive to these drugs. These chronic effects of the gabapentinoids may bear similarity to their acute actions on dorsal horn neurons to explain their cell-type specific actions. Reproduced with permission from Biggs et al, 2014a.

Figure 6-4

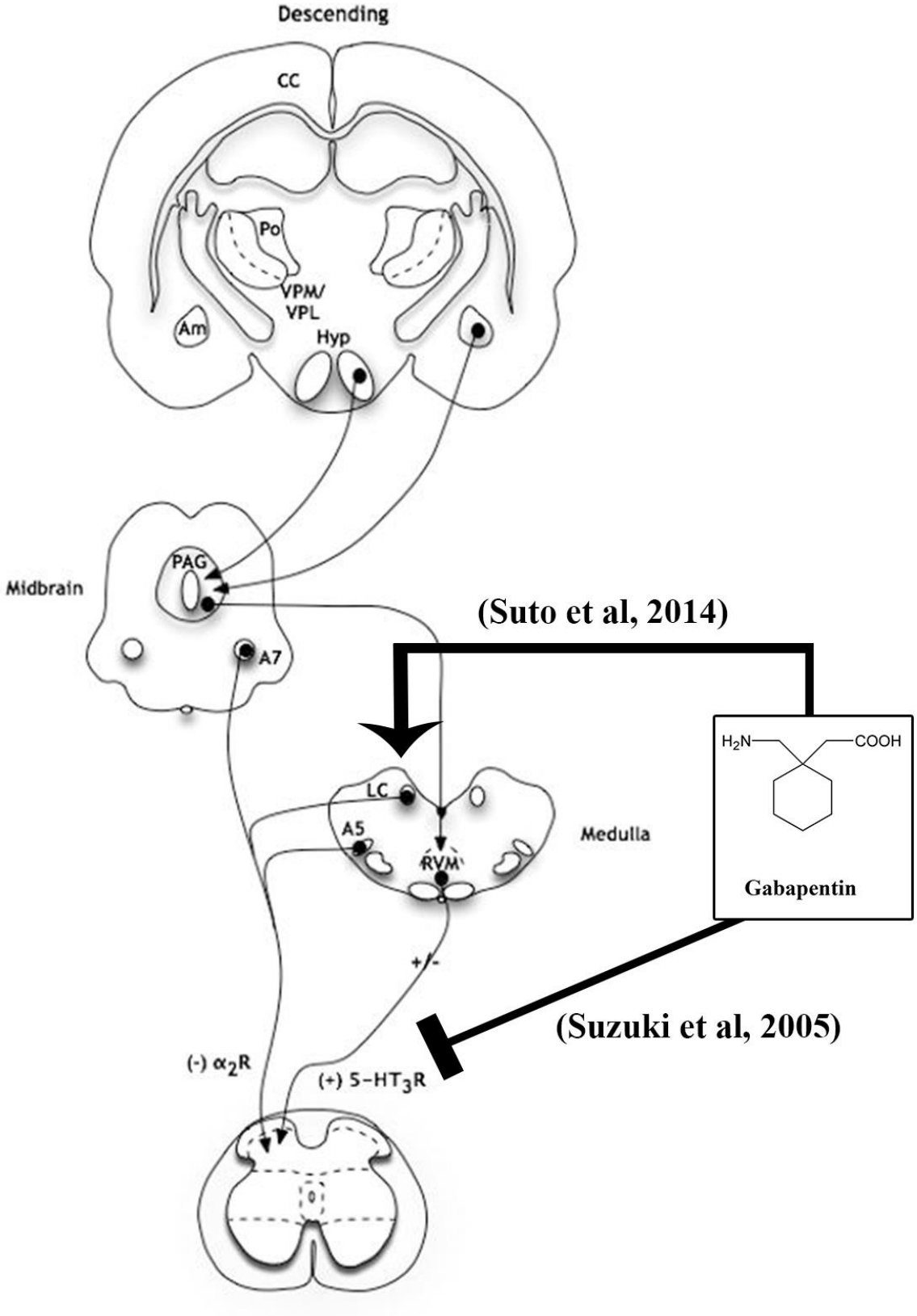
Descending
CC
Po
VPM/
VPL
Am
Hyp
Midbrain
PAG
A7
(Suto et al, 2014)
LC
A5
RVM
Medulla
H_2N
COOH
Gabapentin
+/-
(Suzuki et al, 2005)
(-) α_2R
(+) 5-HT_3R

Figure 6-4. Descending input from higher brain centres to the dorsal spinal cord and targets of gabapentin. Projections are integrated in the midbrain and brainstem, while inhibition is mediated by pre- and postsynaptic α2-adrenergic receptors in the dorsal horn (shown in A5, locus coeruleus, A7). Descending input from the rostral ventromedial medulla (RVM) is either excitatory or inhibitory. Suzuki et al., 2005 have shown that gabapentin (GBP) inhibits $5HT_3$-mediated pathways from the brain to spinal cord in neuropathic rats. Suto et al., 2014 have shown that GBP increases glutamate release in the locus coeruleus (LC) via astroglial glutamate-transporter-1 (GLT-1) dependent mechanisms. (Am: amygdala; Hyp: hypothalamus; VPM and VPL: thalamic nuclei; Po: posterior thalamic nuclei; CC: cingulate cortex; LC: locus coeruleus; PAG: periaqueductal grey). Modified with permission from Sikandar and Dickenson, 2012.

Figure 6-5

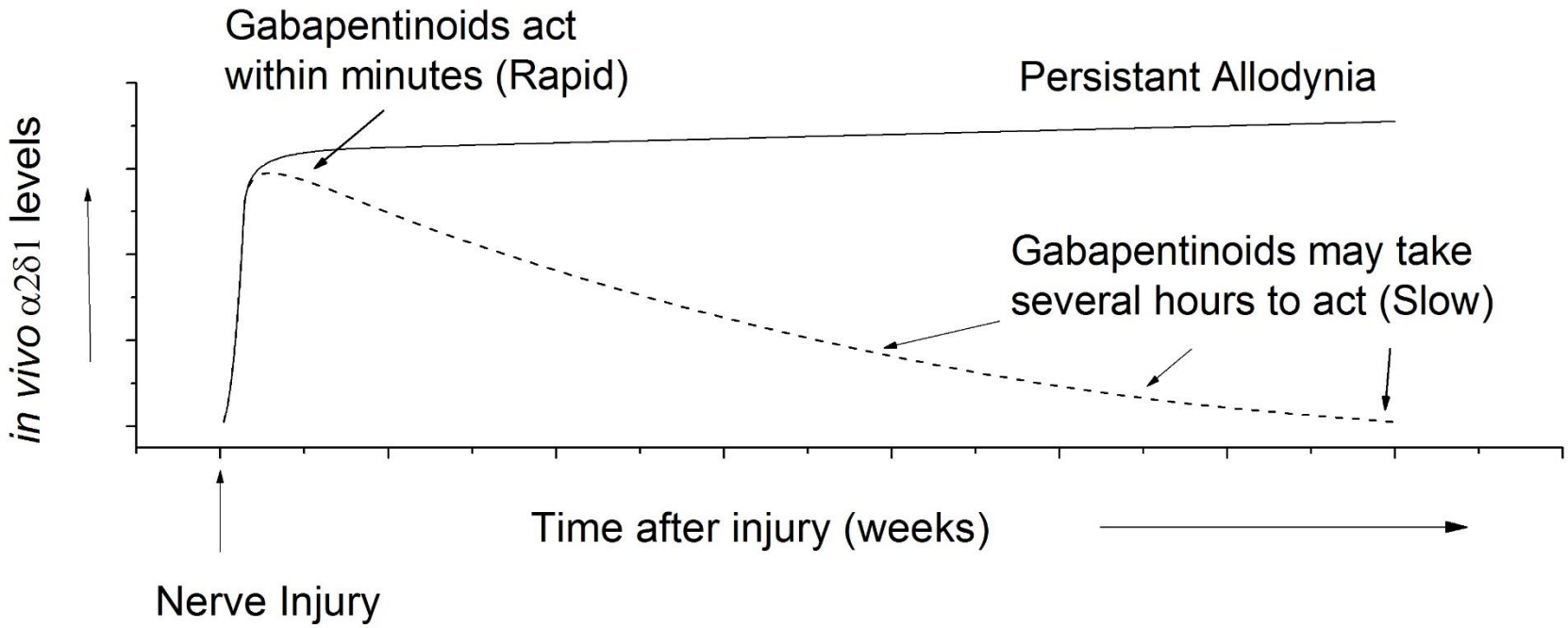

Figure 6-5. Proposed effectiveness of acute GBP with time post-injury and relationship to *in vivo* α2δ-1 levels. In the days or weeks following injury, α2δ levels are increased and gabapentinoids act rapidly. Although allodynia may persist indefinitely after injury, α2δ levels may return to control levels, this would predict slowly developing effects of gabapentinoids that may parallel the clinical situation. Reproduced with permission from Alles and Smith, 2016.

References

INTRODUCTION

ABDULLA, F. A. & SMITH, P. A. 1998. Axotomy reduces the effect of analgesic opioids yet increases the effect of nociceptin on dorsal root ganglion neurons. *J Neurosci,* 18**,** 9685-94.

ABDULLA, F. A. & SMITH, P. A. 2001a. Axotomy- and autotomy-induced changes in Ca2+ and K+ channel currents of rat dorsal root ganglion neurons. *J Neurophysiol,* 85**,** 644-58.

ABDULLA, F. A. & SMITH, P. A. 2001b. Axotomy- and autotomy-induced changes in the excitability of rat dorsal root ganglion neurons. *J Neurophysiol,* 85**,** 630-43.

ABDULLA, F. A. & SMITH, P. A. 2002. Changes in Na(+) channel currents of rat dorsal root ganglion neurons following axotomy and axotomy-induced autotomy. *J Neurophysiol,* 88**,** 2518-29.

ALLES, S.R.A. and SMITH, P.A. 2016. The anti-allodynic gabapentinoids: myths, paradoxes and acute effects. *Neuroscientist* (in press)

ARIKKATH, J. & CAMPBELL, K. P. 2003. Auxiliary subunits: essential components of the voltage-gated calcium channel complex. *Curr Opin Neurobiol,* 13**,** 298-307.

BALASUBRAMANYAN, S., STEMKOWSKI, P. L., STEBBING, M. J. & SMITH, P. A. 2006. Sciatic chronic constriction injury produces cell-type-specific changes in the electrophysiological properties of rat substantia gelatinosa neurons. *J Neurophysiol,* 96**,** 579-90.

BALIKI, M. N., CHIALVO, D. R., GEHA, P. Y., LEVY, R. M., HARDEN, R. N., PARRISH, T. B. & APKARIAN, A. V. 2006. Chronic pain and the emotional brain: specific brain

activity associated with spontaneous fluctuations of intensity of chronic back pain. *J Neurosci,* 26**,** 12165-73.

BAUER, C. S., NIETO-ROSTRO, M., RAHMAN, W., TRAN-VAN-MINH, A., FERRON, L., DOUGLAS, L., KADURIN, I., SRI RANJAN, Y., FERNANDEZ-ALACID, L., MILLAR, N. S., DICKENSON, A. H., LUJAN, R. & DOLPHIN, A. C. 2009. The increased trafficking of the calcium channel subunit alpha2delta-1 to presynaptic terminals in neuropathic pain is inhibited by the alpha2delta ligand pregabalin. *J Neurosci,* 29**,** 4076-88.

BAUER, C. S., RAHMAN, W., TRAN-VAN-MINH, A., LUJAN, R., DICKENSON, A. H. & DOLPHIN, A. C. 2010a. The anti-allodynic alpha(2)delta ligand pregabalin inhibits the trafficking of the calcium channel alpha(2)delta-1 subunit to presynaptic terminals in vivo. *Biochem Soc Trans,* 38**,** 525-8.

BAUER, C. S., TRAN-VAN-MINH, A., KADURIN, I. & DOLPHIN, A. C. 2010b. A new look at calcium channel alpha2delta subunits. *Curr Opin Neurobiol,* 20**,** 563-71.

BEAR, M. F., CONNORS, B. W. & PARADISO, M. A. 2007. *Neuroscience : exploring the brain,* Philadelphia, PA, Lippincott Williams & Wilkins.

BENNETT, G. J. & XIE, Y. K. 1988. A peripheral mononeuropathy in rat that produces disorders of pain sensation like those seen in man. *Pain,* 33**,** 87-107.

BIGGS, J. E., BOAKYE, P. A., GANESAN, N., STEMKOWSKI, P. L., GARCIA, A. L., BALLANYI, K. & SMITH, P. A. 2014a. Analysis of the Long-Term Actions of Gabapentin and Pregabalin in Dorsal Root Ganglia and Substantia Gelatinosa. *J Neurophysiol*.

BIGGS, J. E., STEMKOWSKI, P. L., KNAUS, E. E., CHOWDHURY, M. A., BALLANYI, K. & SMITH, P. A. 2014b. Suppression of network activity in dorsal horn by gabapentin permeation of TRPV1 channels: Implications for drug access to cytoplasmic targets. *Neurosci Lett*.

BINSHTOK, A. M., WANG, H., ZIMMERMANN, K., AMAYA, F., VARDEH, D., SHI, L., BRENNER, G. J., JI, R. R., BEAN, B. P., WOOLF, C. J. & SAMAD, T. A. 2008. Nociceptors are interleukin-1beta sensors. *J Neurosci,* 28**,** 14062-73.

BOCCARD, S. G., PEREIRA, E. A. & AZIZ, T. Z. 2015. Deep brain stimulation for chronic pain. *J Clin Neurosci*.

BOROUJERDI, A., KIM, H. K., LYU, Y. S., KIM, D. S., FIGUEROA, K. W., CHUNG, J. M. & LUO, Z. D. 2008. Injury discharges regulate calcium channel alpha-2-delta-1 subunit upregulation in the dorsal horn that contributes to initiation of neuropathic pain. *Pain,* 139**,** 358-66.

BOURINET, E., ALTIER, C., HILDEBRAND, M. E., TRANG, T., SALTER, M. W. & ZAMPONI, G. W. 2014. Calcium-permeable ion channels in pain signaling. *Physiol Rev,* 94**,** 81-140.

BRIL, V., ENGLAND, J., FRANKLIN, G. M., BACKONJA, M., COHEN, J., DEL TORO, D., FELDMAN, E., IVERSON, D. J., PERKINS, B., RUSSELL, J. W. & ZOCHODNE, D. 2011. Evidence-based guideline: Treatment of painful diabetic neuropathy: report of the American Academy of Neurology, the American Association of Neuromuscular and Electrodiagnostic Medicine, and the American Academy of Physical Medicine and Rehabilitation. *Neurology,* 76**,** 1758-65.

CAO, Y. Q. & TSIEN, R. W. 2010. Different relationship of N- and P/Q-type Ca2+ channels to channel-interacting slots in controlling neurotransmission at cultured hippocampal synapses. *J Neurosci,* 30**,** 4536-46.

CAROZZI, V. A., CANTA, A. & CHIORAZZI, A. 2015. Chemotherapy-induced peripheral neuropathy: What do we know about mechanisms? *Neurosci Lett,* 596**,** 90-107.

CASSIDY, J. S., FERRON, L., KADURIN, I., PRATT, W. S. & DOLPHIN, A. C. 2014. Functional exofacially tagged N-type calcium channels elucidate the interaction with auxiliary alpha2delta-1 subunits. *Proc Natl Acad Sci U S A,* 111**,** 8979-84.

CHAPLAN, S. R., GUO, H. Q., LEE, D. H., LUO, L., LIU, C., KUEI, C., VELUMIAN, A. A., BUTLER, M. P., BROWN, S. M. & DUBIN, A. E. 2003. Neuronal hyperpolarization-activated pacemaker channels drive neuropathic pain. *J Neurosci,* 23**,** 1169-78.

CHEN, Y., BALASUBRAMANYAN, S., LAI, A. Y., TODD, K. G. & SMITH, P. A. 2009. Effects of sciatic nerve axotomy on excitatory synaptic transmission in rat substantia gelatinosa. *J Neurophysiol,* 102**,** 3203-15.

CHESHIRE, W. P., JR. 2002. Defining the role for gabapentin in the treatment of trigeminal neuralgia: a retrospective study. *J Pain,* 3**,** 137-42.

CHRISTOPHERSON, K. S., ULLIAN, E. M., STOKES, C. C., MULLOWNEY, C. E., HELL, J. W., AGAH, A., LAWLER, J., MOSHER, D. F., BORNSTEIN, P. & BARRES, B. A. 2005. Thrombospondins are astrocyte-secreted proteins that promote CNS synaptogenesis. *Cell,* 120**,** 421-33.

CODERRE, T. J., KUMAR, N., LEFEBVRE, C. D. & YU, J. S. 2005. Evidence that gabapentin reduces neuropathic pain by inhibiting the spinal release of glutamate. *J Neurochem,* 94**,** 1131-9.

COSTIGAN, M., SCHOLZ, J. & WOOLF, C. J. 2009. Neuropathic pain: a maladaptive response of the nervous system to damage. *Annu Rev Neurosci,* 32**,** 1-32.

COULL, J. A., BEGGS, S., BOUDREAU, D., BOIVIN, D., TSUDA, M., INOUE, K., GRAVEL, C., SALTER, M. W. & DE KONINCK, Y. 2005. BDNF from microglia causes the shift in neuronal anion gradient underlying neuropathic pain. *Nature,* 438**,** 1017-21.

COULL, J. A., BOUDREAU, D., BACHAND, K., PRESCOTT, S. A., NAULT, F., SIK, A., DE KONINCK, P. & DE KONINCK, Y. 2003. Trans-synaptic shift in anion gradient in spinal lamina I neurons as a mechanism of neuropathic pain. *Nature,* 424**,** 938-42.

CROSBY, N. D., ZAUCKE, F., KRAS, J. V., DONG, L., LUO, Z. D. & WINKELSTEIN, B. A. 2015. Thrombospondin-4 and excitatory synaptogenesis promote spinal sensitization after painful mechanical joint injury. *Exp Neurol,* 264**,** 111-20.

DAVIES, A., KADURIN, I., ALVAREZ-LAVIADA, A., DOUGLAS, L., NIETO-ROSTRO, M., BAUER, C. S., PRATT, W. S. & DOLPHIN, A. C. 2010. The alpha2delta subunits of voltage-gated calcium channels form GPI-anchored proteins, a posttranslational modification essential for function. *Proc Natl Acad Sci U S A,* 107**,** 1654-9.

DECOSTERD, I. & WOOLF, C. J. 2000. Spared nerve injury: an animal model of persistent peripheral neuropathic pain. *Pain,* 87**,** 149-58.

DEVOR, M. 1991a. Neuropathic pain and injured nerve: peripheral mechanisms. *Br Med Bull,* 47**,** 619-30.

DEVOR, M. 1991b. Sensory basis of autotomy in rats. *Pain,* 45**,** 109-10.

DEVOR, M. 2006. Centralization, central sensitization and neuropathic pain. Focus on "sciatic chronic constriction injury produces cell-type-specific changes in the electrophysiological properties of rat substantia gelatinosa neurons". *J Neurophysiol,* 96**,** 522-3.

DEVOR, M. & GOVRIN-LIPPMANN, R. 1983. Axoplasmic transport block reduces ectopic impulse generation in injured peripheral nerves. *Pain,* 16**,** 73-85.

DEVOR, M. & WALL, P. D. 1978. Reorganisation of spinal cord sensory map after peripheral nerve injury. *Nature,* 276**,** 75-6.

DEVOR, M., WALL, P. D. & CATALAN, N. 1992. Systemic lidocaine silences ectopic neuroma and DRG discharge without blocking nerve conduction. *Pain,* 48**,** 261-8.

DIB-HAJJ, S. D., BLACK, J. A. & WAXMAN, S. G. 2015. Na1.9: a sodium channel linked to human pain. *Nat Rev Neurosci*.

DICKMAN, D. K., KURSHAN, P. T. & SCHWARZ, T. L. 2008. Mutations in a Drosophila alpha2delta voltage-gated calcium channel subunit reveal a crucial synaptic function. *J Neurosci,* 28**,** 31-8.

DODGE, F. A., JR. & RAHAMIMOFF, R. 1967. Co-operative action a calcium ions in transmitter release at the neuromuscular junction. *J Physiol,* 193**,** 419-32.

DOLPHIN, A. C. 2013. The alpha2delta subunits of voltage-gated calcium channels. *Biochim Biophys Acta,* 1828**,** 1541-9.

EHDE, D. M., DILLWORTH, T. M. & TURNER, J. A. 2014. Cognitive-behavioral therapy for individuals with chronic pain: efficacy, innovations, and directions for research. *Am Psychol,* 69**,** 153-66.

EMERY, E. C., YOUNG, G. T., BERROCOSO, E. M., CHEN, L. & MCNAUGHTON, P. A. 2011. HCN2 ion channels play a central role in inflammatory and neuropathic pain. *Science,* 333**,** 1462-6.

EROGLU, C., ALLEN, N. J., SUSMAN, M. W., O'ROURKE, N. A., PARK, C. Y., OZKAN, E., CHAKRABORTY, C., MULINYAWE, S. B., ANNIS, D. S., HUBERMAN, A. D.,

GREEN, E. M., LAWLER, J., DOLMETSCH, R., GARCIA, K. C., SMITH, S. J., LUO, Z. D., ROSENTHAL, A., MOSHER, D. F. & BARRES, B. A. 2009. Gabapentin receptor alpha2delta-1 is a neuronal thrombospondin receptor responsible for excitatory CNS synaptogenesis. *Cell,* 139**,** 380-92.

ERTEL, E. A., CAMPBELL, K. P., HARPOLD, M. M., HOFMANN, F., MORI, Y., PEREZ-REYES, E., SCHWARTZ, A., SNUTCH, T. P., TANABE, T., BIRNBAUMER, L., TSIEN, R. W. & CATTERALL, W. A. 2000. Nomenclature of voltage-gated calcium channels. *Neuron,* 25**,** 533-5.

FIELD, M. J., COX, P. J., STOTT, E., MELROSE, H., OFFORD, J., SU, T. Z., BRAMWELL, S., CORRADINI, L., ENGLAND, S., WINKS, J., KINLOCH, R. A., HENDRICH, J., DOLPHIN, A. C., WEBB, T. & WILLIAMS, D. 2006. Identification of the alpha2-delta-1 subunit of voltage-dependent calcium channels as a molecular target for pain mediating the analgesic actions of pregabalin. *Proc Natl Acad Sci U S A,* 103**,** 17537-42.

FRIED, K. & DEVOR, M. 1988. End-structure of afferent axons injured in the peripheral and central nervous system. *Somatosens Mot Res,* 6**,** 79-99.

FRIEDLE, S. A., CURET, M. A. & WATTERS, J. J. 2010. Recent patents on novel P2X(7) receptor antagonists and their potential for reducing central nervous system inflammation. *Recent Pat CNS Drug Discov,* 5**,** 35-45.

GAO, F. & ZHENG, Z. M. 2014. Animal models of diabetic neuropathic pain. *Exp Clin Endocrinol Diabetes,* 122**,** 100-6.

GARCIA-LARREA, L. & PEYRON, R. 2013. Pain matrices and neuropathic pain matrices: a review. *Pain,* 154 Suppl 1**,** S29-43.

GEE, N. S., BROWN, J. P., DISSANAYAKE, V. U., OFFORD, J., THURLOW, R. & WOODRUFF, G. N. 1996. The novel anticonvulsant drug, gabapentin (Neurontin), binds to the alpha2delta subunit of a calcium channel. *J Biol Chem,* 271**,** 5768-76.

GILRON, I., BARON, R. & JENSEN, T. 2015. Neuropathic pain: principles of diagnosis and treatment. *Mayo Clin Proc,* 90**,** 532-45.

GILRON, I. & DICKENSON, A. H. 2014. Emerging drugs for neuropathic pain. *Expert Opin Emerg Drugs,* 19**,** 329-41.

GILRON, I., WATSON, C. P., CAHILL, C. M. & MOULIN, D. E. 2006. Neuropathic pain: a practical guide for the clinician. *CMAJ,* 175**,** 265-75.

GOTTRUP, H., JUHL, G., KRISTENSEN, A. D., LAI, R., CHIZH, B. A., BROWN, J., BACH, F. W. & JENSEN, T. S. 2004. Chronic oral gabapentin reduces elements of central sensitization in human experimental hyperalgesia. *Anesthesiology,* 101**,** 1400-8.

GRACE, P. M., HUTCHINSON, M. R., MAIER, S. F. & WATKINS, L. R. 2014. Pathological pain and the neuroimmune interface. *Nat Rev Immunol,* 14**,** 217-31.

GUEDON, J. M., WU, S., ZHENG, X., CHURCHILL, C. C., GLORIOSO, J. C., LIU, C. H., LIU, S., VULCHANOVA, L., BEKKER, A., TAO, Y. X., KINCHINGTON, P. R., GOINS, W. F., FAIRBANKS, C. A. & HAO, S. 2015. Current gene therapy using viral vectors for chronic pain. *Mol Pain,* 11**,** 27.

HEBLICH, F., TRAN VAN MINH, A., HENDRICH, J., WATSCHINGER, K. & DOLPHIN, A. C. 2008. Time course and specificity of the pharmacological disruption of the trafficking of voltage-gated calcium channels by gabapentin. *Channels (Austin),* 2**,** 4-9.

HENDRICH, J., BAUER, C. S. & DOLPHIN, A. C. 2012. Chronic pregabalin inhibits synaptic transmission between rat dorsal root ganglion and dorsal horn neurons in culture. *Channels (Austin),* 6**,** 124-32.

HENDRICH, J., VAN MINH, A. T., HEBLICH, F., NIETO-ROSTRO, M., WATSCHINGER, K., STRIESSNIG, J., WRATTEN, J., DAVIES, A. & DOLPHIN, A. C. 2008. Pharmacological disruption of calcium channel trafficking by the alpha2delta ligand gabapentin. *Proc Natl Acad Sci U S A,* 105**,** 3628-33.

HILDEBRAND, M. E., SMITH, P. L., BLADEN, C., EDULJEE, C., XIE, J. Y., CHEN, L., FEE-MAKI, M., DOERING, C. J., MEZEYOVA, J., ZHU, Y., BELARDETTI, F., PAJOUHESH, H., PARKER, D., ARNERIC, S. P., PARMAR, M., PORRECA, F., TRINGHAM, E., ZAMPONI, G. W. & SNUTCH, T. P. 2011. A novel slow-inactivation-specific ion channel modulator attenuates neuropathic pain. *Pain,* 152**,** 833-43.

HOLTZMAN, S. & BEGGS, R. T. 2013. Yoga for chronic low back pain: a meta-analysis of randomized controlled trials. *Pain Res Manag,* 18**,** 267-72.

HOPPA, M. B., LANA, B., MARGAS, W., DOLPHIN, A. C. & RYAN, T. A. 2012. alpha2delta expression sets presynaptic calcium channel abundance and release probability. *Nature,* 486**,** 122-5.

HUNT, S. P. & MANTYH, P. W. 2001. The molecular dynamics of pain control. *Nat Rev Neurosci,* 2**,** 83-91.

HUNTER, J. C., GOGAS, K. R., HEDLEY, L. R., JACOBSON, L. O., KASSOTAKIS, L., THOMPSON, J. & FONTANA, D. J. 1997. The effect of novel anti-epileptic drugs in rat experimental models of acute and chronic pain. *Eur J Pharmacol,* 324**,** 153-60.

IOM 2011. *Relieving Pain in America: A Blueprint for Transforming Prevention, Care, Education, and Research.* Washington (DC): The National Academies Press.

JENSEN, T. S., BARON, R., HAANPAA, M., KALSO, E., LOESER, J. D., RICE, A. S. & TREEDE, R. D. 2011. A new definition of neuropathic pain. *Pain,* 152**,** 2204-5.

JONES, A. K., KULKARNI, B. & DERBYSHIRE, S. W. 2003. Pain mechanisms and their disorders. *Br Med Bull,* 65**,** 83-93.

KANDEL, E. R., SCHWARTZ, J. H. & JESSELL, T. M. 2000. *Principles of neural science,* New York, McGraw-Hill, Health Professions Division.

KIM, D. S., LI, K. W., BOROUJERDI, A., PETER YU, Y., ZHOU, C. Y., DENG, P., PARK, J., ZHANG, X., LEE, J., CORPE, M., SHARP, K., STEWARD, O., EROGLU, C., BARRES, B., ZAUCKE, F., XU, Z. C. & LUO, Z. D. 2012. Thrombospondin-4 contributes to spinal sensitization and neuropathic pain states. *J Neurosci,* 32**,** 8977-87.

KIM, K. J., YOON, Y. W. & CHUNG, J. M. 1997. Comparison of three rodent neuropathic pain models. *Exp Brain Res,* 113**,** 200-6.

KIM, S. H. & CHUNG, J. M. 1992. An experimental model for peripheral neuropathy produced by segmental spinal nerve ligation in the rat. *Pain,* 50**,** 355-63.

KOHNO, T., JI, R. R., ITO, N., ALLCHORNE, A. J., BEFORT, K., KARCHEWSKI, L. A. & WOOLF, C. J. 2005. Peripheral axonal injury results in reduced mu opioid receptor pre- and post-synaptic action in the spinal cord. *Pain,* 117**,** 77-87.

KUMAR, N., CHERKAS, P. S., VARATHAN, V., MIYAMOTO, M., CHIANG, C. Y., DOSTROVSKY, J. O., SESSLE, B. J. & CODERRE, T. J. 2013. Systemic pregabalin attenuates facial hypersensitivity and noxious stimulus-evoked release of glutamate in

medullary dorsal horn in a rodent model of trigeminal neuropathic pain. *Neurochem Int,* 62**,** 831-5.

LANNEAU, C., GREEN, A., HIRST, W. D., WISE, A., BROWN, J. T., DONNIER, E., CHARLES, K. J., WOOD, M., DAVIES, C. H. & PANGALOS, M. N. 2001. Gabapentin is not a GABAB receptor agonist. *Neuropharmacology,* 41**,** 965-75.

LEE, J. H., PARK, C. K., CHEN, G., HAN, Q., XIE, R. G., LIU, T., JI, R. R. & LEE, S. Y. 2014. A monoclonal antibody that targets a NaV1.7 channel voltage sensor for pain and itch relief. *Cell,* 157**,** 1393-404.

LEITNER, J., WESTERHOLZ, S., HEINKE, B., FORSTHUBER, L., WUNDERBALDINGER, G., JAGER, T., GRUBER-SCHOFFNEGGER, D., BRAUN, K. & SANDKUHLER, J. 2013. Impaired excitatory drive to spinal GABAergic neurons of neuropathic mice. *PLoS One,* 8**,** e73370.

LEUNG, A., FALLAH, A. & SHUKLA, S. 2014. Transcutaneous magnetic stimulation (TMS) in alleviating post-traumatic peripheral neuropathic pain States: a case series. *Pain Med,* 15**,** 1196-9.

LI, K. W., YU, Y. P., ZHOU, C., KIM, D. S., LIN, B., SHARP, K., STEWARD, O. & LUO, Z. D. 2014. Calcium channel alpha2delta1 proteins mediate trigeminal neuropathic pain states associated with aberrant excitatory synaptogenesis. *J Biol Chem,* 289**,** 7025-37.

LI, Z., TAYLOR, C. P., WEBER, M., PIECHAN, J., PRIOR, F., BIAN, F., CUI, M., HOFFMAN, D. & DONEVAN, S. 2011. Pregabalin is a potent and selective ligand for alpha(2)delta-1 and alpha(2)delta-2 calcium channel subunits. *Eur J Pharmacol,* 667**,** 80-90.

LIU, C. N., WALL, P. D., BEN-DOR, E., MICHAELIS, M., AMIR, R. & DEVOR, M. 2000. Tactile allodynia in the absence of C-fiber activation: altered firing properties of DRG neurons following spinal nerve injury. *Pain,* 85**,** 503-21.

LU, V. B., BALLANYI, K., COLMERS, W. F. & SMITH, P. A. 2007. Neuron type-specific effects of brain-derived neurotrophic factor in rat superficial dorsal horn and their relevance to 'central sensitization'. *J Physiol,* 584**,** 543-63.

LU, V. B., BIGGS, J. E., STEBBING, M. J., BALASUBRAMANYAN, S., TODD, K. G., LAI, A. Y., COLMERS, W. F., DAWBARN, D., BALLANYI, K. & SMITH, P. A. 2009. Brain-derived neurotrophic factor drives the changes in excitatory synaptic transmission in the rat superficial dorsal horn that follow sciatic nerve injury. *J Physiol,* 587**,** 1013-32.

LUO, C., KUNER, T. & KUNER, R. 2014. Synaptic plasticity in pathological pain. *Trends Neurosci,* 37**,** 343-55.

LUO, Z. D., CALCUTT, N. A., HIGUERA, E. S., VALDER, C. R., SONG, Y. H., SVENSSON, C. I. & MYERS, R. R. 2002. Injury type-specific calcium channel alpha 2 delta-1 subunit up-regulation in rat neuropathic pain models correlates with antiallodynic effects of gabapentin. *J Pharmacol Exp Ther,* 303**,** 1199-205.

LUO, Z. D., CHAPLAN, S. R., HIGUERA, E. S., SORKIN, L. S., STAUDERMAN, K. A., WILLIAMS, M. E. & YAKSH, T. L. 2001. Upregulation of dorsal root ganglion (alpha)2(delta) calcium channel subunit and its correlation with allodynia in spinal nerve-injured rats. *J Neurosci,* 21**,** 1868-75.

MARAIS, E., KLUGBAUER, N. & HOFMANN, F. 2001. Calcium channel alpha(2)delta subunits-structure and Gabapentin binding. *Mol Pharmacol,* 59**,** 1243-8.

MATHIE, A. & VEALE, E. L. 2015. Two-pore domain potassium channels: potential therapeutic targets for the treatment of pain. *Pflugers Arch,* 467**,** 931-43.

MELZACK, R. & WALL, P. D. 1965. Pain mechanisms: a new theory. *Science,* 150**,** 971-9.

MERSKEY, H., BOGDUK, N. & INTERNATIONAL ASSOCIATION FOR THE STUDY OF PAIN. TASK FORCE ON TAXONOMY. 1994. *Classification of chronic pain : descriptions of chronic pain syndromes and definitions of pain terms,* Seattle, IASP Press.

MOORE, K. A., BABA, H. & WOOLF, C. J. 2002. Gabapentin-- actions on adult superficial dorsal horn neurons. *Neuropharmacology,* 43**,** 1077-81.

MOORE, R. A., WIFFEN, P. J., DERRY, S., TOELLE, T. & RICE, A. S. 2014. Gabapentin for chronic neuropathic pain and fibromyalgia in adults. *Cochrane Database Syst Rev,* 27.

MOSCONI, T. & KRUGER, L. 1996. Fixed-diameter polyethylene cuffs applied to the rat sciatic nerve induce a painful neuropathy: ultrastructural morphometric analysis of axonal alterations. *Pain,* 64**,** 37-57.

MOULIN, D. E., CLARK, A. J., GILRON, I., WARE, M. A., WATSON, C. P., SESSLE, B. J., CODERRE, T., MORLEY-FORSTER, P. K., STINSON, J., BOULANGER, A., PENG, P., FINLEY, G. A., TAENZER, P., SQUIRE, P., DION, D., CHOLKAN, A., GILANI, A., GORDON, A., HENRY, J., JOVEY, R., LYNCH, M., MAILIS-GAGNON, A., PANJU, A., ROLLMAN, G. B., VELLY, A. & CANADIAN PAIN, S. 2007. Pharmacological management of chronic neuropathic pain - consensus statement and guidelines from the Canadian Pain Society. *Pain Res Manag,* 12**,** 13-21.

NAGY, J. I. & HUNT, S. P. 1982. Fluoride-resistant acid phosphatase-containing neurones in dorsal root ganglia are separate from those containing substance P or somatostatin. *Neuroscience,* 7**,** 89-97.

NARITA, N., KUMAR, N., CHERKAS, P. S., CHIANG, C. Y., DOSTROVSKY, J. O., CODERRE, T. J. & SESSLE, B. J. 2012. Systemic pregabalin attenuates sensorimotor responses and medullary glutamate release in inflammatory tooth pain model. *Neuroscience,* 218**,** 359-66.

NGUYEN, D., DENG, P., MATTHEWS, E. A., KIM, D. S., FENG, G., DICKENSON, A. H., XU, Z. C. & LUO, Z. D. 2009. Enhanced pre-synaptic glutamate release in deep-dorsal horn contributes to calcium channel alpha-2-delta-1 protein-mediated spinal sensitization and behavioral hypersensitivity. *Mol Pain,* 5**,** 6.

NOH, S., KUMAR, N., BUKHANOVA, N., CHEN, Y., STEMKOWSI, P. L. & SMITH, P. A. 2014. The heart-rate-reducing agent, ivabradine, reduces mechanical allodynia in a rodent model of neuropathic pain. *Eur J Pain,* 18**,** 1139-47.

NORRBRINK, C. & LUNDEBERG, T. 2011. Acupuncture and massage therapy for neuropathic pain following spinal cord injury: an exploratory study. *Acupunct Med,* 29**,** 108-15.

PAN, B., YU, H., PARK, J., YU, Y. P., LUO, Z. D. & HOGAN, Q. H. 2015. Painful nerve injury upregulates thrombospondin-4 expression in dorsal root ganglia. *J Neurosci Res,* 93**,** 443-53.

PATEL, R., BAUER, C. S., NIETO-ROSTRO, M., MARGAS, W., FERRON, L., CHAGGAR, K., CREWS, K., RAMIREZ, J. D., BENNETT, D. L., SCHWARTZ, A., DICKENSON, A. H. & DOLPHIN, A. C. 2013. alpha2delta-1 gene deletion affects somatosensory neuron function and delays mechanical hypersensitivity in response to peripheral nerve damage. *J Neurosci,* 33**,** 16412-26.

PITCHER, G. M. & HENRY, J. L. 2008. Governing role of primary afferent drive in increased excitation of spinal nociceptive neurons in a model of sciatic neuropathy. *Exp Neurol,* 214**,** 219-28.

POLOMANO, R. C., MANNES, A. J., CLARK, U. S. & BENNETT, G. J. 2001. A painful peripheral neuropathy in the rat produced by the chemotherapeutic drug, paclitaxel. *Pain,* 94**,** 293-304.

PORRECA, F., OSSIPOV, M. H. & GEBHART, G. F. 2002. Chronic pain and medullary descending facilitation. *Trends Neurosci,* 25**,** 319-25.

PUNNAKKAL, P., VON SCHOULTZ, C., HAENRAETS, K., WILDNER, H. & ZEILHOFER, H. U. 2014. Morphological, biophysical and synaptic properties of glutamatergic neurons of the mouse spinal dorsal horn. *J Physiol,* 592**,** 759-76.

RETTIG, J., SHENG, Z. H., KIM, D. K., HODSON, C. D., SNUTCH, T. P. & CATTERALL, W. A. 1996. Isoform-specific interaction of the alpha1A subunits of brain Ca2+ channels with the presynaptic proteins syntaxin and SNAP-25. *Proc Natl Acad Sci U S A,* 93**,** 7363-8.

REXED, B. 1952. The cytoarchitectonic organization of the spinal cord in the cat. *J Comp Neurol,* 96**,** 414-95.

RIVARA, M. & ZULIANI, V. 2015. Novel sodium channel antagonists in the treatment of neuropathic pain. *Expert Opin Investig Drugs*.

ROTSHENKER, S. 2011. Wallerian degeneration: the innate-immune response to traumatic nerve injury. *J Neuroinflammation,* 8**,** 109.

RUSCHEWEYH, R. & SANDKUHLER, J. 2002. Lamina-specific membrane and discharge properties of rat spinal dorsal horn neurones in vitro. *J Physiol,* 541**,** 231-44.

RUSSO, C. M. & BROSE, W. G. 1998. Chronic pain. *Annu Rev Med,* 49**,** 123-33.

SAEGUSA, H., KURIHARA, T., ZONG, S., KAZUNO, A., MATSUDA, Y., NONAKA, T., HAN, W., TORIYAMA, H. & TANABE, T. 2001. Suppression of inflammatory and neuropathic pain symptoms in mice lacking the N-type Ca2+ channel. *EMBO J,* 20**,** 2349-56.

SANDKUHLER, J. 2009. Models and mechanisms of hyperalgesia and allodynia. *Physiol Rev,* 89**,** 707-58.

SCHMIDT, P. C., RUCHELLI, G., MACKEY, S. C. & CARROLL, I. R. 2013. Perioperative gabapentinoids: choice of agent, dose, timing, and effects on chronic postsurgical pain. *Anesthesiology,* 119**,** 1215-21.

SELTZER, Z., DUBNER, R. & SHIR, Y. 1990. A novel behavioral model of neuropathic pain disorders produced in rats by partial sciatic nerve injury. *Pain,* 43**,** 205-18.

SHAMASH, S., REICHERT, F. & ROTSHENKER, S. 2002. The cytokine network of Wallerian degeneration: tumor necrosis factor-alpha, interleukin-1alpha, and interleukin-1beta. *J Neurosci,* 22**,** 3052-60.

SHARMA, U., GRIESING, T., EMIR, B. & YOUNG, J. P., JR. 2010. Time to onset of neuropathic pain reduction: A retrospective analysis of data from nine controlled trials of pregabalin for painful diabetic peripheral neuropathy and postherpetic neuralgia. *Am J Ther,* 17**,** 577-85.

SHENG, Z. H., RETTIG, J., TAKAHASHI, M. & CATTERALL, W. A. 1994. Identification of a syntaxin-binding site on N-type calcium channels. *Neuron,* 13**,** 1303-13.

SNIDER, W. D. & MCMAHON, S. B. 1998. Tackling pain at the source: new ideas about nociceptors. *Neuron,* 20**,** 629-32.

SORGE, R. E., MAPPLEBECK, J. C., ROSEN, S., BEGGS, S., TAVES, S., ALEXANDER, J. K., MARTIN, L. J., AUSTIN, J. S., SOTOCINAL, S. G., CHEN, D., YANG, M., SHI, X. Q., HUANG, H., PILLON, N. J., BILAN, P. J., TU, Y., KLIP, A., JI, R. R., ZHANG, J., SALTER, M. W. & MOGIL, J. S. 2015. Different immune cells mediate mechanical pain hypersensitivity in male and female mice. *Nat Neurosci,* 18**,** 1081-3.

STEBBING, M.J., BALASUBRAMANYAN and SMITH, P.A. 2016. Calbindin-D-28k-like immunoreactivity in superficial dorsal horn neurons and effects of sciatic chronic constriction injury. *Neuroscience.* (in revision)

STEMKOWSKI, P. L., NOH, M. C., CHEN, Y. & SMITH, P. A. 2015. Increased excitability of medium-sized dorsal root ganglion neurons by prolonged interleukin-1beta exposure is K(+) channel dependent and reversible. *J Physiol,* 593**,** 3739-55.

STEMKOWSKI, P. L. & SMITH, P. A. 2012. Long-term IL-1beta exposure causes subpopulation-dependent alterations in rat dorsal root ganglion neuron excitability. *J Neurophysiol,* 107**,** 1586-97.

STUCKY, C. L. & LEWIN, G. R. 1999. Isolectin B(4)-positive and -negative nociceptors are functionally distinct. *J Neurosci,* 19**,** 6497-505.

SUN, J. H., YANG, B., DONNELLY, D. F., MA, C. & LAMOTTE, R. H. 2006. MCP-1 enhances excitability of nociceptive neurons in chronically compressed dorsal root ganglia. *J Neurophysiol,* 96**,** 2189-99.

SUTTON, K. G., MARTIN, D. J., PINNOCK, R. D., LEE, K. & SCOTT, R. H. 2002. Gabapentin inhibits high-threshold calcium channel currents in cultured rat dorsal root ganglion neurones. *Br J Pharmacol,* 135**,** 257-65.

SUZUKI, R., RYGH, L. J. & DICKENSON, A. H. 2004. Bad news from the brain: descending 5-HT pathways that control spinal pain processing. *Trends Pharmacol Sci,* 25**,** 613-7.

TAJERIAN, M., ALVARADO, S., MILLECAMPS, M., VACHON, P., CROSBY, C., BUSHNELL, M. C., SZYF, M. & STONE, L. S. 2013. Peripheral nerve injury is associated with chronic, reversible changes in global DNA methylation in the mouse prefrontal cortex. *PLoS One,* 8**,** e55259.

TAYLOR, C. P., ANGELOTTI, T. & FAUMAN, E. 2007. Pharmacology and mechanism of action of pregabalin: the calcium channel alpha2-delta (alpha2-delta) subunit as a target for antiepileptic drug discovery. *Epilepsy Res,* 73**,** 137-50.

TAYLOR, C. P., GEE, N. S., SU, T. Z., KOCSIS, J. D., WELTY, D. F., BROWN, J. P., DOOLEY, D. J., BODEN, P. & SINGH, L. 1998. A summary of mechanistic hypotheses of gabapentin pharmacology. *Epilepsy Res,* 29**,** 233-49.

TODD, A. J. 2010. Neuronal circuitry for pain processing in the dorsal horn. *Nat Rev Neurosci,* 11**,** 823-36.

TORRANCE, N., FERGUSON, J. A., AFOLABI, E., BENNETT, M. I., SERPELL, M. G., DUNN, K. M. & SMITH, B. H. 2013. Neuropathic pain in the community: more under-treated than refractory? *Pain,* 154**,** 690-9.

TORRANCE, N., SMITH, B. H., BENNETT, M. I. & LEE, A. J. 2006. The epidemiology of chronic pain of predominantly neuropathic origin. Results from a general population survey. *J Pain,* 7**,** 281-9.

TRACEY, I. 2005. Nociceptive processing in the human brain. *Curr Opin Neurobiol,* 15**,** 478-87.

TRACEY, I. & MANTYH, P. W. 2007. The cerebral signature for pain perception and its modulation. *Neuron,* 55**,** 377-91.

TRANG, T., BEGGS, S., WAN, X. & SALTER, M. W. 2009. P2X4-receptor-mediated synthesis and release of brain-derived neurotrophic factor in microglia is dependent on calcium and p38-mitogen-activated protein kinase activation. *J Neurosci,* 29**,** 3518-28.

TREEDE, R. D., JENSEN, T. S., CAMPBELL, J. N., CRUCCU, G., DOSTROVSKY, J. O., GRIFFIN, J. W., HANSSON, P., HUGHES, R., NURMIKKO, T. & SERRA, J. 2008. Neuropathic pain: redefinition and a grading system for clinical and research purposes. *Neurology,* 70**,** 1630-5.

TSANTOULAS, C. 2015. Emerging potassium channel targets for the treatment of pain. *Curr Opin Support Palliat Care,* 9**,** 147-54.

TSUDA, M., SHIGEMOTO-MOGAMI, Y., KOIZUMI, S., MIZOKOSHI, A., KOHSAKA, S., SALTER, M. W. & INOUE, K. 2003. P2X4 receptors induced in spinal microglia gate tactile allodynia after nerve injury. *Nature,* 424**,** 778-83.

TSUDA, M., TOYOMITSU, E., KOMATSU, T., MASUDA, T., KUNIFUSA, E., NASU-TADA, K., KOIZUMI, S., YAMAMOTO, K., ANDO, J. & INOUE, K. 2008. Fibronectin/integrin system is involved in P2X(4) receptor upregulation in the spinal cord and neuropathic pain after nerve injury. *Glia,* 56**,** 579-85.

ULETT, G. A. 1999. Acupuncture and amitriptyline for HIV-related peripheral neuropathic pain. *JAMA,* 281**,** 1270-1; author reply 1271-2.

ULMANN, L., HATCHER, J. P., HUGHES, J. P., CHAUMONT, S., GREEN, P. J., CONQUET, F., BUELL, G. N., REEVE, A. J., CHESSELL, I. P. & RASSENDREN, F. 2008. Up-regulation of P2X4 receptors in spinal microglia after peripheral nerve injury mediates BDNF release and neuropathic pain. *J Neurosci,* 28**,** 11263-8.

USUNOFF, K. G., POPRATILOFF, A., SCHMITT, O. & WREE, A. 2006. *Functional Neuroanatomy of the Pain System*, Springer.

WALL, P. D. & DEVOR, M. 1983. Sensory afferent impulses originate from dorsal root ganglia as well as from the periphery in normal and nerve injured rats. *Pain,* 17**,** 321-39.

WALL, P. D., DEVOR, M., INBAL, R., SCADDING, J. W., SCHONFELD, D., SELTZER, Z. & TOMKIEWICZ, M. M. 1979. Autotomy following peripheral nerve lesions: experimental anaesthesia dolorosa. *Pain,* 7**,** 103-11.

WALL, P. D. & GUTNICK, M. 1974. Properties of afferent nerve impulses originating from a neuroma. *Nature,* 248**,** 740-3.

WALL, P. D., MELZACK, R. & BONICA, J. J. 1994. *Textbook of pain,* Edinburgh ; New York, Churchill Livingstone.

WALLER, A. 1850. Experiments on the Section of the Glossopharyngeal and Hypoglossal Nerves of the Frog, and Observations of the Alterations Produced Thereby in the Structure of Their Primitive Fibres. *Philosophical Transactions of the Royal Society of London,* 140**,** 423-429.

WAXMAN, S. G. & ZAMPONI, G. W. 2014. Regulating excitability of peripheral afferents: emerging ion channel targets. *Nat Neurosci,* 17**,** 153-63.

WESTENBROEK, R. E., HELL, J. W., WARNER, C., DUBEL, S. J., SNUTCH, T. P. & CATTERALL, W. A. 1992. Biochemical properties and subcellular distribution of an N-type calcium channel alpha 1 subunit. *Neuron,* 9**,** 1099-115.

WHITTAKER, C. A. & HYNES, R. O. 2002. Distribution and evolution of von Willebrand/integrin A domains: widely dispersed domains with roles in cell adhesion and elsewhere. *Mol Biol Cell,* 13**,** 3369-87.

WOOLF, C. J. 1983. Evidence for a central component of post-injury pain hypersensitivity. *Nature,* 306**,** 686-8.

WOOLF, C. J., BENNETT, G. J., DOHERTY, M., DUBNER, R., KIDD, B., KOLTZENBURG, M., LIPTON, R., LOESER, J. D., PAYNE, R. & TOREBJORK, E. 1998. Towards a mechanism-based classification of pain? *Pain,* 77**,** 227-9.

WOOLF, C. J. & MANNION, R. J. 1999. Neuropathic pain: aetiology, symptoms, mechanisms, and management. *Lancet,* 353**,** 1959-64.

WOOLF, C. J. & THOMPSON, S. W. 1991. The induction and maintenance of central sensitization is dependent on N-methyl-D-aspartic acid receptor activation; implications for the treatment of post-injury pain hypersensitivity states. *Pain,* 44**,** 293-9.

WOOLF, C. J. & WALTERS, E. T. 1991. Common patterns of plasticity contributing to nociceptive sensitization in mammals and Aplysia. *Trends Neurosci,* 14**,** 74-8.

YAN, P. Z., BUTLER, P. M., KUROWSKI, D. & PERLOFF, M. D. 2014. Beyond neuropathic pain: gabapentin use in cancer pain and perioperative pain. *Clin J Pain,* 30**,** 613-29.

YANG, L., ZHANG, F. X., HUANG, F., LU, Y. J., LI, G. D., BAO, L., XIAO, H. S. & ZHANG, X. 2004. Peripheral nerve injury induces trans-synaptic modification of channels, receptors and signal pathways in rat dorsal spinal cord. *Eur J Neurosci,* 19**,** 871-83.

YASAKA, T., TIONG, S. Y., HUGHES, D. I., RIDDELL, J. S. & TODD, A. J. 2010. Populations of inhibitory and excitatory interneurons in lamina II of the adult rat spinal dorsal horn revealed by a combined electrophysiological and anatomical approach. *Pain,* 151**,** 475-88.

YOUNG, G. T., EMERY, E. C., MOONEY, E. R., TSANTOULAS, C. & MCNAUGHTON, P. A. 2014. Inflammatory and neuropathic pain are rapidly suppressed by peripheral block of hyperpolarisation-activated cyclic nucleotide-gated ion channels. *Pain,* 155**,** 1708-19.

ZAMPONI, G. W., STRIESSNIG, J., KOSCHAK, A. & DOLPHIN, A. C. 2015. The Physiology, Pathology, and Pharmacology of Voltage-Gated Calcium Channels and Their Future Therapeutic Potential. *Pharmacol Rev,* 67**,** 821-70.

ZEILHOFER, H. U., WILDNER, H. & YEVENES, G. E. 2012. Fast synaptic inhibition in spinal sensory processing and pain control. *Physiol Rev,* 92**,** 193-235.

ZHANG, X. & XIAO, H. S. 2005. Gene array analysis to determine the components of neuropathic pain signaling. *Curr Opin Mol Ther,* 7**,** 532-7.

ZHOU, C. & LUO, Z. D. 2014. Electrophysiological characterization of spinal neuron sensitization by elevated calcium channel alpha-2-delta-1 subunit protein. *Eur J Pain,* 18**,** 649-58.

ZHOU, C. & LUO, Z. D. 2015. Nerve injury-induced calcium channel alpha-2-delta-1 protein dysregulation leads to increased pre-synaptic excitatory input into deep dorsal horn neurons and neuropathic allodynia. *Eur J Pain*.

ZOCHODNE, D. W. 2015. Diabetes and the plasticity of sensory neurons. *Neurosci Lett,* 596**,** 60-5.

METHODS

BALASUBRAMANYAN, S., STEMKOWSKI, P. L., STEBBING, M. J. & SMITH, P. A. 2006. Sciatic chronic constriction injury produces cell-type-specific changes in the electrophysiological properties of rat substantia gelatinosa neurons. *J Neurophysiol,* 96**,** 579-90.

BIGGS, J. E., B. LU, KIM, H. J., LAI, A., TODD, K. G., BALLANYI, K., COLMERS, W. F. & SMITH, P. A. 2012. Defined Medium Organotypic Cultures of Spinal Cord Put 'Pain in a Dish' #. *T Isolated Central Nervous System Circuits.*

CHEN, T. W., WARDILL, T. J., SUN, Y., PULVER, S. R., RENNINGER, S. L., BAOHAN, A., SCHREITER, E. R., KERR, R. A., ORGER, M. B., JAYARAMAN, V., LOOGER, L. L., SVOBODA, K. & KIM, D. S. 2013. Ultrasensitive fluorescent proteins for imaging neuronal activity. *Nature,* 499**,** 295-300.

DOETSCH, G. S. 2000. Patterns in the brain. Neuronal population coding in the somatosensory system. *Physiol Behav,* 69**,** 187-201.

EDWARDS, F. A., KONNERTH, A. & SAKMANN, B. 1990. Quantal analysis of inhibitory synaptic transmission in the dentate gyrus of rat hippocampal slices: a patch-clamp study. *J Physiol,* 430**,** 213-49.

ERICKSON, R. P. 1986. A neural metric. *Neurosci Biobehav Rev,* 10**,** 377-86.

KERLIN, A. M., ANDERMANN, M. L., BEREZOVSKII, V. K. & REID, R. C. 2010. Broadly tuned response properties of diverse inhibitory neuron subtypes in mouse visual cortex. *Neuron,* 67**,** 858-71.

LI, Y., LU, H., CHENG, P. L., GE, S., XU, H., SHI, S. H. & DAN, Y. 2012. Clonally related visual cortical neurons show similar stimulus feature selectivity. *Nature,* 486**,** 118-21.

MORAN, T. D. & SMITH, P. A. 2002. Morphine-3beta-D-glucuronide suppresses inhibitory synaptic transmission in rat substantia gelatinosa. *J Pharmacol Exp Ther,* 302**,** 568-76.

MOSCONI, T. & KRUGER, L. 1996. Fixed-diameter polyethylene cuffs applied to the rat sciatic nerve induce a painful neuropathy: ultrastructural morphometric analysis of axonal alterations. *Pain,* 64**,** 37-57.

NIMMERJAHN, A., KIRCHHOFF, F., KERR, J. N. & HELMCHEN, F. 2004. Sulforhodamine 101 as a specific marker of astroglia in the neocortex in vivo. *Nat Methods,* 1**,** 31-7.

OHKI, K., CHUNG, S., CH'NG, Y. H., KARA, P. & REID, R. C. 2005. Functional imaging with cellular resolution reveals precise micro-architecture in visual cortex. *Nature,* 433**,** 597-603.

PERKINS, M. N. & STONE, T. W. 1982. An iontophoretic investigation of the actions of convulsant kynurenines and their interaction with the endogenous excitant quinolinic acid. *Brain Res,* 247**,** 184-7.

SCHUMMERS, J., YU, H. & SUR, M. 2008. Tuned responses of astrocytes and their influence on hemodynamic signals in the visual cortex. *Science,* 320**,** 1638-43.

STOSIEK, C., GARASCHUK, O., HOLTHOFF, K. & KONNERTH, A. 2003. In vivo two-photon calcium imaging of neuronal networks. *Proc Natl Acad Sci U S A,* 100**,** 7319-24.

VAN DER KLOOT, W. 1991. The regulation of quantal size. *Prog Neurobiol,* 36**,** 93-130.

WINSHIP, I. R. & MURPHY, T. H. 2008. In vivo calcium imaging reveals functional rewiring of single somatosensory neurons after stroke. *J Neurosci,* 28**,** 6592-606.

WINSHIP, I. R., PLAA, N. & MURPHY, T. H. 2007. Rapid astrocyte calcium signals correlate with neuronal activity and onset of the hemodynamic response in vivo. *J Neurosci,* 27**,** 6268-72.

CHAPTER 3

BACKONJA, M. & GLANZMAN, R. L. 2003. Gabapentin dosing for neuropathic pain: evidence from randomized, placebo-controlled clinical trials. *Clin Ther,* 25**,** 81-104.

BEN-MENACHEM, E., PERSSON, L. I. & HEDNER, T. 1992. Selected CSF biochemistry and gabapentin concentrations in the CSF and plasma in patients with partial seizures after a single oral dose of gabapentin. *Epilepsy Res,* 11**,** 45-9.

BIGGS, J. E., BOAKYE, P. A., GANESAN, N., STEMKOWSKI, P. L., GARCIA, A. L., BALLANYI, K. & SMITH, P. A. 2014a. Analysis of the Long-Term Actions of Gabapentin and Pregabalin in Dorsal Root Ganglia and Substantia Gelatinosa. *J Neurophysiol*.

BIGGS, J. E., STEMKOWSKI, P. L., KNAUS, E. E., CHOWDHURY, M. A., BALLANYI, K. & SMITH, P. A. 2014b. Suppression of network activity in dorsal horn by gabapentin permeation of TRPV1 channels: Implications for drug access to cytoplasmic targets. *Neurosci Lett*.

BOCCARD, S. G., PEREIRA, E. A., MOIR, L., VAN HARTEVELT, T. J., KRINGELBACH, M. L., FITZGERALD, J. J., BAKER, I. W., GREEN, A. L. & AZIZ, T. Z. 2014. Deep brain stimulation of the anterior cingulate cortex: targeting the affective component of chronic pain. *Neuroreport,* 25**,** 83-8.

CHESHIRE, W. P., JR. 2002. Defining the role for gabapentin in the treatment of trigeminal neuralgia: a retrospective study. *J Pain,* 3**,** 137-42.

CHRISTOPHERSON, K. S., ULLIAN, E. M., STOKES, C. C., MULLOWNEY, C. E., HELL, J. W., AGAH, A., LAWLER, J., MOSHER, D. F., BORNSTEIN, P. & BARRES, B. A. 2005.

Thrombospondins are astrocyte-secreted proteins that promote CNS synaptogenesis. *Cell,* 120**,** 421-33.

CODERRE, T. J., KUMAR, N., LEFEBVRE, C. D. & YU, J. S. 2005. Evidence that gabapentin reduces neuropathic pain by inhibiting the spinal release of glutamate. *J Neurochem,* 94**,** 1131-9.

EROGLU, C., ALLEN, N. J., SUSMAN, M. W., O'ROURKE, N. A., PARK, C. Y., OZKAN, E., CHAKRABORTY, C., MULINYAWE, S. B., ANNIS, D. S., HUBERMAN, A. D., GREEN, E. M., LAWLER, J., DOLMETSCH, R., GARCIA, K. C., SMITH, S. J., LUO, Z. D., ROSENTHAL, A., MOSHER, D. F. & BARRES, B. A. 2009. Gabapentin receptor alpha2delta-1 is a neuronal thrombospondin receptor responsible for excitatory CNS synaptogenesis. *Cell,* 139**,** 380-92.

FIELD, M. J., COX, P. J., STOTT, E., MELROSE, H., OFFORD, J., SU, T. Z., BRAMWELL, S., CORRADINI, L., ENGLAND, S., WINKS, J., KINLOCH, R. A., HENDRICH, J., DOLPHIN, A. C., WEBB, T. & WILLIAMS, D. 2006. Identification of the alpha2-delta-1 subunit of voltage-dependent calcium channels as a molecular target for pain mediating the analgesic actions of pregabalin. *Proc Natl Acad Sci U S A,* 103**,** 17537-42.

FUCHS, P. N., PENG, Y. B., BOYETTE-DAVIS, J. A. & UHELSKI, M. L. 2014. The anterior cingulate cortex and pain processing. *Front Integr Neurosci,* 8**,** 35.

HAYASHIDA, K., OBATA, H., NAKAJIMA, K. & EISENACH, J. C. 2008. Gabapentin acts within the locus coeruleus to alleviate neuropathic pain. *Anesthesiology,* 109**,** 1077-84.

HENDRICH, J., BAUER, C. S. & DOLPHIN, A. C. 2012. Chronic pregabalin inhibits synaptic transmission between rat dorsal root ganglion and dorsal horn neurons in culture. *Channels (Austin),* 6**,** 124-32.

HENDRICH, J., VAN MINH, A. T., HEBLICH, F., NIETO-ROSTRO, M., WATSCHINGER, K., STRIESSNIG, J., WRATTEN, J., DAVIES, A. & DOLPHIN, A. C. 2008. Pharmacological disruption of calcium channel trafficking by the alpha2delta ligand gabapentin. *Proc Natl Acad Sci U S A,* 105**,** 3628-33.

HUNTER, J. C., GOGAS, K. R., HEDLEY, L. R., JACOBSON, L. O., KASSOTAKIS, L., THOMPSON, J. & FONTANA, D. J. 1997. The effect of novel anti-epileptic drugs in rat experimental models of acute and chronic pain. *Eur J Pharmacol,* 324**,** 153-60.

JONES, A. K., KULKARNI, B. & DERBYSHIRE, S. W. 2003. Pain mechanisms and their disorders. *Br Med Bull,* 65**,** 83-93.

JUENKE, J. M., BROWN, P. I., JOHNSON-DAVIS, K. L. & MCMILLIN, G. A. 2011. Simultaneous quantification of levetiracetam and gabapentin in plasma by ultra-pressure liquid chromatography coupled with tandem mass spectrometry detection. *Ther Drug Monit,* 33**,** 209-13.

KAYSER, V. & CHRISTENSEN, D. 2000. Antinociceptive effect of systemic gabapentin in mononeuropathic rats, depends on stimulus characteristics and level of test integration. *Pain,* 88**,** 53-60.

KUMAR, N., CHERKAS, P. S., VARATHAN, V., MIYAMOTO, M., CHIANG, C. Y., DOSTROVSKY, J. O., SESSLE, B. J. & CODERRE, T. J. 2013. Systemic pregabalin attenuates facial hypersensitivity and noxious stimulus-evoked release of glutamate in medullary dorsal horn in a rodent model of trigeminal neuropathic pain. *Neurochem Int,* 62**,** 831-5.

LARSEN, M. S., KEIZER, R., MUNRO, G., MORK, A., HOLM, R., SAVIC, R. & KREILGAARD, M. 2016. Pharmacokinetic/Pharmacodynamic Relationship of Gabapentin in a CFA-induced Inflammatory Hyperalgesia Rat Model. *Pharm Res*.

MELZACK, R. & EISENBERG, H. 1968. Skin sensory afterglows. *Science,* 159**,** 445-7.

MOORE, K. A., BABA, H. & WOOLF, C. J. 2002. Gabapentin-- actions on adult superficial dorsal horn neurons. *Neuropharmacology,* 43**,** 1077-81.

MOSCONI, T. & KRUGER, L. 1996. Fixed-diameter polyethylene cuffs applied to the rat sciatic nerve induce a painful neuropathy: ultrastructural morphometric analysis of axonal alterations. *Pain,* 64**,** 37-57.

NAVARRO, X., VIVO, M. & VALERO-CABRE, A. 2007. Neural plasticity after peripheral nerve injury and regeneration. *Prog Neurobiol,* 82**,** 163-201.

PEREIRA, E. A., PARANATHALA, M., HYAM, J. A., GREEN, A. L. & AZIZ, T. Z. 2014. Anterior cingulotomy improves malignant mesothelioma pain and dyspnoea. *Br J Neurosurg,* 28**,** 471-4.

PURVES, D. 2008. *Neuroscience,* Sunderland, Mass., Sinauer.

RADULOVIC, L. L., TURCK, D., VON HODENBERG, A., VOLLMER, K. O., MCNALLY, W. P., DEHART, P. D., HANSON, B. J., BOCKBRADER, H. N. & CHANG, T. 1995. Disposition of gabapentin (neurontin) in mice, rats, dogs, and monkeys. *Drug Metab Dispos,* 23**,** 441-8.

SANDERSON, C., QUINN, S. J., AGAR, M., CHYE, R., CLARK, K., DOOGUE, M., FAZEKAS, B., LEE, J., LOVELL, M. R., ROWETT, D., SPRUYT, O. & CURROW, D. C. 2014. Pharmacovigilance in hospice/palliative care: net effect of gabapentin for neuropathic pain. *BMJ Support Palliat Care*.

SHARMA, T. 1973. Absence of cognitive deficits from bilateral cingulotomy for intractable pain in humans. *Tex Med,* 69**,** 79-82.

SHARMA, U., GRIESING, T., EMIR, B. & YOUNG, J. P., JR. 2010. Time to onset of neuropathic pain reduction: A retrospective analysis of data from nine controlled trials of pregabalin for painful diabetic peripheral neuropathy and postherpetic neuralgia. *Am J Ther,* 17**,** 577-85.

SU, T. Z., LUNNEY, E., CAMPBELL, G. & OXENDER, D. L. 1995. Transport of gabapentin, a gamma-amino acid drug, by system l alpha-amino acid transporters: a comparative study in astrocytes, synaptosomes, and CHO cells. *J Neurochem,* 64**,** 2125-31.

TAYLOR, K. S., ANASTAKIS, D. J. & DAVIS, K. D. 2009. Cutting your nerve changes your brain. *Brain,* 132**,** 3122-33.

TODD, A. J. 2010. Neuronal circuitry for pain processing in the dorsal horn. *Nat Rev Neurosci,* 11**,** 823-36.

VONSY, J. L., GHANDEHARI, J. & DICKENSON, A. H. 2009. Differential analgesic effects of morphine and gabapentin on behavioural measures of pain and disability in a model of osteoarthritis pain in rats. *Eur J Pain,* 13**,** 786-93.

WALPOLE, S. C., PRIETO-MERINO, D., EDWARDS, P., CLELAND, J., STEVENS, G. & ROBERTS, I. 2012. The weight of nations: an estimation of adult human biomass. *BMC Public Health,* 12**,** 439.

WOOLF, C. J. 1993. The pathophysiology of peripheral neuropathic pain--abnormal peripheral input and abnormal central processing. *Acta Neurochir Suppl (Wien),* 58**,** 125-30.

YUAN, W., DAN, L., NETRA, R., SHAOHUI, M., CHENWANG, J. & MING, Z. 2013. A pharmaco-fMRI study on pain networks induced by electrical stimulation after sumatriptan injection. *Exp Brain Res,* 226**,** 15-24.

ZHOU, C. & LUO, Z. D. 2015. Nerve injury-induced calcium channel alpha-2-delta-1 protein dysregulation leads to increased pre-synaptic excitatory input into deep dorsal horn neurons and neuropathic allodynia. *Eur J Pain*.

ZHUO, M. 2011. Cortical plasticity as a new endpoint measurement for chronic pain. *Mol Pain,* 7**,** 54.

CHAPTER 4

ALBUQUERQUE, C., LEE, C. J., JACKSON, A. C. & MACDERMOTT, A. B. 1999. Subpopulations of GABAergic and non-GABAergic rat dorsal horn neurons express Ca2+-permeable AMPA receptors. *Eur J Neurosci,* 11**,** 2758-66.

BALASUBRAMANYAN, S., STEMKOWSKI, P. L., STEBBING, M. J. & SMITH, P. A. 2006. Sciatic chronic constriction injury produces cell-type-specific changes in the electrophysiological properties of rat substantia gelatinosa neurons. *J Neurophysiol,* 96**,** 579-90.

BENARROCH, E. E. 2013. HCN channels: function and clinical implications. *Neurology,* 80**,** 304-10.

BIGGS, J. E., BOAKYE, P. A., GANESAN, N., STEMKOWSKI, P. L., GARCIA, A. L., BALLANYI, K. & SMITH, P. A. 2014. Analysis of the Long-Term Actions of Gabapentin and Pregabalin in Dorsal Root Ganglia and Substantia Gelatinosa. *J Neurophysiol*.

CUI, L., KIM, Y. R., KIM, H. Y., LEE, S. C., SHIN, H. S., SZABO, G., ERDELYI, F., KIM, J. & KIM, S. J. 2011. Modulation of synaptic transmission from primary afferents to spinal substantia gelatinosa neurons by group III mGluRs in GAD65-EGFP transgenic mice. *J Neurophysiol,* 105**,** 1102-11.

DOLPHIN, A. C., WYATT, C. N., RICHARDS, J., BEATTIE, R. E., CRAIG, P., LEE, J. H., CRIBBS, L. L., VOLSEN, S. G. & PEREZ-REYES, E. 1999. The effect of alpha2-delta and other accessory subunits on expression and properties of the calcium channel alpha1G. *J Physiol,* 519 Pt 1**,** 35-45.

DUBEL, S. J., ALTIER, C., CHAUMONT, S., LORY, P., BOURINET, E. & NARGEOT, J. 2004. Plasma membrane expression of T-type calcium channel alpha(1) subunits is modulated by high voltage-activated auxiliary subunits. *J Biol Chem,* 279**,** 29263-9.

EDWARDS, F. A., KONNERTH, A. & SAKMANN, B. 1990. Quantal analysis of inhibitory synaptic transmission in the dentate gyrus of rat hippocampal slices: a patch-clamp study. *J Physiol,* 430**,** 213-49.

GEE, N. S., BROWN, J. P., DISSANAYAKE, V. U., OFFORD, J., THURLOW, R. & WOODRUFF, G. N. 1996. The novel anticonvulsant drug, gabapentin (Neurontin), binds to the alpha2delta subunit of a calcium channel. *J Biol Chem,* 271**,** 5768-76.

HE, C., CHEN, F., LI, B. & HU, Z. 2014. Neurophysiology of HCN channels: from cellular functions to multiple regulations. *Prog Neurobiol,* 112**,** 1-23.

HEBLICH, F., TRAN VAN MINH, A., HENDRICH, J., WATSCHINGER, K. & DOLPHIN, A. C. 2008. Time course and specificity of the pharmacological disruption of the trafficking of voltage-gated calcium channels by gabapentin. *Channels (Austin),* 2**,** 4-9.

HEINKE, B., RUSCHEWEYH, R., FORSTHUBER, L., WUNDERBALDINGER, G. & SANDKUHLER, J. 2004. Physiological, neurochemical and morphological properties of a subgroup of GABAergic spinal lamina II neurones identified by expression of green fluorescent protein in mice. *J Physiol,* 560**,** 249-66.

HENDRICH, J., BAUER, C. S. & DOLPHIN, A. C. 2012. Chronic pregabalin inhibits synaptic transmission between rat dorsal root ganglion and dorsal horn neurons in culture. *Channels (Austin),* 6**,** 124-32.

HENDRICH, J., VAN MINH, A. T., HEBLICH, F., NIETO-ROSTRO, M., WATSCHINGER, K., STRIESSNIG, J., WRATTEN, J., DAVIES, A. & DOLPHIN, A. C. 2008.

Pharmacological disruption of calcium channel trafficking by the alpha2delta ligand gabapentin. *Proc Natl Acad Sci U S A,* 105**,** 3628-33.

HOPPA, M. B., LANA, B., MARGAS, W., DOLPHIN, A. C. & RYAN, T. A. 2012. alpha2delta expression sets presynaptic calcium channel abundance and release probability. *Nature,* 486**,** 122-5.

HUANG, H. & TRUSSELL, L. O. 2014. Presynaptic HCN channels regulate vesicular glutamate transport. *Neuron,* 84**,** 340-6.

KERR, R. C., MAXWELL, D. J. & TODD, A. J. 1998. GluR1 and GluR2/3 subunits of the AMPA-type glutamate receptor are associated with particular types of neurone in laminae I-III of the spinal dorsal horn of the rat. *Eur J Neurosci,* 10**,** 324-33.

LI, C. Y., ZHANG, X. L., MATTHEWS, E. A., LI, K. W., KURWA, A., BOROUJERDI, A., GROSS, J., GOLD, M. S., DICKENSON, A. H., FENG, G. & LUO, Z. D. 2006. Calcium channel alpha2delta1 subunit mediates spinal hyperexcitability in pain modulation. *Pain,* 125**,** 20-34.

LIU, Y., QIN, N., REITZ, T., WANG, Y. & FLORES, C. M. 2006. Inhibition of the rat brain sodium channel Nav1.2 after prolonged exposure to gabapentin. *Epilepsy Res,* 70**,** 263-8.

LUO, Z. D., CALCUTT, N. A., HIGUERA, E. S., VALDER, C. R., SONG, Y. H., SVENSSON, C. I. & MYERS, R. R. 2002. Injury type-specific calcium channel alpha 2 delta-1 subunit up-regulation in rat neuropathic pain models correlates with antiallodynic effects of gabapentin. *J Pharmacol Exp Ther,* 303**,** 1199-205.

LUO, Z. D., CHAPLAN, S. R., HIGUERA, E. S., SORKIN, L. S., STAUDERMAN, K. A., WILLIAMS, M. E. & YAKSH, T. L. 2001. Upregulation of dorsal root ganglion

(alpha)2(delta) calcium channel subunit and its correlation with allodynia in spinal nerve-injured rats. *J Neurosci,* 21**,** 1868-75.

MELNICK, I. V., SANTOS, S. F., SZOKOL, K., SZUCS, P. & SAFRONOV, B. V. 2004. Ionic basis of tonic firing in spinal substantia gelatinosa neurons of rat. *J Neurophysiol,* 91**,** 646-55.

MIXCOATL-ZECUATL, T., MEDINA-SANTILLAN, R., REYES-GARCIA, G., VIDAL-CANTU, G. C. & GRANADOS-SOTO, V. 2004. Effect of K+ channel modulators on the antiallodynic effect of gabapentin. *Eur J Pharmacol,* 484**,** 201-8.

MOORE, K. A., BABA, H. & WOOLF, C. J. 2002. Gabapentin-- actions on adult superficial dorsal horn neurons. *Neuropharmacology,* 43**,** 1077-81.

NOH, S., KUMAR, N., BUKHANOVA, N., CHEN, Y., STEMKOWSI, P. L. & SMITH, P. A. 2014. The heart-rate-reducing agent, ivabradine, reduces mechanical allodynia in a rodent model of neuropathic pain. *Eur J Pain,* 18**,** 1139-47.

PATEL, M. K., GONZALEZ, M. I., BRAMWELL, S., PINNOCK, R. D. & LEE, K. 2000. Gabapentin inhibits excitatory synaptic transmission in the hyperalgesic spinal cord. *Br J Pharmacol,* 130**,** 1731-4.

POLGAR, E., WATANABE, M., HARTMANN, B., GRANT, S. G. & TODD, A. J. 2008. Expression of AMPA receptor subunits at synapses in laminae I-III of the rodent spinal dorsal horn. *Mol Pain,* 4**,** 5.

PUNNAKKAL, P., VON SCHOULTZ, C., HAENRAETS, K., WILDNER, H. & ZEILHOFER, H. U. 2014. Morphological, biophysical and synaptic properties of glutamatergic neurons of the mouse spinal dorsal horn. *J Physiol,* 592**,** 759-76.

RUSCHEWEYH, R. & SANDKUHLER, J. 2002. Lamina-specific membrane and discharge properties of rat spinal dorsal horn neurones in vitro. *J Physiol,* 541**,** 231-44.

SANTOS, S. F., REBELO, S., DERKACH, V. A. & SAFRONOV, B. V. 2007. Excitatory interneurons dominate sensory processing in the spinal substantia gelatinosa of rat. *J Physiol,* 581**,** 241-54.

SINGH, N. S., PAUL, R. K., TORJMAN, M. C. & WAINER, I. W. 2013. Gabapentin and (S)-pregabalin decrease intracellular D-serine concentrations in PC-12 cells. *Neurosci Lett,* 535**,** 90-4.

SUTO, T., SEVERINO, A. L., EISENACH, J. C. & HAYASHIDA, K. 2014. Gabapentin increases extracellular glutamatergic level in the locus coeruleus via astroglial glutamate transporter-dependent mechanisms. *Neuropharmacology,* 81**,** 95-100.

TAKASU, K., ONO, H. & TANABE, M. 2008. Gabapentin produces PKA-dependent pre-synaptic inhibition of GABAergic synaptic transmission in LC neurons following partial nerve injury in mice. *J Neurochem,* 105**,** 933-42.

TAKASU, K., ONO, H. & TANABE, M. 2010. Spinal hyperpolarization-activated cyclic nucleotide-gated cation channels at primary afferent terminals contribute to chronic pain. *Pain,* 151**,** 87-96.

TODD, A. J. 2010. Neuronal circuitry for pain processing in the dorsal horn. *Nat Rev Neurosci,* 11**,** 823-36.

VERSTREKEN, P. & BELLEN, H. J. 2001. Neuroscience. The meaning of a mini. *Science,* 293**,** 443-4.

WAXMAN, S. G. & ZAMPONI, G. W. 2014. Regulating excitability of peripheral afferents: emerging ion channel targets. *Nat Neurosci,* 17**,** 153-63.

YANG, R. H., WANG, W. T., CHEN, J. Y., XIE, R. G. & HU, S. J. 2009. Gabapentin selectively reduces persistent sodium current in injured type-A dorsal root ganglion neurons. *Pain,* 143**,** 48-55.

YASAKA, T., HUGHES, D. I., POLGAR, E., NAGY, G. G., WATANABE, M., RIDDELL, J. S. & TODD, A. J. 2009. Evidence against AMPA receptor-lacking glutamatergic synapses in the superficial dorsal horn of the rat spinal cord. *J Neurosci,* 29**,** 13401-9.

YASAKA, T., TIONG, S. Y., HUGHES, D. I., RIDDELL, J. S. & TODD, A. J. 2010. Populations of inhibitory and excitatory interneurons in lamina II of the adult rat spinal dorsal horn revealed by a combined electrophysiological and anatomical approach. *Pain,* 151**,** 475-88.

YOSHIZUMI, M., PARKER, R. A., EISENACH, J. C. & HAYASHIDA, K. 2012. Gabapentin inhibits gamma-amino butyric acid release in the locus coeruleus but not in the spinal dorsal horn after peripheral nerve injury in rats. *Anesthesiology,* 116**,** 1347-53.

YOUNG, G. T., EMERY, E. C., MOONEY, E. R., TSANTOULAS, C. & MCNAUGHTON, P. A. 2014. Inflammatory and neuropathic pain are rapidly suppressed by peripheral block of hyperpolarisation-activated cyclic nucleotide-gated ion channels. *Pain,* 155**,** 1708-19.

ZAMPONI, G. W., STRIESSNIG, J., KOSCHAK, A. & DOLPHIN, A. C. 2015. The Physiology, Pathology, and Pharmacology of Voltage-Gated Calcium Channels and Their Future Therapeutic Potential. *Pharmacol Rev,* 67**,** 821-70.

ZEILHOFER, H. U., WILDNER, H. & YEVENES, G. E. 2012. Fast synaptic inhibition in spinal sensory processing and pain control. *Physiol Rev,* 92**,** 193-235.

ZHOU, C. & LUO, Z. D. 2014. Electrophysiological characterization of spinal neuron sensitization by elevated calcium channel alpha-2-delta-1 subunit protein. *Eur J Pain,* 18**,** 649-58.

ZHOU, C. & LUO, Z. D. 2015. Nerve injury-induced calcium channel alpha-2-delta-1 protein dysregulation leads to increased pre-synaptic excitatory input into deep dorsal horn neurons and neuropathic allodynia. *Eur J Pain*.

ZHOU, Q., LAI, Y., BACAJ, T., ZHAO, M., LYUBIMOV, A. Y., UERVIROJNANGKOORN, M., ZELDIN, O. B., BREWSTER, A. S., SAUTER, N. K., COHEN, A. E., SOLTIS, S. M., ALONSO-MORI, R., CHOLLET, M., LEMKE, H. T., PFUETZNER, R. A., CHOI, U. B., WEIS, W. I., DIAO, J., SUDHOF, T. C. & BRUNGER, A. T. 2015. Architecture of the synaptotagmin-SNARE machinery for neuronal exocytosis. *Nature,* 525**,** 62-7.

CHAPTER 5

ALLES, S.R.A. & SMITH, P.A. 2016. The anti-allodynic gabapentinoids: myths, paradoxes and acute effects. *Neuroscientist*. (in press)

BAYER, K., AHMADI, S. & ZEILHOFER, H. U. 2004. Gabapentin may inhibit synaptic transmission in the mouse spinal cord dorsal horn through a preferential block of P/Q-type Ca2+ channels. *Neuropharmacology,* 46**,** 743-9.

BIGGS, J. E., BOAKYE, P. A., GANESAN, N., STEMKOWSKI, P. L., GARCIA, A. L., BALLANYI, K. & SMITH, P. A. 2014. Analysis of the Long-Term Actions of Gabapentin and Pregabalin in Dorsal Root Ganglia and Substantia Gelatinosa. *J Neurophysiol*.

BRYANS, J. S. & WUSTROW, D. J. 1999. 3-Substituted GABA analogs with central nervous system activity: A review. *Medicinal Research Reviews,* 19**,** 149-177.

CAO, Y. Q. & TSIEN, R. W. 2010. Different relationship of N- and P/Q-type Ca2+ channels to channel-interacting slots in controlling neurotransmission at cultured hippocampal synapses. *J Neurosci,* 30**,** 4536-46.

CHENG, J. K. & CHIOU, L. C. 2006. Mechanisms of the antinociceptive action of gabapentin. *J Pharmacol Sci,* 100**,** 471-86.

CORDEIRA, J. W., FELSTED, J. A., TEILLON, S., DAFTARY, S., PANESSITI, M., WIRTH, J., SENA-ESTEVES, M. & RIOS, M. 2014. Hypothalamic dysfunction of the thrombospondin receptor alpha2delta-1 underlies the overeating and obesity triggered by brain-derived neurotrophic factor deficiency. *J Neurosci,* 34**,** 554-65.

COULL, J. A., BEGGS, S., BOUDREAU, D., BOIVIN, D., TSUDA, M., INOUE, K., GRAVEL, C., SALTER, M. W. & DE KONINCK, Y. 2005. BDNF from microglia causes the shift in neuronal anion gradient underlying neuropathic pain. *Nature,* 438**,** 1017-21.

DODGE, F. A., JR. & RAHAMIMOFF, R. 1967. Co-operative action a calcium ions in transmitter release at the neuromuscular junction. *J Physiol,* 193**,** 419-32.

FINK, K., MEDER, W., DOOLEY, D. J. & GOTHERT, M. 2000. Inhibition of neuronal Ca(2+) influx by gabapentin and subsequent reduction of neurotransmitter release from rat neocortical slices. *Br J Pharmacol,* 130**,** 900-6.

HAYASHIDA, K. & EISENACH, J. C. 2011. A tropomyosine receptor kinase inhibitor blocks spinal neuroplasticity essential for the anti-hypersensitivity effects of gabapentin and clonidine in rats with peripheral nerve injury. *J Pain,* 12**,** 94-100.

HEBLICH, F., TRAN VAN MINH, A., HENDRICH, J., WATSCHINGER, K. & DOLPHIN, A. C. 2008. Time course and specificity of the pharmacological disruption of the trafficking of voltage-gated calcium channels by gabapentin. *Channels (Austin),* 2**,** 4-9.

HENDRICH, J., VAN MINH, A. T., HEBLICH, F., NIETO-ROSTRO, M., WATSCHINGER, K., STRIESSNIG, J., WRATTEN, J., DAVIES, A. & DOLPHIN, A. C. 2008. Pharmacological disruption of calcium channel trafficking by the alpha2delta ligand gabapentin. *Proc Natl Acad Sci U S A,* 105**,** 3628-33.

HOPPA, M. B., LANA, B., MARGAS, W., DOLPHIN, A. C. & RYAN, T. A. 2012. alpha2delta expression sets presynaptic calcium channel abundance and release probability. *Nature,* 486**,** 122-5.

LU, V. B., BIGGS, J. E., STEBBING, M. J., BALASUBRAMANYAN, S., TODD, K. G., LAI, A. Y., COLMERS, W. F., DAWBARN, D., BALLANYI, K. & SMITH, P. A. 2009. Brain-derived neurotrophic factor drives the changes in excitatory synaptic transmission in the rat superficial dorsal horn that follow sciatic nerve injury. *J Physiol,* 587**,** 1013-32.

LUO, Z. D., CALCUTT, N. A., HIGUERA, E. S., VALDER, C. R., SONG, Y. H., SVENSSON, C. I. & MYERS, R. R. 2002. Injury type-specific calcium channel alpha 2 delta-1 subunit up-regulation in rat neuropathic pain models correlates with antiallodynic effects of gabapentin. *J Pharmacol Exp Ther,* 303**,** 1199-205.

MOORE, K. A., BABA, H. & WOOLF, C. J. 2002. Gabapentin-- actions on adult superficial dorsal horn neurons. *Neuropharmacology,* 43**,** 1077-81.

PATEL, M. K., GONZALEZ, M. I., BRAMWELL, S., PINNOCK, R. D. & LEE, K. 2000. Gabapentin inhibits excitatory synaptic transmission in the hyperalgesic spinal cord. *Br J Pharmacol,* 130**,** 1731-4.

ZHOU, C. & LUO, Z. D. 2015. Nerve injury-induced calcium channel alpha-2-delta-1 protein dysregulation leads to increased pre-synaptic excitatory input into deep dorsal horn neurons and neuropathic allodynia. *Eur J Pain*.

ABE, K., KATO, G., KATAFUCHI, T., TAMAE, A., FURUE, H. & YOSHIMURA, M. 2009. Responses to 5-HT in morphologically identified neurons in the rat substantia gelatinosa in vitro. *Neuroscience,* 159**,** 316-24.

ALLES, S.R.A. and SMITH, P.A. 2016. The anti-allodynic gabapentinoids: myths, paradoxes and acute effects. *Neuroscientist* (in press)

ANTAL, M., PAPP, I., BAHAERGULI, N., VERESS, G. & VEREB, G. 2004. Expression of hyperpolarization-activated and cyclic nucleotide-gated cation channel subunit 2 in axon terminals of peptidergic nociceptive primary sensory neurons in the superficial spinal dorsal horn of rats. *Eur J Neurosci,* 19**,** 1336-42.

ANTAL, M., PETKO, M., POLGAR, E., HEIZMANN, C. W. & STORM-MATHISEN, J. 1996. Direct evidence of an extensive GABAergic innervation of the spinal dorsal horn by fibres descending from the rostral ventromedial medulla. *Neuroscience,* 73**,** 509-18.

BALASUBRAMANYAN, S., STEMKOWSKI, P. L., STEBBING, M. J. & SMITH, P. A. 2006. Sciatic chronic constriction injury produces cell-type-specific changes in the electrophysiological properties of rat substantia gelatinosa neurons. *J Neurophysiol,* 96**,** 579-90.

BAUER, C. S., NIETO-ROSTRO, M., RAHMAN, W., TRAN-VAN-MINH, A., FERRON, L., DOUGLAS, L., KADURIN, I., SRI RANJAN, Y., FERNANDEZ-ALACID, L., MILLAR, N. S., DICKENSON, A. H., LUJAN, R. & DOLPHIN, A. C. 2009. The increased trafficking of the calcium channel subunit alpha2delta-1 to presynaptic terminals in neuropathic pain is inhibited by the alpha2delta ligand pregabalin. *J Neurosci,* 29**,** 4076-88.

BAUER, C. S., TRAN-VAN-MINH, A., KADURIN, I. & DOLPHIN, A. C. 2010. A new look at calcium channel alpha2delta subunits. *Curr Opin Neurobiol,* 20**,** 563-71.

BIGGS, J. E., BOAKYE, P. A., GANESAN, N., STEMKOWSKI, P. L., GARCIA, A. L., BALLANYI, K. & SMITH, P. A. 2014a. Analysis of the Long-Term Actions of Gabapentin and Pregabalin in Dorsal Root Ganglia and Substantia Gelatinosa. *J Neurophysiol*.

BIGGS, J. E., LU, V. B., STEBBING, M. J., BALASUBRAMANYAN, S. & SMITH, P. A. 2010. Is BDNF sufficient for information transfer between microglia and dorsal horn neurons during the onset of central sensitization? *Mol Pain,* 6**,** 44.

BIGGS, J. E., STEMKOWSKI, P. L., KNAUS, E. E., CHOWDHURY, M. A., BALLANYI, K. & SMITH, P. A. 2014b. Suppression of network activity in dorsal horn by gabapentin permeation of TRPV1 channels: Implications for drug access to cytoplasmic targets. *Neurosci Lett*.

BOROUJERDI, A., KIM, H. K., LYU, Y. S., KIM, D. S., FIGUEROA, K. W., CHUNG, J. M. & LUO, Z. D. 2008. Injury discharges regulate calcium channel alpha-2-delta-1 subunit upregulation in the dorsal horn that contributes to initiation of neuropathic pain. *Pain,* 139**,** 358-66.

CANTI, C., NIETO-ROSTRO, M., FOUCAULT, I., HEBLICH, F., WRATTEN, J., RICHARDS, M. W., HENDRICH, J., DOUGLAS, L., PAGE, K. M., DAVIES, A. & DOLPHIN, A. C. 2005. The metal-ion-dependent adhesion site in the Von Willebrand factor-A domain of alpha2delta subunits is key to trafficking voltage-gated Ca2+ channels. *Proc Natl Acad Sci U S A,* 102**,** 11230-5.

CASSIDY, J. S., FERRON, L., KADURIN, I., PRATT, W. S. & DOLPHIN, A. C. 2014. Functional exofacially tagged N-type calcium channels elucidate the interaction with auxiliary alpha2delta-1 subunits. *Proc Natl Acad Sci U S A,* 111**,** 8979-84.

CHAPLAN, S. R., GUO, H. Q., LEE, D. H., LUO, L., LIU, C., KUEI, C., VELUMIAN, A. A., BUTLER, M. P., BROWN, S. M. & DUBIN, A. E. 2003. Neuronal hyperpolarization-activated pacemaker channels drive neuropathic pain. *J Neurosci,* 23**,** 1169-78.

CHESHIRE, W. P., JR. 2002. Defining the role for gabapentin in the treatment of trigeminal neuralgia: a retrospective study. *J Pain,* 3**,** 137-42.

CHRISTOPHERSON, K. S., ULLIAN, E. M., STOKES, C. C., MULLOWNEY, C. E., HELL, J. W., AGAH, A., LAWLER, J., MOSHER, D. F., BORNSTEIN, P. & BARRES, B. A. 2005. Thrombospondins are astrocyte-secreted proteins that promote CNS synaptogenesis. *Cell,* 120**,** 421-33.

CODERRE, T. J., KUMAR, N., LEFEBVRE, C. D. & YU, J. S. 2005. Evidence that gabapentin reduces neuropathic pain by inhibiting the spinal release of glutamate. *J Neurochem,* 94**,** 1131-9.

COULL, J. A., BEGGS, S., BOUDREAU, D., BOIVIN, D., TSUDA, M., INOUE, K., GRAVEL, C., SALTER, M. W. & DE KONINCK, Y. 2005. BDNF from microglia causes the shift in neuronal anion gradient underlying neuropathic pain. *Nature,* 438**,** 1017-21.

CROSBY, N. D., ZAUCKE, F., KRAS, J. V., DONG, L., LUO, Z. D. & WINKELSTEIN, B. A. 2015. Thrombospondin-4 and excitatory synaptogenesis promote spinal sensitization after painful mechanical joint injury. *Exp Neurol,* 264**,** 111-20.

DOETSCH, G. S. 2000. Patterns in the brain. Neuronal population coding in the somatosensory system. *Physiol Behav,* 69**,** 187-201.

EIPE, N., PENNING, J., YAZDI, F., MALLICK, R., TURNER, L., AHMADZAI, N. & ANSARI, M. T. 2015. Perioperative use of pregabalin for acute pain-a systematic review and meta-analysis. *Pain,* 156**,** 1284-300.

EMERY, E. C., YOUNG, G. T., BERROCOSO, E. M., CHEN, L. & MCNAUGHTON, P. A. 2011. HCN2 ion channels play a central role in inflammatory and neuropathic pain. *Science,* 333**,** 1462-6.

EMERY, E. C., YOUNG, G. T. & MCNAUGHTON, P. A. 2012. HCN2 ion channels: an emerging role as the pacemakers of pain. *Trends Pharmacol Sci,* 33**,** 456-63.

ERICKSON, R. P. 1986. A neural metric. *Neurosci Biobehav Rev,* 10**,** 377-86.

EROGLU, C., ALLEN, N. J., SUSMAN, M. W., O'ROURKE, N. A., PARK, C. Y., OZKAN, E., CHAKRABORTY, C., MULINYAWE, S. B., ANNIS, D. S., HUBERMAN, A. D., GREEN, E. M., LAWLER, J., DOLMETSCH, R., GARCIA, K. C., SMITH, S. J., LUO, Z. D., ROSENTHAL, A., MOSHER, D. F. & BARRES, B. A. 2009. Gabapentin receptor alpha2delta-1 is a neuronal thrombospondin receptor responsible for excitatory CNS synaptogenesis. *Cell,* 139**,** 380-92.

FIELD, M. J., COX, P. J., STOTT, E., MELROSE, H., OFFORD, J., SU, T. Z., BRAMWELL, S., CORRADINI, L., ENGLAND, S., WINKS, J., KINLOCH, R. A., HENDRICH, J., DOLPHIN, A. C., WEBB, T. & WILLIAMS, D. 2006. Identification of the alpha2-delta-1 subunit of voltage-dependent calcium channels as a molecular target for pain mediating the analgesic actions of pregabalin. *Proc Natl Acad Sci U S A,* 103**,** 17537-42.

GASSNER, M., RUSCHEWEYH, R. & SANDKUHLER, J. 2009. Direct excitation of spinal GABAergic interneurons by noradrenaline. *Pain,* 145**,** 204-10.

GEE, N. S., BROWN, J. P., DISSANAYAKE, V. U., OFFORD, J., THURLOW, R. & WOODRUFF, G. N. 1996. The novel anticonvulsant drug, gabapentin (Neurontin), binds to the alpha2delta subunit of a calcium channel. *J Biol Chem,* 271**,** 5768-76.

GOTTRUP, H., JUHL, G., KRISTENSEN, A. D., LAI, R., CHIZH, B. A., BROWN, J., BACH, F. W. & JENSEN, T. S. 2004. Chronic oral gabapentin reduces elements of central sensitization in human experimental hyperalgesia. *Anesthesiology,* 101**,** 1400-8.

GOVERNO, R. J., MORRIS, P. G., MARSDEN, C. A. & CHAPMAN, V. 2008. Gabapentin evoked changes in functional activity in nociceptive regions in the brain of the anaesthetized rat: an fMRI study. *Br J Pharmacol,* 153**,** 1558-67.

HEBLICH, F., TRAN VAN MINH, A., HENDRICH, J., WATSCHINGER, K. & DOLPHIN, A. C. 2008. Time course and specificity of the pharmacological disruption of the trafficking of voltage-gated calcium channels by gabapentin. *Channels (Austin),* 2**,** 4-9.

HEINKE, B., RUSCHEWEYH, R., FORSTHUBER, L., WUNDERBALDINGER, G. & SANDKUHLER, J. 2004. Physiological, neurochemical and morphological properties of a subgroup of GABAergic spinal lamina II neurones identified by expression of green fluorescent protein in mice. *J Physiol,* 560**,** 249-66.

HENDRICH, J., VAN MINH, A. T., HEBLICH, F., NIETO-ROSTRO, M., WATSCHINGER, K., STRIESSNIG, J., WRATTEN, J., DAVIES, A. & DOLPHIN, A. C. 2008. Pharmacological disruption of calcium channel trafficking by the alpha2delta ligand gabapentin. *Proc Natl Acad Sci U S A,* 105**,** 3628-33.

HOPPA, M. B., LANA, B., MARGAS, W., DOLPHIN, A. C. & RYAN, T. A. 2012. alpha2delta expression sets presynaptic calcium channel abundance and release probability. *Nature,* 486**,** 122-5.

HUNTER, J. C., GOGAS, K. R., HEDLEY, L. R., JACOBSON, L. O., KASSOTAKIS, L., THOMPSON, J. & FONTANA, D. J. 1997. The effect of novel anti-epileptic drugs in rat experimental models of acute and chronic pain. *Eur J Pharmacol,* 324**,** 153-60.

KIM, D. S., LI, K. W., BOROUJERDI, A., PETER YU, Y., ZHOU, C. Y., DENG, P., PARK, J., ZHANG, X., LEE, J., CORPE, M., SHARP, K., STEWARD, O., EROGLU, C., BARRES, B., ZAUCKE, F., XU, Z. C. & LUO, Z. D. 2012. Thrombospondin-4 contributes to spinal sensitization and neuropathic pain states. *J Neurosci,* 32**,** 8977-87.

KUMAR, N., CHERKAS, P. S., VARATHAN, V., MIYAMOTO, M., CHIANG, C. Y., DOSTROVSKY, J. O., SESSLE, B. J. & CODERRE, T. J. 2013. Systemic pregabalin attenuates facial hypersensitivity and noxious stimulus-evoked release of glutamate in medullary dorsal horn in a rodent model of trigeminal neuropathic pain. *Neurochem Int,* 62**,** 831-5.

LANNEAU, C., GREEN, A., HIRST, W. D., WISE, A., BROWN, J. T., DONNIER, E., CHARLES, K. J., WOOD, M., DAVIES, C. H. & PANGALOS, M. N. 2001. Gabapentin is not a GABAB receptor agonist. *Neuropharmacology,* 41**,** 965-75.

LI, C. Y., SONG, Y. H., HIGUERA, E. S. & LUO, Z. D. 2004. Spinal dorsal horn calcium channel alpha2delta-1 subunit upregulation contributes to peripheral nerve injury-induced tactile allodynia. *J Neurosci,* 24**,** 8494-9.

LI, C. Y., ZHANG, X. L., MATTHEWS, E. A., LI, K. W., KURWA, A., BOROUJERDI, A., GROSS, J., GOLD, M. S., DICKENSON, A. H., FENG, G. & LUO, Z. D. 2006. Calcium channel alpha2delta1 subunit mediates spinal hyperexcitability in pain modulation. *Pain,* 125**,** 20-34.

LI, K. W., YU, Y. P., ZHOU, C., KIM, D. S., LIN, B., SHARP, K., STEWARD, O. & LUO, Z. D. 2014. Calcium channel alpha2delta1 proteins mediate trigeminal neuropathic pain states associated with aberrant excitatory synaptogenesis. *J Biol Chem,* 289**,** 7025-37.

LIN, H. C., HUANG, Y. H., CHAO, T. H., LIN, W. Y., SUN, W. Z. & YEN, C. T. 2014. Gabapentin reverses central hypersensitivity and suppresses medial prefrontal cortical glucose metabolism in rats with neuropathic pain. *Mol Pain,* 10**,** 63.

LU, V. B., BALLANYI, K., COLMERS, W. F. & SMITH, P. A. 2007. Neuron type-specific effects of brain-derived neurotrophic factor in rat superficial dorsal horn and their relevance to 'central sensitization'. *J Physiol,* 584**,** 543-63.

LU, V. B., BIGGS, J. E., STEBBING, M. J., BALASUBRAMANYAN, S., TODD, K. G., LAI, A. Y., COLMERS, W. F., DAWBARN, D., BALLANYI, K. & SMITH, P. A. 2009. Brain-derived neurotrophic factor drives the changes in excitatory synaptic transmission in the rat superficial dorsal horn that follow sciatic nerve injury. *J Physiol,* 587**,** 1013-32.

LUO, L., CHANG, L., BROWN, S. M., AO, H., LEE, D. H., HIGUERA, E. S., DUBIN, A. E. & CHAPLAN, S. R. 2007. Role of peripheral hyperpolarization-activated cyclic nucleotide-modulated channel pacemaker channels in acute and chronic pain models in the rat. *Neuroscience,* 144**,** 1477-85.

LUO, Z. D., CALCUTT, N. A., HIGUERA, E. S., VALDER, C. R., SONG, Y. H., SVENSSON, C. I. & MYERS, R. R. 2002. Injury type-specific calcium channel alpha 2 delta-1 subunit up-regulation in rat neuropathic pain models correlates with antiallodynic effects of gabapentin. *J Pharmacol Exp Ther,* 303**,** 1199-205.

LUO, Z. D., CHAPLAN, S. R., HIGUERA, E. S., SORKIN, L. S., STAUDERMAN, K. A., WILLIAMS, M. E. & YAKSH, T. L. 2001. Upregulation of dorsal root ganglion

(alpha)2(delta) calcium channel subunit and its correlation with allodynia in spinal nerve-injured rats. *J Neurosci,* 21**,** 1868-75.

MOGIL, J. S. 2009. Animal models of pain: progress and challenges. *Nat Rev Neurosci,* 10**,** 283-94.

MOGIL, J. S. & CRAGER, S. E. 2004. What should we be measuring in behavioral studies of chronic pain in animals? *Pain,* 112**,** 12-5.

MOORE, A., WIFFEN, P. & KALSO, E. 2014. Antiepileptic drugs for neuropathic pain and fibromyalgia. *JAMA,* 312**,** 182-3.

MOORE, K. A., BABA, H. & WOOLF, C. J. 2002. Gabapentin-- actions on adult superficial dorsal horn neurons. *Neuropharmacology,* 43**,** 1077-81.

MUNRO, G., ERICHSEN, H. K. & MIRZA, N. R. 2007. Pharmacological comparison of anticonvulsant drugs in animal models of persistent pain and anxiety. *Neuropharmacology,* 53**,** 609-18.

NARITA, N., KUMAR, N., CHERKAS, P. S., CHIANG, C. Y., DOSTROVSKY, J. O., CODERRE, T. J. & SESSLE, B. J. 2012. Systemic pregabalin attenuates sensorimotor responses and medullary glutamate release in inflammatory tooth pain model. *Neuroscience,* 218**,** 359-66.

NOH, S., KUMAR, N., BUKHANOVA, N., CHEN, Y., STEMKOWSI, P. L. & SMITH, P. A. 2014. The heart-rate-reducing agent, ivabradine, reduces mechanical allodynia in a rodent model of neuropathic pain. *Eur J Pain,* 18**,** 1139-47.

PAN, B., YU, H., PARK, J., YU, Y. P., LUO, Z. D. & HOGAN, Q. H. 2015. Painful nerve injury upregulates thrombospondin-4 expression in dorsal root ganglia. *J Neurosci Res,* 93**,** 443-53.

PAPP, I., SZUCS, P., HOLLO, K., ERDELYI, F., SZABO, G. & ANTAL, M. 2006. Hyperpolarization-activated and cyclic nucleotide-gated cation channel subunit 2 ion channels modulate synaptic transmission from nociceptive primary afferents containing substance P to secondary sensory neurons in laminae I-IIo of the rodent spinal dorsal horn. *Eur J Neurosci,* 24**,** 1341-52.

PARSONS, B., EMIR, B. & CLAIR, A. 2015. Temporal analysis of pain responders and common adverse events: when do these first appear following treatment with pregabalin. *J Pain Res,* 8**,** 303-9.

PATEL, M. K., GONZALEZ, M. I., BRAMWELL, S., PINNOCK, R. D. & LEE, K. 2000. Gabapentin inhibits excitatory synaptic transmission in the hyperalgesic spinal cord. *Br J Pharmacol,* 130**,** 1731-4.

PUNNAKKAL, P., VON SCHOULTZ, C., HAENRAETS, K., WILDNER, H. & ZEILHOFER, H. U. 2014. Morphological, biophysical and synaptic properties of glutamatergic neurons of the mouse spinal dorsal horn. *J Physiol,* 592**,** 759-76.

RAUCK, R., COFFEY, R. J., SCHULTZ, D. M., WALLACE, M. S., WEBSTER, L. R., MCCARVILLE, S. E., GRIGSBY, E. J. & PAGE, L. M. 2013. Intrathecal gabapentin to treat chronic intractable noncancer pain. *Anesthesiology,* 119**,** 675-86.

SCHMIDT, P. C., RUCHELLI, G., MACKEY, S. C. & CARROLL, I. R. 2013. Perioperative gabapentinoids: choice of agent, dose, timing, and effects on chronic postsurgical pain. *Anesthesiology,* 119**,** 1215-21.

SHARMA, U., GRIESING, T., EMIR, B. & YOUNG, J. P., JR. 2010. Time to onset of neuropathic pain reduction: A retrospective analysis of data from nine controlled trials of pregabalin

for painful diabetic peripheral neuropathy and postherpetic neuralgia. *Am J Ther,* 17**,** 577-85.

SIKANDAR, S. & DICKENSON, A. H. 2012. Visceral pain: the ins and outs, the ups and downs. *Curr Opin Support Palliat Care,* 6**,** 17-26.

SUTO, T., SEVERINO, A. L., EISENACH, J. C. & HAYASHIDA, K. 2014. Gabapentin increases extracellular glutamatergic level in the locus coeruleus via astroglial glutamate transporter-dependent mechanisms. *Neuropharmacology,* 81**,** 95-100.

SUTTON, K. G., MARTIN, D. J., PINNOCK, R. D., LEE, K. & SCOTT, R. H. 2002. Gabapentin inhibits high-threshold calcium channel currents in cultured rat dorsal root ganglion neurones. *Br J Pharmacol,* 135**,** 257-65.

SUZUKI, R., RAHMAN, W., RYGH, L. J., WEBBER, M., HUNT, S. P. & DICKENSON, A. H. 2005. Spinal-supraspinal serotonergic circuits regulating neuropathic pain and its treatment with gabapentin. *Pain,* 117**,** 292-303.

TAYLOR, C. P., ANGELOTTI, T. & FAUMAN, E. 2007. Pharmacology and mechanism of action of pregabalin: the calcium channel alpha2-delta (alpha2-delta) subunit as a target for antiepileptic drug discovery. *Epilepsy Res,* 73**,** 137-50.

TODD, A. J. 2010. Neuronal circuitry for pain processing in the dorsal horn. *Nat Rev Neurosci,* 11**,** 823-36.

TRAN-VAN-MINH, A. & DOLPHIN, A. C. 2010. The alpha2delta ligand gabapentin inhibits the Rab11-dependent recycling of the calcium channel subunit alpha2delta-2. *J Neurosci,* 30**,** 12856-67.

WALL, P. D., MELZACK, R. & BONICA, J. J. 1994. *Textbook of pain,* Edinburgh ; New York, Churchill Livingstone.

XIE, J. Y., QU, C., PATWARDHAN, A., OSSIPOV, M. H., NAVRATILOVA, E., BECERRA, L., BORSOOK, D. & PORRECA, F. 2014. Activation of mesocorticolimbic reward circuits for assessment of relief of ongoing pain: a potential biomarker of efficacy. *Pain,* 155**,** 1659-66.

YEZIERSKI, R. P., GREEN, M., MURPHY, K. & VIERCK, C. J. 2013. Effects of gabapentin on thermal sensitivity following spinal nerve ligation or spinal cord compression. *Behav Pharmacol,* 24**,** 598-609.

YOSHIZUMI, M., PARKER, R. A., EISENACH, J. C. & HAYASHIDA, K. 2012. Gabapentin inhibits gamma-amino butyric acid release in the locus coeruleus but not in the spinal dorsal horn after peripheral nerve injury in rats. *Anesthesiology,* 116**,** 1347-53.

YOUNG, G. T., EMERY, E. C., MOONEY, E. R., TSANTOULAS, C. & MCNAUGHTON, P. A. 2014. Inflammatory and neuropathic pain are rapidly suppressed by peripheral block of hyperpolarisation-activated cyclic nucleotide-gated ion channels. *Pain,* 155**,** 1708-19.

ZEILHOFER, H. U., WILDNER, H. & YEVENES, G. E. 2012. Fast synaptic inhibition in spinal sensory processing and pain control. *Physiol Rev,* 92**,** 193-235.

ZHOU, C. & LUO, Z. D. 2014. Electrophysiological characterization of spinal neuron sensitization by elevated calcium channel alpha-2-delta-1 subunit protein. *Eur J Pain,* 18**,** 649-58.

ZHOU, C. & LUO, Z. D. 2015. Nerve injury-induced calcium channel alpha-2-delta-1 protein dysregulation leads to increased pre-synaptic excitatory input into deep dorsal horn neurons and neuropathic allodynia. *Eur J Pain*.